Technische Universität München

Fakultät für Physik
T70 Theoretische Physik des frühen Universums

Quantum mechanical field fluctuations about inhomogeneous backgrounds

Juan Sebastián Cruz Avendaño

Vollständiger Abdruck der von der Fakultät für Physik der Technischen Universität München zur Erlangung des akademischen Grades eines

Doktors der Naturwissenschaften (Dr. rer. nat.)

genehmigten Dissertation.

Vorsitzender:	Prof. Dr. Peter Fierlinger
Prüfer der Dissertation:	1. Prof. Dr. Björn Garbrecht 2. Prof. Dr. Martin Beneke

Die Dissertation wurde am 31.08.2021 bei der Technischen Universität München eingereicht und durch die Fakultät für Physik am 22.11.2021 angenommen.

Abstract

Mathematical methods and applications aimed at understanding the effects of inhomogeneous backgrounds in the context of quantum field theory are presented. The first part introduces the reader to the necessary mathematical tools given a graduate-level knowledge of theoretical physics. The second describes applications to the electroweak vacuum decay of the Standard Model of particle physics. The work ends with the demonstration of how similar mathematical methods can be employed to include instanton effects and track down CP-violating phases in the context of QCD.

Kurzfassung

Es werden mathematische Methoden und Anwendungen vorgestellt, die darauf abzielen, die Auswirkungen inhomogener Hintergründe im Kontext der Quantenfeldtheorie zu verstehen. Der erste Teil führt den Leser in die notwendigen mathematischen Werkzeuge ein, wobei ein Absolventenniveau der theoretischen Physik vorausgesetzt wird. Die zweite beschreibt Anwendungen auf den elektroschwachen Vakuumzerfall des Standardmodells der Teilchenphysik. Die Arbeit endet mit der Demonstration, wie ähnliche mathematische Methoden verwendet werden können, um Instanton-Effekte einzubeziehen und CP-verletzende Phasen im Kontext von QCD aufzuspüren.

Contents

Preface

Allow me a few words about the purpose and making of this document. Put shortly, it is the love for challenges, comparable to the thrill provided by a roller-coaster. A roller-coaster of feelings of successes and failures, which serves to describe what doing research in physics seems to be. I have written it first to me, then for the physics community, with the hope of contributing to something bigger than what a single man can be. To me, this document will be forever a weird superposition of a beginning, of a deeper adventure, and the end of a journey. Hence, I must observe.

And with the fear of words being friendlier than formulas here it goes...

Juan S. Cruz
December 17, 2021

Introduction

One of the most striking things among the features of quantum mechanics is the nature of the vacuum. The idea of nothingness has accompanied humankind since the very far back in time and has evolved along with us through time. However, with the establishment of quantum mechanics in the early 20^{th} century, the classical notions of vacuum as just "emptiness" were not able to stand any longer.

According to quantum mechanics, one of the simplest systems we can think of, the harmonic oscillator, already presents a lowest-energy state which we call vacuum, to which it corresponds a non-zero energy. Moreover, the idea that all other states of the system are excitations of the vacuum acquires much importance since it promotes the vacuum from a sterile and spectating entity to one of the main characters in the history of the universe.

This thesis pretends to expose and hopefully deepen the understanding of some characteristics of the quantum field theoretical vacuum from the point of view of current physics and mathematics. Although the latter is the language used to describe the ideas that follow, it is the physical intuition and the careful experimental observation, the elements that guide our studies. That is the attitude we want to maintain among the different views within science itself.

This document is by no means a mathematics thesis, so we will not claim to derive the most general results starting with rigorous axioms; on the contrary, we study specific cases where we find interesting features and try to understand, with all the formality available to us, what their implications are to the current mainstream models.

The thesis is divided into three parts. They attempt to be as self-consistent as possible but, they do assume the background knowledge of a graduate-level physics student. The necessary tools are presented so that the reader attains a full grasp of the techniques that the author has learned in the last four years while doing research at the Technical University of Munich.

Part I of this document has the purpose of introducing the reader to the set of techniques we use in our computations. To do that, we start reviewing the path integral formulation while showing an explicit example of its usage and at the same time using many of the ideas that will be central in later chapters. Therein, a brief presentation of the construction of the effective action in the context of statistical mechanics is given. We also go over the concept of renormalization, which will also be needed in later stages of the document and is essential to extract physical quantities from quantum field theory computations. Finally, Part I ends with the application of the presented tools to quantum tunneling, which will be a central topic in part II.

The second part of this work deals with the stability of the electroweak vacuum. A question that arises naturally once a field configuration acquires a non-zero expectation value is; whether the vacuum can somehow decay into a configuration with even lower energy within the current Standard Model (SM) of particle physics. It has been known since the late 70s that there are non-perturbative euclidean solutions that may contribute

to vacuum decay [1]. At that time, this feature might have looked like a curiosity since the Standard Model of particle physics did not contain the Higgs boson; it was just a theoretical suggestion.
Things changed after 2012 when the discovery of the Higgs boson at LHC [2, 3] established the existence of a scalar particle, which we know today has the expected properties of the sought Higgs boson with a mass of $m_h = 125.18 \pm 0.16$ GeV [4]. This observation together with the improvements in the determination of the mass of the top quark, $m_t = 173.0 \pm 0.4$ GeV [4], puts the SM in a metastable phase [5]. Therefore, it is of much relevance to understand and compute not only the tree-level decay rate of the vacuum but possible corrections from higher-order effects as well, such as those coming from traditional one-loop diagrams or the gradients of an inhomogeneous background. We summarize previous studies and elaborate on the published work produced by our group[6] concerning this topic. In addition, we include some newly developed techniques that allow us to estimate gradient contributions utilizing a gradient expansion and which will be later published.
The last part, Part III, of this work is concerned with the computation of correlation functions over an instanton background[7]. These considerations have, in turn, led us to interesting implications to the *strong CP problem*. First, we review the pertaining interactions in the SM and then describe the low-energy quantum chromodynamics (QCD) effective models that are important for our discussion of instantons as well as their relation with the chiral anomaly[8, 9] and to the mesons η and η' known from the "U(1)-problem"[10]. We then describe how to derive Minkowskian or real-time versions of the fields and correlation functions needed, usually found in the literature written in Euclidean space. We compute correlation functions for fermions in QCD using a spectral decomposition which will allow us to study complex phases and draw conclusions on the relative phases contributing to CP-violation effects. We conclude by deriving consistent results from the point of view of the cluster decomposition principle, which supports our conclusions previously obtained using instantons.

Conventions and Notation

Minkowski metric	$\mathrm{diag}(+,-,-,-)$
Lorentz indices	$\mu = 0,1,2,3$
Euclidean indices	$\mu = 1,2,3,4$
Wick Rotation	$x^4 = -ix^0$

Lie Groups & Algebras

Unitary group	$U(N)$
Unitary Lie algebra	$\mathfrak{u}(N)$
Special Unitary group	$SU(N)$
Special Unitary Lie alg.	$\mathfrak{su}(N)$

Pauli Matrices (basis for $\mathfrak{su}(2)$)

$$\sigma_1 = \begin{pmatrix} 0 & 1 \\ 1 & 0 \end{pmatrix}$$

$$\sigma_2 = \begin{pmatrix} 0 & -i \\ i & 0 \end{pmatrix}$$

$$\sigma_3 = \begin{pmatrix} 1 & 0 \\ 0 & -1 \end{pmatrix}$$

Dirac Matrices Weyl representation (basis for $\mathfrak{so}^{\uparrow}_{+}(1,3)$)

$$\gamma^0 = \begin{pmatrix} 0 & -\mathbb{1}_2 \\ -\mathbb{1}_2 & 0 \end{pmatrix}$$

$$\gamma^k = \begin{pmatrix} 0 & \sigma^k \\ -\sigma^k & 0 \end{pmatrix}$$

$$\gamma^5 = \begin{pmatrix} \mathbb{1}_2 & 0 \\ 0 & -\mathbb{1}_2 \end{pmatrix}$$

Gell-Mann matrices (basis for $\mathfrak{su}(3)$)

$$\lambda^1 = \begin{pmatrix} 0 & 1 & 0 \\ 1 & 0 & 0 \\ 0 & 0 & 0 \end{pmatrix} \qquad \lambda^2 = \begin{pmatrix} 0 & -i & 0 \\ i & 0 & 0 \\ 0 & 0 & 0 \end{pmatrix}$$

$$\lambda^3 = \begin{pmatrix} 1 & 0 & 0 \\ 0 & -1 & 0 \\ 0 & 0 & 0 \end{pmatrix} \qquad \lambda^4 = \begin{pmatrix} 0 & 0 & 1 \\ 0 & 0 & 0 \\ 1 & 0 & 0 \end{pmatrix}$$

$$\lambda^5 = \begin{pmatrix} 0 & 0 & -i \\ 0 & 0 & 0 \\ i & 0 & 0 \end{pmatrix} \qquad \lambda^6 = \begin{pmatrix} 0 & 0 & 0 \\ 0 & 0 & 1 \\ 0 & 1 & 0 \end{pmatrix}$$

$$\lambda^7 = \begin{pmatrix} 0 & 0 & 0 \\ 0 & 0 & -i \\ 0 & i & 0 \end{pmatrix} \qquad \lambda^8 = \frac{1}{\sqrt{3}} \begin{pmatrix} 1 & 0 & 0 \\ 0 & 1 & 0 \\ 0 & 0 & -2 \end{pmatrix}$$

Gauge fields matrix notation with generators T^a	$\boldsymbol{A}_\mu = \sum_a A^a_\mu T^a$
Chiral projectors	$P_{\substack{L \\ R}} = \frac{(1 \mp \gamma^5)}{2}$

Part I

Mathematical Background

1

The path integral and the effective action

Quantum mechanics can be formulated in several ways. A traditional starting point is the treatment of the harmonic oscillator via canonical quantization, which is the algebraic approach of using creation and annihilation operators which diagonalize the Hamiltonian and capture the non-commutativity of observables such as position and momentum. Although this procedure lets itself generalize to multi-particle systems, in what is historically referred to as second quantization and the Fock space construction, it is not always suitable, in the context of field theory, for the computation of non-perturbative effects, which are often not captured by usual Feynman diagram techniques. For this reason, we employ the path integral formulation. Historically the idea of summing over paths was used for the study of Brownian motion and was much later shown by Feynman[11] to be completely equivalent to the canonical formulation of quantum mechanics. Here we review such formulation and expand by illustrating more modern techniques suited to the computation of effective actions over non-standard backgrounds. We follow the expositions of [12–15].

1.1 The Path Integral Formulation

Let us begin the discussion by obtaining the known quantum mechanics oscillator propagator by using the path integral. Then, we will show a generic construction that will highlight why the propagator is an essential building block giving out the transition amplitude connecting two states. Allow us to label such states generically by their degrees of freedom and an external time parameter, $|q_0, t_0\rangle$ and $|q_f, t_f\rangle$, via the evolution operator of the system, $\hat{U}(t, t')$:

$$K(q_f, t_f, q_0, t_0) \equiv \langle q_f, t_f | \, \hat{U}(t_f, t_0) \, | q_0, t_0 \rangle \, . \tag{1.1.1}$$

Let us then consider a one dimensional quantum mechanical system with describing some particle of mass m, whose dynamics are governed by the following Hamiltonian:

$$\hat{H} = \frac{\hat{p}^2}{2m} + V(\hat{x}). \tag{1.1.2}$$

In this simple case $\hat{U}(t_f, t_0)$ is related to the Hamiltonian of the system by

$$\hat{U}(t, t') = \exp\left(-\mathrm{i}\frac{(t - t')}{\hbar}\hat{H}\right). \tag{1.1.3}$$

Recall that the propagator is the integral kernel that allows us to obtain the wavefunction of the system at time t, $\psi(t)$, given as input the wavefunction of the system at an earlier time t_0, $\psi(t_0)$:

$$\psi(y;t) = \langle y|\psi(t)\rangle = \langle y|\,\hat{U}(t,t_0)\,|\psi(t_0)\rangle = \int \mathrm{d}x\, K(y,t,x,t_0)\psi(x,t_0), \tag{1.1.4}$$

where we have inserted a completeness relation and the definition in Eq. (1.1.1) to write down the last line. Now we will use the composition law for the evolution operator to rewrite the propagator as a sum over paths. We remind ourselves of said composition law,

$$\hat{U}(t_f,t_0) = \hat{U}(t_f,t')\hat{U}(t',t_0), \tag{1.1.5}$$

which evolves the system from time t_0 to time t_f in two steps, first evolving the system to some intermediate time $t' > t_0$ and then evolving it to $t_f > t'$. A repeated application of such law allows us to break down any time interval into arbitrarily many time steps Δt. Let us split the time interval $[t_0, t_f]$ into $N \in \mathbb{Z}$ equal sub-intervals, so that we can write the transition amplitude between two wavefunctions as

$$\langle x_f,t_f|\hat{U}(t_f,t_0)|x_0,t_0\rangle = \langle x_f,t_f|\hat{U}(t_f,t_{N-1})\hat{U}(t_f,t_{N-2})\cdots\hat{U}(t_1,t_0)|x_0,t_0\rangle. \tag{1.1.6}$$

Let us insert a completeness relation $\int |x\rangle\langle x|\,\mathrm{d}x$ between the application of each evolution operator and notice that for Hamiltonian operators without an explicit time dependence, the evolution operator, $\hat{u}(t,t')$, depends only on the time difference $t-t'$, so that we can write

$$\begin{aligned}
&\left\langle x_f,t_f|\hat{U}(t_f,t_0)|x_0,t_0\right\rangle \\
&\quad= \int \mathrm{d}x_{N-1}\,\mathrm{d}x_{N-2}\cdots\mathrm{d}x_1\langle x_f,t_f|\hat{U}(\Delta t)|x_{N-1}\rangle \prod_{i=1}^{N-2}\left\langle x_{i+1}|\hat{U}(\Delta t)|x_i\right\rangle\langle x_1|\hat{U}(\Delta t)|x_0,t_0\rangle \\
&\quad= \int \tilde{\mathcal{D}}x\langle x_f,t_f|\hat{U}(\Delta t)|x_{N-1}\rangle \prod_{i=1}^{N-2}\left\langle x_{i+1}|\hat{U}(\Delta t)|x_i\right\rangle\langle x_1|\hat{U}(\Delta t)|x_0,t_0\rangle,
\end{aligned} \tag{1.1.7}$$

where we have abbreviated the measure by $\tilde{\mathcal{D}}x = \mathrm{d}x_1\cdots\mathrm{d}x_{N-1}$. Now we can use the relation between the coordinate basis, $|x\rangle$, and the momentum basis $|p\rangle$, to make contact with the classical action, i.e. $\langle x|p\rangle = \mathrm{e}^{\mathrm{i}px/\hbar}$. By inserting closure relations for momentum space to the left of every evolution operator

$$\begin{aligned}
\langle x_f,t_f|\hat{U}(t_f,t_0)|x_0,t_0\rangle = \int \tilde{\mathcal{D}}x\mathcal{D}p\langle x_f,t_f|p_N\rangle\langle p_N|\hat{U}(\Delta t)|x_{N-1}\rangle \\
\prod_{i=1}^{N-2}\langle x_{i+1}|p_{i+1}\rangle\langle p_{i+1}|\hat{U}(\Delta t)|x_i\rangle\langle x_1|p_1\rangle\langle p_1|\hat{U}(\Delta t)|x_0,t_0\rangle,
\end{aligned} \tag{1.1.8}$$

where $\mathcal{D}p = \mathrm{d}p_1 \cdots \mathrm{d}p_N/(2\pi\hbar)^N$. Let us estimate the expected values containing the evolution operator

$$\langle p_{i+1}|\hat{U}(\Delta t)|x_i\rangle \approx \left\langle p_{i+1}\left|\mathbb{1} - \frac{\mathrm{i}}{\hbar}\Delta t\hat{H}\right|x_i\right\rangle \tag{1.1.9}$$

$$\approx \left\langle p_{i+1}\left|\mathbb{1} - \frac{\mathrm{i}}{\hbar}\Delta t\left(\frac{\hat{p}^2}{2m} + V(\hat{x})\right)\right|x_i\right\rangle \tag{1.1.10}$$

$$\approx \langle p_{i+1}|x_i\rangle \exp\left(-\frac{\mathrm{i}}{\hbar}\Delta t\left(\frac{p_{i+1}^2}{2m} + V(x_i)\right)\right) \tag{1.1.11}$$

$$\equiv \langle p_{i+1}|x_i\rangle \exp\left(-\frac{\mathrm{i}}{\hbar}\Delta t H(p_{i+1}, x_i)\right), \tag{1.1.12}$$

note that the expression above does not contain operators anymore. We can write the factors $\langle x_i|p_i\rangle$ as exponentials to obtain

$$\langle x_f, t_f|\hat{U}(t_f, t_0)|x_0, t_0\rangle = \int \tilde{\mathcal{D}}x\mathcal{D}p \exp\left\{\frac{\mathrm{i}\Delta t}{\hbar}\left[\frac{p_N(x_f - x_{N-1})}{\Delta t} + \frac{p_{N-1}(x_{N-1} - x_{N-2})}{\Delta t} + \right.\right.$$

$$\left.\left. \cdots + \frac{p_1(x_2 - x_0)}{\Delta t} - H(p_N, x_{N-1}) - H(p_{N-1}, x_{N-2}) - \cdots - H(p_1, x_0)\right]\right\}. \tag{1.1.13}$$

Let us perform the momentum integrals to simplify the exponent. They are all of the following form and can be computed by completing the binomial in the exponent into a perfect square

$$\int \frac{\mathrm{d}p_i}{2\pi\hbar} \exp\left\{\frac{\mathrm{i}}{\hbar}\Delta t\left(p_i\frac{(x_i - x_{i-1})}{\Delta t} - \frac{p_i^2}{2m}\right)\right\} = \sqrt{\frac{m}{2\pi\hbar\mathrm{i}\Delta t}} \exp\left[\frac{\mathrm{i}}{\hbar}\Delta t\frac{m}{2}\left(\frac{x_i - x_{i-1}}{\Delta t}\right)^2\right]. \tag{1.1.14}$$

With this last expression we can take the limit of $N \longrightarrow \infty$, which is the same as taking $\Delta t \longrightarrow 0$ and thus

$$\frac{x_i - x_{i-1}}{\Delta t} \approx \dot{x}_i, \tag{1.1.15}$$

while making the sum over sub-intervals an integral,

$$\langle x_f, t_f|\hat{U}(t_f, t_0)|x_0, t_0\rangle = \lim_{N\to\infty} \int \mathcal{D}x \exp\left\{\frac{\mathrm{i}}{\hbar}\sum_{i=1}^{N}\Delta t\left(\frac{m}{2}\left(\frac{x_i - x_{i-1}}{\Delta t}\right)^2 - V(x_{i-1})\right)\right\}$$

$$= \int \mathcal{D}x \exp\left\{\frac{\mathrm{i}}{\hbar}\int_{t_0}^{t_f} \mathrm{d}t\left(\frac{m}{2}\dot{x}^2(t) - V(x(t))\right)\right\}, \tag{1.1.16}$$

where

$$\mathcal{D}x = \lim_{N\to\infty} \sqrt{\frac{m}{2\pi\mathrm{i}\hbar\Delta t}} \prod_{i=1}^{N} \mathrm{d}x_i \sqrt{\frac{m}{2\pi\mathrm{i}\hbar\Delta t}}. \tag{1.1.17}$$

We can see that the exponential contains nothing else but the Lagrangian of the system which after integration gives us its action and the path integral

$$\langle x_f, t_f|\hat{U}(t_f, t_0)|x_0, t_0\rangle = \int \mathcal{D}x \ \mathrm{e}^{\frac{\mathrm{i}}{\hbar}S[x(t)]}, \tag{1.1.18}$$

which summarizes the idea of summing paths weighted by their action contribution, Fig. 1.1 illustrates what we have done by discretization through a fixed time interval and what formulas Eq. (1.1.7) and briefly in Eq. (1.1.18).

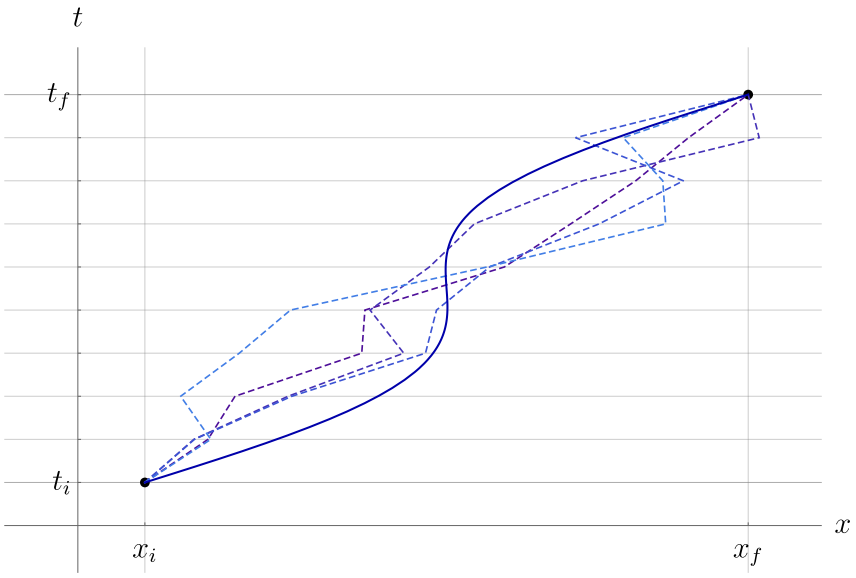

Figure 1.1: Depiction of several discrete paths (dashed) and a limiting path (solid line) joining the initial and final points considered in the path integral formulation.

1.1.1 The free particle revisited

As an example of the spoken formulation, let us consider a non-relativistic free particle of mass m, for which we only need to employ Eq. (1.1.18) with $V = 0$, and compute the propagator,

$$\langle x_f, t_f | U(\Delta t) | x_i, t_i \rangle = \int_{x(t_i)=x_i}^{x(t_f)=x_f} \mathcal{D}x \; \mathrm{e}^{\frac{\mathrm{i}}{\hbar}\int \mathrm{d}t \left(\frac{m}{2}\dot{x}^2\right)}. \tag{1.1.19}$$

The path can be split into sub-intervals as described previously and together with Eq. (1.1.14) one can arrive to the equation

$$\begin{aligned}\langle x_f, t_f | U(\Delta t) | x_i, t_i \rangle &= \sqrt{\frac{m}{2\pi \mathrm{i}\hbar(t_f - t_i)}} \exp\left\{ (t_f - t_i) \frac{\mathrm{i}m}{2\hbar} \left(\frac{x_f - x_i}{(t_f - t_i)} \right)^2 \right\} + \mathcal{O}((t_f - t_i)^2) \\ &= \sqrt{\frac{m}{2\pi \mathrm{i}\hbar(t_f - t_i)}} \exp\left\{ \frac{\mathrm{i}m}{2\hbar} \frac{(x_f - x_i)^2}{(t_f - t_i)} \right\} + \mathcal{O}((t_f - t_i)^2). \end{aligned} \tag{1.1.20}$$

This result can be further interpreted in relation to the action evaluated on a classical solution. That is, a free particle moves with constant speed and if we require the boundary conditions above, we have the following classical path,

$$x_{cl}(t) = \frac{1}{t_f - t_i} \left((t - t_i) x_f - (t - t_f) x_i \right). \tag{1.1.21}$$

Evaluating the action over such path, we have

$$\begin{aligned} S[x_{cl}] &= \frac{m}{2} \int_{t_i}^{t_f} \mathrm{d}t (\dot{x}_{cl}(t))^2 = \frac{m}{2} \int_{t_i}^{t_f} \mathrm{d}t \frac{1}{(t_f - t_i)^2} (x_f - x_i)^2 \\ &= \frac{m}{2} \int_{t_i}^{t_f} \mathrm{d}t \frac{1}{(t_f - t_i)^2} (x_f - x_i)^2 = \frac{m}{2} \frac{(x_f - x_i)^2}{t_f - t_i}. \end{aligned} \tag{1.1.22}$$

Observe as well that

$$\frac{\partial^2 S[x_{cl}]}{\partial x_f \partial x_i} = -m\frac{1}{t_f - t_i}, \tag{1.1.23}$$

which hints at the formula

$$\langle x_f, t_f | U(\Delta t) | x_i, t_i \rangle = \sqrt{\frac{\mathrm{i}}{2\pi\hbar}\frac{\partial^2 S[x_{cl}]}{\partial x_f \partial x_i}} \exp\left(\frac{\mathrm{i}}{\hbar} S[x_{cl}]\right). \tag{1.1.24}$$

1.1.2 The harmonic oscillator revisited

For the harmonic oscillator of mass m and natural frequency ω, we take Eq. (1.1.2) with $V(\hat{x}) = m\omega^2\hat{x}^2$ and attempt to compute the propagator as in Eq. (1.1.18). We follow closely the arguments exposed in Section 2.7 from [15]. We will already employ here some of the common methods used for the calculation of fluctuations in field theory. In order to deal with the oscillatory behavior displayed by the exponential of the action, we perform a Wick rotation, i.e. $t \to -\mathrm{i}\tau$. Doing this leads us to

$$\langle x_f | U(\tau_f, \tau_i) | x_i \rangle = \int_{x(\tau_i)=x_i}^{x(\tau_f)=x_f} \mathcal{D}[x]\, \mathrm{e}^{-S_E[x]/\hbar}, \tag{1.1.25}$$

with

$$S_E[x] = \int_{\tau_i}^{\tau_f} \mathrm{d}\tau \frac{1}{2}\left(m\dot{x}^2(\tau) + m\omega^2 x^2(\tau)\right). \tag{1.1.26}$$

The next step is to expand the path integration around a classical solution, $x_c(\tau)$, which satisfies the classical equation of motion,

$$m\ddot{x}_c - m\omega^2 x_c = 0, \tag{1.1.27}$$

where the dot means derivative with respect to τ. We then integrate over a new set of paths,

$$x(\tau) = x_c(\tau) + r(\tau), \tag{1.1.28}$$

which corresponds to a translation at every point in Euclidean time. These means that the following boundary conditions are to be met

$$x_c(\tau_i) = x_i, \qquad x_c(\tau_f) = x_f, \qquad \text{and} \qquad r(\tau_i) = r(\tau_f) = 0, \tag{1.1.29}$$

while the path integral measure changes from $\mathcal{D}[x] = \mathcal{D}[r]$, since translations in functional space have a Jacobian of 1. The action is in turn expanded as

$$S_E[x] = S_E[x_c] + \int_{\tau_i}^{\tau_f} \mathrm{d}\tau\, m\left(\dot{r}(\tau)\dot{x}_c(\tau) + \omega^2 r(\tau) x_c(\tau)\right) + S_E[r]. \tag{1.1.30}$$

We observe that by means of integration by parts we can identify the second term of the right hand side as nothing else than the equations of motion evaluated at x_c, which vanishes according to Eq. (1.1.27). We have reduced the propagator, Eq. (1.1.25), to

$$\langle x_f | U(\tau_f, \tau_i) | x_i \rangle = N(\omega, m, \tau)\, \mathrm{e}^{-S_E[x_c]/\hbar}, \tag{1.1.31}$$

with

$$N(\omega, m, \Delta\tau) = \int_{r(\tau_i)=0}^{r(\tau_f)=0} \mathcal{D}[r] \exp\left\{-\frac{m}{2\hbar}\int_{\tau_i}^{\tau_f} \mathrm{d}\tau \left(\dot{r}^2(\tau) + \omega^2 r^2(\tau)\right)\right\}. \tag{1.1.32}$$

Which is expected already from the Eq. (1.1.24), we learn that the exponential factor will contain the classical action while the normalization will depend on the fluctuations around it. At this point we can solve the equation of motion, Eq. (1.1.27), subject to the given boundary conditions in order to obtain a closed form for the classical action $S_E[x_c]$. It is immediate to verify that

$$x_c(\tau) = \frac{1}{\sinh(\omega(\tau_f - \tau_i))}\left[x_i \sinh(\omega(\tau_f - \tau)) + x_f \sinh(\omega(\tau - \tau_i))\right] \tag{1.1.33}$$

solves such equation and satisfies the boundary conditions. Let us now evaluate the action on this solution:

$$\begin{aligned} S_E[x_c] &= \frac{m}{2}\int_{\tau_i}^{\tau_f} \mathrm{d}\tau \left(\dot{x}_c^2(\tau) + \omega^2 x_c^2(\tau)\right) = \frac{m}{2}\left[x_c\dot{x}_c\Big|_{\tau_i}^{\tau_f} + \int_{\tau_i}^{\tau_f} \mathrm{d}\tau x_c\left(-\ddot{x}_c(\tau) + \omega^2 x_c(\tau)\right)\right] \\ &= \frac{m}{2}\left[x_c(\tau_f)\dot{x}_c(\tau_f) - x_c(\tau_i)\dot{x}_c(\tau_i)\right] \\ &= \frac{m\omega}{2\sinh(\omega\Delta\tau)}\left[(x_f^2 + x_i^2)\cosh(\omega\Delta\tau) - 2x_f x_i\right]. \end{aligned} \tag{1.1.34}$$

At this point the the integral over fluctuations r is missing, however it does not depend on the boundary conditions anymore and will produce a normalization factor, which we can compute as follows. Let us introduce the partition function

$$Z(\beta) = \mathrm{tr}\left(\mathrm{e}^{-\beta H}\right), \tag{1.1.35}$$

where β is conventionally related with temperature in statistical systems, here it serves for book-keeping of the boundary conditions, $x_f = x(\hbar\beta/2)$ and $x_i = x(-\hbar\beta/2)$. We can relate the partition function with the normalization by choosing periodic boundary conditions $x_f = x_i = x_b$, in which case we can take the trace of Eq. (1.1.31),

$$Z(\beta) = \int \mathrm{d}x_b \, \langle x_b|U(\beta/2, -\beta/2)|x_b\rangle \tag{1.1.36}$$

$$= N(m,\omega,\beta)\int \mathrm{d}x_b \, \mathrm{e}^{-S_E[x_c(\tau)]/\hbar} \tag{1.1.37}$$

$$= N(m,\omega,\beta)\int \mathrm{d}x_b \, \exp\left(-\frac{m\omega x_b^2}{\hbar\sinh(\omega\hbar\beta)}(\cosh(\omega\hbar\beta) - 1)\right) \tag{1.1.38}$$

$$= N(m,\omega,\beta)\int \mathrm{d}x_b \, \exp\left(-\frac{m\omega}{\hbar}x_b^2 \tanh\left(\frac{\omega\hbar\beta}{2}\right)\right) \tag{1.1.39}$$

$$= N(m,\omega,\beta)\sqrt{\frac{\pi\hbar}{m\omega\tanh(\beta\hbar\omega/2)}}, \tag{1.1.40}$$

where we have used the result of Eq. (1.1.34) before computing the last Gaussian integral. At this point we have that

$$N(m,\omega,\beta) = Z(\beta)\sqrt{\frac{m\omega\tanh(\beta\hbar\omega/2)}{\pi\hbar}}. \tag{1.1.41}$$

Let us now compute $Z(\beta)$ using spectral techniques which will be often used in later chapters. We consider first a discrete version of the problem (with $\hbar = 1$ and $m = 1$), where one has initially a finite number of sub-intervals:

$$Z(\beta,\epsilon) = \left(\frac{1}{2\pi\epsilon}\right)^{n/2} \int \mathrm{d}x_0\, \mathrm{d}x_n \delta(x_n - x_0) \int \prod_{k=1}^{n-1} \mathrm{d}x_k\, \mathrm{e}^{-S_E(x,\epsilon)}, \tag{1.1.42}$$

with a discrete version of the action

$$S_E(x,\epsilon) = \sum_{k=1}^{n} \left[\frac{(x_k - x_{k-1})^2}{2\epsilon} + \frac{1}{2}\epsilon\omega^2 x_k^2\right]. \tag{1.1.43}$$

Let us decompose x_k into discrete mode expansion

$$x_k = \frac{1}{\sqrt{n}} \sum_{\ell=0}^{n-1} \mathrm{e}^{2\mathrm{i}\pi k\ell/n} c_\ell, \tag{1.1.44}$$

with the convention that ℓ is a periodic integer modulo n, i.e. $-\ell \sim n-\ell$, demanding that x_k is real, so that we have the condition $c_\ell = \bar{c}_{-\ell}$, and remembering the relation

$$\frac{1}{n} \sum_{k=0}^{n-1} \mathrm{e}^{2\pi\mathrm{i}k\ell/n} = \delta_{0,\ell}, \tag{1.1.45}$$

the action takes the form

$$S_E(x,\epsilon) = \sum_{\ell=0}^{n-1} \bar{c}_\ell \left[\frac{1}{\epsilon}\left(1 - \cos\left(\frac{2\pi\ell}{n}\right)\right) + \frac{1}{2}\omega^2\epsilon\right] c_\ell. \tag{1.1.46}$$

We can recognize this as a change of variables, through transformation which is unitary and with a Jacobian which is just a phase. Coming back to the partition function, we will need the known result for Gaussian integrals (see Appendix A.)

$$\int \left(\prod_{i=1}^{n} \frac{\mathrm{d}z_i\, \mathrm{d}\bar{z}_i}{2\mathrm{i}\pi}\right) \exp\left[-\mathbf{A}(\bar{\mathbf{z}},\mathbf{z}) + \bar{\mathbf{b}}\cdot\mathbf{z} + \bar{\mathbf{z}}\cdot\mathbf{b}\right] = \frac{1}{\det \mathbf{A}}\, \mathrm{e}^{\bar{\mathbf{b}}\,\mathbf{A}^{-1}\,\mathbf{b}}, \tag{1.1.47}$$

where $\mathbf{A}$ is a quadratic form on $\bar{\mathbf{z}}$ and $\mathbf{z}$. For our case we have $\mathbf{b} = 0$ and that the integration has $n/2$ independent directions because of the reality condition means we get a square root over the determinant,

$$\begin{aligned} Z(\beta,\epsilon) &= \left(\frac{1}{2\pi\epsilon}\right)^{\frac{n}{2}} \int \mathrm{d}c_0 \int \left(\prod_{k=1}^{n-1} \mathrm{d}c_\ell\, \mathrm{d}\bar{c}_\ell\right) \prod_{\ell=0}^{n-1} \exp\left(-\bar{c}_\ell \left[\frac{1}{\epsilon}\left(1 - \cos\left(\frac{2\pi\ell}{n}\right)\right) + \frac{1}{2}\omega^2\epsilon\right] c_\ell\right) \\ &= \left(\frac{1}{2\epsilon}\right)^{n/2} \left(\prod_{\ell=0}^{n-1} \left[\frac{1}{\epsilon}\left(1 - \cos\left(\frac{2\pi\ell}{n}\right)\right) + \frac{1}{2}\omega^2\epsilon\right]\right)^{-1/2} \qquad (1.1.48) \\ &= \left(\frac{1}{2}\right)^{n/2} \left(\prod_{\ell=0}^{n-1} 1 + \frac{1}{2}\omega^2\epsilon^2 - \cos\left(\frac{2\pi\ell}{n}\right)\right)^{-1/2}. \qquad (1.1.49) \end{aligned}$$

We can parameterize $1+\omega^2\epsilon^2/2 = \cosh\theta = \cos(\mathrm{i}\theta)$ and prove the following trigonometric identity:

$$\prod_{k=0}^{n-1} \cos(\mathrm{i}\theta) - \cos(2\pi\ell/n) = \prod_{k=0}^{n-1} 2\sin\left(\frac{\pi\ell}{n} + \frac{\mathrm{i}\theta}{2}\right)\sin\left(\frac{\pi\ell}{n} - \frac{\mathrm{i}\theta}{2}\right) \tag{1.1.50}$$

$$= 2^n\left(\frac{1}{2^{n-1}}\sin\left(\frac{\mathrm{i}n\theta}{2}\right)\right)\left(\frac{-1}{2^{n-1}}\sin\left(\frac{\mathrm{i}n\theta}{2}\right)\right) \tag{1.1.51}$$

$$= -\frac{2}{2^{n-1}}\frac{1-\cos(\mathrm{i}n\theta)}{2} \tag{1.1.52}$$

$$= \frac{1}{2^{n-1}}(\cosh(n\theta)-1), \tag{1.1.53}$$

where we have used the following multiple angle product formula for the Sine to obtain the second line of the above computation:

$$\frac{1}{2^{n-1}}\sin(nx) = \prod_{k=0}^{n-1}\sin\left(x+\frac{k\pi}{n}\right). \tag{1.1.54}$$

Applying the result from Eq. (1.1.53) to the last expression in Eq. (1.1.49),

$$Z(\beta,\epsilon) = \left(\frac{1}{2}\right)^{n/2}\left(\frac{2}{2^n}(\cosh(n\theta)-1)\right)^{-1/2}. \tag{1.1.55}$$

In order to finally obtain the partition function we must take $\epsilon\to 0$ and $n\to\infty$ simultaneously, meaning that $n\epsilon=\beta$ remains fixed. For small ϵ we have from our parametrization, $\theta\approx\omega\epsilon$ and $n\theta\to\beta\omega$ hence

$$Z(\beta) = \lim_{\substack{\epsilon\to 0\\ n\to\infty}} Z(\beta,\epsilon) = \frac{1}{\sqrt{2(\cosh(\beta\omega)-1)}} = \frac{1}{2\sinh\left(\frac{\omega\beta}{2}\right)} = \frac{\mathrm{e}^{-\beta\omega/2}}{1-\mathrm{e}^{-\beta\omega}}. \tag{1.1.56}$$

We can make an analogous computation without discretization to illustrate the appearance of an infinite factor coming from the measure and to confirm the above equation. Let us consider again an expansion in modes for the paths $x(\tau)$, notice the sum will still be discrete given the boundary conditions,

$$x(\tau) = \frac{1}{\sqrt{\beta}}\sum_{\ell>0}^{\infty} c_\ell\,\mathrm{e}^{2\mathrm{i}\pi\ell.\tau/\beta} \tag{1.1.57}$$

Again the Jacobian amounts to an overall phase and the measure is then

$$\mathcal{D}[x] = \mathrm{d}x_0\prod_{\ell>0}\mathrm{d}c_\ell\,\mathrm{d}\bar{c}_\ell, \tag{1.1.58}$$

where the reality condition is the same as before, $c_{-\ell}=\bar{c}_\ell$. The action for the Euclidean operator (after one integration by parts) is $-\mathrm{d}^2/\mathrm{d}\tau^2+\omega^2$ and in these new coordinates becomes

$$S_E[c_\ell,\bar{c}_\ell] = \sum_{\ell\geq 1}\bar{c}_\ell\left(\omega^2 + 4\frac{\pi^2\ell^2}{\beta^2}\right)c_\ell + \frac{1}{2}\omega^2 c_0^2, \tag{1.1.59}$$

after having integrated over τ and used the orthogonality of the modes. The partition function is then

$$Z(\beta) = \int \mathrm{d}x_0 \prod_{k>0} \mathrm{d}c_k \; \mathrm{d}\bar{c}_k \, \mathrm{e}^{-S_E/\hbar} = \mathcal{N}' \frac{1}{\omega} \prod_{\ell>0} \left(\omega^2 + \frac{4\pi^2\ell^2}{\beta^2} \right)^{-1}, \tag{1.1.60}$$

where there are an infinite number of factors being absorbed in $\mathcal{N}'$. In order to extract physical information from determinants of operators, called functional determinants, it is necessary to compare against a reference case, usually the free case, however in this case it is easier to use theories with different ω parameters. A formal mathematical definition for these determinants and the equivalence to what we have described above can be found in[16], but the intuitive picture of a product of eigenvalues will suffice. Let us then consider the logarithmic derivative to check that we indeed make contact with Eq. (1.1.56);

$$\begin{aligned} \frac{\partial}{\partial\omega} \ln Z(\beta) &= -\frac{\partial}{\partial\omega} \ln\omega - \frac{1}{2} \sum_{\ell>0}^{\infty} \frac{\partial}{\partial\omega} \ln \left(\omega^2 + \frac{4\pi^2\ell^2}{\beta^2} \right) \\ &= -\frac{1}{\omega} - \frac{1}{2} \sum_{\ell>0}^{\infty} \frac{2\omega}{\omega^2 + \frac{4\pi^2\ell^2}{\beta^2}} = -\frac{\beta}{2\tanh(\beta\omega/2)}, \end{aligned} \tag{1.1.61}$$

where the last equality can be proven using the following factorization of $\sin(\pi z)$ coming from the *Weierstrass factorization theorem*,

$$\sin(\pi z) = \pi z \prod_{n=1}^{\infty} \left(1 - \left(\frac{z}{n} \right)^2 \right), \tag{1.1.62}$$

and then taking a logarithmic derivative. The result in Eq. (1.1.61) agrees with the previous discrete calculation, from which we can finish the computation of the normalization for the propagator. Using the result for the partition function, Eq. (1.1.56), and plugging it in Eq. (1.1.41) we can fully write down the propagator for the Euclidean harmonic oscillator. Restoring factors of $\hbar$ the propagator is

$$\langle x_f | U(\tau_f, \tau_i) | x_i \rangle = \sqrt{\frac{m\omega}{2\hbar\sinh(\omega\Delta\tau)}} \exp\left(\frac{-m\omega}{2\hbar\sinh(\omega\Delta\tau)} \left[(x_f^2 + x_i^2)\cosh(\omega\Delta\tau) - 2x_f x_i \right] \right). \tag{1.1.63}$$

In order to obtain the real time propagator we need to Wick rotate back, $\tau \to \mathrm{i}t$,

$$\langle x_f | U(t_f, t_i) | x_i \rangle = \sqrt{\frac{m\omega}{2\hbar\mathrm{i}\sin(\omega\Delta t)}} \exp\left(\frac{\mathrm{i}m\omega}{2\hbar\sin(\omega\Delta t)} \left[(x_f^2 + x_i^2)\cos(\omega\Delta t) - 2x_f x_i \right] \right). \tag{1.1.64}$$

As a bonus, we remark that the knowledge of the propagator allowed us, in this case, to compute the partition function, and with it extract the energy levels of the system without any a priori knowledge about them or the use of the traditional algebraic techniques that use creation and annihilation operators. Expression Eq. (1.1.56) can be written down as a series for large enough β and with $\hbar$ restored, as

$$Z(\beta) = \frac{\mathrm{e}^{-\beta\hbar\omega/2}}{1 - \mathrm{e}^{-\beta\hbar\omega}} = \sum_{n=0}^{\infty} \mathrm{e}^{-\beta\hbar\omega(n+1/2)}, \tag{1.1.65}$$

meaning

$$E_n = \hbar\omega\left(n + \frac{1}{2}\right) \qquad \text{for} \quad n \in \mathbb{N}. \tag{1.1.66}$$

Of course, this is not the simplest method for the quantum harmonic oscillator, but it has the advantage that it can be generalized to more complicated situations.

Comments on the harmonic oscillator example

The purpose of the last example is to demonstrate several techniques that will be used later in our studies, in a case where all computations can be done analytically and closed expressions are known for the quantities of interest such as the propagator or the partition function.
Therefore, it is crucial to highlight the central role played by the path integral formulation in connection with statistical ensembles. They together allow us to compute expectation values for desired observables. Another powerful tool is Gaussian integration. At the end of the day, in the context of quantum field theory, Gaussian integrals are the only functional integral which we can perform exactly, especially when dealing with more spatial dimensions. Therefore, handling them in all their possible forms is a must, for example, the fermionic case, the diagonalization operators appearing in the exponents, etc.
We will often use the exposed expansion around a classical solution to the equations of motion, which is generally referred to as the semi-classical expansion, where the perturbation parameter is to be understood to be $\hbar$. As we will see later in Sec. 1.2.2, this expansion coincides in the quantum field theoretic setting with an expansion in loops. We will concern ourselves with ways to compute fluctuation effects, that is, effects that appear at one-loop order in the traditional perturbative expansion in terms of the interaction couplings.

1.1.3 Connecting the dots towards Quantum Field Theory (QFT)

We now take the task of applying the previous techniques for a case closer to the main topics of the present document. Let us show a possible use of the path integral methods for the case of a real scalar field. For this purpose, we follow closely Fujikawa's book on path integrals[14] and Zinn-Justin's[12] as well as [13]. We introduce the generating functional which will frequently appear in our computations and show how it can be used to obtain the propagator for this model and give some comments about the iϵ prescription often found in traditional approaches to QFT. Let us consider the action for a free real scalar field in 4 dimensional Minkowski space in natural units $c = \hbar = 1$,

$$S[\phi] = \int \mathrm{d}^4x\, \mathcal{L} = \int \mathrm{d}^4x\, \frac{1}{2}\partial_\mu\phi\partial^\mu\phi - \frac{1}{2}m^2\phi^2 \tag{1.1.67}$$

$$= \int_{\mathscr{T}} \mathrm{d}t \int \mathrm{d}^3\vec{x}\, -\frac{1}{2}\phi(t,\vec{x})(\Box + m^2)\phi(t,\vec{x}), \tag{1.1.68}$$

where we have written the arguments for time and space explicitly in the second line and added the $\mathscr{T} \equiv (t_i, t_f)$ subscript to label the specific boundary conditions. If we were interested in vacuum to vacuum transitions within a certain time window for example, we would have to look at the set of fields

$$\mathscr{D}(t_i,t_f) = \left\{\phi(t,\vec{x}) : \mathbb{R}^4 \to \mathbb{R} \;\middle|\; \phi(t_i,\vec{x}) = \phi_{\text{asymp.}}(\vec{x}) \quad \text{and} \quad \phi(t_f,\vec{x}) = \phi_{\text{asymp.}}(\vec{x})\right\}, \tag{1.1.69}$$

where the free configurations above are eigenvalues of the free field operator

$$\hat{\phi}_{\text{asymp.}}(\vec{x}) = \int \frac{\mathrm{d}^3\vec{p}}{(2\pi)^3}\frac{1}{\sqrt{2E_p}}\left(a_{\vec{p}}\,\mathrm{e}^{\mathrm{i}\vec{p}\cdot\vec{x}} + a^\dagger_{\vec{p}}\,\mathrm{e}^{-\mathrm{i}\vec{p}\cdot\vec{x}}\right), \tag{1.1.70}$$

with $E_p = \sqrt{m^2+\vec{p}^2}$. We can employ the canonical quantization prescription, to write down a Hamiltonian and build the path integral from the evolution operator. For that purpose we will need the conjugated momentum field obtained by

$$\hat{\pi}_{\text{asymp.}}(\vec{x}) = \frac{\partial\mathcal{L}}{\partial\dot{\phi}(\vec{x})}\bigg|_{\text{asymp.}} = -\mathrm{i}\int\frac{\mathrm{d}^3\vec{p}}{(2\pi)^3}\sqrt{\frac{E_p}{2}}\left(a_{\vec{p}}\,\mathrm{e}^{\mathrm{i}\vec{p}\cdot\vec{x}} - a^\dagger_{\vec{p}}\,\mathrm{e}^{-\mathrm{i}\vec{p}\cdot\vec{x}}\right), \tag{1.1.71}$$

where $\dot{}$ means derivative with respect to time, together with the canonical commutation relations (CCR) at fixed time

$$[\hat{\phi}(\vec{x}),\hat{\pi}(\vec{y})] = \mathrm{i}\delta^3(\vec{x}-\vec{y}). \tag{1.1.72}$$

The associated Hilbert space of states can be spanned by a set of eigen-field configurations:

$$\begin{aligned}\hat{\phi}(\vec{x})\,|\Phi\rangle &= \Phi(\vec{x})\,|\Phi\rangle\,,\\ \hat{\pi}(\vec{x})\,|\Pi\rangle &= \Pi(\vec{x})\,|\Pi\rangle\,.\end{aligned} \tag{1.1.73}$$

which allow us to change from momentum to configuration space representation with the formula

$$\langle\Pi|\Phi\rangle = \mathrm{e}^{-\mathrm{i}\int\mathrm{d}^3x\,\Pi(\vec{x})\Phi(\vec{x})}. \tag{1.1.74}$$

The Hamiltonian density is computed using the Legendre transform with the free operators defined in Eqs. (1.1.70),(1.1.71), to arrive to

$$\hat{H} = \int\mathrm{d}^3\vec{x}\,\mathcal{H} = \int\mathrm{d}^3\vec{x}\,\frac{1}{2}\hat{\pi}^2 + \frac{1}{2}(\nabla\hat{\phi})^2 + \frac{1}{2}m^2\hat{\phi}^2. \tag{1.1.75}$$

As in previous sections, we use the Hamiltonian to evolve states. As an example, we consider the vacuum to vacuum transition amplitude, evolved in time steps of Δt:

$$\begin{aligned}\langle 0,t_f|U(t_f,t_i)|0,t_i\rangle = \int\mathcal{D}\Phi_1(x)\cdots\mathcal{D}\Phi_n(x)\left\langle 0\right|\mathrm{e}^{-\mathrm{i}\frac{\Delta t}{\hbar}\hat{H}(t_n)}\left|\Phi_n\right\rangle\left\langle\Phi_n\right|\mathrm{e}^{-\mathrm{i}\frac{\Delta t}{\hbar}\hat{H}(t_{n-1})}\left|\Phi_{n-1}\right\rangle\cdots\\ \left\langle\Phi_1\right|\mathrm{e}^{-\mathrm{i}\frac{\Delta t}{\hbar}\hat{H}(t_0)}\left|0\right\rangle.\end{aligned} \tag{1.1.76}$$

We can compute each of these expectation values as follows

$$\begin{aligned}\langle\Phi_{j+1}|\,\mathrm{e}^{-\mathrm{i}\frac{\Delta t}{\hbar}\hat{H}(t_j)}|\Phi_j\rangle &= \int\mathcal{D}\Pi\,\langle\Phi_{j+1}|\Pi\rangle\,\langle\Pi|\exp\left(-\mathrm{i}\frac{\Delta t}{\hbar}\int\mathrm{d}^3x\,\mathcal{H}(t_j)\right)|\Phi_j\rangle\\ &= \int\mathcal{D}\Pi\exp\left(\mathrm{i}\int\mathrm{d}^3\vec{x}\,\Pi(\vec{x})(\Phi_{j+1}(\vec{x})-\Phi_j(\vec{x}))\right)\\ &\quad\times\exp\left(\mathrm{i}\frac{\Delta t}{\hbar}\int\mathrm{d}^3\vec{x}\,\left(\frac{1}{2}\Pi^2(\vec{x})+\frac{1}{2}(\nabla\Phi_j)^2+\frac{1}{2}m^2\Phi_j^2\right)\right),\end{aligned} \tag{1.1.77}$$

where we have used Eq. (1.1.74). We can now perform the Gaußian integral and get

$$\langle\Phi_{j+1}|\,\mathrm{e}^{-\mathrm{i}\frac{\Delta t}{\hbar}\hat{H}(t_j)}|\Phi_j\rangle = N\exp\left(\mathrm{i}\frac{\Delta t}{\hbar}\int \mathrm{d}^3\vec{x}\;\mathcal{L}[\Phi_j,\partial_t\Phi_j]\right). \tag{1.1.78}$$

Next, using this result in Eq. (1.1.76) we arrive to the conventional expression of the amplitude as a path integral over a phase given by the action,

$$\langle 0,t_f|0,t_i\rangle \equiv \langle 0,t_f|U(t_f,t_i)|0,t_i\rangle = \int_{\mathscr{D}(t_i,t_f)}\mathcal{D}\Phi\;\mathrm{e}^{\frac{\mathrm{i}}{\hbar}S[\Phi]} \tag{1.1.79}$$

and for the case of S-matrix elements:

$$\langle 0,-\infty|0,\infty\rangle = \int_{\mathscr{D}(-\infty,\infty)}\mathcal{D}\Phi\;\mathrm{e}^{\frac{\mathrm{i}}{\hbar}S[\Phi]}. \tag{1.1.80}$$

For interacting theories we must define an interacting vacuum state $|\Omega\rangle$ which takes care of removing vacuum-bubble diagrams. For this vacuum state we demand

$$1 = \langle\Omega|\Omega\rangle, \tag{1.1.81}$$

which implies the following general formula for correlation functions

$$\langle\Omega\big|T\{\hat{\phi}_1(x_1)\cdots\hat{\phi}_n(x_n)\}\big|\Omega\rangle = \frac{\int\mathcal{D}\phi_1\cdots\mathcal{D}\phi_n\,\mathrm{e}^{\frac{\mathrm{i}}{\hbar}S}\phi_1(x_1)\cdots\phi_n(x_n)}{\int\mathcal{D}\phi_1\cdots\mathcal{D}\phi_n\,\mathrm{e}^{\frac{\mathrm{i}}{\hbar}S}}. \tag{1.1.82}$$

Notice that we have added the time-ordering prescription for the quantum fields appearing on the left-hand side, while within the path integral, only classical fields appear. We will provide more details concerning the iϵ prescription, which will confirm that the equation above indeed holds.

One way to compute such correlations in practice is by means of the generating functional. Let us add an external classical source to the exponent in Eq.(1.1.79). We call the following functional of a current, the generating functional

$$Z[J] = \int\mathcal{D}\Phi\exp\left(\frac{\mathrm{i}}{\hbar}S[\phi] + \frac{\mathrm{i}}{\hbar}\int\mathrm{d}^4x\,J(x)\phi(x)\right). \tag{1.1.83}$$

From functional calculus we have

$$\frac{\delta J(x)}{\delta J(y)} = \delta^4(x-y), \tag{1.1.84}$$

which allows us to express Eq. (1.1.82) in terms of functional derivatives of the generating functional $Z[J]$ (for the case of only one field) as

$$\frac{(-\mathrm{i})^n}{\hbar^n}\frac{1}{Z[0]}\frac{\delta^n}{\delta J(x_1)\cdots\delta J(x_n)}Z[J]\bigg|_{J=0} = \langle\Omega\big|T\{\hat{\phi}(x_1)\cdots\hat{\phi}(x_n)\}\big|\Omega\rangle. \tag{1.1.85}$$

We use the above formula to verify a matching result for the case of the two-point correlation function in the free theory. That is, we should obtain the Feynman propagator when we take $n=2$,

$$Z_{\text{free}}[J] = \int\mathcal{D}\phi\exp\left[\frac{\mathrm{i}}{\hbar}\int\mathrm{d}^4x\,\left(-\frac{1}{2}\phi(x)(\Box_x+m^2)\phi(x)+J(x)\phi(x)\right)\right]. \tag{1.1.86}$$

Using the result from the Appendix on Gaußian integrals Eq. (A.10), we have for the Klein-Gordon operator $\mathrm{i}(\Box_x + m^2)$,

$$Z_{\text{free}}[J] = N \exp\left[\mathrm{i}\int \mathrm{d}^4x \int \mathrm{d}^4y \,\frac{1}{2}J(x)G(x-y)J(y)\right], \tag{1.1.87}$$

where G is its Green's function, i.e. observes $\mathrm{i}(\Box_x + m^2)G(x-y) = \delta^4(x-y)$, and can be written as

$$G(x-y) = \mathrm{i}\int \frac{\mathrm{d}^4p}{(2\pi)^4}\frac{\mathrm{e}^{\mathrm{i}p(x-y)}}{p^2-m^2}. \tag{1.1.88}$$

Then we using the functional derivatives prescription described, Eq. (1.1.85), we get

$$\langle 0|T\{\hat{\phi}(x)\hat{\phi}(y)\}|0\rangle = \frac{(-\mathrm{i})^2}{\hbar^2}\frac{1}{Z[0]}\frac{\delta^2}{\delta J(x)\delta J(y)}Z[J]\bigg|_{J=0} = \mathrm{i}G(x-y), \tag{1.1.89}$$

as expected. So far we have not been explicit enough with the boundary conditions and the time ordering which is the reason why we do not have the $\mathrm{i}\epsilon$ in the Feynman propagator. We recall the $\mathrm{i}\epsilon$ is related with causality and specifies which type of Green's function is to be considered. The Feynman propagator is the Green's function complying with causality and therefore compliant with time ordering. Let us now consider explicitly an S-matrix element to see how the $\mathrm{i}\epsilon$ prescription shows up from the path integral formulation.
We follow the explanations from Refs. [13, 17] to see how imposing a projection on states with appropriate boundary conditions, we can understand the appearance of the $\mathrm{i}\epsilon$ prescription. Let us remark its importance by noting that from a mathematical perspective, the path integral does not converge without any imaginary part in the action. Consider then a matrix element

$$\langle f|S|i\rangle = \int_{\phi(t\to\pm\infty)=\phi_{\text{asymp.}}} \mathcal{D}\phi\, \mathrm{e}^{\mathrm{i}S[\phi]}. \tag{1.1.90}$$

Another way to impose the boundary conditions is to write explicit projectors in the integrand while leaving the integration constraints unspecified:

$$\langle f|S|i\rangle = \int \mathcal{D}\phi\ \mathrm{e}^{\mathrm{i}S[\phi]}\,\langle f|\Phi(t=\infty)\rangle\,\langle\Phi(t=-\infty)|i\rangle\,. \tag{1.1.91}$$

Let us consider the vacuum-to-vacuum transition amplitude in a free theory. Given the mode expansion a free scalar field and denoting with boldface letters the spatial components of vectors, we have

$$\hat{\phi}(t,\mathbf{x}) = \int \frac{\mathrm{d}^3\mathbf{p}}{(2\pi)^3}\frac{1}{\sqrt{2E_{\mathbf{p}}}}\left(a_{\mathbf{p}}\,\mathrm{e}^{-\mathrm{i}p\cdot x} + a^\dagger_{\mathbf{p}}\,\mathrm{e}^{\mathrm{i}p\cdot x}\right)\Big|_{p^0=E_{\mathbf{p}}}, \tag{1.1.92}$$

with $E_{\mathbf{p}} = \sqrt{\mathbf{p}^2+m^2}$ and where we have included the time dependence in contrast to the asymptotic expressions written before. Recalling the definition of the conjugated momentum field:

$$\hat{\pi}(t,\mathbf{x}) \equiv \partial_t\hat{\phi}(t,\mathbf{x}) = -\mathrm{i}\int \frac{\mathrm{d}^3\mathbf{p}}{(2\pi)^3}\sqrt{\frac{E_{\mathbf{p}}}{2}}\left(a_{\mathbf{p}}\,\mathrm{e}^{-\mathrm{i}p\cdot x} - a^\dagger_{\mathbf{p}}\,\mathrm{e}^{\mathrm{i}p\cdot x}\right)\Big|_{p^0=E_{\mathbf{p}}}, \tag{1.1.93}$$

we can write the creation and annihilation operators in terms of the field and its conjugated momentum by first inverting the Fourier transform and then writing down an appropriate linear combination:

$$\begin{aligned} a_{\mathbf{p}} &= \frac{1}{\sqrt{2}} \int \mathrm{d}^3\mathbf{x}\, \mathrm{e}^{\mathrm{i}p\cdot x} \left(\sqrt{E_{\mathbf{p}}}\, \hat{\phi}(t,\mathbf{x}) + \frac{\mathrm{i}}{\sqrt{E_{\mathbf{p}}}}\, \hat{\pi}(t,\mathbf{x}) \right) \Big|_{p^0=E_{\mathbf{p}}}, \\ a^\dagger_{\mathbf{p}} &= \frac{1}{\sqrt{2}} \int \mathrm{d}^3\mathbf{x}\, \mathrm{e}^{-\mathrm{i}p\cdot x} \left(\sqrt{E_{\mathbf{p}}}\, \hat{\phi}(t,\mathbf{x}) - \frac{\mathrm{i}}{\sqrt{E_{\mathbf{p}}}}\, \hat{\pi}(t,\mathbf{x}) \right) \Big|_{p^0=E_{\mathbf{p}}}. \end{aligned} \tag{1.1.94}$$

Let us keep the notation given in Eq. (1.1.73) while noticing that the operators at a given t have a given field configuration $\Phi(\mathbf{x})$ as eigenvalue. We can understand the action of $\hat{\pi}(t,\mathbf{x})$ as an operator acting on eigenstates of $\hat{\phi}$ as follows,

$$\hat{\pi}(t,\mathbf{x})|\Phi\rangle = \int \mathcal{D}\Pi\, \hat{\pi}(t,\mathbf{x})|\Pi\rangle\, \langle\Pi|\Phi\rangle = \int \mathcal{D}\Pi\, \Pi(\mathbf{x})\, \mathrm{e}^{-\mathrm{i}\int \mathrm{d}^3\mathbf{y}\Pi(\mathbf{y})\mathbf{\Phi}(\mathbf{y})}|\Pi\rangle \tag{1.1.95}$$

$$= \int \mathcal{D}\Pi\, \mathrm{i}\frac{\delta}{\delta\Phi(\mathbf{x})}\, \mathrm{e}^{-\mathrm{i}\int \mathrm{d}^3\mathbf{y}\Pi(\mathbf{y})\mathbf{\Phi}(\mathbf{y})}|\Pi\rangle = \mathrm{i}\frac{\delta}{\delta\Phi(\mathbf{x})}|\Phi\rangle. \tag{1.1.96}$$

We can obtain a differential equation for the transition amplitude $\langle\Phi|0\rangle$ by using the annihilation of the vacuum property of $a_{\mathbf{p}}$. Explicitly, for a given $\mathbf{p}$ and field configuration Φ it holds that

$$0 = \langle\Phi|a_{\mathbf{p},\mathrm{asymp.}}|0\rangle = \langle\Phi| \int \mathrm{d}^3\mathbf{x}\, \mathrm{e}^{\mathrm{i}p\cdot x} \left(\sqrt{E_{\mathbf{p}}}\hat{\phi}_{\mathrm{free}}(\mathbf{x}) + \frac{\mathrm{i}}{\sqrt{E_{\mathbf{p}}}}\hat{\pi}_{\mathrm{free}}(\mathbf{x}) \right) \Big|_{p^0=E_{\mathbf{p}}} |0\rangle, \tag{1.1.97}$$

for $t \to \pm\infty$, so that the operators inside the parenthesis are the free ones and only depend on space. Multiplying the equation above by $\mathrm{e}^{-\mathrm{i}E_{\mathbf{p}}t}\sqrt{E_{\mathbf{p}}}$,

$$0 = \int \mathrm{d}^3\mathbf{x}\, \mathrm{e}^{\mathrm{i}\mathbf{p}\cdot\mathbf{x}} \left(E_{\mathbf{p}}\Phi(\mathbf{x}) + \frac{\delta}{\delta\Phi(\mathbf{x})} \right) \langle\Phi|0\rangle. \tag{1.1.98}$$

In analogy with the quantum harmonic oscillator, we take a Gaußian state as an Ansatz

$$\langle\Phi|0\rangle \propto \exp\left(-\frac{1}{2} \int \mathrm{d}^3\mathbf{x}\, \mathrm{d}^3\mathbf{y}\, \mathcal{G}(\mathbf{x},\mathbf{y})\Phi(\mathbf{x})\Phi(\mathbf{y}) \right), \tag{1.1.99}$$

with some symmetric kernel, $\mathcal{G}(\mathbf{x},\mathbf{y})$, to be determined and plug it in the differential equation Eq. (1.1.98), to get

$$\begin{aligned} 0 &= \int \mathrm{d}^3\mathbf{z}\, \mathrm{e}^{\mathrm{i}\mathbf{p}\cdot\mathbf{z}} \left(E_{\mathbf{p}}\Phi(\mathbf{z}) + \frac{\delta}{\delta\Phi(\mathbf{z})} \right) \exp\left(-\frac{1}{2} \int \mathrm{d}^3\mathbf{x}\, \mathrm{d}^3\mathbf{y}\, \mathcal{G}(\mathbf{x},\mathbf{y})\Phi(\mathbf{x})\Phi(\mathbf{y}) \right) \\ &= \int \mathrm{d}^3\mathbf{z}\, \mathrm{e}^{\mathrm{i}\mathbf{p}\cdot\mathbf{z}} \left(E_{\mathbf{p}}\Phi(\mathbf{z}) - \left[\int \mathrm{d}^3\mathbf{x}\, \mathcal{G}(\mathbf{z},\mathbf{x})\Phi(\mathbf{x}) \right] \right) \exp\left(-\frac{1}{2} \int \mathrm{d}^3\mathbf{x}\, \mathrm{d}^3\mathbf{y}\, \mathcal{G}(\mathbf{x},\mathbf{y})\phi(\mathbf{x})\phi(\mathbf{y}) \right) \\ &= \int \mathrm{d}^3\mathbf{z}\, \mathrm{e}^{\mathrm{i}\mathbf{p}\cdot\mathbf{z}} E_{\mathbf{p}}\Phi(\mathbf{z}) - \int \mathrm{d}^3\mathbf{z}\, \mathrm{e}^{\mathrm{i}\mathbf{p}\cdot\mathbf{z}} \left[\int \mathrm{d}^3\mathbf{x}\, \mathcal{G}(\mathbf{z},\mathbf{x})\Phi(\mathbf{x}) \right] \\ &= \int \mathrm{d}^3\mathbf{z}\, \mathrm{e}^{\mathrm{i}\mathbf{p}\cdot\mathbf{z}} E_{\mathbf{p}}\Phi(\mathbf{z}) - \int \mathrm{d}^3\mathbf{z} \left[\int \mathrm{d}^3\mathbf{z}'\, \mathrm{e}^{\mathrm{i}\mathbf{p}\cdot\mathbf{z}'} \mathcal{G}(\mathbf{z}',\mathbf{z})\Phi(\mathbf{z}) \right], \end{aligned}$$

where we relabeled the variables to obtain the last line. It follows that $\mathcal{G}(\mathbf{z}', \mathbf{z})$ is a solution for any $\Phi(\mathbf{x})$ if it observes

$$0 = \mathrm{e}^{\mathrm{i}\mathbf{p}\cdot\mathbf{z}} E_{\mathbf{p}} - \int \mathrm{d}^3\mathbf{z}'\, \mathrm{e}^{\mathrm{i}\mathbf{p}\cdot\mathbf{z}'} \mathcal{G}(\mathbf{z}', \mathbf{z}), \tag{1.1.100}$$

or clearly

$$\mathcal{G}(\mathbf{x}, \mathbf{y}) = \frac{1}{(2\pi)^3} \int \mathrm{d}^3\mathbf{p}\, \mathrm{e}^{\mathrm{i}\mathbf{p}\cdot(\mathbf{x}-\mathbf{y})} E_{\mathbf{p}} = \frac{1}{(2\pi)^3} \int \mathrm{d}^3\mathbf{p}\, \mathrm{e}^{\mathrm{i}\mathbf{p}\cdot(\mathbf{x}-\mathbf{y})} \sqrt{\mathbf{p}^2 + m^2}. \tag{1.1.101}$$

This integral is obviously divergent and formally is only defined in the sense of distributions, but can be regulated to express it in terms of a Bessel function which serves perhaps to the intuition around this Gaußian solution for $\langle\Phi|0\rangle$. Consider $r = |\mathbf{x} - \mathbf{y}|$ and choosing spherical coordinates for the momentum integration, whose polar axis is aligned with $\mathbf{x} - \mathbf{y}$ one can perform the angular integration

$$\begin{aligned} \mathcal{G}(\mathbf{x}, \mathbf{y}) &= \frac{1}{(2\pi)^3} \int_0^\infty \mathrm{d}p\, \mathrm{d}\Omega_2\, p^2\, \mathrm{e}^{\mathrm{i}rp\cos\theta} \sqrt{p^2 + m^2} \\ &= \frac{4\pi}{(2\pi)^3} \int_0^\infty \mathrm{d}p\, \frac{p\sqrt{m^2 + p^2}\sin(pr)}{r}. \end{aligned} \tag{1.1.102}$$

Using Basset's integral for modified Bessel functions[18, Eq. 10.32.11], (however outside of its domain of validity)

$$K_\nu(xz) = \frac{\Gamma\left(\nu + \frac{1}{2}\right)(2z)^\nu}{\pi^{\frac{1}{2}} x^\nu} \int_0^\infty \frac{\cos(xt)\,\mathrm{d}t}{(t^2 + z^2)^{\nu + \frac{1}{2}}}, \quad \text{for} \quad \mathfrak{Re}\nu > -\frac{1}{2}, |\arg z| < \frac{\pi}{2} \tag{1.1.103}$$

so that

$$\frac{\mathrm{d}}{\mathrm{d}x}\left(x^\nu K_\nu(xz)\right) = -\frac{\Gamma\left(\nu + \frac{1}{2}\right)(2z)^\nu}{\pi^{\frac{1}{2}}} \int_0^\infty \frac{t\sin(xt)\,\mathrm{d}t}{(t^2 + z^2)^{\nu + \frac{1}{2}}}. \tag{1.1.104}$$

Setting $\nu = -1$ and identifying variables we have

$$\mathcal{G}(r) = \frac{1}{2\pi^2} \frac{m}{r} \frac{\mathrm{d}}{\mathrm{d}r}\left(\frac{1}{r} K_{-1}(mr)\right). \tag{1.1.105}$$

The graphs corresponding to this integration kernel are shown in Fig. (1.2) as a function of the distance between the points $\mathbf{x}$ and $\mathbf{y}$. We can see how higher masses make the curve steeper and more and more concentrated at $r = 0$.

Let us go back to computing the vacuum-to-vacuum matrix element of Eq. (1.1.91), first let us analyze the projectors using the Gaußian form of $\mathcal{G}(\mathbf{x}, \mathbf{y})$,

$$\begin{aligned} \langle 0|\Phi(t=\infty)\rangle \langle\Phi(t=-\infty)|0\rangle \propto \exp\Bigg(-\frac{1}{2}\int \mathrm{d}^3\mathbf{x}\, \mathrm{d}^3\mathbf{y}\, \mathcal{G}(\mathbf{x}, \mathbf{y}) \left[\Phi(t=\infty, \mathbf{x})\Phi(t=\infty, \mathbf{y})\right. \\ \left. + \Phi(t=-\infty, \mathbf{x})\Phi(t=-\infty, \mathbf{y})\right]\Bigg), \end{aligned} \tag{1.1.106}$$

where we have made explicit that the field configurations are to be evaluated at infinite past/future. Assuming the field configurations are smooth and have such limit one can prove that

$$f(\infty) + f(-\infty) = \lim_{\epsilon \to 0^+} \epsilon \int_{-\infty}^\infty \mathrm{d}\tau f(\tau)\, \mathrm{e}^{-\epsilon|\tau|}, \tag{1.1.107}$$

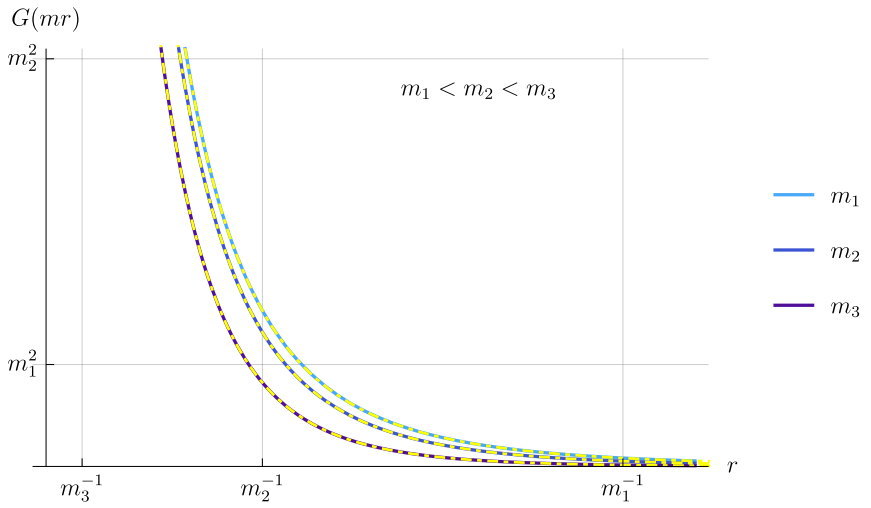

Figure 1.2: Plot of $\mathcal{G}(\mathbf{x}-\mathbf{y})$ for different increasing masses inserted in Eq. (1.1.105) (blue tones) and the corresponding plot from Eq. (1.1.102) made by using Riemann's Zeta function regularization, that is introducing $-\exp(-\varepsilon E_{\mathbf{p}})$ into the integrand and taking the limit $\varepsilon \to 0$.

via splitting the integral at $\tau = 0$ and an integration by parts given $|f(0)| < \infty$. This allows us to write down the projectors including an integral over time

$$\langle 0|\Phi(t=\infty)\rangle \, \langle \Phi(t=-\infty)|0\rangle \propto \exp\left(-\frac{1}{2}\epsilon \int_{-\infty}^{\infty} \mathrm{d}t \int \mathrm{d}^3\mathbf{x}\, \mathrm{d}^3\mathbf{y}\, \mathcal{G}(\mathbf{x},\mathbf{y})\Phi(t,\mathbf{x})\Phi(t,\mathbf{y})\right), \tag{1.1.108}$$

where terms going like $\mathcal{O}(\epsilon^2)$ have not been written. Using the above formula in Eq. (1.1.91), we get the full S-matrix element

$$\langle 0|0\rangle = \lim_{\epsilon\to 0^+} \int \mathcal{D}\Phi \exp\left\{ \mathrm{i}S[\Phi] - \frac{1}{2}\epsilon \int_{-\infty}^{\infty} \mathrm{d}t \int \mathrm{d}^3\mathbf{x}\, \mathrm{d}^3\mathbf{y}\, \mathcal{G}(\mathbf{x},\mathbf{y})\Phi(t,\mathbf{x})\Phi(t,\mathbf{y})\right\}, \tag{1.1.109}$$

up to order ϵ. Simplifying this by using the specific action for the free case and Eq.(1.1.101), with $\epsilon E_{\mathbf{p}} \to \epsilon$, we obtain

$$\begin{aligned}\langle 0|0\rangle &= \lim_{\epsilon\to 0^+} \int \mathcal{D}\Phi \exp\left\{ -\frac{\mathrm{i}}{2} \int_{-\infty}^{\infty} \mathrm{d}t \int \mathrm{d}^3\mathbf{x}\, \mathrm{d}^3\mathbf{y} \int \frac{\mathrm{d}^3\mathbf{p}}{(2\pi)^3}\, \mathrm{e}^{\mathrm{i}\mathbf{p}\cdot(\mathbf{x}-\mathbf{y})}\Phi(t,\mathbf{y})(\Box + m^2 - \mathrm{i}\epsilon)\Phi(t,\mathbf{x})\right\} \\ &= \lim_{\epsilon\to 0^+} \int \mathcal{D}\Phi \exp\left\{ -\frac{\mathrm{i}}{2} \int \mathrm{d}^4x\, \Phi(t,\mathbf{x})(\Box + m^2 - \mathrm{i}\epsilon)\Phi(t,\mathbf{x})\right\},\end{aligned} \tag{1.1.110}$$

where we have integrated over $\mathbf{p}$ and over $\mathbf{y}$ thereafter. The last equation recovers already the action including the $\mathrm{i}\epsilon$ prescription, coming from the fact that we want to deal with local theories, where field are to interact at the same space-time point, this locality is what Eq. (1.1.107) encapsulates, and has the effect of choosing the Feynman propagator for the theory. Employing this careful projection over the boundary configurations, the generating functional in Eq. (1.1.87) acquires the usual $+\mathrm{i}\epsilon$ leading to the correct Feynman propagator

$$G(x-y) = \mathrm{i}\int \frac{\mathrm{d}^4p}{(2\pi)^4} \frac{\mathrm{e}^{\mathrm{i}p(x-y)}}{p^2 - m^2 + \mathrm{i}\epsilon}. \tag{1.1.111}$$

Although we computed only the vacuum-to-vacuum transition in a free scalar theory, the arguments can be translated verbatim to other models. Even more care must be taken when dealing when curved spacetimes. For more details about imposing boundary conditions in the path integral formalism, see Ref.[19].

1.2 The Effective Action

Although classical field theory is successful in describing many degrees of freedom and allows for models that can avoid the concept of *action at a distance*, with the most famous example probably being electromagnetism, it does not incorporate quantum mechanics. In other words, for cases where we are interested in describing a large and possibly changing number of particles, while at the same time taking into account their causal interactions and their quantum aspects, we are lead to work within the quantum field theory framework. Such a framework is vast and contains an enormous amount of tools that have been developed over time to address different situations. One such tool was already presented in the previous section, the path integral, which allows us to employ functional calculus to obtain correlation functions. Here we will introduce the effective action, whose objective is to incorporate one-loop or radiative corrections (or even higher-order corrections) on top of the classical contributions. The following exposition is based on these references [20, Ch. 11.3], [21, Ch. 16] and [12, Ch. 7].
There are several ways to motivate the introduction of the effective action. On the one hand, it can be understood as the resulting action when external fields are present. On the other, it is meant to be an effective description after certain loop effects have been resummed. For the studies presented in this document, we are mainly focused on computing the effective action for the computation of vacuum expectation values of different fields. It is known that classical expectation values are altered by means of quantum corrections. Hence the stationary points of the action do not provide the correct expectation values. The effective action, $\Gamma[\phi]$, plays the role of such a functional, one whose minimum corresponds to the quantum corrected $\langle\phi\rangle$.
It is because of that reason that the effective action is particularly relevant for phenomena surrounding spontaneous symmetry breaking. It is only after the effective potential is calculated that the local and global minima of the theory can be studied. In practice, one does not have access to the full effective potential since that would mean having solved the theory completely and having taken into account corrections of all orders. Therefore we are forced to truncate the computation at a given order in an expansion in terms of some perturbative parameter, the most common one perhaps being an expansion in $\hbar$. We will show how $\hbar$ serves as a bookkeeping parameter for the number of loops being included in the effective potential.

1.2.1 Effective action

To explain the construction of the effective action, let us consider a field theory in an unbounded flat spacetime of dimension d, featuring field content Φ^a, where a is a label running over the fields of the theory. Assume we are dealing with scalars to be able to write down the kinetic term explicitly. Then it suffices to substitute such term with the kinetic term of a spinor or a gauge boson accordingly. Assume as well that the model may have a local scalar potential for certain fields which we will denote $U_a(x) = U_a(\Phi^a(x))$, for certain a's. Lastly, assume the model is specified through a Lagrangian density $\mathcal{L}$ which may include polynomial interactions, $\mathcal{L}_{\text{int}}$ among the fields. The full Lagrangian of the

theory has the form:

$$\mathcal{L}(\Phi^a) = \sum_a \frac{1}{2}(\partial_\mu \Phi^a)^2 + U(\Phi^a) + \mathcal{L}_{\text{int}}. \tag{1.2.112}$$

The partition function as explained in the previous section can be interpreted as a generating functional when extended by terms containing auxiliary external sources $J_a(x)$, abbreviating the set of external sources by J we have that the generating functional is

$$Z[J] = \left\langle \Omega \left| \, \mathrm{e}^{-\mathrm{i}HT} \right| \Omega \right\rangle = \int \left(\prod_a \mathcal{D}[\Phi^a] \right) \exp\left(\frac{\mathrm{i}}{\hbar} \left[S[\Phi^a] + \int \mathrm{d}^d x J_a(x) \Phi^a(x) \right] \right), \tag{1.2.113}$$

where H is the Hamiltonian of the theory and T represents the time window over which the system is studied and

$$S[\Phi^a] = \int \mathrm{d}^d x \mathcal{L}(\Phi^a). \tag{1.2.114}$$

We can now introduce

$$\mathcal{W}[J] \equiv -\mathrm{i}\hbar \log\left(Z[J]\right), \tag{1.2.115}$$

the *generating functional of connected diagrams* as an analogue of the Helmholtz free energy in thermodynamic systems. It is useful to give some comments pertaining $\mathcal{W}$ in order to develop some intuition about what it describes, which seems at glance obscure in its definition. From quantum field theory, we know that the partition function is understood as the vacuum-to-vacuum transition amplitude, which could in principle be obtained exactly if one could sum over all vacuum diagrams, that is, over all connected and disconnected Feynman diagrams that have no external legs. A neat interpretation for $\mathcal{W}$ was provided by Weinberg in [21], where simply put, while Z sums over all possible diagrams, $\mathcal{W}$ only sums over connected diagrams (see [15] for a proof). By letting N be the number of connected components of a given diagram, we see how Z counts all components, while avoiding possible over counting produced by permuting vertices within a component, through the formula

$$Z[J] = \sum_{N=0}^{\infty} \frac{1}{N!} \left(\frac{\mathrm{i}}{\hbar} \mathcal{W}[J] \right)^N = \exp\left(\frac{\mathrm{i}}{\hbar} \mathcal{W}[J] \right). \tag{1.2.116}$$

We can also see already that the generating functional would factorize into an integral over each sector if it were not for the interactions. In order to obtain the effective action, it is convenient to define new fields which follow the one-point expectation values of the original fields Φ^a, let

$$\varphi^a_J(x) \equiv \langle \Omega | \Phi^a(x) | \Omega \rangle \, \big|_J = -\frac{\mathrm{i}\hbar}{Z[J]} \frac{\delta Z[J]}{\delta J_a(x)} = \frac{\delta \mathcal{W}[J]}{\delta J_a(x)}, \tag{1.2.117}$$

creating a correspondence

$$\varphi^a_J(x) \quad \Longleftrightarrow \quad J^a_\varphi(x). \tag{1.2.118}$$

The φ^a_J's are commonly referred to as the classical fields. The effective action corresponds to the Legendre transform of $\mathcal{W}$, (using the sign convention from [21])

$$\Gamma[\varphi^a] = \mathcal{W}[\tilde{J}] - \sum_a \int \mathrm{d}^d x \, \tilde{J}_a(x) \varphi^a(x), \tag{1.2.119}$$

where $\tilde{J}^a$ is obtained by inverting Eq. (1.2.117), or in other words using the correspondence written above (possible under the assumption of convexity on $\mathcal{W}$). In other words, given a configuration $\varphi^b(x)$, $\tilde{J}_b$ is the current that satisfies Eq. (1.2.117). This procedure returns the convex hull of the initial functional, which is at the same time a functional, although now dependent on the new fields. It is the effective action in the sense that it has the properties we seek:

1. It provides us with quantum corrected field equations.

2. It is an action from which Feynman rules can be extracted. In the case of truncating $\mathcal{W}$ to first order in $\hbar$, the tree-level diagrams will include all one-loop effects of the original theory.

We can show the first property by showing how to obtain the equations of motion for the fields φ^a and realizing that a solution to such equation for vanishing sources becomes an extremum of the action automatically. Let us compute the variation with respect to some new field φ^b of the effective action Γ:

$$\begin{aligned}\frac{\delta\Gamma[\varphi^a]}{\delta\varphi^b(x)} &= \frac{\delta\mathcal{W}[\tilde{J}]}{\delta\varphi^b(x)} - \sum_a \int \mathrm{d}^d y\, \frac{\delta\tilde{J}_a(y)}{\delta\varphi^b(x)}\varphi^a(y) - \sum_a \int \mathrm{d}^d y\, \tilde{J}_a(y)\frac{\delta\varphi^a(y)}{\delta\varphi^b(x)} \\ &= \sum_c \int \mathrm{d}^d y \left(\frac{\delta\mathcal{W}[\tilde{J}]}{\delta J_c(y)}\right)\Big|_{J_c=\tilde{J}} \frac{\delta\tilde{J}_c(y)}{\delta\varphi^b(x)} - \sum_a \int \mathrm{d}^d y\, \frac{\delta\tilde{J}_a(y)}{\delta\varphi^b(x)}\varphi^a(y) - \tilde{J}_b(x),\end{aligned}$$

which after using Eq. (1.2.117) gives

$$\frac{\delta\Gamma[\varphi^a]}{\delta\varphi^b(x)} = -\tilde{J}_b(x). \tag{1.2.120}$$

This last expression indeed tells us that the configuration solving it for vanishing sources is a stationary point.
Let us know understand how the lowest order of Γ includes corrections from one-loop Feynman diagrams. The exact effective action, as defined in Eq. (1.2.119), can be expanded in powers of the fields, let us assume for simplicity that the theory contains only one field– although the expansion may be also done for multiple fields,

$$\Gamma[\varphi] = \sum_n \frac{1}{n!}\int \mathrm{d}^d x^1 \cdots \mathrm{d}^d x^n\, \varphi(x^1)\cdots\varphi(x^n)\Gamma^{(n)}(x_1,\ldots,x_n), \tag{1.2.121}$$

where the coefficients are

$$\Gamma^{(n)}(x^1,\ldots,x^n) = \frac{\delta^n\Gamma[\varphi]}{\delta\varphi(x^1)\delta\varphi(x^2)\cdots\delta\varphi(x^n)} \tag{1.2.122}$$

and receive the name of proper vertices or 1PI diagrams (one-particle irreducible, meaning that cutting any internal propagator line disconnects the diagram), having n external insertion points, by convention they are taken to be amputated.

1.2.2 The semi-classical (or loop) expansion

Let us use $\hbar$ as a book-keeping device and perform a saddle point expansion on Γ. It is worth noting that a priori, the steepest descent approach, does not work for a theory on Minkowski space because of the oscillatory exponent in the path integral. To overcome

such an obstacle and still be able to extract physical information from vacuum expectation values, we again use a Wick rotation as illustrated for the harmonic oscillator previously. Therefore we assume in this section that the spacetime is $O(d)$ symmetric so that no imaginary units appear in the exponents. We begin by finding the saddle point of the exponential of the path integral Eq. (1.2.113), that is, assume φ_c satisfies:

$$\frac{\delta S[\varphi_{c,J}(x)]}{\delta\varphi(x)} = J(x) \qquad \text{such that} \qquad \varphi_c = 0 \quad \text{when} \quad J(x) = 0, \tag{1.2.123}$$

and without loss of generality, we can adjust S such that for $\phi_c = 0$, $S = 0$. So to the lowest order we get

$$\mathcal{W}_0[J] = S[\varphi_{c,J}] + \int \mathrm{d}^d x' J(x')\varphi_{c,J}(x'), \tag{1.2.124}$$

meaning that the lowest order of $\mathcal{W}$ is the Legendre transform of the action, provided equation Eq. (1.2.123) holds. This in turn means that the effective action to lowest order is

$$\Gamma^{(0)}[\varphi] = S[\varphi], \tag{1.2.125}$$

which contains the usual vertices and corresponding Feynman diagrams, and is valid for a field, φ, with no reference to external currents J. In order to include the next order corrections in $\hbar$ we proceed along the same lines as in the exposition of the path integral in earlier sections. Consider the effective action now for a field expanded around the classical solution,

$$\Phi^{(1)}(x) = \varphi_{c,J}(x) + \sqrt{\hbar}\,\chi(x) \tag{1.2.126}$$

and expand the action together with the external source accordingly to get

$$\begin{aligned} S[\Phi^{(1)}] - \int \mathrm{d}^d x'\, J(x')\Phi^{(1)}(x') = S[\varphi_{c,J}] - \int \mathrm{d}^d x' J(x')\varphi_{c,J}(x') \\ + \frac{\hbar}{2}\int \mathrm{d}^d x_1\, \mathrm{d}^d x_2\, \chi(x_1)\Delta^{-1}(\varphi_{c,J}; x_1, x_2)\chi(x_2) + \mathcal{O}(\hbar^{3/2}), \end{aligned} \tag{1.2.127}$$

with

$$\Delta^{-1}(\varphi_{c,J}; x, x') = \left.\frac{\delta^2 S[\Phi]}{\delta\Phi(x)\delta\Phi(x')}\right|_{\Phi=\varphi_{c,J}}. \tag{1.2.128}$$

Computing the path integral using the expression above leads to

$$Z[J] = Z_0[J]\int \mathcal{D}[\chi]\, \exp\left(-\frac{1}{2}\int \mathrm{d}^d x_1\, \mathrm{d}^d x_2\, \chi(x_1)\Delta^{-1}(\varphi_{c,J}; x_1, x_2)\chi(x_2)\right), \tag{1.2.129}$$

modulo a normalization factor and where $Z_0[J]$ is the part involving only $\varphi_{c,J}$. It is possible to perform the Gaußian integral on χ, which together with the normalization condition $Z[0] = 1$ gives

$$Z[J] \propto Z_0[J]\sqrt{\frac{\det\Delta^{-1}(\varphi_{c,0}; x_1, x_2)}{\det\Delta^{-1}(\varphi_{c,J}(x); x_1, x_2)}}, \tag{1.2.130}$$

using this result in the definition of $\mathcal{W}$– technically the Euclidean version of Eq. (1.2.115) where there is no factor of "i", and exchanging log det with tr log

$$\mathcal{W}[J] = \mathcal{W}_0[J] + \hbar\mathcal{W}_1[J] + \mathcal{O}(\hbar^2), \tag{1.2.131}$$

with

$$\mathcal{W}_0[J] = -\hbar\log(Z_0[J]) = S[\varphi_{c,J}] + \int \mathrm{d}^d x J(x)\varphi_{c,J}(x) \tag{1.2.132}$$

and

$$\mathcal{W}_1[J] = \frac{1}{2}\left(\mathrm{tr}\log\Delta^{-1}(\varphi_{c,J}(x);x_1,x_2) - \mathrm{tr}\log\Delta^{-1}(\varphi_{c,0};x_1,x_2)\right) \tag{1.2.133}$$

$$= \frac{1}{2}\int \mathrm{d}^d x\, \log\left(\frac{\Delta^{-1}(\varphi_{c,J}(x);x,x)}{\Delta^{-1}(\varphi_{c,0};x,x)}\right). \tag{1.2.134}$$

To understand the previous term, let us expand the two point correlation function written in Eq. (1.2.128) in terms of a free part and an the terms of the action containing interactions, S_{int},

$$\Delta^{-1}(\varphi_{c,J}(x);x,x') = \Delta^{-1}(\varphi_{c,0};x,x') + \frac{\delta^2 S_{int}}{\delta\Phi(x)\delta\Phi(x')}\bigg|_{\Phi=\varphi_c}, \tag{1.2.135}$$

then we have

$$\mathcal{W}_1[J] = \frac{1}{2}\int \mathrm{d}^d x\, \log\left(\mathbb{1} + \int \mathrm{d}^d x'\, \Delta(\varphi_{c,0};x,x')\frac{\delta^2 S_{int}}{\delta\Phi(x')\delta\Phi(x)}\bigg|_{\Phi=\varphi_c}\right). \tag{1.2.136}$$

Assuming the interactions can be treated perturbatively we can expand the logarithm in its series expansion

$$\mathcal{W}_1[J] = -\frac{1}{2}\int \mathrm{d}^d x \sum_{n=1}^{\infty}(-1)^n\frac{1}{n}\left(\int \mathrm{d}^d x'\, \Delta(\varphi_{c,0};x,x')\frac{\delta^2 S_{int}}{\delta\Phi(x')\delta\Phi(x)}\bigg|_{\Phi=\varphi_c}\right)^n, \tag{1.2.137}$$

where the notation $\mathcal{O}^n(x,x)$ for operators of two-points means each factor is chained with the next one by integration. Before giving a particular diagrammatic illustration let us write down the effective action to this order. From the definition of the effective action Eq. (1.2.119), we have that the following relation must hold for any external parameter on which Γ and $\mathcal{W}$ may depend on, in particular for $\hbar$:

$$\frac{\partial\mathcal{W}}{\partial\hbar} - \frac{\partial\Gamma}{\partial\hbar} = 0. \tag{1.2.138}$$

So up to order $\hbar$, using the results for $\mathcal{W}_1$ above we obtain finally the one-loop effective action which will be used throughout this document

$$\Gamma(\varphi) = S[\varphi] + \frac{1}{2}\int \mathrm{d}^d x\, \log\left(\frac{\Delta^{-1}(\varphi(x);x,x)}{\Delta^{-1}(\varphi_0;x,x)}\right) + \mathcal{O}(\hbar^2). \tag{1.2.139}$$

Before moving on, let us provide an example for the case of a Φ^3 interaction

$$S_{int}[\Phi] = \frac{\lambda}{3!}\int \mathrm{d}^d x\, \Phi^3(x) \Longrightarrow \frac{\delta^2 S_{int}}{\delta\Phi(x')\delta\Phi(x)}\bigg|_{\Phi=\varphi_c} = \lambda\varphi_c(x)\delta(x-x'), \tag{1.2.140}$$

then up to second order in the interaction

$$\mathcal{W}_1[J] = -\frac{\lambda}{2}\int \mathrm{d}^d x\, \Delta(\varphi_{c,0}; x, x)\varphi_c(x) + \frac{\lambda^2}{4}\int \mathrm{d}^d x\, \mathrm{d}^d x' \Delta(\varphi_{c,0}; x, x')\varphi_c(x')\Delta(\varphi_{c,0}; x', x)\varphi_c(x) + \cdots,$$

to which we can already give a diagrammatic interpretation

$\mathcal{W}_1[J] =$ 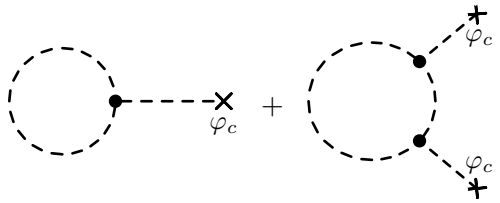

(1.2.141)

where dashed lines are the propagators, and the external lines with crosses represent insertions of the background (with no propagator included if the line ends in a cross). We can now understand visually what the n-th term of Eq. (1.2.137) for this theory, looks like:

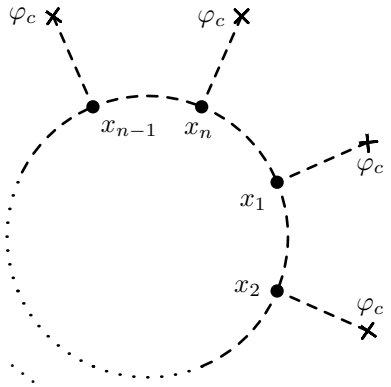

,
(1.2.142)

which illustrates the claim that Γ_1 sums up the contributions up to 1PI (one-particle irreducible). The statement can be made more precise[22] by counting powers of $\hbar$. We can see from Eq. (1.2.127) that the propagator appears with a linear power of $\hbar$, that is $\hbar\Delta^{-1}$, while interaction vertices will appear always proportional to $\hbar_{-1}$. If we count the powers of $\hbar$ in the amplitude corresponding to a 1PI diagram, having I internal lines and V vertices will have

$$P = I - V, \tag{1.2.143}$$

while the number of loops is equal to the number of free remaining momentum integrals. Each internal line contributes one integral while each vertex comes with a δ which cancels one. The minimal loop consists, however, of only one internal line and one vertex, which must be counted separately, and any additional loop is one of three cases: it is anchored in an existing vertex and the new internal line comes back to it increasing I by 1, or it is anchored in an existing vertex and a new one and thus increases I by two and V by

1, or the loop comes from two new vertices thus increasing I by three and V by 2. In either case, an extra loop implies that $I - V$ increases by one. We have that the number of independent momentum integrals left, or equivalently the number of loops, is

$$L = I - V + 1. \tag{1.2.144}$$

We can write down the powers of $\hbar$ of a given 1PI diagram (with no external lines) in terms of the number of loops to find

$$P = L - 1. \tag{1.2.145}$$

So we can conclude that an expansion in powers of $\hbar$ corresponds indeed one-to-one to summing contributions of increasing order of loops. Where $\hbar^{-1}$ corresponds to the tree-level diagrams, contributions proportional to $\hbar$ come then from one-loop 1PI diagrams, etc.

1.3 Computing and Renormalizing the one-Loop effective action

1.3.1 Computing the Coleman-Weinberg potential

We can make the arguments of the previous section even more explicit by directly computing the effective potential up to one-loop for a scalar theory with a ϕ^4 self-interaction. We follow Coleman and Weinberg's original paper[22] to obtain the one-loop effective potential for a constant vacuum expectation value, named thereafter the Coleman-Weinberg potential (CW). The Lagrangian density for this simplest case is the following:

$$\mathcal{L} = \frac{1}{2}(\partial_\mu\phi)^2 - \lambda\frac{1}{4!}\phi^4 + \frac{1}{2}\delta Z(\partial_\mu\phi)^2 - \frac{1}{2}\delta m^2\phi^2 - \frac{1}{4!}\delta\lambda\phi^4, \tag{1.3.146}$$

where δZ, δm^2 and $\delta\lambda$ are counterterms related to the renormalization of the theory and will be specified later. We can build then the effective one-loop potential by adding all contributions from tree-level diagrams and 1PI diagrams. For this theory, at tree level we have only the term already appearing in the Lagrangian, which becomes

$$V_{\text{tree}} = \frac{\lambda}{4!}\varphi^4, \qquad \text{for} \qquad \varphi(x) = \frac{\delta\mathcal{W}[J]}{\delta J(x)} = \left.\frac{\langle t=\infty,0|\phi(x)|t=-\infty,0\rangle}{\langle t=\infty,0|t=-\infty,0\rangle}\right|_J. \tag{1.3.147}$$

Then we have to add all contributions coming from diagrams with one loop but an arbitrary number of field insertions. In the ϕ^4 theory specifically, we have a minimal of 2 insertions and a single diagram for every even number onward, the so-called *polygon graphs* (see Fig. 1.3), these diagrams produce then effective one-loop vertices for all orders, hence

$$V_{\text{one-loop}} = \mathrm{i}\int\frac{\mathrm{d}^4k}{(2\pi)^4}\sum_{n=1}^{\infty}\frac{1}{2n}\left(\frac{1}{2}\lambda\varphi^2\,\frac{1}{k^2+\mathrm{i}\epsilon}\right)^n, \tag{1.3.148}$$

where the i in front enters in the definition of $\mathcal{W}$, the $\frac{1}{2}$ in front of φ occurs because interchanging two φ's (bosonic) at a given vertex does not generate a new diagram.
Formula (1.3.148) already includes the geometry factors for each order: a factor of $(1/2)^n$ for interchanging two sources at a given vertex and a factor of $1/2n$ from rotations and reflections (see [20, Sec 9.5] for a more modern explanation.). We can observe how this contribution corresponds to the Taylor series of the natural logarithm and exactly matches

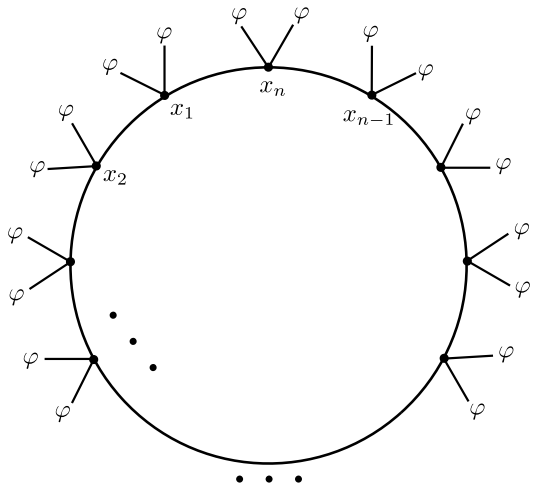

Figure 1.3: Feynman diagram corresponding to one of the 1PI one-loop diagrams displaying n vertices and $2n$ insertions of φ in the ϕ^4 theory.

what we expected from the general case, Eq. (1.2.136). All contributions up to one-loop order, including counterterms for the theory, can be written down as follows, where we can neglect the $i\epsilon$ and perform the integral appearing in the last term in Euclidean space:

$$V_{\mathrm{CW}}(\varphi) = \frac{\lambda}{4!}\varphi^4 - \frac{1}{2}\delta m^2\varphi^2 - \frac{1}{4!}\delta\lambda\varphi^4 + \frac{1}{2}\int \frac{\mathrm{d}^4k}{(2\pi)^4}\log\left(1+\lambda\frac{\varphi^2}{2k^2}\right). \tag{1.3.149}$$

By performing the momentum integral in the last term up to some cutoff Λ, we can see that the apparent infrared divergences are resummed into something finite, viz.

$$\begin{aligned}
&\int_{B(\Lambda)} \frac{\mathrm{d}^4k}{(2\pi)^4}\log\left(k^2+f(\varphi)\right) \\
&\qquad = \frac{2\pi^2}{(2\pi)^4}\int_0^\Lambda \mathrm{d}|k|\,|k|^3\log\left(|k|^2+f(\varphi)\right) \\
&\qquad = \frac{1}{16\pi^2}\int_{f(\varphi)}^{\Lambda^2+f(\varphi)} \mathrm{d}z\,(z-f(\varphi))\log(z) \\
&\qquad = \frac{1}{16\pi^2}\left[\int_{f(\varphi)}^{\Lambda^2+f(\varphi)} \mathrm{d}z\,z\log(z) - \int_{f(\varphi)}^{\Lambda^2+f(\varphi)} \mathrm{d}z\,f(\varphi)\log(z)\right] \\
&\qquad = \frac{1}{16\pi^2}\left[\frac{\Lambda^4}{2}\log(\Lambda^2+f(\varphi)) - \frac{\Lambda^4}{4} + \frac{f^2(\varphi)}{2}\log\left(\frac{f(\varphi)}{\Lambda^2+f(\varphi)}\right) + \frac{\Lambda^2 f(\varphi)}{2}\right] \\
&\qquad \overset{\Lambda^2\gg f(\varphi)}{\longrightarrow} \frac{1}{16\pi^2}\left[\frac{\Lambda^4}{2}\log(\Lambda^2) - \frac{1}{4}f^2(\varphi) - \frac{\Lambda^4}{4} + \frac{f^2(\varphi)}{2}\log\left(\frac{f(\varphi)}{\Lambda^2+f(\varphi)}\right) + \Lambda^2 f(\varphi)\right],
\end{aligned} \tag{1.3.150}$$

with $f(\varphi) = \frac{1}{2}\lambda\varphi^2$ we get for the effective potential for large but still finite Λ

$$V_{\mathrm{CW}}(\varphi) = \frac{\lambda}{4!}\varphi^4 - \frac{1}{2}\delta m^2\varphi^2 - \frac{1}{4!}\delta\lambda\varphi^4 - \frac{1}{32\pi^2}\left(\frac{\lambda^2\varphi^4}{16} - \frac{\lambda^2\varphi^4}{8}\log\left(\frac{\frac{\lambda}{2}\varphi^2}{\Lambda^2}\right) - \Lambda^2\frac{\lambda\varphi^2}{2}\right), \tag{1.3.151}$$

where terms vanishing in the limit $\Lambda \to \infty$ have been omitted and the log expanded assuming $f(\varphi) \ll \Lambda^2$. Before dealing with renormalization and finding the determining the counterterms, let us generalize the above expression to a scalar field subject to an arbitrary potential by making contact with the functional tools explained in Sec. 1.2.2.
Let us now consider a more general case, which will serve us later, consider a potential term $U(\phi)$ in the Lagrangian density, which contains all polynomial self-interaction terms in the field ϕ, including possibly a mass term and satisfies $U(\varphi = 0) = 0$. We expand the field ϕ around the expectation value φ, so that we can use Eq. (1.2.134) to compute the one-loop contributions in general,

$$\mathcal{W}_1[J=0] = -\frac{1}{2}\int \mathrm{d}^4x \, \log\left(\frac{\Delta^{-1}(\varphi(x);x,x)}{\Delta^{-1}(0;x,x)}\right) = -\frac{1}{2}\int \mathrm{d}^4x \, \frac{\mathrm{d}^4k}{(2\pi)^4}\log\left(\frac{k^2+U''(\varphi)}{k^2+U''(0)}\right), \tag{1.3.152}$$

where $U''(\varphi)$ means the second derivative with respect to ϕ, evaluated at φ and where we have inserted a complete set of states of momentum to be able to compute the log, recall this expression is already in its Euclidean form[1]. With the extra assumption that φ is to be fixed an therefore space-time independent, we can perform the momentum integral, using the formula in Eq. (1.3.150), while extracting a space-time volume factor Ω and identifying the Coleman-Weinberg potential:

$$\mathcal{W}_1[J=0] = -\Omega V_{\mathrm{CW}}(\varphi) = -\frac{\Omega}{32\pi^2}\left(\frac{U''(\varphi)}{4} - \frac{U''(\varphi)^2}{2}\log\left(\frac{U''(\varphi)}{\Lambda^2}\right) - \Lambda^2 U''(\varphi)\right). \tag{1.3.153}$$

Having derived the above expression, which will be applied several times in later chapters, we go ahead and describe the procedure of renormalization for the above case.

1.3.2 Renormalization

Historically, renormalization was a prescription that allowed us to address certain divergent results appearing in quantum field theory. Since its introduction by Stückelberg and Petermann[23], it has been employed to build counterterms, examples are δm^2 and $\delta\lambda$ in the previous section, which are additional terms for the Lagrangian density, whose job is to absorb the divergent behavior coming out of the perturbative treatment of the theory by means of Feynman diagrams presenting loops. Depending on the context and the specific theory we might be looking at, they might play specific roles, e.g., mass renormalization, vacuum polarization, charge renormalization, etc.
Renormalization has been, since its introduction, a very relevant guideline for constructing theories. It used to stand at the same level, compared to Poincaré symmetry and gauge symmetry, when model building. However, later on, with the appearance of Wilsonian renormalization group ideas[24, 25], together with more modern views on effective field theories, renormalizability became no longer a requirement, as long as the model under consideration is understood as an effective description of phenomena below a certain energy scale.
In this section, we intend to describe the basic ideas concerning renormalization. We will go over the construction of the counterterms for the example theory of the previous section and take the chance to speak about renormalization schemes that will be used in later applications. Not pretending to review the topic of renormalization in its full detail and

[1]Starting from the Minkowskian action, there is an i in the definition of the generating functional and another one coming from the measure after doing the Wick rotation.

generality, we show in the present section how to impose basic renormalization conditions and how to employ the so-called WKB expansion to compute the divergent contributions often appearing in one-loop effective actions.

Let us make some comments on the steps already taken to get the CW effective potential in the previous section. In actuality, we have only postponed the issue of dealing with divergent contributions. This has been done by employing a hard cutoff, Λ, that is restricting the integrals over all momentum space to a ball of radius Λ. This procedure, as it stands, for example, breaks translation symmetry, so without taking the limit $\Lambda \to \infty$, we can not make any statement about the initial theory we started with. Any prescription whose objective is to extract finite pieces from divergent integrals receives the name of regularization and constitutes the first step in renormalizing a field theory. Although different techniques exist for this purpose, we will mostly employ hard momentum cutoffs which will suffice for our purposes.

Once divergent quantities have been regularized, we must choose a renormalization scheme. That is, we must impose certain renormalization conditions that will allow us to fully determine the counterterms in terms of the regularizing parameter.

For the purpose of illustration, we use the following conditions,

$$\left.\frac{\mathrm{d}^2 V_{\mathrm{CW}}}{\mathrm{d}\varphi^2}\right|_{\varphi=M} = m_0, \tag{1.3.154}$$

$$\left.\frac{\mathrm{d}^4 V_{\mathrm{CW}}}{\mathrm{d}\varphi^4}\right|_{\varphi=M} = \lambda, \tag{1.3.155}$$

which are arbitrary and up to us to choose, however, motivated by keeping the effective parameters appearing in the one-loop potential equal to the bare parameters, very similar to what is known as the on-shell scheme, where the pole mass is required to match the effective mass. It is typical, but not necessary, to choose the scale M to be such that the log's are minimized so that if our scalar had a non-zero mass, typical values for the field should oscillate in its vicinity and choosing M close to the tree-level mass would ensure logarithms are small. In our case, m_0 was taken to be 0 in the previous section, so we will see that choosing $M = 0$ is possible in the first condition, Eq. (1.3.154), but not for the second one Eq. (1.3.155). In general, we would need to consider a counterterm for the normalization of the field itself, using canonical normalization, the terms proportional to $(\partial\phi)^2/2$ should add up to one, in our notation and up to one-loop

$$1 + \delta Z(M) = 1, \tag{1.3.156}$$

at mass/energy scale M. With this additional condition, we are able to determine δZ in Eq. (1.3.146). However, we postpone this issue and deal with it when we speak about the WKB expansion.

For definiteness let us follow the original exposition by Coleman and Weinberg[22] and take the renormalization scale in Eq. (1.3.154) in the limit $M \to 0$. Imposing this in our toy CW potential in Eq. (1.3.151) we get the following result

$$\delta m^2 = \frac{\lambda}{32\pi^2}\Lambda^2. \tag{1.3.157}$$

For the condition in Eq. (1.3.155) we must choose a different renormalization scale, let it be some chosen scale M to arrive to

$$\delta\lambda = \frac{11}{32\pi^2} + \frac{3}{32\pi^2}\lambda^2 \log\left(\frac{\lambda}{2}\frac{M^2}{\Lambda^2}\right). \tag{1.3.158}$$

Plugging in these quantities back in the CW potential, we obtain an expression,

$$V_{\mathrm{CW}}^{\mathrm{ren}}(\varphi) = \frac{\lambda}{4!}\varphi^4 - \frac{25}{64\cdot 4!}\lambda^2\varphi^4 + \frac{1}{4!}\frac{3}{32}\lambda^2\varphi^4 \log\left(\frac{\varphi^2}{M^2}\right). \tag{1.3.159}$$

which becomes predictive once observations have set the value of λ at scale M within the full Lagrangian density of the model.
The last observation concerning this model is that of the symmetry-breaking process that occurred when including one-loop effects. The original potential was fully symmetric in the sense that no explicit mass term was included and the theory only possessed one minimum. Nonetheless, the one-loop logarithms are negative for values of $\varphi < M$ and thus lifts the minimum at the origin while generating a new minimum displaced from the origin at a non-zero value of φ. We can state that such a model suffers spontaneous symmetry breaking (SSB) coming from radiative effects, this is a particular case of SSB about which we will expand in a coming chapter. We must mention a caveat in the above interpretation. The new minima can actually occur at large field values, moreover, values that are beyond the perturbative regime in which the one-loop effective potential was computed. In order to address the validity of the model, we must make sure that large field values do not interfere with the perturbation theory. This is remedied by the renormalization group improvement, which will be explained in the next section.
Before we describe the renormalization group improvement, let us attempt to address the renormalization procedure by computing the divergences occurring in the Greens' functions of the model directly by employing the so-called WKB expansion[26–28] (named after its authors Wentzel–Kramers–Brillouin). The method has already been applied in previous studies[29–31], where it has been used in the context of non-homogeneous backgrounds. Given its generality and usefulness, we describe the generic results applied to Greens' functions found in QFT here, to which we will refer to in later, more specific applications. Thus, bear in mind that the method works for a more general class of differential equations. Let us consider finding the Green's function for a fluctuation operator, corresponding to the differential operator shown in Eq. (1.2.135) when the theory is expanded around a given VEV, φ. Let us consider the problem in its minimal version. That is, let us assume it has been reduced to one direction, e.g., in the case of a system enjoying a $O(4)$ symmetry in four-dimensional Euclidean space. Then the Green's equation will look like

$$G_x^{-1}G(x,y) = \left[-\partial_x^2 + \mathcal{V}(\varphi(x))\right] G(x,y) = \delta(x-y), \tag{1.3.160}$$

where $\mathcal{V}(\varphi(x))$ can be thought of as a point-dependent effective mass and $\delta(x)$ is the Dirac delta distribution. We start by considering a specific form for the Green's function, where we decompose G as follows

$$G(x,y) = \Theta(x-y)f^{>}(x)g^{<}(y) + \Theta(y-x)g^{>}(y)f^{<}(x), \tag{1.3.161}$$

where

$$\Theta(x) = \begin{cases} 1 & \text{if } x > 0 \\ 1/2 & \text{if } x = 0 \\ 0 & \text{if } x < 0 \end{cases}, \tag{1.3.162}$$

is the Heaviside step function, which has been regularized at $x = 0$ and we use as such in numerical computations in the applications (Part II). Plugging Eq. (1.3.161) into Eq. (1.3.160) we get, for $x \neq y$, two ordinary differential equations to be solved separately

$$\left[-\partial_x^2 + \mathcal{V}(\varphi(x))\right] f^{\lessgtr}(x) = 0. \tag{1.3.163}$$

Let us consider boundary conditions were the Green's function itself vanishes at infinity, so we will impose

$$\lim_{x\to\infty} f^{>}(x) = 0, \tag{1.3.164}$$

$$\lim_{x\to-\infty} f^{<}(x) = 0. \tag{1.3.165}$$

These are technically the conditions associated to the Feynman propagator which can be understood as the average between retarded and advanced Green's functions where each satisfies only one of the above. The WKB Ansatz tells us to take $f^{\lessgtr}$ in the following form,

$$f^{\lessgtr}(x) = \frac{1}{\sqrt{2W(x)}}\, \mathrm{e}^{\pm\int_{-\infty}^{x} \mathrm{d}x'\, W(x')}, \tag{1.3.166}$$

for some function, $W(x)$ in the exponential, to be determined. The pre-factor has been chosen for convenience and where there is no i in the exponential because we are working in Euclidean space. Observe as well that if $\mathcal{V}$ were independent of x then the Ansatz above already gives the exact solution. Before continuing the computation let us obtain conditions of validity for the procedure in general.
Consider then the simpler Ansatz of an exponential function with a position dependent exponent, $f(x) = \mathrm{e}^{\frac{S(x)}{\epsilon}}$, where we have introduced an auxiliary parameter, ϵ which can be taken as a scale related to $\mathcal{V}$, so let us re-scale it and express such term as $\mathcal{V}_\epsilon = \epsilon^2\mathcal{V}$. Using this form in Eq. (1.3.163):

$$-\frac{S''(x)}{\epsilon} - \frac{(S'(x))^2}{\epsilon^2} + \mathcal{V}(x) = 0, \tag{1.3.167}$$

or in other words

$$(S'(x))^2 = \mathcal{V}_\epsilon(x) - \epsilon S''(x). \tag{1.3.168}$$

We can be solve it perturbatively, by an expansion of the type

$$S(x) = S^{(0)}(x) + \epsilon S^{(1)}(x) + \epsilon^2 S^{(2)}(x) + \cdots, \tag{1.3.169}$$

which leads to the following equations by collecting orders in ϵ,

$$\epsilon^0: \quad (S'^{(0)}(x))^2 = \mathcal{V}_\epsilon(x), \tag{1.3.170}$$

$$\epsilon^1: \quad 2S'^{(0)}(x)S'^{(1)}(x) = -S''^{(0)}(x), \tag{1.3.171}$$

$$\epsilon^2: \quad 2S'^{(0)}(x)S'^{(2)}(x) + (S'^{(1)}(x))^2 = -S''^{(1)}(x), \tag{1.3.172}$$

$$\vdots$$

so we can now estimate when the expansion above is convergent and when it is not. The set of equations above lead to a convergent sum if they satisfy the necessary condition of each order being smaller than the one immediately before, in terms of the first derivative:

$$|S'^{(0)}(x)| > |S'^{(1)}(x)| > |S'^{(2)}(x)| > \cdots. \tag{1.3.173}$$

Examining Eqs. (1.3.170)-(1.3.172), we see that we have the conditions

$$\left|\frac{S''^{(0)}(x)}{(S'^{(0)}(x))^2}\right| < 1, \tag{1.3.174}$$

$$(S'^{(1)}(x))^2 = \left(\frac{S''^{(0)}(x)}{2S'^{(0)}(x)}\right)^2 < (S'^{(0)}(x))^2 = \mathcal{V}_\epsilon(x), \tag{1.3.175}$$

$$(S'^{(2)}(x))^2 = \left(\frac{S''^{(1)}(x) + (S'^{(1)}(x))^2}{2S'^{(0)}(x)}\right)^2 < (S'^{(1)}(x))^2 < \mathcal{V}_\epsilon(x), \tag{1.3.176}$$

$$\vdots$$

where the first condition is the one allowing us to start the chain and where the last condition can be cleaned up to find

$$\left|\frac{S''^{(1)}(x)}{2S'^{(0)}(x)}\right|^2 < |S'^{(1)}(x)|^2 \Longrightarrow \left|\frac{S''^{(1)}(x)}{2S'^{(1)}(x)}\right|^2 < |S'^{(0)}(x)|^2 \sim \mathcal{V}_\epsilon. \tag{1.3.177}$$

This procedure can be continued to higher orders to find analogous relations even when $\epsilon \to 1$. These conditions, although not sufficient, provide us with a quick test of whether the WKB expansion is sensible. We can observe that solving Eq. (1.3.170) leads exactly to

$$S^{(0)}(x) = C\int_{-\infty}^{x} \mathrm{d}x'\sqrt{\mathcal{V}(x')}, \tag{1.3.178}$$

which explains the exponent chosen in Eq. (1.3.166). The factor sitting in front of the exponential is a convenient modification of the method that ensures a constant Wronskian, as we will soon see. The last observation of the method itself concerns the classical turning points, namely the x's where $\mathcal{V}$ vanishes. Close to these points, $S^{(0)}$ becomes extremely small and the inequalities above will not necessarily hold any longer, so we cannot expect the WKB expansion to be reliable close to such points.
Coming back to our problem, to determine $W(x)$ we plug in the Ansatz for $f^{\lessgtr}(x)$ in Eq. (1.3.163), to find

$$W^2(x) = \mathcal{V}(x) - \frac{3}{4}\left(\frac{W'(x)}{W(x)}\right)^2 + \frac{1}{2}\frac{W''(x)}{W(x)}. \tag{1.3.179}$$

Depending on $\mathcal{V}$, this equation might not be solvable in closed form, so we often resort to perturbative treatments. Consider expanding the square of $W(x)$ rather than $W(x)$ itself

$$W(x)^2 = (W^{(0)}(x))^2 + \epsilon(W^{(1)}(x))^2 + \cdots, \tag{1.3.180}$$

using ϵ as a bookkeeping device. Given that we know from Eq.(1.3.178), that $(W^{(0)}(x))^2 = \mathcal{V}(x)$, we can subsequently compute the next order in the series following the assumption that higher order derivatives are smaller and smaller, thus

$$W'(x) = W'^{(0)}(x) + \epsilon W'^{(1)}(x)\left(\frac{W^{(1)}(x)}{W^{(0)}(x)}\right) - \frac{\epsilon}{2}W'^{(0)}(x)\left(\frac{(W^{(1)}(x))}{(W^{(0)}(x))}\right)^2 + \mathcal{O}(\epsilon^2), \tag{1.3.181}$$

which leads to an equation for the next order of the form

$$(W^{(1)}(x))^2 = -\frac{3}{4}\left(\frac{W'^{(0)}(x)}{W^{(0)}(x)}\right)^2 + \frac{1}{2}\frac{W''^{(0)}(x)}{W^{(0)}(x)}\bigg|_{W^{(0)}=\sqrt{\mathcal{V}}}. \tag{1.3.182}$$

This already constitutes the WKB method. Let us now finish writing down the Green's function for which we need to impose, in this case, the conditions of continuity of the 0-th derivative and an appropriate discontinuity in the 1-st derivative.
Continuity of Eq. (1.3.161) is ensured at the coincident point if we demand the we reach the same value from both sides, that is

$$f^{>}(x)g^{<}(x) = g^{>}(x)f^{<}(x). \tag{1.3.183}$$

while the discontinuity in the 1-st derivative is obtained by integrating one of the variables in Eq. (1.3.160) in an interval around the coincident point and then taking the limit of the interval going to zero length to arrive to

$$f'^{>}(x)g^{<}(x) - g^{>}(x)f'^{<}(x) = -1. \tag{1.3.184}$$

The two conditions above allow us to determine $g^{\lessgtr}$ in terms of $f^{\lessgtr}$ and $f'^{\lessgtr}$,

$$g^{\lessgtr}(x) = \frac{f^{\lessgtr}(x)}{\mathrm{Wr}[f^{>}, f^{<}](x)}, \tag{1.3.185}$$

where Wr stands for the Wronskian of the two functions and is defined as

$$\mathrm{Wr}[f_1, f_2](x) = f_1(x)f_2'(x) - f_2(x)f_1'(x), \tag{1.3.186}$$

and for $f^{\lessgtr}$ as in Eq. (1.3.166), we actually have $\mathrm{Wr}[f^{>}, f^{<}](x) = 1$. Collecting all the results, we have for the Green's function and its coincident limit:

$$G(x,y) = \frac{1}{\mathrm{Wr}[f^{>}, f^{<}](y)}\left(\Theta(x-y)f^{>}(x)f^{<}(y) + \Theta(y-x)f^{>}(y)f^{<}(x)\right) \tag{1.3.187}$$

$$\xrightarrow{y\to x} \frac{f^{>}(x)f^{<}(x)}{\mathrm{Wr}[f^{>}, f^{<}](x)} = f^{>}(x)f^{<}(x) = \frac{1}{2W(x)}. \tag{1.3.188}$$

The last expression can be estimated up to the desired order by using the corresponding WKB equations obtained previously, for illustration purposes we go up to order (1), using Eq. (1.3.180),

$$G(x,x) = \frac{1}{2W(x)} = \frac{1}{2W^{(0)}(x)}\left(1 + \epsilon\left(\frac{W^{(1)}(x)}{W^{(0)}(x)}\right)^2 + \mathcal{O}(\epsilon^2)\right)^{-1/2} \tag{1.3.189}$$

$$\approx \frac{1}{2W^{(0)}(x)} + \frac{3}{16}\frac{(W'^{(0)}(x))^2}{(W^{(0)}(x))^5} - \frac{1}{8}\frac{W''^{(0)}(x)}{(W^{(4)}(x))^4}. \tag{1.3.190}$$

We can finally use this expression to estimate the possible wavefunction divergence in the present toy theory, but also in more complicated scenarios later on. For a model such us the ϕ^4 we have been treating,

$$\mathcal{V}(x)\big|_{\phi=\varphi} = \frac{\mathrm{d}^2 V_{\mathrm{tree}}}{\mathrm{d}\phi^2}\bigg|_{\phi=\varphi} = \frac{\lambda}{2}\varphi^2, \tag{1.3.191}$$

so that for a fixed φ we will find no divergent term proportional to $(\partial_\mu\phi)^2$ and thus no infinite wavefunction renormalization coming from one-loop contributions. As long as there are no other fields, such as gauge or fermionic fields, and the VEV is constant, this will be the case. Finite pieces will be fixed by the subtraction scheme adopted and do not have an impact on the extraction of physical statements from our studies. We can then pick $\delta Z = 0$ for this particular example to one-loop, which is a known feature of the ϕ^4 theory (see [20, Ch. 10.2]).
We will later see how to express the one-loop contributions to the effective action in terms of the coincident Green's functions, which will complete the argument and show explicitly how the possible scale dependence can show up.

1.3.3 Renormalization Group Improvement

Besides the renormalization procedure carried on in the previous subsection, we would like to have an effective potential that is valid for high field values, provided the values of the couplings remain in the perturbation regime. As it stands, the one-loop effective action does not enjoy that feature. Hence we would like to improve on the one-loop effective Lagrangian to avoid the fact that the logarithmic terms might become large. In other words, after having picked a renormalization scale M, if the range of ϕ is too large, we might leave the perturbative regime because of the combination $\lambda^2\log(\phi^2/M^2)$. To address such failure, we describe the renormalization group improvement.
The main observation is that in a finite theory describing phenomena at a certain energy scale $E < \Lambda$, for some UV cutoff Λ, observables cannot depend on the renormalization conditions chosen. Once a theory has been renormalized and a certain subtraction scheme has been chosen, leading to some scale M as in the previous subsection, we should be able to demand that observables do not change whenever M is varied. These ideas are summarized in the Callan-Symanzik equation[32, 33].
Mathematically, the renormalized n-point functions are then a rescaling of the bare ones, by an appropriate power of the wavefunction normalization factor, Z which renormalizes the field. $\phi(x) = Z^{-1/2}\phi_0$, and we have implicitly written as $Z = 1 + \delta Z + \cdots$,

$$G^n(x_1, x_2, \ldots, x_n) \equiv \langle\Omega|T\phi(x_1)\phi(x_2)\cdots\phi(x_n)|\Omega\rangle = Z^{-n/2}\,\langle\Omega|T\phi_0(x_1)\phi_0(x_2)\cdots\phi_0(x_n)|\Omega\rangle\,. \tag{1.3.192}$$

Since these n-point functions are the building blocks of observables, they must be independent of the renormalization scale chosen. This means that considering renormalized n-point functions as functions of the couplings and the renormalization scale, as they would be when computed from for example a renormalized one-loop effective potential, the following equation– Callan-Symanzik Equation– must hold

$$\left[M\frac{\partial}{\partial M} + \beta_j(\{\lambda_i\})\frac{\partial}{\partial\lambda_j} + n\gamma\right] G^n(x_1, x_2, \cdots, x_n) = 0, \tag{1.3.193}$$

where λ_i are the couplings of the theory, the β's are the so-called beta-functions or renormalization group equation, there is one for each coupling and they track the running of the couplings with respect to the renormalization scale and are often defined as

$$\beta_j(\{\lambda_i\}) = \frac{\mathrm{d}}{\mathrm{d}\log M}\lambda_j(M). \tag{1.3.194}$$

The other as of yet undefined quantity is γ which receives the name of anomalous dimension and encodes the deviations from the expected scaling of the n-point function according

to mass-dimensions of the fields appearing in the n-point function. The Callan-Symanzik equation will have a term for each type of field appearing on the given n-point function, which can be written as

$$\gamma(Z) \equiv -\frac{\mathrm{d}}{\mathrm{d}\log M}\log(\sqrt{Z}) = -\frac{1}{2Z}\frac{\mathrm{d}}{\mathrm{d}\log M}Z(M). \tag{1.3.195}$$

These two equations give out how the theory changes when different renormalization scales are chosen. In practice, to find out how a theory responds to a change in scale, the β-functions and the anomalous dimensions are approximated to a certain order in the couplings with which the two differential equations above can be used to predict the running of the couplings by using a chosen scale, where the couplings are known, as an initial condition.

Let us then close the chapter by obtaining the running for λ in our ϕ^4 theory. This will explicitly show us how the coupling λ runs; up to this order, and clarify where we can expect the approximations made to start to break down.

Following the explanation of Coleman and Weinberg [22], let us consider the coincident 2-point and 4-point functions of the renormalized theory having $V_{\mathrm{CW}}^{\mathrm{ren}}$ as its potential and apply to them the Callan-Symanzik Equation, Eq. (1.3.193). For that purpose let us define:

$$\mathscr{G} = G^{(4)}(x,x,x,x) = \frac{\partial^4 V_{\mathrm{CW}}^{\mathrm{ren}}}{\partial\varphi^4}, \tag{1.3.196}$$

$$\mathscr{Z} = \frac{G^{(2)}(x,x)}{\langle\phi(x)\phi(x)\rangle} = Z \tag{1.3.197}$$

and observe that both $\mathscr{G}$ and $\mathscr{Z}$ are functions solely of the couplings, in this case λ alone and implicitly on the ratio $\log(\varphi/M)$ and the Callan-Symanzik equation for them is

$$\left(-\frac{\partial}{\partial t} + \beta(\lambda)\frac{\partial}{\partial\lambda} + 4\gamma\right)\mathscr{G} = 0, \tag{1.3.198}$$

$$\left(-\frac{\partial}{\partial t} + \beta(\lambda)\frac{\partial}{\partial\lambda} + 2\gamma\right)\mathscr{Z} = 0, \tag{1.3.199}$$

where we have written the first term also in terms of the logarithm of the renormalization scale, $t = \log M$. From our computations from the last section, we have to one-loop

$$\frac{\partial^4 V_{\mathrm{CW}}^{\mathrm{ren}}}{\partial\varphi^4} = \lambda + \frac{3}{16\pi^2}\lambda^2 t, \tag{1.3.200}$$

$$Z = 1. \tag{1.3.201}$$

We can plug Z into the Eq. (1.3.199) to find that $\gamma = 0$ and consequently Eq. (1.3.198) gives

$$\beta = \frac{\partial}{\partial t}\mathscr{G} = \frac{3\lambda^2}{16\pi^2}. \tag{1.3.202}$$

With the beta-function to second order in the coupling, we can write down and solve the renormalization group equation, Eq. (1.3.194):

$$\frac{\mathrm{d}\lambda'(t)}{\mathrm{d}t} = \frac{3\lambda'^2(t)}{16\pi^2} \Rightarrow \lambda'(t) = \frac{\lambda}{1 - \dfrac{3\lambda t}{16\pi^2}}. \tag{1.3.203}$$

We can now build an effective potential by using the running coupling λ',

$$V_{\mathrm{RG}}(\varphi) = \frac{\lambda}{1 - \dfrac{3\lambda t}{16\pi^2}}\varphi^4, \tag{1.3.204}$$

which recovers the CW potential of the last section, whenever $\lambda \ll 1$ and $\lambda t \ll 1$, but is additionally well defined for large negative values of t which supports the conclusions regarding spontaneous symmetry breaking coming from radiative corrections.

2

Decay by tunneling

2.1 Quantum mechanical illustration of tunneling

It is known that certain processes within the quantum field theory framework are not fully captured by traditional perturbative expansions for small couplings such as quantum tunneling processes (also known as barrier penetration). These require then a different treatment, the so-called semi-classical expansions, where the perturbation parameter is $\hbar$. In this section, we illustrate the main computational technique of our work. In order to do this, we start by examining a classical quantum mechanical system by means of its path integral formulation to arrive at its WKB-approximation result via a semi-classical approach. For this, we closely follow Coleman's book[34]. Let us then begin by considering a one-dimensional quantum mechanical system of a particle subject to a potential well $V(x)$. This system can be described by the following Hamiltonian operator:

$$H = \frac{p^2}{2} + V(x). \tag{2.1.1}$$

Our objective is to obtain the ground state energy of this system by using the path integral, a Wick rotation and an appropriate limit. Let the position basis consist of $|x\rangle$ for $x \in \mathbb{R}$. We can compute the probability amplitude for finding the system in state $|x_f\rangle$, given that it is prepared in the state $|x_i\rangle$ by letting the evolution operator $\exp(-\mathrm{i}Ht/\hbar)$ act on the initial state and projecting into the final state, that is:

$$\left\langle x_f \left| \, \mathrm{e}^{-\mathrm{i}Ht/\hbar} \right| x_i \right\rangle = N \int_{\substack{x(0)=x_i \\ x(t)=x_f}} \mathcal{D}[x(t)] \, \mathrm{e}^{\mathrm{i}S/\hbar}, \tag{2.1.2}$$

where $t > 0$ and N is some normalization constant. Each side of the equation above must be elaborated on to understand the present methodology. Let us consider first the left hand side of the equation. Suppose there exists a complete[1] basis of eigenfunctions for the Hamiltonian, $|n\rangle$, labeled discretely for simplicity and with corresponding eigenvalues E_n, so inserting the identity to the left of $|x_i\rangle$, the left hand side can be written as

$$\left\langle x_f \left| \, \mathrm{e}^{-\mathrm{i}Ht/\hbar} \right| x_i \right\rangle = \sum_n \mathrm{e}^{-\mathrm{i}E_n t/\hbar} \left\langle x_f | n \right\rangle \left\langle n | x_i \right\rangle . \tag{2.1.3}$$

By performing a Wick rotation, $t \to -\mathrm{i}\tau$ with τ commonly referred to as Euclidean time or imaginary time, of the expression above, we can exchange the oscillatory behavior of

[1] In the physics sense, it is to be understood as satisfying the closure property, i.e. $\mathbb{1} = \sum_n |n\rangle \langle n|$.

the exponential with a decaying one:

$$\left\langle x_f \left| \mathrm{e}^{-H\tau/\hbar} \right| x_i \right\rangle = \sum_n \mathrm{e}^{-E_n\tau/\hbar} \langle x_f|n\rangle \langle n|x_i\rangle \,. \tag{2.1.4}$$

If we were to consider large imaginary times, $\tau \gg 1$, the expression above should have an asymptotic behavior that allows us to extract the ground state energy. For example by taking $|x_f\rangle = |x_i\rangle = |0\rangle$ we would obtain this formula for the ground state

$$E_0 = -\lim_{\tau\to\infty} \frac{\hbar}{\tau} \log\left(\frac{\left\langle 0 \left| \mathrm{e}^{-H\tau/\hbar} \right| 0 \right\rangle}{|\langle 0|0\rangle|^2} \right) = -\lim_{\tau\to\infty} \frac{\hbar}{\tau} \log\left(\left\langle 0 \left| \mathrm{e}^{-H\tau/\hbar} \right| 0 \right\rangle \right), \tag{2.1.5}$$

meaning that if we are able to compute the Wick rotated probability amplitude, without having full knowledge of $|0\rangle$, we can still obtain the ground state energy.
Let us now return to the right-hand side of Eq. 2.1.2. We are interested in its Wick-rotation as well, for the same reasons as before, it allows us to obtain a decaying behavior, thus:

$$N \int_{\substack{x(0)=x_i \\ x(t)=x_f}} \mathcal{D}[x(t)]\, \mathrm{e}^{-S_E[x(t)]/\hbar}, \tag{2.1.6}$$

where S_E stands for the Wick-rotated action of the problem and is by convention defined to be positive (an overall minus is therefore explicitly written in front as in the previous formula)

$$S_E[x(\tau)] \equiv \int_0^{\mathcal{T}} \mathrm{d}\tau \left(\frac{1}{2} \left(\frac{\mathrm{d}x}{\mathrm{d}\tau} \right)^2 + V(x(\tau)) \right). \tag{2.1.7}$$

Observe that the potential V appears with the opposite sign in the Euclidean version and that we have labeled the upper limit of Euclidean time by $\mathcal{T}$. In order to approximate the path-integral and illustrate the technique, let us assume the potential has only one saddle-point, that is there exists some path $\bar{x}(\tau)$ that minimizes the action. We can then expand the integration path as follows:

$$x(\tau) = \bar{x}(\tau) + \sqrt{\hbar}\Delta x(\tau). \tag{2.1.8}$$

The action functional can be expanded using a functional Taylor series:

$$\begin{aligned} S_E[x(\tau)] = S_E[\bar{x}(\tau)] &+ \int_0^{\mathcal{T}} \mathrm{d}\tau\, \frac{\delta S_E}{\delta x(\tau)}[\bar{x}(\tau)]\Delta x(\tau) \\ &+ \frac{\hbar}{2} \int_0^{\mathcal{T}} \mathrm{d}\tau\, \mathrm{d}\tau'\, \frac{\delta^2 S_E[\bar{x}(\tau)]}{\delta x(\tau)\delta x(\tau')} \Delta x(\tau)\Delta x(\tau') + \mathcal{O}[\Delta^3 x]. \end{aligned} \tag{2.1.9}$$

In the case of $\bar{x}(\tau)$ being a saddle-point, the second term of the expansion vanishes and one is left with

$$S_E[x(\tau)] = S_E[\bar{x}(\tau)] + \frac{\hbar}{2} \int_0^{\mathcal{T}} \mathrm{d}\tau\, \mathrm{d}\tau'\, \Delta x(\tau) \frac{\delta^2 S_E[\bar{x}(\tau)]}{\delta x(\tau)\delta x(\tau')} \Delta x(\tau'), \tag{2.1.10}$$

up to quadratic variations. The second functional derivative of the action is known as the fluctuations operator, since it can be interpreted as a propagator for the variations of the

path as we will later see in the case of field theories. Let us then compute such operator for the case at hand. We obtain

$$\frac{\delta^2 S_E[\bar{x}(\tau)]}{\delta x(\tau)\delta x(\tau')} = \delta(\tau-\tau')\left(-\frac{\mathrm{d}^2}{\mathrm{d}\tau'^2}+V''(\bar{x}(\tau'))\right), \tag{2.1.11}$$

where $V''(x)$ is the second derivative with respect to x. Using this result in Eq. (2.1.10) and performing the τ' integration we have:

$$S_E[x(\tau)] = S_E[\bar{x}(\tau)] + \frac{\hbar}{2}\int_0^{\mathcal{T}} \mathrm{d}\tau\, \Delta x(\tau)\left(-\frac{\mathrm{d}^2}{\mathrm{d}\tau^2}+V''(\bar{x}(\tau))\right)\Delta x(\tau). \tag{2.1.12}$$

We can now pick an orthonormal basis of normalizable eigenfunctions of the fluctuations operator as to decompose the fluctuations, Δx, as

$$\Delta x(\tau) = \sum_m c_m \Delta x_m(\tau), \tag{2.1.13}$$

for some appropriate index m which can be either discrete, continuous or a mixture of both, and Δx_m satisfies

$$\left(-\frac{\mathrm{d}^2}{\mathrm{d}\tau^2}+V''(\bar{x}(\tau))\right)\Delta x_m(\tau) = \lambda_m \Delta x_m(\tau). \tag{2.1.14}$$

This expansion allows us to trade the integral over all fluctuation paths for integration over the coefficients of the linear combination in Eq. (2.1.13), to do that let us plug the expansion of the action, Eq. (2.1.12), into the Wick rotated Eq. (2.1.2):

$$\left\langle x_f \left| \mathrm{e}^{-H\mathcal{T}/\hbar} \right| x_i \right\rangle = N\int_{\substack{x(0)=x_i\\ x(t)=x_f}} \mathcal{D}[x(\tau)] \exp\left(-\frac{1}{\hbar}S_E[x(\tau)]\right) \tag{2.1.15}$$

$$= N\int_{\substack{\Delta x(0)=0\\ \Delta x(\mathcal{T})=0}} \mathcal{D}[\Delta x(\tau)] \exp\left[-\frac{1}{\hbar}S_E[\bar{x}(\tau)] - \frac{1}{2}\int_0^{\mathcal{T}} \mathrm{d}\tau\, \Delta x(\tau)\left(-\frac{\mathrm{d}^2}{\mathrm{d}\tau^2}+V''(\bar{x}(\tau))\right)\Delta x(\tau)\right] \tag{2.1.16}$$

$$= N\int_{\substack{\Delta x(0)=0\\ \Delta x(\mathcal{T})=0}} \prod_m \mathrm{d}c_m \exp\left[-\frac{1}{\hbar}S_E[\bar{x}(\tau)] - \sum_m \frac{c_m^2}{2}\lambda_m |\Delta x_m|^2\right] \tag{2.1.17}$$

$$= N\,\mathrm{e}^{-S_E[\bar{x}]/\hbar}\int_{\substack{\Delta x(0)=0\\ \Delta x(\mathcal{T})=0}} \prod_m \mathrm{d}c_m \exp\left[-\sum_m \frac{c_m^2}{2}\lambda_m\right] \tag{2.1.18}$$

$$= N\,\mathrm{e}^{-S_E[\bar{x}]/\hbar}\prod_m \sqrt{\frac{2\pi}{\lambda_m}}. \tag{2.1.19}$$

Rewriting the above in a general form

$$\left\langle x_f \left| \mathrm{e}^{-H\mathcal{T}/\hbar} \right| x_i \right\rangle = N\mathcal{V}\,\mathrm{e}^{-S_E[\bar{x}]/\hbar}(\det \mathcal{M}^{-1})^{-1/2} \tag{2.1.20}$$

where $\mathcal{V}$ is an infinite volume factor and we have named the fluctuations operator $\mathcal{M}^{-1}$ and assumed for the time being that all eigenvalues are positive.
We can interpret this result as leading to a non-zero probability of finding our particle in the vicinity of x_f when it started closely localized at x_i. Independently of a classical barrier separating both points, we can see that the quantity above is not zero and lends itself to the interpretation of the particle tunneling through the barrier itself. In the following, we extend these notions to the field theory setting. Nonetheless, the interpretation remains the same.

2.2 False vacuum decay in field theory

We can now utilize the tools of the previous section in the framework of field theory, which we will use for the rest of the document. In particular, we will be interested in applying such tools for the study of transitions between vacua so that x_i and x_f now adopt the meaning of minima of the potential. For this, we summarize Coleman's original paper[1]. Let us then consider a scalar field ϕ on four-dimensional space-time, subject to a potential U having two local minima as the one drawn in Fig. 2.1, which is such that $U(\varphi_+) = 0$, and has been sketched inverted to make an analogy with mechanical systems. The corresponding Euclidean equation of motion for such a field is

$$\frac{\mathrm{d}^2\phi}{\mathrm{d}\tau^2} + \nabla^2\phi = \frac{\mathrm{d}U}{\mathrm{d}\phi}. \tag{2.2.21}$$

The boundary conditions for a bounce-like solution are analogously

$$\begin{aligned} \phi(\tau, \mathbf{x}) &\underset{\tau\to\pm\infty}{\longrightarrow} \varphi_+, \\ \frac{\mathrm{d}\phi}{\mathrm{d}\tau}(0, \mathbf{x}) &= 0, \end{aligned}$$

and

$$\phi(\tau, |\mathbf{x}|) \underset{|x|\to\infty}{\longrightarrow} \varphi_+, \tag{2.2.22}$$

where the last condition is needed when we demand that the action evaluated at such configuration remains finite. As shown in Fig. 2.1, a way to think about this type of configurations is in analogy to mechanical systems. A system described by Eq. (2.2.21) can be thought of as a particle rolling down an inverted potential, if one in addition imposes the boundary conditions above we can imagine a particle starting on φ_+ and rolling back and forth. This matches graciously with the picture of a bubble appearing in some region whose inside experiences true vacuum, φ_+, and where outer far away regions experience false vacuum, φ_-.
As before the 0-th order contribution to the action from bounce configuration satisfying Eqs. (2.2.21),(2.2.22)

$$B \equiv S_E^{(0)} = \int \mathrm{d}\tau\, \mathrm{d}^3x \left[\frac{1}{2}\left(\frac{\mathrm{d}\phi}{\mathrm{d}\tau}\right)^2 + \frac{1}{2}\left(\nabla^2\phi\right)^2 + U(\phi)\right]. \tag{2.2.23}$$

After observing that the differential equation determining the bounce configuration is translation invariant, and more over $O(4)$ symmetric, we can perform a coordinate change

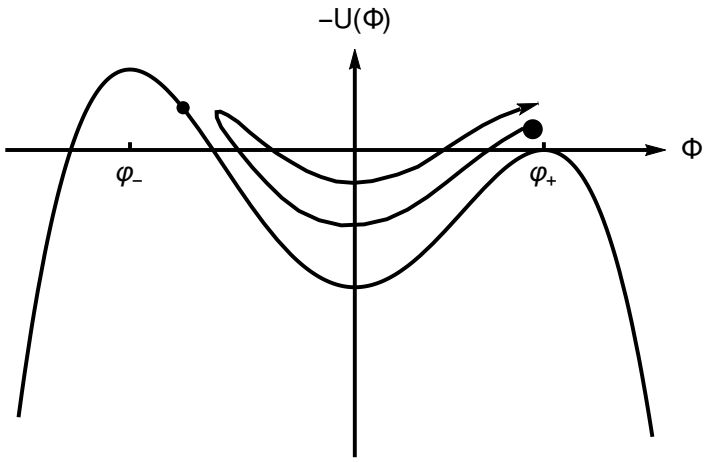

Figure 2.1: Depiction of the bounce solution as a mechanical system, rolling down an inverted potential having several local minima.

to exploit such property. Let us introduce $r^2 = \tau^2 + \mathbf{x}^2$ and assume that $\phi = \phi(r)$, this renders Eq. (2.2.21) into the following form:

$$-\frac{\mathrm{d}^2\varphi}{\mathrm{d}r^2} - \frac{3}{r}\frac{\mathrm{d}\varphi}{\mathrm{d}r} + U'(\varphi) = 0, \tag{2.2.24}$$

and the boundary conditions to be met become only the following two equations:

$$\begin{aligned} \varphi(r) &\underset{r\to\infty}{\longrightarrow} \varphi_+, \\ \frac{\mathrm{d}\varphi}{\mathrm{d}r}(0) &= 0, \end{aligned} \tag{2.2.25}$$

where the second condition ensures that the field configuration is non-singular at $r = 0$. Coleman argues and proves[35] that an $O(4)$-symmetric solution would correspond to a minimum, thus we adopt the above conditions.

A second look at Eq. (2.2.24), using the mechanical system analogy of a particle rolling down a potential, calls for the interpretation of the second term on the left-hand side as a friction term or viscous force. Under this perspective, one can understand the existence of the sought configuration via the traditional argument of overshooting and undershooting. If we were to release our particle from a given point in the vicinity of φ_- (see Fig. (2.1)), too far to the right, the particle will not have enough energy to climb up to φ_+, especially not since friction is always dissipating energy. Along the continuous process of moving the release point to the left, Coleman[1] proves that even when considering friction, if a hypothetical particle is released from too close to φ_-, it will roll down, then up and go past φ_+, i.e., it will overshoot. Since the dependence of the solution to Eq. (2.2.24) on the release point is continuous, there must exist at least one point between both behaviors, where there is a solution that exactly stops at φ_+, which is the bounce configuration we seek.

Having argued in favor of the existence of such configuration in general, we now elaborate on the treatable case where we neglect the friction term, the so-called thin-wall approximation. Let us for that purpose begin with a symmetric potential U_{sym}, such that $U_{\mathrm{sym}}(\phi) = U_{\mathrm{sym}}(-\phi)$, with minima at field values $\pm\varphi_{\mathrm{sym}}$, let its second derivative at the minima be $U''_{\mathrm{sym}}(\pm\varphi_{\mathrm{sym}}) = \mu^2$ and consider a perturbation breaking the $\mathbb{Z}_2$-symmetry, so

that our new potential is

$$U(\phi) = U_{\rm sym}(\phi) + \frac{\epsilon}{2\varphi_{\rm sym}}(\phi - \varphi_{\rm sym}). \tag{2.2.26}$$

Under the current approximations, we can divide the behavior of the solution into three pieces, inside the bubble $r \ll R$, near the bubble-wall $r \sim R$ and outside the bubble $r \gg R$, where R is the location of the bubble wall. For $\epsilon \ll 1$, we have that the field spends a large amount of time at the top before rolling down the valley. That is, we expect R to be generally large and to be able to neglect the friction term for regions far away from the wall. This makes Eq. (2.2.24) into the equation of a one-dimensional soliton over the potential $U_{\rm sym}$, whose solution can be written in implicit form by

$$r = \int_0^{\varphi} \frac{{\rm d}\tilde{\phi}}{\sqrt{2U_{\rm sym}(\tilde{\phi})}}. \tag{2.2.27}$$

We can compute an approximation to the classical action

$$S_{\rm wall}[\varphi] = \int {\rm d}r \left[\frac{1}{2} \left(\frac{{\rm d}\varphi}{{\rm d}r} \right)^2 + U_{\rm sym}(\varphi) \right] = \int_{-\varphi_{\rm sym}}^{+\varphi_{\rm sym}} {\rm d}\varphi \sqrt{2U_{\rm sym}(\varphi)}. \tag{2.2.28}$$

Under the current approximation we have the following piece-wise profile for the bounce configuration

$$\phi_{\rm bounce} = \begin{cases} -\varphi_{\rm sym} & \text{if} \quad r \gg R \\ \varphi(r - R) & \text{if} \quad r \approx R \\ \varphi_{\rm sym} & \text{if} \quad r \ll R \end{cases} . \tag{2.2.29}$$

The Euclidean action can then be evaluated over the bounce configuration by splitting the contributions into the one coming from the interior and the one coming from the wall's tension:

$$B = S_E(\phi_{\rm bounce}) = 2\pi^2 \int_0^{\infty} r^3 \, {\rm d}r \left[\frac{1}{2} \left(\frac{{\rm d}\phi_{\rm bounce}}{{\rm d}r} + U(\phi_{\rm bounce}) \right)^2 \right] \tag{2.2.30}$$

$$= -\frac{1}{2}\pi^2 R^4 \epsilon + \pi^2 R^3 S_{\rm wall}. \tag{2.2.31}$$

The location of the wall can then be specified by finding the extreme point of the expression above, leading immediately to $R = 3S_{\rm wall}/\epsilon$. This is in agreement with the picture of a large bubble for degenerate potentials, i.e. $\epsilon \to 0$ and gives

$$B = \frac{27\pi^2 S_{\rm wall}^4}{2\epsilon^3} \tag{2.2.32}$$

for such cases.
From Eq. (2.2.27) one can obtain a condition for the validity of the thin-wall approximation, the relevant scale is μr for the asymptotic behavior used, and it corresponds to $\mu r \gg 1$ thus we have the condition

$$\mu R = \frac{3\mu \, S_{\rm wall}}{\epsilon} \gg 1. \tag{2.2.33}$$

For example, for a Mexican-hat type of potential of the form

$$U_{\text{sym}} = -\frac{1}{2}\mu^2\phi^2 + \frac{1}{4!}\lambda\phi^4 + \text{const.}, \tag{2.2.34}$$

the thin-wall condition becomes

$$\frac{12\mu^4}{\lambda\epsilon} \gg 1, \tag{2.2.35}$$

which we can take to mean that the asymmetry multiplied with the quartic self-coupling is small when compared to the tree-level mass, which we can consider as a rule of thumb for later cases.

In order to relate the saddle-point expansion of the action with a decay rate, we can use exactly the arguments used in the previous section of the quantum mechanical case. Coleman's argument[34], that under the view of turning-on perturbations adiabatically, we may see that the ground state may be displaced to an unstable state, which acquires a negative imaginary part which we just witnessed above, and then decays exponentially. At this point, it is natural to ask ourselves how to improve on the estimation of the tunneling rate and maintain the interpretation of a decay rate when an imaginary part of the energy is not possible or not clear enough. It can be argued[36] via Picard-Lifschitz theory that the decay rate per unit volume and time expression,

$$\frac{\gamma}{\mathcal{V}} = -\frac{2}{\mathcal{V}\hbar}\mathfrak{Im}E_0 = \frac{2}{\mathcal{V}T\hbar}\mathfrak{Im}\log\left(\frac{Z_{\text{bounce}}}{Z_{\text{f.v}}}\right), \tag{2.2.36}$$

is indeed correct and in agreement with other approaches, by means of a proper analytical continuation, that takes the results from their Euclidean to their Minkowskian version.

2.2.1 Subtleties when including higher-order corrections

As we saw in Eq. (2.1.20), we need to not only evaluate the action at the interpolating solution but also need to compute the prefactor in front of the exponential. For fluctuation operators that are positive-definite, the computation can be done straightforwardly as we did before. However, it is often the case that the fluctuation operator will have certain symmetry leading to zero eigenvalues, in which case we must be careful when using Eq. (2.1.20). Furthermore, besides zero-modes, we must also be careful with negative modes associated with tunneling and with the type of spectrum of the fluctuations operator, which might have a discrete part and a continuum part, or a mixture, that must be dealt with carefully in a case by case basis. Let us here discuss the impact of possible zero-modes before moving on to the computation of higher-order corrections.

Precisely this phenomenon would have occurred in the case of study of the previous section, were we to choose the polynomial potential in Eq. (2.2.34)[37]. For such a case, the potential respects an $O(4)$ and a translations symmetry, implying there are four directions in which we can translate the bounce configuration without incurring additional contributions to the fluctuation operator, or in other words, the bounce configuration constitutes a saddle-point of the action and there are flat-directions around it corresponding to the normalizable configurations proportional to $\partial_\mu\phi_{\text{bounce}}$ for $\mu = 1, \ldots, 4$.

In computing the Gaussian path integral for the fluctuation operator, it was required for us to consider a decomposition in eigenfunctions, Eq. (2.1.13). However, this made no mention of possible zero eigenvalues. In such a case, we may exchange such directions for integrals over collective coordinates[38], which represent the symmetries associated with the zero-modes.

For the case of the translations symmetry the path integral is computed by using a decomposition (assuming a discrete spectrum), analogous to the one in Eq. (2.1.13),

$$\delta\phi(x) = \sum_{\mu=1}^{4} c_{\mu,0}\,\delta\phi_{\mu,0}(x) + \sum_{\substack{n \\ c_n\neq 0}} c_n\delta\phi_n(x) = \sum_{\mu=1}^{4} \delta_\mu x\,\partial_\mu\phi_{\text{bounce}}(x) + \sum_{\substack{n \\ c_n\neq 0}} c_n\delta\phi_n(x), \tag{2.2.37}$$

where $\delta_\mu x$ represents an infinitesimal displacement in the μ direction, $\delta\phi_{\mu,0}$ are the four zero-modes and where the $\delta_n\phi$ as before, represent the orthonormal set of eigenfunctions of the fluctuation operator with eigenvalues c_n respectively. The arrow in the equation above means we have changed our basis from the one including $\delta\phi_{\mu,0}$ to one including $\partial_\mu\phi_{\text{bounce}}(x)$ instead. We identify then a variation of the coefficients of the normalized zero-modes with a translation displacement

$$\mathrm{d}c_{\mu,0}\,\delta\phi_{\mu,0}(x) = \mathrm{d}c_{\mu,0}\,\mathcal{N}_\mu\partial_\mu\,\phi_{\text{bounce}}(x) = \mathrm{d}\delta_\mu x\,\partial_\mu\phi_{\text{bounce}}(x), \tag{2.2.38}$$

for some normalization factor $\mathcal{N}_\mu$. We can thus identify $\mathrm{d}c_{\mu,0} = \mathrm{d}\delta_\mu x/\mathcal{N}_\mu$. Performing such an exchange, we transform the integration measure accordingly, that is, we integrate over the coefficients of the non-zero modes and over the infinitesimal displacements for the zero-modes, namely

$$\mathcal{D}[\delta\phi] = \prod_{\mu=1}^{4}\frac{\mathrm{d}c_{\mu,0}}{\sqrt{2\pi\hbar}}\prod_{\substack{n \\ c_n\neq 0}}\frac{\mathrm{d}c_n}{\sqrt{2\pi\hbar}} \longrightarrow \prod_{\mu=1}^{4}\frac{\mathrm{d}\delta_\mu x}{\sqrt{2\pi\hbar}\mathcal{N}_\mu}\prod_{\substack{n \\ c_n\neq 0}}\frac{\mathrm{d}c_n}{\sqrt{2\pi\hbar}}, \tag{2.2.39}$$

that way we manage to trade the integrals over zero eigenvalues for integrals over the collective coordinates, $\delta_\mu x$, which represent an infinite set of bounces centered at different locations, thus their name. All that remains is to compute the normalization and proceed to compute integrals that are now independent of the zero-mode directions. To obtain the normalization, recall $\phi_{\text{bounce}}(x)$ satisfies the equation of motion and corresponds to a solution which has 0 energy-momentum, since we set the false vacuum at zero potential at the starting point, ϕ_+, the trace of the stress-energy momentum tensor evaluated on the bounce implies:

$$0 = -\int \mathrm{d}^4x\,\partial_\mu\phi_{\text{bounce}}\partial^\mu\phi_{\text{bounce}} + 4U(\phi_{\text{bounce}}). \tag{2.2.40}$$

Be means of isotropy we can state that each direction then contributes a fourth of U, so for a given fixed μ,

$$\int \mathrm{d}^4x\,\partial_\mu\phi_{\text{bounce}}\partial^\mu\phi_{\text{bounce}} = -\int \mathrm{d}^4x\,U(\phi_{\text{bounce}}). \tag{2.2.41}$$

where no Einstein summation is implied. Then we have, by applying Eq. (2.2.40), that

$$\begin{aligned} S_{\text{tree}} &= \int \mathrm{d}^4x\left[\frac{1}{2}\partial_\mu\phi_{\text{bounce}}\partial^\mu\phi_{\text{bounce}} + U(\phi_{\text{bounce}})\right] \\ &= \int \mathrm{d}^4x\; -2U(\phi_{\text{bounce}}) + U(\phi_{\text{bounce}}) \\ &= -\int \mathrm{d}^4x\,U(\phi_{\text{bounce}}), \end{aligned}$$

and comparing Eq. (2.2.41) and Eq. (2.2.42) we can conclude that $\mathcal{N}_\mu = (S_{\rm tree})^{-1/2}$. The integration measure gets then an overall factor of $(\sqrt{S_{\rm tree}})^{-4}$, and we can write down a formula with this correction as follows

$$\frac{\gamma}{\mathcal{V}} = \frac{S_{\rm tree}^2}{4\pi^2\hbar^2}\, {\rm e}^{-S_{\rm tree}/\hbar} \left|\frac{\det'[-\Delta_4 + U''(\phi_{\rm bounce})]}{\det[-\Delta_4 + U''(\phi_+)]}\right|^{-1/2} + \mathcal{O}(\hbar), \tag{2.2.42}$$

where the $'$ indicates that the zero-modes have been extracted. We observe that all prefactors are dimensionless and given that the eigenvalues of the operators inside the determinants have units of length^{-2}, extracting four of them leaves an excess of length^{-4} as the overall units of $\gamma/\mathcal{V}$, which agrees with a decay rate per unit time and volume.
Besides extracting the zero-modes of the fluctuation operator, we must expect at least a possible negative mode, responsible for the imaginary piece of the action. Coleman and Callan's[37] argument ensures the existence of at least one mode but is not really conclusive concerning the question of the existence of multiple negative modes in the case of a four-dimensional field theory. Some can be found by studying the thin-wall limit, where if they do exist, they must belong to the $\ell = 0$ sector of an expansion in hyper-spherical harmonics, with ℓ being the generalization of angular momentum to four-dimensional space. We will attempt to extract the negative modes on a case-by-case basis.
The last but not least important matter to discuss, before suggesting our own methods, is that of renormalization and higher-order corrections. Already in Coleman and Callan's paper[1] and in Coleman's book[34], it is suggested that we replace the action with the renormalized action plus some given order of loop-diagrams. Substituting $S[\phi]$ for

$$S_R[\phi] = S[\phi] + S_{\rm ct}[\phi] + \sum_{m=1}^{n} \hbar^n S^{(m)}[\phi], \tag{2.2.43}$$

which is the renormalized action and has been broken down into: a bare piece[2] S, a piece containing the counterterms required to renormalize the theory, i.e. absorb all divergences, $S_{\rm ct}$ and contributions from higher number of loops $S^{(m)}$, which stands for those coming from m-loop diagrams.
An improvement on the computations of the present section is achieved already by including one-loop diagrams. We can actually follow the same path we have followed, but compute a bounce for the action $S[\phi] + S_{\rm ct}[\phi]$, $\phi_{\rm bounce}$, and obtain the following formula for the decay rate which would include one-loop contributions

$$\frac{\gamma}{\mathcal{V}} = \frac{S^2}{4\pi^2\hbar^2}\, {\rm e}^{-S_{\rm tree}-(S^{(1)}[\phi_{\rm bounce}]-S^{(1)}[\varphi_+])} \left|\frac{\det'[-\Delta_4 + U''(\phi_{\rm bounce})]}{\det[-\Delta_4 + U''(\phi_+)]}\right|^{-1/2}. \tag{2.2.44}$$

This expression coincides with a renormalized effective action to one-loop level as we explained in Sec.1.2. In the first set of applications, related to the electroweak sector and the vacuum stability, we focus on computing the exponent appearing in the decay rate not only to one-loop order but also including the gradients of the bounce solution. That is, accounting for the non-homogeneity of the bounce. The prescription demonstrating how to do such a thing is what is presented in the following subsection.

2.2.2 Green's function and self-consistent method

In this subsection, we introduce the prescription we will follow in order to include the effects of gradient corrections from the background, besides the already mentioned radiative

[2] Corrected so that the whole action still vanishes at φ_+, by possibly adding a constant

corrections of the one-loop diagrams. The proposal is later applied to specific sectors which serve the role of test grounds for the methods here presented. We follow the exposition of the methods as introduced by Garbrecht and Millington[30],[39]. Therein the method is applied for a ϕ^4 toy model, similar to what we have used in this chapter to illustrate most of the mathematical tools. We do not pretend to reproduce the paper in full detail but to highlight the steps that need to be followed in order to include the effects of gradients into the computation of the exponents appearing in the formula for the vacuum decay rate, Eq. (2.2.44).

The method consists of using a saddle-point expansion as we have done to compute the action and possible higher-order corrections to it. Once we have found the saddle-point, e.g., the bounce, we compute the Green's functions for the fluctuations operators. These allow us, in turn, to compute the functional determinants appearing in the prefactor of the exponential as well as the one-loop contributions. In a self-consistent manner, the Green's functions can be used in the one-loop effective action to obtain a corrected equation of motion for the saddle-point configuration. The corrected bounce can be used to estimate $\hbar^2$ contributions, which may be particularly relevant in certain models. We describe here the missing steps not yet covered to compute the effects described above.

The whole prescription relies heavily on the availability of the Green's functions, so let us begin by going over that point in view of its applications to vacuum decay. Given a fluctuation operator $\mathcal{M}_x^{-1}$, which consists of derivatives and functionals on configurations depending on the coordinate x, the Green's function problem is then

$$\mathcal{M}_x^{-1}\mathcal{M}(x,x') = \delta(x-x'), \tag{2.2.45}$$

where $\mathcal{M}$ is to be found, as already postulated when explaining the WKB method in Subsec. 1.3.2. As described there, the WKB-method is one possible method to approximate the Green's function $\mathcal{M}$, which is useful under specific conditions and is known to be insufficient for others. Specifically, the WKB approximation fails to account correctly for the inhomogeneity of the background. That is the reason we are interested in looking for alternatives.

We do not pretend to give a compilation of methods here but only mention some possibilities in passing and make some comments about this point. For specific models, we might even be able to solve for the Green's function analytically (see [30] and [31]) when the bounce configuration itself has been found in closed analytical form. In such cases, exploiting the $SO(4)$ symmetry permits an expansion in hyperspherical harmonics, which can be truncated at a given order and proceed with the program described above. However, that will not be the case for more realistic cases and the bounce configuration must be found using numerical methods. For such cases, we will attempt to find the Green's function as well by using computational methods. From this point on and until the end of this subsection, we assume $\mathcal{M}(x,x')$ has been found in some way.

We need then only answer how the Green's functions allow us to compute functional determinants and the quantum corrected equation of motion. In this subsection, we try to remain fairly general as the same methods will be employed later in the next chapter, where the specific models of a fermion sector and a gauge sector are addressed.

The functional determinants can be expressed in terms of Green's functions, $\mathcal{M}(x,x')$, through the resolvent method which exploits the spectral decomposition of an operator, as shown on Refs. [31, 40–42]. We summarize the procedure here. Given a hermitian and positive-definite operator between Hilbert spaces, $\mathcal{M}^{-1}:\mathcal{H}\to\mathcal{H}$, with a continuous spectrum, and a basis for $\mathcal{H}$ consisting of orthogonal eigenfunctions, $\{f_\lambda\}_{\lambda\in\mathbb{R}^+}$ of $\mathcal{M}^{-1}$,

we can employ the spectral theorem to decompose its Green's functions $\mathcal{M}$ as follows:

$$\mathcal{M}(x,y) = \int \mathrm{d}\lambda \frac{f_\lambda(x) f_\lambda^*(y)}{\lambda}. \tag{2.2.46}$$

It is immediate to verify that the expression above does indeed solve the Green's function equation. A deformation of the operator, $\mathcal{M}^{-1}$, can be made by means of the addition of an auxiliary parameter $s \in \mathbb{R}$,

$$\mathcal{M}_s^{-1}(x,y) \equiv \mathcal{M}^{-1}(x,y) + s\mathbb{1}, \tag{2.2.47}$$

so that the corresponding Green's function is now

$$\mathcal{M}_s(x,y) = \int \mathrm{d}\lambda \frac{f_\lambda(x) f_\lambda^*(y)}{\lambda + s}. \tag{2.2.48}$$

The integration over the auxiliary parameter to obtain the logarithm of the operator $\mathcal{M}^{-1}$ does not converge when the parameter s is integrated up to infinity, however the ratio of the logarithms of two operators $\mathcal{M}_1$ and $\mathcal{M}_2$, with eigenfunctions $f_{\lambda,1}$ and $f_{\lambda,2}$ respectively, and having the same continuous spectrum of eigenvalues, does:

$$\begin{aligned}
\log \frac{\mathcal{M}_1^{-1}(x,y)}{\mathcal{M}_2^{-1}(x,y)} &= \int \mathrm{d}\lambda \, \log(\lambda) f_{\lambda,1}(x) f_{\lambda,1}^*(y) - \int \mathrm{d}\lambda \, \log(\lambda) f_{\lambda,2}(x) f_{\lambda,2}^*(y) \\
&= -\int \mathrm{d}\lambda \left(\int_0^\infty \mathrm{d}s \, \frac{f_{\lambda,1}(x) f_{\lambda,1}^*(y)}{\lambda + s} - \int_0^\infty \mathrm{d}s \, \frac{f_{\lambda,2}(x) f_{\lambda,2}^*(y)}{\lambda + s} \right) \\
&= -\int_0^\infty \mathrm{d}s \, \mathcal{M}_{1_s}(x,y) - \mathcal{M}_{2_s}(x,y),
\end{aligned}$$

where we have used Eq. (2.2.48) to get to the last line. Then taking a full trace leads us to the equation:

$$\log \frac{\det \mathcal{M}_1^{-1}(x,y)}{\det \mathcal{M}_2^{-1}(x,y)} = \operatorname{tr} \log \frac{\mathcal{M}_1^{-1}(x,y)}{\mathcal{M}_2^{-1}(x,y)} = -\operatorname{tr}_{\mathrm{dis}} \int \mathrm{d}x \int_0^\infty \mathrm{d}s \, \mathcal{M}_{1_s}(x,x) - \mathcal{M}_{2_s}(x,x). \tag{2.2.49}$$

where $\operatorname{tr}_{\mathrm{dis}}$ denotes a trace over possible remaining indices, such as Lorentz or color. The formula above shows how to compute the one-loop contribution terms by using the Green's functions for the deformed operators. In the next part of the document we will adapt this formula given some extra assumptions and obtain with it an estimate of the size of the gradient effects compared to the CW version.

The next observations pertain to the so-called tadpole contributions, which usually are diagrammatically represented by a loop with one insertion of the background or external leg. In general, their mathematical expression might not correspond only to such diagram, but may also contain more insertions depending on the specific potential of the model. What is important nonetheless is that their relation to the Green's function remains the same, which we then can take as a definition. We will call tadpole contributions from field X, to those coming from a functional derivative of the logarithm of the one-loop diagrams $\mathcal{W}^{(1)}[J=0]$, with respect to X (see Eq. (1.2.134)),

$$\Pi_X(\psi,x)\varphi(x) \equiv \frac{\delta}{\delta\varphi(x)} B_X^{(1)} = g_X \frac{\delta}{\delta\varphi(x)} \log \frac{\det' \mathcal{M}_X^{-1}(\varphi; x', x'')}{\det \mathcal{M}_X^{-1}(\varphi_+; x', x'')}\bigg|_{\varphi=\psi}, \tag{2.2.50}$$

where g_X is generally associated to the degrees of freedom of the field and is negative for fermions, while the origin of the logarithm is the use of the generating functional of connected diagrams (see 1.2) for computing the one-loop effective action. We then compute the corresponding corrected equation of motion in a self-consistent manner, that is we find the equation of motion for a bounce subject to the one-loop effective potential. Mathematically we do this by expanding the effective action Eq. (1.2.139) around the classical bounce $\varphi^{(1)} = \varphi + \hbar\delta\varphi$, the quantum corrected bounce, and subsequently by taking a functional derivative with respect to it to obtain a corrected equation of motion:

$$0 = \frac{\delta}{\delta\varphi(x)}\Gamma^{(1)}[\varphi^{(1)}] = -\partial^2\varphi^{(1)}(x) + V'_{\text{eff}}(\varphi^{(1)}; x), \tag{2.2.51}$$

where V_{eff} is the collection of terms appearing in $\Gamma^{(1)}$ other than the kinetic term and with the present notation we have

$$V'_{\text{eff}}(\varphi^{(1)}; x) = V_{\text{tree}}(\varphi^{(1)}; x) + \sum_X \hbar\,\Pi_X(\varphi; x)\varphi(x), \tag{2.2.52}$$

where X runs over the field content of the model. We then have some $\hbar^2$ corrections appearing when we evaluate the effective action on the quantum corrected bounce. The first corrections will come from the tree-level action and the second from the variation of the one-loop terms as above. In the case more fields are involved, each term will have such a contribution and all must be added. We only collect the results here, which have been derived already in [30, 31]. The contribution from the tree-level action for the scalar case is

$$\hbar^2\delta S_\varphi = \frac{1}{2}\int \mathrm{d}^4x\,\delta\varphi(x)\mathcal{M}_\varphi^{-1}(\varphi; x, x)\delta\varphi(x) = -\frac{1}{2}\int \mathrm{d}^4x\,\delta\varphi(x)\Pi_\varphi(\varphi; x)\varphi(x) \tag{2.2.53}$$

and the one from the variations within the one-loop term are

$$\hbar^2\delta B_\varphi^{(1)} = \frac{1}{2}\int \mathrm{d}^4x\,\delta\varphi(x)\frac{\delta}{\delta\varphi(x)}\log\det{}'\mathcal{M}_\varphi(\varphi; x', x'') \tag{2.2.54}$$

$$= \int \mathrm{d}^4x\,\delta\varphi(x)\Pi_\varphi(\varphi; x)\varphi(x). \tag{2.2.55}$$

The total contribution of order $\hbar^2$ appearing in the one-loop effective action evaluated at the quantum corrected bounce is, for the case of a single scalar field,

$$B_\varphi^{(2)} \equiv \delta S_\varphi + \delta B_\varphi^{(1)} = -\delta S. \tag{2.2.56}$$

Collecting the different contributions we have seen, we have a final expression for the exponent of the decay rate

$$\frac{\gamma}{\mathcal{V}} \propto \exp\left\{-\frac{1}{\hbar}\left(S_{\text{tree}}[\varphi] + \hbar B_\varphi^{(1)} + \hbar^2 B_\varphi^{(2)}\right)\right\}, \tag{2.2.57}$$

where the constant of proportionality is given by the factors coming out of the integration over collective coordinates and the negative mode.

Having reached this point, we believe the main mathematical tools for the studies that follow have been discussed, and we consider we can now elaborate on the specific applications pursued.

Part II

Applications related to the electroweak vacuum

3

The Electroweak sector of the minimal Standard Model

3.1 The electroweak sector

The electroweak (EW) sector we know today was suggested in the 1960s, known as the GWS after its creators [43–45] for which they were later awarded the 1979 Nobel prize in physics. Here we present the ingredients needed to understand the current knowledge concerning vacuum stability. Thus we begin by motivating our studies by using the mathematical tools available to summarize and obtain a one-loop improved scalar potential for the SM. Although our specific toy model on which we elaborate later does not correspond to the current SM, it serves as a testing ground for the functional techniques used and to examine possible contributions that are usually neglected in traditional computations of the effective scalar potential.

For this short presentation of the EW sector, we will follow closely what has been exposed in the review by Sher [46] and in the book by Donoghue [47]. The GWS model mixes the electromagnetic interaction and the weak interactions under a single framework. Formally we say the EW sector corresponds to a gauge field theory with gauge group $SU_L(2) \times U_Y(1)$. Matter fields are, in contrast, described by massless spin one-half fermions. The group factor $SU_L(2)$ is referred to as (weak) isospin and the $U_Y(1)$ factor as the (weak) hypercharge. The subscript L highlights the fact that only the left-handed components of the fermions have non-trivial isospin, opposed to the right-handed components, which are isospin singlets. The subscript Y denotes the weak hypercharge that is possessed by all leptons and quarks (not counting possible right-handed neutrinos).

The last field in the model is the Higgs field which, as is now known[2, 3], is responsible for the mechanism of spontaneous symmetry breaking (SSB) which provides the fermions and the gauge bosons with mass. It is this field about which we will generally speak when referring to vacuum because it is a scalar of the model and hence is allowed to have a non-trivial potential without disrupting the condition of renormalizability. The SSB mechanism as such requires just one such field as a $SU_L(2)$-doublet (or isospin 1/2 representation), although modern theories aiming to extend the standard model may include more such fields (see Ref. [48] for a review).

The model consists of a Lagrangian density,

$$\mathcal{L}_{EW} = \mathcal{L}_{\mathrm{k.G}} + \mathcal{L}_{\mathrm{k.F}} + \mathcal{L}_{\mathrm{H}} + \mathcal{L}_{\mathrm{HF}}, \tag{3.1.1}$$

which can be split into the four terms above: a kinetic term for the gauge fields, a kinetic term for the fermions, the Higgs sector and an interactions part between the Higgs field

and the fermions.
Fermions are split between leptons and quarks, the latter carrying also color corresponding to the $SU(3)$ symmetry or strong sector, which is not relevant for the present discussion. Leptons consist of neutrinos and electrons from three families which differ only in their mass, the label f will denote the field's family. The fields themselves are generally denoted by

$$L_f = \begin{pmatrix} \nu_{L_f} \\ e_{L_f} \end{pmatrix} \quad \text{and} \quad e_{R_f}. \tag{3.1.2}$$

Similarly the quarks are denoted by

$$Q_f = \begin{pmatrix} u_{L_f} \\ d_{L_f} \end{pmatrix}, \quad u_{R_f} \quad \text{and} \quad d_{R_f}. \tag{3.1.3}$$

The gauge field components are commonly denoted by W^a_μ and B_μ, corresponding to the $SU(2)_L$ and the $U_Y(1)$, respectively. This implies we will have in principle four real gauge fields, three corresponding to the infinitesimal generators of $SU_L(2)$ and one for the infinitesimal generator of $U_Y(1)$. We may make use of a slight abuse of notation and denote their field strength tensors by using the same letter, however attaching two indices since they are second-order tensors,

$$W^a_{\mu\nu} = \partial_\mu W^a_\nu - \partial_\nu W^a_\mu + g\varepsilon^{abc} W^b_\mu W^c_\nu \tag{3.1.4}$$

$$B_{\mu\nu} = \partial_\mu B_\nu - \partial_\nu B_\mu \tag{3.1.5}$$

where $a = 1, 2, 3$ and we have chosen the generators of $SU_L(2)$ to be $\sigma_i/2$ with σ_i the Pauli matrices, which leads to the structure constants appearing above, $2\mathrm{i}\varepsilon_{ijk}\sigma_k = [\sigma_i, \sigma_j]$. We can now write down the kinetic term for the gauge fields,

$$\mathcal{L}_{\mathrm{k.G}} = -\frac{1}{4} W^{a\,\mu\nu} W^a_{\mu\nu} - \frac{1}{4} B^{\mu\nu} B_{\mu\nu} \tag{3.1.6}$$

and the kinetic terms of the fermions

$$\mathcal{L}_{\mathrm{k.F}} = \sum_{f=1}^{3} \sum_{X \in \mathscr{F}} \bar{X}_f \mathrm{i} \not{D}_{X_f} X_f, \tag{3.1.7}$$

where $\mathscr{F} = \{Q_f, L_f, e_{R_f}, u_{R_f}, d_{R_f}\}$ are all the matter fields of the model and where the covariant derivative, D, appears already contracted with the Gamma matrices, γ^μ. It is given by the general expression

$$\not{D}_{X_f} = \gamma^\mu D_{\mu_{X_f}} = \gamma^\mu \left[\left(\partial_\mu + \mathrm{i}\frac{g'}{2} Y_{X_f} B_\mu \right) \otimes \mathbb{1}_{\dim R_I(X_f)} + \mathrm{i}g \frac{\sigma_a}{2} W^a_\mu P_L \right] \tag{3.1.8}$$

where the hypercharge, Y, as well as the isospin representation, $R_I(X_f)$, can depend on the family but as it turns out, measurements show they remain the same across families, we have used $\dim R_I(X_f)$ to denote the dimension of the isospin representation and included an identity matrix which is formally present. For that reason we have fixed the representation for the field X_f to be an isospin $1/2$ representation, provided the field is left-handed, as indicated by the projector $P_L = (1 - \gamma^5)/2$ in the last term, meaning all right-handed fields simply do not couple to the W_μ.

So far, we have described the gauge bosons and the fermions of the theory, but then the Electroweak sector would consist only of massless particles if that were the full story, given that no mass terms are allowed that respect the imposed symmetries. In order to give them mass and for unitarity reasons, the model needs a scalar particle that can implement the SSB mechanism. In its minimal version, the Higgs field is an $SU_L(2)$ doublet with hypercharge $1/2$, labeled by H with the following Lagrangian density:

$$\mathcal{L}_{\rm H} = (D_{\mu_H} H)^\dagger D_{\mu_H} H - V_{\rm tree}(H^\dagger H) \equiv (D_\mu H)^\dagger D_\mu H + \mu^2 H^\dagger H - \lambda (H^\dagger H)^2, \tag{3.1.9}$$

where

$$D_{\mu_H} = \left(\partial_\mu + \frac{1}{2} \mathrm{i} g' B_\mu\right) \otimes \mathbb{1}_{\dim R_I(H)} + \mathrm{i} g \frac{\sigma_a}{2} W^a_\mu \quad \text{and} \quad H = \begin{pmatrix} H^+ \\ H^0 \end{pmatrix} \tag{3.1.10}$$

The specific form of the potential is chosen as to respect the gauge symmetries, be renormalizable and to present a $U(1)$ degenerate minima. In order for the fermions of the theory to acquire mass, they must also be coupled to the Higgs field, this is done via Yukawa type interactions,

$$\mathcal{L}_{\rm HF} = \sum_{f,f'} -Y^u_{ff'} \bar{Q}_f \tilde{H} u_{R'_f} - Y^d_{ff'} \bar{Q}_f H d_{R'_f} - Y^e_{ff'} \bar{L}_f H e_{R'_f} + \text{h.c}, \tag{3.1.11}$$

where $\tilde{H} = \mathrm{i}\frac{\sigma_2}{2} H^*$ and the Y's are the coupling matrices which mix the families and are a priori not diagonal. The Yukawa couplings form matrices of dimensions $N_f \times N_f$ that are responsible for introducing flavor mixing, which we wont be discussing further in this document.
For the sake of completeness, we summarize the charges of the different fields in Table 3.1, where the numbers shown specify then the representation, T_W, and the conserved charge in the $T_{W3} = \sigma_3/2$ direction for the $SU_L(2)$ part. Finally, the last line is assigned with $\mathscr{Q}$ the electromagnetic charge operator and the stated convention, which can be obtained after anomaly cancellation, as explained in most QFT and SM books [13, 17, 47].

	Leptons			Quarks				Higgs
	L		R	L		R		-
Field / Generator	ν_{L_f}	e_{L_f}	e_{R_f}	u_{L_f}	d_{L_f}	u_{R_f}	d_{R_f}	H^0
T_W	$\frac{1}{2}$	$\frac{1}{2}$	0	$\frac{1}{2}$	$\frac{1}{2}$	0	0	$\frac{1}{2}$
T_{W3}	$\frac{1}{2}$	$-\frac{1}{2}$	0	$\frac{1}{2}$	$-\frac{1}{2}$	0	0	$-\frac{1}{2}$
$Y_{X_f} = 2(\mathscr{Q} - T_{W3})$	-1	-1	-2	$\frac{1}{3}$	$\frac{1}{3}$	$\frac{4}{3}$	$-\frac{2}{3}$	1

Table 3.1: Assignment of charges for the fermions in the EW sector, where $\mathscr{Q}$ represents the electromagnetic charge.

3.1.1 Spontaneous symmetry breaking (SSB)

Here we summarize the SSB mechanism in relation to the masses of bosons and fermions, which is relevant in the discussion on electroweak effective potential. Let us begin by

observing that the scalar potential depends only on $|H|^2$, which implies that minimizing the scalar potential with respect to it, we can find a value for $|H|^2$, while nothing fixes its phase. Minimizing $V(H^\dagger H)$ in Eq. (3.1.9), we find that the minimum is at

$$|H|^2 = \frac{v^2}{2} \quad \text{with} \quad v \equiv \sqrt{\frac{\mu^2}{\lambda}}., \tag{3.1.12}$$

which is still $U(1)$ symmetric (see Fig. 3.1). Thus v referred to as a vacuum expectation value (VEV) since it coincides with $\langle 0|\mathfrak{Re}H^0|0\rangle$. Experimentally its value is computed via the Fermi coupling constant G_F which is measured by looking at muon decays[13], and is known to be $v = \sqrt{\frac{1}{\sqrt{2}G_F}} \approx 246.22\,\text{GeV}$[49].

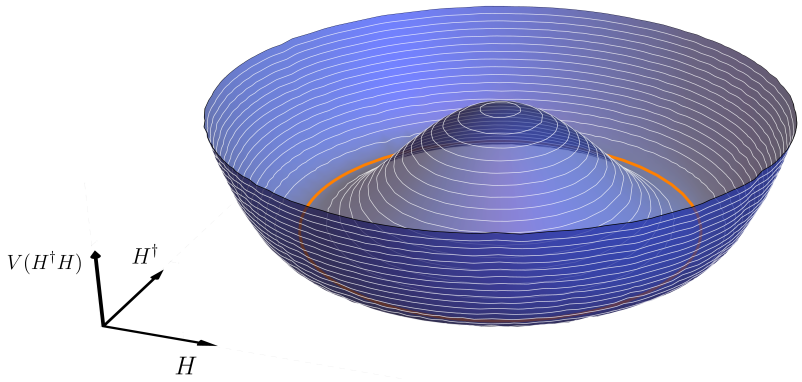

Figure 3.1: Sketch of the potential for the Higgs field, $V(H^\dagger H)$, from Eq. (3.1.9). The orange solid line depicts the Goldstone directions which remain symmetric under translations.

After choosing a phase for the H, we can then find out the mass spectrum of the theory by performing an expansion of the Higgs field around a minimum. That is, we take the above to be the expectation value of the Higgs field in a classical setting and study the fluctuations around it, explicitly

$$H(x) = \frac{1}{\sqrt{2}} \exp\left(\frac{\mathrm{i}}{v}\sum_{j=1}^{3}\chi_j(x)\frac{\sigma_j}{2}\right)\begin{pmatrix}0\\ v+h(x)\end{pmatrix}. \tag{3.1.13}$$

We can see how the mass terms for the gauge bosons is generated already from the constant part of H, that is, from the first term in the right-hand side of the expansion

$$H(x) \approx \frac{v}{\sqrt{2}}\begin{pmatrix}0\\ 1\end{pmatrix} + \frac{1}{\sqrt{2}}\begin{pmatrix}0\\ h(x)\end{pmatrix} + \frac{\mathrm{i}}{\sqrt{2}v}\sum_{j=1}^{3}\chi_j(x)\frac{\sigma_j}{2}\begin{pmatrix}0\\ v+h(x)\end{pmatrix}, \tag{3.1.14}$$

where $h(x)$ is now a real scalar field referred to as Higgs boson. Let us first compute the mass of the Higgs boson to lowest order, by implementing the above expansion in the potential for the Higgs field Eq. (3.1.9):

$$V_{\text{tree}}(H) \approx -\frac{\mu^2}{2}(v+h(x))^2 + \frac{\lambda}{4}(v+h(x))^4 \tag{3.1.15}$$

$$\approx \text{const.} - \frac{\mu^2}{2}h^2 + \frac{3}{2}\lambda v^2 h^2 + \mathcal{O}(h^3) \tag{3.1.16}$$

where we have use that v minimizes the potential and thus we can recognize the mass of the real scalar field h to be

$$m_{\mathrm{H}} = \sqrt{2\lambda}v, \tag{3.1.17}$$

at tree-level. Analogously, we find the mass terms for the gauge fields by means of expanding the Higgs field's kinetic term:

$$|D_{\mu_H} H|^2 = g^2 \frac{v^2}{8} \left\{ (W_\mu^1)^2 + (W_\mu^2)^2 + \left(\frac{g'}{g} B_\mu - W_\mu^3 \right)^2 \right\} + \mathcal{O}(h(x)^2). \tag{3.1.18}$$

The interplay between the weak isospin and the weak hypercharge implies that there is some mixing of components pertaining to B_μ and W_μ^3. Therefore, in order to diagonalize these mass terms fully, we need to perform an additional transformation while keeping the gauge fields canonically normalized. We perform an orthogonal transformation of a pair of real fields, i.e., a rotation into new fields:

$$Z_\mu \equiv \cos\theta_W W_\mu^3 - \sin\theta_W B_\mu \tag{3.1.19}$$

$$A_\mu \equiv \sin\theta_W W_\mu^3 + \cos\theta_W B_\mu. \tag{3.1.20}$$

If $\tan\theta_W = \frac{g'}{g}$, is the weak mixing angle, then one arrives to the following kinetic terms:

$$\mathcal{L}_{\mathrm{EW}} \supseteq -\frac{1}{4}F_{\mu\nu}^2 - \frac{1}{2}Z_{\mu\nu}^2 + \frac{1}{2}\left(\frac{gv}{2\cos\theta_W}\right)^2 Z^\mu Z_\mu + \frac{1}{2}\left(\frac{vg}{2}\right)^2 ((W_\mu^1)^2 + (W_\mu^2)^2) \tag{3.1.21}$$

where $F_{\mu\nu}$ and $Z_{\mu\nu}$ are the field strength tensors of the newly defined fields A_μ and Z_μ. From here although the charged W's and the interactions are not obvious, we can already identify

$$\begin{aligned} m_A &= 0, \\ m_Z &= \frac{gv}{2\cos\theta_W}, \\ m_W &= \frac{vg}{2}, \end{aligned} \tag{3.1.22}$$

these results are obtained from the expansion of the kinetic terms too lowest order in fluctuations of the Higgs field.

Let us now consider what happens with the fermions, it suffices to describe the case of the top quark which is the heaviest of them, with an experimentally observed mass of around $m_t = 173\,\mathrm{GeV}$, and will contribute the most to the effective action as we will later witness. The Yukawa terms are after symmetry breaking in the notation above, $Y_{tt}^u \bar{u}_{L_3} \sigma u_{R_3}/\sqrt{2} + \text{h.c.}$ from which we can recognize

$$m_t = Y_{tt}^u \frac{v}{\sqrt{2}}. \tag{3.1.23}$$

The previous results do not depend on any gauge choice up to this point. However, in order to study the stability of the model, we need to be able to go beyond tree-level and include higher loop-order corrections.

However, this is a good point to mention that by choosing a good gauge, we can usually get rid of the χ_j fields in Eq. (3.1.13). This is the so-called unitary gauge, where the Goldstone field directions disappear, specifically the kinetic mixing between the gauge

field components and the Goldstone bosons is also zero so that the quadratic terms for the gauge bosons are diagonal in the fields. Explicitly let $U(\chi) = \exp(-\mathrm{i}\sum_j \chi_j \sigma_j/(2v))$, we can bring our Lagrangian to the $SU_L(2)$-unitary gauge by transforming the $SU_L(2)$ charged fields as follows:

$$\begin{aligned} H'(x) &= U(\chi)H = \frac{1}{\sqrt{2}}\begin{pmatrix} 0 \\ v + h(x) \end{pmatrix} \\ X'_L(x) &= U(\chi)X_L(x) \quad \text{for} \quad X \in \{Q_f, L_f\} \\ \frac{1}{2}\vec{\sigma}_a \cdot W'^a_\mu(x) &= \frac{1}{2}U(\chi)\sigma_a W^a_\mu(x)U^{-1}(\chi) + \frac{\mathrm{i}}{g}\partial_\mu U(\chi)\cdot U^{-1}(\chi). \end{aligned} \tag{3.1.24}$$

Choosing the above gauge makes the physical degrees of freedom of the fields manifest. In other words, all internal lines in Feynman diagrams correspond to physical particles. Unfortunately, it is not always useful in computations since the gauge boson propagator and, in general, Green's functions are not renormalizable[50]. We take the opportunity to mention a family of gauges, the R_ξ-gauges family, which have the useful property of depending on one parameter, ξ, which can continuously be adjusted to reach different well-known cases, e.g., Feynman, R, Landau gauges. The fixing of the gauge is usually done by adding a term to the Lagrangian density, for a model with a gauge field A_μ coupled with scalars, $\vec{\phi}$, with an $O(N)$ symmetry, one has for example[51]

$$\mathcal{L}_{\text{gf.}} = -\frac{1}{2\xi}(\partial_\mu A^\mu + \vec{\zeta}\cdot\vec{\phi})^2. \tag{3.1.25}$$

where ξ is to be chosen between 0 and ∞ and $\vec{\zeta}$ is also arbitrary. The R_ξ family occurs when $\zeta_n u \propto \delta_{0\nu}/\xi$. This topic will be relevant for our specific toy model in an application reported later. From this form, we can recover the following gauges:

Unitary gauge:	$\xi \longrightarrow \infty$	there are no Goldstone bosons present but calculations are cumbersome.
Feynman Gauge:	$\xi = 1$	Propagators have a simple algebraic form in momentum space.
Landau Gauge:	$\xi \longrightarrow 0$	Has massless Goldstone bosons which are decoupled from physical scalars.

3.2 The effective potential to one-loop order

We will now attempt to study the stability of the SM by considering the effective potential to one-loop order. For the discussion in this section pertaining to the SM, the Landau gauge will be employed. Let us then apply the methods explained in Sec. 1.3. In addition to the one-loop diagrams formed by the scalar acquiring the VEV in the model, we must also deal with gauge bosons, fermions and other possible scalars in the EW sector. By employing the same techniques[22], we determine the effective potentials for the other field types. Let us then recall that the effective potential, $V_{\text{eff}}(\varphi_{\text{cl}})$, gives the energy density of the system on state ψ, $\langle\psi|H|\psi\rangle$, provided $\varphi_{\text{cl}} = \langle\psi|\phi(x)|\psi\rangle$. one can first obtain the one-loop contributions to the potential from a gauge boson in an Abelian theory (see Ref. [46]

for an extended review)

$$V_{\text{gb Abelian}} = \frac{3e^4}{64\pi^2}\,\varphi_{\text{cl}}^4\,\log\left(\frac{\varphi_{\text{cl}}^2}{M_\Lambda^2}\right), \tag{3.2.26}$$

where M_Λ is the renormalization scale for the theory. For non-Abelian gauge groups, where the effective mass of the gauge boson comes from terms of the form

$$\frac{1}{2}\sum_{a,b} M_{ab}^2(\varphi_{\text{cl}})A_\mu^a A^{\mu\,b}, \tag{3.2.27}$$

where a and b run over the infinitesimal generators of the gauge group, we have

$$V_{\text{gb non-Abelian}} = 3\,\frac{1}{64\pi^2}\,\text{tr}\left\{M(\varphi_{\text{cl}})^4\,\log\left(\frac{M(\varphi_{\text{cl}})^2}{M_\Lambda^2}\right)\right\}, \tag{3.2.28}$$

where the gauge couplings are included within the effective mass matrix M_{ab}. In case the theory is extended to have additional scalars, we might then find the following contribution from such fields

$$V_{\text{s non-Abelian}} = \frac{1}{64\pi^2}\,\text{tr}\left\{\mathbf{M}(\varphi_{\text{cl}})^4\,\log\left(\frac{\mathbf{M}(\varphi_{\text{cl}})^2}{M_\Lambda^2}\right)\right\}, \tag{3.2.29}$$

where $\mathbf{M}_{ab}^2(\varphi_{\text{cl}}) = \frac{\mathrm{d}^2 V_{\text{tree}}}{\mathrm{d}\phi_a \mathrm{d}\phi_b}$.
Let us now include the contribution from the fermionic fields. As we saw in the previous section, the Yukawa terms will imply masses after symmetry breaking of the form

$$-\sum_{a,b}\bar{\psi}\,m_{ab}(\varphi_{\text{cl}})\psi_b \tag{3.2.30}$$

where m_{ab} is obtained after switching to the mass basis and is in general complex. Then

$$V_f = -\frac{1}{64\pi^2}\left(\frac{m_f}{v}\,\varphi_{\text{cl}}\right)^4\,\text{tr}\left\{(mm^\dagger)^2\log\left(\frac{mm^\dagger}{M_\Lambda^2}\right)\right\} \tag{3.2.31}$$

We are now in a position to collect all the contributions and write down the one-loop effective potential for the EW sector, where we neglect all fermions other than the top quark,

$$V_{\text{eff}} \approx V_{\text{tree}} + V_{\text{Z,W,A}} + V_{\text{Higgs}} + V_{\text{top}} \tag{3.2.32}$$

where

$$\begin{aligned}
V_{\text{tree}} &= -\frac{1}{2}\mu^2\varphi_{\text{cl}}^2 + \frac{1}{4}\lambda\varphi_{\text{cl}}^4 \\
V_{\text{Z,W,A}} &= \frac{3}{1024\pi^2}(2g^4 + (g^2+g'^2)^2)\varphi_{\text{cl}}^4\log\left(\frac{\varphi_{\text{cl}}^2}{M_\Lambda^2}\right) \\
V_{\text{H,G}} &= \frac{1}{64\pi^2}(\mu^2+3\lambda\varphi_{\text{cl}}^2)^2\log\left(\frac{\mu^2+3\lambda\varphi_{\text{cl}}^2}{M_\Lambda^2}\right) + \frac{3}{64\pi^2}(\mu^2+\lambda\varphi_{\text{cl}}^2)^2\log\left(\frac{\mu^2+\lambda\varphi_{\text{cl}}^2}{M_\Lambda^2}\right) \\
V_{\text{t}} &= -\frac{3}{64\pi^2}Y_{tt}^{u\,2}\,\varphi_{\text{cl}}^4\log\left(\frac{\varphi_{\text{cl}}^2}{M_\Lambda^2}\right).
\end{aligned} \tag{3.2.33}$$

Historically the masses of the top quark and the Higgs boson were not known with good enough precision, so that one was led to consider different possibilities. Let us comment here on one of these possibilities, although not realized in nature, for the sake of studying the behavior of the minima of the effective potential. For such purpose, let us assume that the mass of the Higgs and its self-interaction are small, i.e., μ^2 and λ, so that we can neglect the contributions from the scalars. The potential then takes a simpler form

$$V = V_{\text{tree}} + B\,\varphi_{\text{cl}}^4 \log\left(\frac{\varphi_{\text{cl}}^2}{M_\Lambda^2}\right) \tag{3.2.34}$$

where

$$B = \frac{3}{64\pi^2}\left[\frac{1}{16}(3g^4 + 2g^2 g'^2 + g'^4) - Y_{tt}^{u\,2}\right], \tag{3.2.35}$$

and it can be estimated by using experimental observations of the masses and its relation to the couplings, Eqs. 3.1.22(3.1.23). Let us consider a top Quark which is light and thus fix B to be positive. To witness how the potential itself changes, let us pick the renormalization scale to be $M_\Lambda = v$ and fix the relation between μ, λ and B such that $\varphi_{\text{cl}} = v$ always represents the minimum. Fig. 3.2 shows the effective potential obtained for different values for μ^2, where the condition $\lambda = \mu^2 - 2B$ ensures the location of the critical point lies at σ, for μ^2 in Bv^2 units.

$$V(\varphi_{\text{cl}}) = -\frac{1}{2}\mu^2\varphi_{\text{cl}}^2 + \frac{1}{4}(\mu^2 - 2B)\varphi_{\text{cl}}^4 + B\varphi_{\text{cl}}^4 \log\left(\frac{\varphi_{\text{cl}}^2}{v^2}\right) \tag{3.2.36}$$

The different possible shapes of the potential shown in Fig. 3.2 imply very different scenarios from the point of view of vacuum stability. We can mention that the radiative corrections can create a minimum even in the case of $\mu^2 = 0$. Some of the shown values for μ^2 hint tunneling processes between different local minima. For each of the values shown, one can compute the corresponding Higgs boson mass, $m_H = \frac{d^2V(\phi)}{d\phi^2}|_{\phi=v}$. We could subsequently make statements concerning bounds on the mass of the Higgs by demanding certain features of the potential, as was done in the past. Nowadays, the available measurements of the Higgs' boson mass and the top quark can be used to determine the shape of the effective potential instead.

As we know, the top quark's mass is higher than around 83 GeV which would imply in this approximation where scalar loops have been neglected, that B would be negative. For such a case, this very preliminary examination of the effective potential displays an unstable vacuum. This is precisely the central object of the applications of the present chapter.

For illustration purposes, we show how to obtain the renormalization group improved potential to this same order, which has the advantage of being valid as long as we find ourselves in the perturbative regime of the couplings. Without such improvement, it is not really justified to speak about arbitrarily high field values since the actual condition needed by the effective potential to hold, as is, is that $\alpha \log(\varphi_{\text{cl}}^2/M_\Lambda^2) \ll 1$, where α is the largest of the couplings.

3.2.1 Renormalization group improved potential for EW sector

We employ the techniques of Sec.1.3.3 to the effective one-loop potential for the EW sector. We can split the potential into three pieces

$$V = V_{\text{tree}} + V_{\text{loop}}, \tag{3.2.37}$$

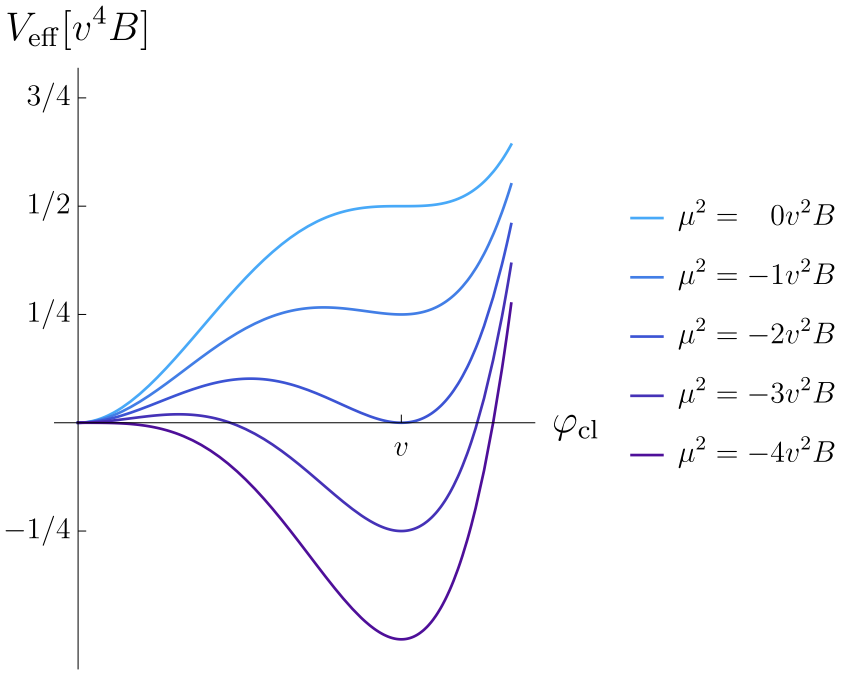

Figure 3.2: Depiction of the one-loop effective potential for different historical scenarios for assuming a light top quark, (see Ref. [46]), for an updated heavy top quark the potential becomes unstable.

where the one loop contributions concerning the running of μ^2 and λ are

$$V_{\text{loop}} = \frac{1}{64\pi^2}\left(B\phi^4 \log\left(\frac{\phi^2}{M^2}\right) + (\mu^2+3\lambda\phi^2)^2 \log\frac{\mu^2+3\lambda\phi^2}{M^2} + 3(\mu^2+\lambda\phi^2)^2 \log\frac{\mu^2+\lambda\phi^2}{M^2}\right) \tag{3.2.38}$$

and the last piece corresponds to the top quark which will ignore in the analysis of the running of μ^2 and λ.
As in the illustration done in the Sec.1.3.3, we can find the beta functions through a bootstrap procedure, where we employ the Callan-Symanzik equation on the effective potential. The information of the one-loop contributions can be used to reconstruct the running of the couplings to build the improved version, that is

$$\left(\beta_\lambda \frac{\partial}{\partial\lambda} + \mu^2\beta_{\mu^2}\frac{\partial}{\partial\mu^2} - \gamma\phi\frac{\partial}{\partial\phi}\right) V_{\text{tree}} = -M\frac{\partial}{\partial M}V_{\text{loop}} \tag{3.2.39}$$

allows us to compare terms proportional in ϕ^2 and ϕ^4 and write down the following expressions for the beta functions[1]

$$\beta_\lambda = 4\lambda\gamma + \frac{1}{8\pi^2}(12\lambda^2 + B), \tag{3.2.40}$$

$$\beta_{\mu^2} = 2\gamma + \frac{3\lambda}{4\pi^2}. \tag{3.2.41}$$

[1]Here we have followed a different definition for the beta functions and anomalous dimension, compared to the one presented in the mathematical background, the beta functions and the anomalous dimensions are related through $\beta = \tilde{\beta}/(1+\tilde{\gamma})$ and $\gamma = \tilde{\gamma}/(1+\tilde{\gamma})$, where $\tilde{}$ represents the quantities we use now. Also a factor of μ^2 has been extracted by convention.

Once we have explicitly computed the beta functions, we must solve the renormalization group equation for a given set of initial conditions to obtain the improved potential

$$V(\varphi) = \frac{1}{2}\mu^2(t)G^2(t)\varphi^2 + \frac{1}{4}\lambda(t)G^4(t)\varphi^4, \qquad \text{for} \quad t = \log(\varphi/M), \tag{3.2.42}$$

where

$$G(t) = \exp\left(-\int_0^t \mathrm{d}t'\gamma(g_i(t'), \lambda(t'))\right). \tag{3.2.43}$$

We need an estimate of the anomalous dimension as well, to be able to write down the RG equations, for that purpose let us consider the two-point function, which to one-loop order implies the following anomalous dimension

$$\gamma = \left(-9g^2 - 3g'^2 + 12Y_{tt}^u\right)/(64\pi^2). \tag{3.2.44}$$

We must also include the running of the Yukawa couplings which to one-loop order have been computed[52] and currently are known to two-loops (see Refs. [53–58] or [59] and more recently to three-loops under certain assumptions[60], while partial results exist for higher loops[61, 62]. For our purposes it will suffice to use

$$\beta_Y = \frac{1}{16\pi^2}\left(\frac{9}{2}g_Y^2 - 8g_s^2 g_Y - \frac{9}{4}g^2 g_Y - \frac{17}{12}g'^2 g_Y\right), \tag{3.2.45}$$

where g_s is the strong sector (QCD) coupling constant. For the gauge couplings we have to one-loop[63]

$$\begin{aligned} \beta_{g_s} &= -\frac{7g_s^3}{16\pi^2}, \\ \beta_g &= -\frac{19g^3}{96\pi^2}, \\ \beta_{g'} &= \frac{41g'^3}{96\pi^2}. \end{aligned} \tag{3.2.46}$$

We can then set the boundary conditions on the gauge couplings, Yukawa couplings and for λ and μ^2. For the gauge couplings we can demand to begin the running at the known values at a typical energy scale. Conventionally this is done at the scale of the Z^0-boson pole mass. The gauge couplings of the EW sector can then be defined through the mass parameters after symmetry breaking, that is in terms of m_Z and m_W which are in turn defined via tree-level relations to: v, θ_W and α_e. The current world averages values, for the fine structure and the strong coupling constants are[49],

$$\alpha(m_Z^2) = \frac{g^2}{4\pi} = \frac{1}{127.952 \pm 0.009} \tag{3.2.47}$$

$$\alpha_s(m_z^2) = \frac{g_s(m_Z^2)^2}{4\pi} = 0.1179 \pm 0.0010 \tag{3.2.48}$$

$$\tag{3.2.49}$$

which together with a starting point for the top Yukawa coupling $Y_{tt}^u(\phi = 4m_t^2) = m_t/175\,\mathrm{GeV}$, and an on shell-scheme as before

$$\left.\frac{\mathrm{d}V}{\mathrm{d}\phi}\right|_{\phi=v} = 0, \tag{3.2.50}$$

$$\left.\frac{\mathrm{d}^2V}{\mathrm{d}\phi^2}\right|_{\phi=v} = m_H^2, \tag{3.2.51}$$

we can run the couplings numerically for given masses of the Higgs boson and the top quark, and thereafter obtain the improved one-loop potential in Eq. (3.2.42). With this we cover the basics of computing effective potentials for the SM and also its possible improved versions.
As we have learned, the effective potential can possess exciting features such as several minima. What is more, this specific feature is the one allowing for scenarios where tunneling phenomena can occur. These, in turn, may have dictated the dynamics of phase transitions in the early days of our Universe. Thus, studying the consequences of the effective potential of the SM in detail comes without question.
Before we move on to our cases of study, we need to relate the effective potential computations with the notion of stability. As was briefly mentioned when we computed a one-loop non-improved effective potential, the coefficient B can become negative enough to imply that the effective potential will not be bounded from below for large field values, instability, which at first glance contradicts our existence.
Ways out of this issue include improving our approximation of the effective potential, that is, increasing the number of loops considered to check whether the instability is still there and this may also be accompanied by the construction of a more precise RG improved potential. In one of the scenarios, the instability remains and we can then require a milder constraint; that of meta-stability, meaning that we can hope that computing the decay rate of the tunneling process from one minimum to the unbounded region gives something smaller than the inverse age of the Universe, $(4.3 \times 10^{17}\,\text{sec})^{-1}$. This idea has been used in the past to put bounds on the masses of certain particles before they were actually experimentally detected[64–66]. Nowadays, after the measurements of the top quark[67, 68] and the Higgs boson[2, 3] masses, we can, on the contrary, estimate the lifetime or equivalently the decay rate of the SM vacuum.
We do not pretend to focus on traditional computations of the effective potential of the SM as described in this section but take the chance to quote the state-of-the-art stability analysis concerning the different stability regions of the SM[5, 69]. Combining the two-loop effective potential, the three-loop beta functions for the relevant couplings and a more detailed determination of matching conditions at the EW scale to two-loops to determine the initial values for the running, it is possible to obtain a full next-to-next-to-leading order computation of the Higgs' boson potential. Fig. 3.3 shows the results of such a study which have become a central motivator for our current research.

3.2.2 Evolution and status of the Field

The mathematical tools and the framework presented in this chapter so far have only opened the doors to deeper and more sophisticated studies concerning the topic of vacuum stability within the SM of particle physics. As already shortly mentioned, the notion of stability has been an interesting and evolving constraint for the masses of the top quark and the Higgs boson[70] before they were accurately measured. More recently, making use of these new measurements, the vacuum stability question has transformed into a question on metastability, and as a consequence, into one about the false vacuum's lifetime[5, 69, 71, 72], given the catastrophic consequences that the occurrence of such a decay could have.
As is usually the case in particle physics, answering questions about the very small leads to clues (and also more questions) about the "very early". The metastability of the SM potential can have consequences that pertain to the very early Universe. Even before the discovery of the Higgs boson, implications to cosmological aspects were already being considered, affecting, for example, inflation [73]. Simultaneously, discussions about the

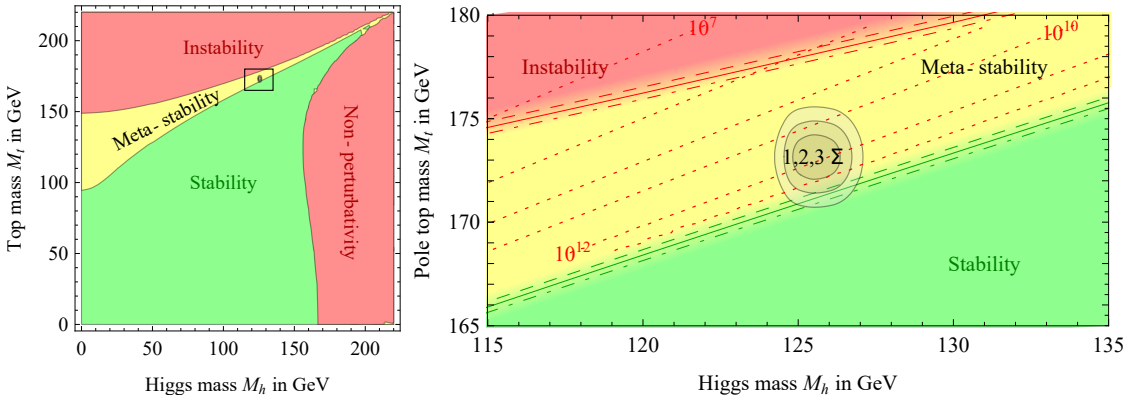

Figure 3.3: (Left) Plot depicting the regions of stability for the NNLO precision scalar potential of the SM in the $m_t - m_H$ plane. (Right) Zoom in around the interesting experimental range for m_H and m_t displaying in gray the best fit regions for $1\sigma, 2\sigma$ and 3σ deviations and where the boundary between regions were obtained using $\alpha_s(m_Z) = 0.1184 \pm 0.0007$. This plot appeared first in [69].

early Universe's phase transitions include suggestions of possible first-order phase transitions that can occur via nucleation of true vacuum bubbles, as has been described in this document. A good review that outlines the current views and aspects possibly interesting to cosmologists related to the Higgs vacuum metastability is Ref. [74]. A very similar set of ideas to what we will consider in the following chapter can also be found in Ref. [75].

The multiple connections to the cosmological evolution make it a "must" to try to understand in detail how higher precision computations modify these quantum tunneling processes. New methodologies are constantly needed to compute the false vacuum decay under different settings, such as different models with varied field content, finite temperatures, at different levels of precision, or even at curved spacetimes.

The initial considerations by Coleman and Callan lead quickly to the realization that bubble nucleation processes can also happen under finite temperature conditions[76], applications to the earlier Universe have since proliferated. One of the most important examples is that of Baryogenesis[77–79], a process in which the matter and anti-matter asymmetry of the Universe is produced. Most models of Baryogenesis require a first-order phase transition[80] which entails the nucleation of vacuum bubbles, increasing, therefore, their relevance, since they may play an essential role in understanding the nature of the EW phase transition.

It is appropriate to mention here the prospects of learning more about the early Universe by means of new observational capabilities such as those presented by the detection of gravitational waves (GWs) with present detectors: GEO600, VIRGO, LIGO, and near-future ones like LISA in outer space. Studies about phase transitions[81–83] feature vacuum bubbles collisions, which are predicted to produce GWs. Hence the detection of specific power spectra from GWs may shed some light on the nature of the EW phase transition.

The examples above constitute compelling reasons to pursue the study of the EW vacuum transitions. Given that most treatments so far focus on including higher-loop corrections or in RG-improving the effective potential to higher orders, we decide to take a different path and consider the impact of the non-homogeneity of the bounce configurations on the decay rate. These gradient effects are generally neglected when computing the CW potential, as we have seen. Therefore an in-detail consideration of the gradients was missing in the literature. The following applications will allow us to have a quantitative

idea of the impact of such effects.
We present first a summary of the work already published by our research group in which the author of this document did not participate. However, the study served as an introduction to the methods and was instrumental to the author's study case, the reason why we have chosen to present them also here. Later, we move to our personal study case, where the methods are extended.

4

Vacuum decay rate including background gradients

Before approaching the more complicated gauge sector, we summarize first how the techniques can is used in a slightly simpler scenario. Thus, we describe the results of [31] in a compressed way as a prelude to our computations. They will also provide a reference point to compare results and observe differences between the two sectors.

4.1 The Higgs-Yukawa sector abridged

Let us begin the discussion by stating exactly the model to be studied. The Euclidean Lagrangian describing the interaction of a Dirac fermion and a real scalar has the form:

$$\mathcal{L} = \bar{\Psi}\gamma_\mu\partial_\mu\Psi + \frac{1}{2}(\partial_\mu\Phi)^2 + \mathcal{L}_{\text{int}} + U(\Phi) \tag{4.1.1}$$

where the scalar potential is given by

$$U(\phi) = -\frac{1}{2}\mu^2\phi^2 + \frac{1}{3!}g\phi^3 + \frac{1}{4!}\lambda\phi^4 + U_0, \tag{4.1.2}$$

with U_0 chosen so that the right minimum is located at 0 potential (see Fig. 4.1) and the interaction is chosen to be of Yukawa type

$$\mathcal{L}_{\text{int}} = \kappa\bar{\Psi}\Phi\Psi. \tag{4.1.3}$$

The scalar potential is build as to present at least two local minima, which will correspond to homogeneous field configuration which we refer to as vacua, true vacuum reserved for the lowest lying one, ϕ_-, and false vacuum to any other local minimum of the potential, in this case denoted ϕ_+ (see Fig. 4.1)

4.1.1 Adapting the decay rate formula for this model

The starting point is, again, the action supplemented with external sources in order to be able to extract correlation functions from the partition function. It takes the form

$$S[\Phi,\Psi,\bar{\Psi}] = \int \mathrm{d}^4x\,\mathcal{L} + \int \mathrm{d}^4x\,J(x)\Phi(x) + \int \mathrm{d}^4x\,\bar{\eta}(x)\Psi(x) + \int \mathrm{d}^4x\,\bar{\Psi}(x)\eta(x) \tag{4.1.4}$$

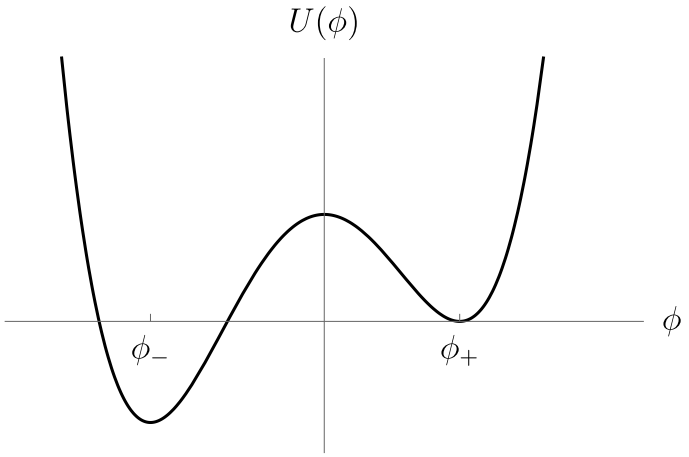

Figure 4.1: Example of a scalar tree level 4th-order polynomial potential displaying the features required for vacuum tunneling to be present.

and we can expand the theory around a background configuration by using the describe semi-classical approximation, $\Phi(x) = \varphi(x) + \hbar^{1/2}\hat{\Phi}(x)$, $\hat{\Psi}(x) = \hat{\psi}(x) + \hbar^{1/2}\hat{\bar{\Psi}}$ and $\Psi(x) = \psi(x) + \hbar^{1/2}\hat{\Psi}(x)$. The action is then up to terms that are quadratic in the fields,

$$S[\Phi,\Psi,\bar{\Psi}] = S[\varphi,0,0] + \hbar^{1/2}\int \mathrm{d}^4x\, J(x)\hat{\Phi}(x) + \hbar^{1/2}\int \mathrm{d}^4x\, \bar{\eta}(x)\hat{\Psi}(x) + \hbar^{1/2}\int \mathrm{d}^4x\, \hat{\bar{\Psi}}(x)\eta(x)$$
$$+ \frac{\hbar}{2}\int \mathrm{d}^4x\ \mathrm{d}^4y\, \hat{\Phi}G^{-1}(\varphi(x);x,y)\hat{\Phi} + \frac{\hbar}{2}\int \mathrm{d}^4x\ \mathrm{d}^4y\, \hat{\bar{\Psi}}D^{-1}(\varphi(x);x,y)\hat{\Psi} \tag{4.1.5}$$

where in general the fields are expanded around configurations that invert the relations with the currents as to cancel linear terms, that is explicitly

$$\varphi(x) = \langle\Omega|\Phi(x)|\Omega\rangle\,\big|_{J,\bar{\eta},\eta} = \hbar\frac{\delta \log Z[J,\bar{\eta},\eta]}{\delta J(x)}, \tag{4.1.6}$$

$$\bar{\psi}(x) = \big\langle\Omega|\bar{\Psi}(x)|\Omega\big\rangle\,\big|_{J,\bar{\eta},\eta} = -\hbar\frac{\delta \log Z[J,\bar{\eta},\eta]}{\delta \eta(x)}, \tag{4.1.7}$$

$$\psi(x) = \langle\Omega|\Psi(x)|\Omega\rangle\,\big|_{J,\bar{\eta},\eta} = \hbar\frac{\delta \log Z[J,\bar{\eta},\eta]}{\delta \bar{\eta}(x)}, \tag{4.1.8}$$

and where

$$G^{-1}(\varphi;x,y) \equiv \frac{\delta^2 S[\Phi,\bar{\Psi},\Psi]}{\delta\Phi(x)\delta\Phi(y)}\bigg|_{\Phi=\varphi,\psi=0,\bar{\psi}=0}$$
$$= \delta^4(x-y)\left[-\Delta_x + U''(\varphi(x))\right] \tag{4.1.9}$$

and

$$D^{-1}(\varphi;x,y) \equiv \frac{\delta^2 S[\Phi,\bar{\Psi},\Psi]}{\delta\Psi(x)\delta\bar{\Psi}}\bigg|_{\Phi=\varphi,\psi=0,\bar{\psi}=0}$$
$$= \delta^4(x-y)\left[\gamma_\mu\partial_\mu + \kappa\varphi(x)\right]. \tag{4.1.10}$$

The associated operators depend on one space-time point only and can be obtained by integration over y. Observe how higher order terms will not contribute at one-loop order as explained when developing the expansion in loops in the mathematical background section. We have also required the tree-level fermion tadpoles to vanish, namely $\psi(x) = 0, \bar{\psi}(x) = 0$. The expansion above is valid for an arbitrary field configuration φ given an appropriate choice for the sources $J, \eta, \bar{\eta}$. Therefore, we proceed to compute the 1-PI effective action evaluated about the configuration φ by including $\hbar$ corrections from the expansion made in Eq. (4.1.5) and building first the path integral, including external sources:

$$Z[J,\eta,\bar{\eta}] = Z_0[J,\eta,\bar{\eta}] \int \mathcal{D}[\hat{\Phi}]\,\mathcal{D}[\hat{\bar{\Psi}}]\,\mathcal{D}[\hat{\Psi}] \exp\Big\{ -\frac{\hbar}{2}\int \mathrm{d}^4x\,\mathrm{d}^4y \hat{\Phi}(x) G^{-1}(\varphi(x);x,y)\hat{\Phi}(y) + \frac{\hbar}{2}\int \mathrm{d}^4\,\mathrm{d}^4y \hat{\bar{\Psi}} D^{-1}(\varphi(x);x,y)\hat{\Psi} + \mathcal{O}(\hbar^{3/2})\Big\}. \tag{4.1.11}$$

performing the Gaussian integrals inside the brackets we arrive to

$$Z[J,\eta,\bar{\eta}] \sim Z_0[J,\eta,\bar{\eta}] \left|\frac{\det G^{-1}(\varphi(x);x,y)}{\det G^{-1}(\varphi_+;x,y)}\right|^{1/2} \left|\frac{\det D^{-1}(\varphi(x);x,y)}{\det D^{-1}(\varphi_+;x,y)}\right|^{-1}. \tag{4.1.12}$$

modulo a normalization constant, set by $Z[\varphi_+,0,0]$. We may now plug in this expression into Eq. (1.2.119) so that up to first order and for vanishing sources, we find the 1-PI effective action,

$$\begin{aligned}\Gamma^{(1)}[\Phi,\Psi,\bar{\Psi}] &= -\hbar\log(Z[J,\eta,\bar{\eta}]) - \int \mathrm{d}^4x\, J(x)\Phi(x) - \int \mathrm{d}^4x\,\bar{\eta}(x)\Psi(x) - \int \mathrm{d}^4x\,\bar{\Psi}(x)\eta(x)\\ &\approx -\hbar\log\left(\exp\left(-\frac{1}{\hbar}S[\varphi,0,0]\right)\right) + \frac{\hbar}{2}\log\left|\frac{\det G^{-1}(\varphi(x);x,y)}{\det G^{-1}(\varphi_+;x,y)}\right|\\ &\quad - \hbar\log\left|\frac{\det D^{-1}(\varphi(x);x,y)}{\det D^{-1}(\varphi_+;x,y)}\right|\\ &= S_0[\varphi,0,0] + \frac{\hbar}{2}\log\left|\frac{\det G^{-1}(\varphi(x);x,y)}{\det G^{-1}(\varphi_+;x,y)}\right| - \hbar\left|\frac{\det D^{-1}(\varphi(x);x,y)}{\det D^{-1}(\varphi_+;x,y)}\right|.\end{aligned} \tag{4.1.13}$$

Adding the quantum corrections

In this subsections we are interested in taking φ to be the quantum corrected bounce configuration, meaning it will consist of two terms, the classical bounce $\varphi^{(0)}$ and its quantum corrections $\delta\varphi$, such that $\varphi^{(1)} \equiv \varphi = \varphi^{(0)} + \delta\varphi$. In order to include such corrections the 1-PI effective action must be evaluated self-consistently at the quantum corrected bounce. Before computing every contribution in detail, let us set up the remaining quantities we are after. Let us then consider expanding Eq. (4.1.6), by decomposing the field configuration into a classical piece and its quantum corrections. We obtain therefore

$$\begin{aligned}\delta\varphi = &-\int \mathrm{d}^4y\, G(\varphi^{(0)};x,y)\Pi_S(\varphi^{(0)};y)\varphi^{(0)}\\ &-\int \mathrm{d}^4y\, G(\varphi^{(0)};x,y)\Pi_D(\varphi^{(0)};y)\varphi^{(0)}\end{aligned} \tag{4.1.14}$$

with the tadpole functions Π_X being defined as

$$\Pi_X(\varphi^{(0)};x)\varphi^{(0)}(x) \equiv \left.\frac{\delta B_X^{(1)}[\varphi]}{\delta\varphi(x)}\right|_{\varphi^{(0)}} \tag{4.1.15}$$

where X denotes either of the fields in the model and where $B_X^{(1)}$ is proportional to the positive-definite part of the one-loop contributions, specifically in this case we have

$$\begin{aligned}\hbar B_S^{(1)} &\equiv \hbar B_S^{(1)}[\varphi^{(0)}] = \hbar g_S \log \frac{\det' G^{-1}(\varphi^{(0)})}{\det' G^{-1}(\varphi_+)} \\ \hbar B_D^{(1)} &\equiv \hbar B_D^{(1)}[\varphi^{(0)}] = \hbar g_D \log \frac{\det D^{-1}(\varphi^{(0)})}{\det D^{-1}(\varphi_+)}\end{aligned} \tag{4.1.16}$$

where $g_S = 1/2$ and $g_D = -1$, where the prime denotes that the negative and zero modes have been extracted about which we expand later. From a 1PI effective action evaluated at a quantum corrected classical configuration we can obtain an approximation to its quantum equation of motion (in the sense of powers of $\hbar$) giving

$$-\Delta_4 \varphi(x) + U'(\varphi(x)) + \hbar \sum_{X\in\{S,D\}} \Pi_X(\varphi^{(0)}; x)\varphi^{(0)}(x) = 0 \tag{4.1.17}$$

where Δ_4 is the four-dimensional Laplacian and where the tadpole functions are evaluated at the bounce configuration. Using the solution to this equation we can estimate the 1PI effective action at the corrected configuration by considering the deviations from the saddle-point. Explicitly, we have some contributions of order $\hbar^2$, on the one hand one coming from the classical action S at φ as well as some coming from the variations of the $B^{(1)}$ terms with respect to φ, since we are considering tadpole functions always on the bounce configuration. The classical action is then

$$S[\varphi] = S[\varphi^{(0)}] + \hbar^2 \delta S + \mathcal{O}(\hbar^3) \tag{4.1.18}$$

where

$$\delta S = -\frac{1}{2}\int \mathrm{d}^4x\, \delta\varphi(x)\Pi(\varphi^{(0)}; x)\varphi^{(0)}(x), \tag{4.1.19}$$

with Π the total tadpole function. This is what the result that was already mentioned briefly in Sec.2.2. Similarly the variation of the $B_X^{(1)}$ terms gives

$$\delta B_S^{(1)} = \frac{1}{2}\int \mathrm{d}^4x \delta\varphi(x) \frac{\delta}{\delta\varphi(x)} \log\det' G^{-1}(\varphi)\Big|_{\varphi^{(0)}} \tag{4.1.20}$$

$$\delta B_D^{(1)} = -\int \mathrm{d}^4x \delta\varphi(x) \frac{\delta}{\delta\varphi(x)} \log\det D^{-1}(\varphi)\Big|_{\varphi^{(0)}} \tag{4.1.21}$$

So for this model the corrections of order $\hbar^2$ add up to

$$B^{(2)} = \delta S + \delta B_S^{(1)} + \delta B_D^{(1)} = -\delta S, \tag{4.1.22}$$

which can be interpreted diagrammatically if we recall that all possible corrections of order $\hbar^2$ are considered within a 2-PI effective action. Explicitly the variations of the one-loop contributions correspond to dumbbell diagrams which is easily seen if we plug Eq. (4.1.14) in Eq. (4.1.19). It can be argued that such a subset of diagrams can be the leading one when the number of degrees of freedom that can run in the loops is large, as might be the case in a model with several spectators fields.

With this, we make contact with the formula advertised earlier, Eq. (2.2.44) for the decay rate. We will now find the prefactor exactly, for which we will have to dive into the computation of the bounce and the functional determinants.

4.1.2 The classical bounce solution

We need to additionally expand around the saddle-point field configuration that interpolates between the two vacua in the scalar potential, i.e., a bounce solution, $\varphi(x)$, which is an inhomogeneous background satisfying the classical equation of motion, Eq. (2.2.24), as in section 2.2. For that purpose, let us now determine the classical contribution to the action coming from the tree-level part. For this particular application, the thin-wall approximation will be used, meaning we take the vacua to be close to degenerate ($g \to 0$) and neglect, as a consequence, the friction term (first-order derivative term). In such case, the bounce configuration is known in closed form (near the wall):

$$\varphi^{(0)}(r) \equiv \begin{cases} -v & r \ll R \\ v \tanh\left(\frac{\mu}{\sqrt{2}}(r-R)\right) \equiv vu & r \approx R \\ v & r \gg R \end{cases}, \tag{4.1.23}$$

where R is interpreted as the radius of the bubble or the location of the wall and $\pm v = \pm\sqrt{6\mu^2/\lambda}$ are the values of the field at the minima in the degenerate case. The following computations will be easier to implement in terms of a new compactified coordinate $u \in (-1, 1)$. However before proceeding, let us determine R as well as the value of the classical action. The wall will be located such that the classical action

$$B \equiv S[\varphi^{(0)}, 0, 0] = \int \mathrm{d}^4x \left[\frac{1}{2}\left(\frac{\mathrm{d}\varphi^{(0)}}{\mathrm{d}r}\right)^2 + U(\varphi^{(0)})\right] \tag{4.1.24}$$

is minimized[1]. To do that we compute B by separating the contributions for $r \ll R$, $r \sim R$ and $r \gg R$, while separating the potential into $U(\phi) = U_{\mathrm{tw}}(\phi) + \frac{g}{3!}\phi^3$. Eq. (4.1.24) then becomes

$$\begin{aligned} B = 2\pi^2 \Bigg\{ & \int_{\ll R} r^3 \,\mathrm{d}r \left[\frac{1}{2}\left(\frac{\mathrm{d}\varphi^{(0)}}{\mathrm{d}r}\right)^2 + U(\varphi^{(0)})\right] \\ & \int_{\approx R} r^3 \,\mathrm{d}r \left[\frac{1}{2}\left(\frac{\mathrm{d}\varphi^{(0)}}{\mathrm{d}r}\right)^2 + U_{\mathrm{tw}}(\varphi^{(0)})\right] \\ & \int_{\gg R} r^3 \,\mathrm{d}r \left[\frac{1}{2}\left(\frac{\mathrm{d}\varphi^{(0)}}{\mathrm{d}r}\right)^2 + U(\varphi^{(0)})\right] \Bigg\}. \end{aligned} \tag{4.1.25}$$

For the first and third line the bounce configuration is already sitting at the minima, therefore its kinetic term does not contribute, so we need just evaluate the potential term at the minima, which leaves the symmetry breaking term $\pm\frac{g}{3!}v^3$ and the constant U_0 so that the region $r \gg R$ completely vanishes. For the middle line we approximate the integral by using a linearized substitute integral

$$\int_{\approx R} r^3 \,\mathrm{d}r \left[\frac{1}{2}\left(\frac{\mathrm{d}\varphi^{(0)}}{\mathrm{d}r}\right)^2 + U(\varphi^{(0)})\right] \sim R^3 \int_{-\infty}^{\infty} \mathrm{d}r \,\frac{1}{2}\left(\frac{\mathrm{d}\varphi^{(0)}}{\mathrm{d}r}\right)^2 + U(\varphi^{(0)}) \tag{4.1.26}$$

For the bounce configuration, φ, we can use the fact that it satisfies the equation of motion, so that by integrating over φ, namely

$$\begin{aligned}
\frac{\mathrm{d}^2\varphi}{\mathrm{d}x^2} &= U'(\varphi) \\
\int \mathrm{d}\varphi \frac{\mathrm{d}^2\varphi}{\mathrm{d}x^2} &= \int \mathrm{d}\varphi\, U'(\varphi) \\
\int \mathrm{d}x \frac{\mathrm{d}\varphi}{\mathrm{d}x}\frac{\mathrm{d}^2\varphi}{\mathrm{d}x^2} &= U(\varphi) \\
\int \mathrm{d}x \frac{1}{2}\frac{\mathrm{d}}{\mathrm{d}x}\left(\frac{\mathrm{d}\varphi}{\mathrm{d}x}\frac{\mathrm{d}\varphi}{\mathrm{d}x}\right) &= U(\varphi) \\
\left(\frac{\mathrm{d}\varphi}{\mathrm{d}x}\right)^2 &= 2U(\varphi).
\end{aligned} \tag{4.1.27}$$

Using this result we can easily compute the integral for the wall region and obtain

$$\int_{\approx R} r^3\,\mathrm{d}r \left[\frac{1}{2}\left(\frac{\mathrm{d}\varphi^{(0)}}{\mathrm{d}r}\right)^2 + U_{\mathrm{tw}}(\varphi^{(0)})\right] \approx R^3 \int_{-\infty}^{\infty} 2U(\varphi^{(0)}) = 4\sqrt{2}\frac{\mu^3 R^3}{\lambda} \tag{4.1.28}$$

Let us now compute explicitly the first line of Eq. (4.1.25), for the region far inside the bubble, the kinetic term vanishes as mentioned and we are left with

$$\int_{\ll R} r^3\,\mathrm{d}r \left[\frac{1}{2}\left(\frac{\mathrm{d}\varphi^{(0)}}{\mathrm{d}r}\right)^2 + U(\varphi^{(0)})\right] = \int_{\ll R} r^3\,\mathrm{d}r\, U(\phi_-) = -2\frac{\sqrt{6}}{4}R^4\frac{g\mu^3}{\lambda^{3/2}}. \tag{4.1.29}$$

With the two results above we can minimize B with respect to R. Taking the corresponding derivative, we get the equation

$$12\sqrt{2}\frac{\mu^3 R^2}{\lambda} - 2\sqrt{6}R^3\frac{g\mu^3}{\lambda^{3/2}} = 0 \tag{4.1.30}$$

$$2\sqrt{6}R\frac{g}{\lambda^{3/2}} = 12\frac{\sqrt{2}}{\lambda} \tag{4.1.31}$$

with which we determine the size of the bubble to be

$$R = 2\frac{\sqrt{3\lambda}}{g}, \tag{4.1.32}$$

and the contribution to the action from the tree-level part, coming from the true vacuum region (pressure) and the surface tension (the wall region), to be

$$B = 48\pi^2\sqrt{6\lambda}\frac{\mu^3}{g^3}. \tag{4.1.33}$$

4.1.3 Zero and Negative modes extraction

For the present case, the operator of fluctuations, $G^{(-1)}(\varphi(x); x, y)$, has to be treated with care, as we know it might present zero-modes corresponding to the symmetries of the model. For the Higgs-Yukawa sector, we still have an $O(4)$ symmetry, meaning we expect four zero-modes from derivatives of the bounce configuration with respect to each possible

direction, i.e., $\partial_\mu\varphi$, as we saw in Sec. 2.2. The results from such section are unaffected by the presence of a fermion and can be repeated verbatim, leading to a prefactor of

$$VT\left(\frac{B}{2\pi\hbar}\right)^2, \tag{4.1.34}$$

after trading zero-mode directions for collective coordinates and where VT is formally an infinite factor representing the full spacetime volume.
Given the tunneling nature of this process, we can also extract a mode proportional to $\partial_r\varphi$, to which corresponds a negative eigenvalue,

$$\lambda_0 = \frac{1}{B}\frac{\partial^2 B}{\partial R^2} = -\frac{3}{R^2}. \tag{4.1.35}$$

This mode is associated to dilatations of the critical bubble and following [1, 37] its contribution to the decay rate formula can be extracted by a careful analytic continuation and gives a factor of $-\mathrm{i}|\lambda_0|^{-1/2}/2$, with this knowledge we can write the functional determinant having extracted the discrete part of its spectrum as

$$\left[\det G^{-1}(\varphi^{(0)})\right]^{-1/2} = -\frac{\mathrm{i}}{2}\frac{1}{\sqrt{|\lambda_0|}}VT\left(\frac{B}{2\pi\hbar}\right)^2\left[\det{}' G^{-1}(\varphi^{(0)})\right]^{-1/2}, \tag{4.1.36}$$

where the $'$ indicates the functional determinant is to be computed for the positive-definite part of the spectrum as wave seen in a couple of examples in PartI. Analogously we must extract from the determinant over the false vacuum, four zero-modes to obtain the well defined ratio of functional determinants[84], hence

$$\left[\det G^{-1}(\varphi_+)\right]^{-1/2} = \frac{1}{(\sqrt{2}\mu)^5}\left[\det{}' G^{-1}(\varphi_+)\right]^{-1/2}. \tag{4.1.37}$$

This is a good point to collect all our definitions for the different contributions and results so far in the formula for the false vacuum decay rate,

$$\frac{\gamma}{V} = \left(\frac{B}{2\pi\hbar}\right)^2\frac{(\sqrt{2}\mu)^5}{\sqrt{|\lambda_0|}}\exp\left[-\frac{1}{\hbar}\left(B + \hbar\sum_{X\in\{S,D\}} B_X^{(1)} + \hbar^2 B^{(2)}\right)\right], \tag{4.1.38}$$

where it can be seen that the extraction of zero and negative modes settles the proportionality factor.

4.1.4 Summary of the computation of the quantities in the decay rate

As described in Sec. 2.2.2, the key idea of the Green's function method is to find all contributions: $B_X^{(1)}$ and $B^{(2)}$ by using the dressed propagators that is, the two-point functions obtained from the 1-PI effective action when expanded around a saddle-point configuration or incidentally the Green's functions of the fluctuations operators.
The first task is then to express the functional determinants in terms of coincident Green's functions, which we have already done for a general case. In order to make progress analytically, we will employ the planar-wall approximation, in which we rewrite the Green's function equation after having applied a Fourier transform to the directions parallel to the bubble wall while considering the remaining direction as flat and containing the radial dependence of the bounce. The derivatives are exchanged by a momentum parameter on which the Green's function will depend:

$$(-\partial_z^2 + \mathbf{k}^2 + U''(\varphi^{(0)}; z))G(\varphi^{(0)}; z, z', \mathbf{k}) = \delta(z - z') \tag{4.1.39}$$

where we have implicitly taken $r \to z$ and we have set the wall at $z = 0$. We can then recover the full Green's function by simply inverting the Fourier transform, i.e.

$$G(z, z') = \int \frac{\mathrm{d}^3\mathbf{k}}{(2\pi)^3} G(\varphi^{(0)}; z, z', \mathbf{k}). \tag{4.1.40}$$

These Green's functions for each field constitute the building blocks for all contributions. As it turns out, obtaining the Green's functions for the deformation of the planar Green's functions (see Eq. (2.2.49)) is very simple if we already have the Green's functions available. With $\mathcal{M}$ representing the Green's function for either the scalar or the Dirac field,

$$\mathcal{M}_{X;\mathbf{k}_s}(\varphi; z, z') \equiv \mathcal{M}_{X;\sqrt{\mathbf{k}^2+s}}(\varphi; z, z') = \mathcal{M}_{X;\mathbf{k}}(\varphi; z, z')\big|_{\mathbf{k}^2 \to \mathbf{k}^2+s}\,. \tag{4.1.41}$$

Applying Eq. (2.2.49) for our planar-wall case means explicitly

$$\begin{aligned}\log \frac{\det \mathcal{M}_X^{-1}(\varphi)}{\det \mathcal{M}_X^{-1}(0)} &= \mathrm{tr} \int \frac{\mathrm{d}^3\mathbf{k}}{(2\pi)^3} \log \frac{\det \mathcal{M}_{X;\mathbf{k}}^{-1}(\varphi)}{\det \mathcal{M}_{X;\mathbf{k}}^{-1}(0)} \\ &= -V \int_{-\infty}^{\infty} \mathrm{d}z \int_0^{\infty} \mathrm{d}s \int \frac{\mathrm{d}^3\mathbf{k}}{(2\pi)^3}\, \mathrm{tr}_{\mathrm{dis}} \left(\mathcal{M}_{X;\sqrt{\mathbf{k}^2+s}}(\varphi; z, z) - \mathcal{M}_{X;\sqrt{\mathbf{k}^2+s}}(0; z, z) \right).\end{aligned} \tag{4.1.42}$$

In the practice this can be carried out for the scalar without a problem, however for the Dirac field, the fluctuation operator is not a differential operator of order two as in Eq. (4.1.39), and some manipulations are required. Given that the Dirac equation can be squared into a Klein-Gordon type equation, we can rewrite the logarithm of the functional determinant as

$$\begin{aligned}\log \det(\gamma_\mu \partial_\mu + m_D(z)) &= \frac{1}{2} \log \det \left[(-\Delta_4 + m_D^2(z)) \mathbb{1}_{4\times 4} + \gamma_4 (\partial_z m_D(z)) \right] \\ &= \log \det \left[-\Delta_4 + m_D^2(z) - \partial_z m_D(z) \right] \\ &\qquad + \log \det \left[-\Delta_4 + m_D^2(z) + \partial_z m_D(z) \right] \\ &\equiv \log \det \left[G_{D_-}^{-1}(\varphi^{(0)}) \right] + \log \det \left[G_{D_+}^{-1}(\varphi^{(0)}) \right]\end{aligned} \tag{4.1.43}$$

where the last term of the right-hand side of the first line appears because of the mass term's non-homogeneity on the bounce background and where the Euclidean version of the Chiral basis for the γ matrices has been used.
Using the definitions in Eq. (4.1.43) above, we have that

$$B_D^{(1)} = B_{D_+}^{(1)} + B_{D_-}^{(1)} \tag{4.1.44}$$

with an analogous definition as in Eq. (4.1.16), for this Klein-Gordon type auxiliary operators:

$$\hbar B_{D_\pm}^{(1)} \equiv -\hbar \log \frac{\det G_{D_\pm}^{-1}(\varphi^{(0)})}{\det G_{D_\pm}^{-1}(\varphi_+)} \tag{4.1.45}$$

and the problem has been reduced to dealing with only scalar type fluctuation operators. So far we can write the functional determinants in terms of the Green's functions, let us now see that the tadpole contributions can also be written in terms of the Green's

functions by performing the functional derivatives appearing in their definition:

$$\Pi_S(\varphi^{(0)};x)\varphi^{(0)}(x) = \left.\frac{\delta B_S^{(1)}[\varphi]}{\delta\varphi}\right|_{\varphi^{(0)}} = \frac{\lambda}{2}G(\varphi^{(0)};x,x)\varphi^{(0)} \tag{4.1.46}$$

$$\Pi_D(\varphi^{(0)};x)\varphi^{(0)}(x) = \left.\frac{\delta B_{D_+}^{(1)}[\varphi]}{\delta\varphi}\right|_{\varphi^{(0)}} + \left.\frac{\delta B_{D_-}^{(1)}[\varphi]}{\delta\varphi}\right|_{\varphi^{(0)}} \tag{4.1.47}$$

where

$$\left.\frac{\delta B_{D_\pm}^{(1)}[\varphi]}{\delta\varphi}\right|_{\varphi^{(0)}} = -2\kappa^2 G_{D_\pm}(\varphi^{(0)};x)\varphi^{(0)} \pm \kappa\partial_z G_{D_\pm}(\varphi^{(0)};x). \tag{4.1.48}$$

These together with Eq.(4.1.14), allow us to compute all desired contributions: B, $B^{(1)}$ and $B^{(2)}$. However we cannot just obtain the decay rate yet, as it happens that some of these quantities are a priori divergent. As we saw in the mathematical background, in dealing with loop contributions we must go through the process of renormalization.

4.1.5 The CW potential and Renormalization

This model's Lagrangian needs to be supplemented with certain counterterms in order to render one-loop contributions finite. This we do by considering counterterms as explained in Sec.1.3.2, for this model we will add

$$\mathcal{L}_{\text{ct}} = \frac{1}{2}\delta Z(\partial_\mu\varphi)^2 + \frac{1}{2}\delta\mu^2\varphi^2 + \frac{1}{4!}\delta\lambda\varphi^4 \tag{4.1.49}$$

and we will use the homogeneous contributions, also referred to as CW-potential, to specify the counterterms. Using the CW potential from Sec.1.3 for this model leads to

$$\begin{aligned} U_{\text{CW}} =& U(\varphi) + \left\{\left[\frac{\Lambda^2}{16\pi^2}\left(-\mu^2+\frac{\lambda}{2}\varphi^2\right) + \frac{1}{64\pi^2}\left(-\mu^2+\frac{\lambda}{2}\varphi^2\right)^2\left(\log\frac{-\mu^2+\frac{\lambda}{2}\varphi^2}{4\Lambda^2}+\frac{1}{2}\right)\right.\right. \\ &\left.\left. -\Lambda^2\frac{\kappa^2\varphi^2}{4\pi^2} - \frac{\kappa^4\varphi^4}{16\pi^2}\left(\log\frac{\kappa^2\varphi^2}{4\Lambda^2}+\frac{1}{2}\right)\right] - (\varphi\to v)\right\} \end{aligned} \tag{4.1.50}$$

as can be obtained by performing first a Fourier transform over all directions while ignoring the spacetime point dependence of the background and then computing the log det terms through tr log and performing $O(4)$ symmetric integrals up to some cutoff Λ. We must also include the counterterms for the terms that are evaluated at v, thus obtaining the renormalized CW potential:

$$U_{\text{CW}}^{\text{ren}} = U_{\text{CW}} + \frac{1}{2}\delta\mu^2(\varphi^2-v^2) + \frac{1}{4!}\delta\lambda(\varphi^4-v^4). \tag{4.1.51}$$

We may now impose renormalization conditions, we take

$$\left.\frac{\partial^2 U_{\text{CW}}^{\text{ren}}(\varphi)}{\partial\varphi^2}\right|_{\varphi=v} = -\mu^2 + \frac{\lambda}{2}v^2 = 2\mu^2 \tag{4.1.52}$$

$$\left.\frac{\partial^4 U_{\text{CW}}^{\text{ren}}(\varphi)}{\partial\varphi^4}\right|_{\varphi=v} = \lambda \tag{4.1.53}$$

which force the renormalized vertices to coincide with the tree-level parameters. We must now find the divergent terms proportional to gradients which may come out of the exact one-loop terms. We use a WKB expansion as shown in Sec. 1.3.2 to find the gradient dependent pieces for the scalar and the fermion in this model. Repeating the aforementioned steps word by word for the Klein-Gordon type operators G and $G_{D_\pm}$ we get the following two results:

$$B_S^{(1)} \supset \int_{-\infty}^{\infty} \mathrm{d}z \int \mathrm{d}^3x \, \frac{1}{384\pi^2} \frac{\lambda^2\varphi^2\varphi'^2}{-\mu^2 + \frac{\lambda}{2}\varphi^2} \tag{4.1.54}$$

and

$$B_D^{(1)} \supset \int_{-\infty}^{\infty} \mathrm{d}z \int \mathrm{d}^3x \, \frac{\kappa^2\varphi^2}{16\pi^2} \left(-\log\frac{\kappa^2\varphi^2}{\Lambda^2} + 2\log 2 - \frac{8}{3} \right). \tag{4.1.55}$$

The third renormalization condition we take as

$$\frac{\partial^2}{\partial(\partial_\mu\varphi)^2} \left[\mathcal{L} + U_{\mathrm{CW}} + \mathcal{L}_{\mathrm{ct}} \right] \Big|_{\varphi=v} = 1 \tag{4.1.56}$$

Imposing the renormalization conditions in Eqs. (4.1.52),(4.1.53) and (4.1.56), we arrive to the following explicit expressions for the counterterms for this model model

$$\delta Z = -\frac{\kappa^2\varphi^2}{16\pi^2} \left(-\log\frac{\kappa^2\varphi^2}{\Lambda^2} + 2\log 2 - \frac{8}{3} \right) - \frac{\lambda}{64\pi^2} \tag{4.1.57}$$

$$\delta\mu^2 = -\frac{\lambda\mu^2}{32\pi^2} \left(\frac{2\Lambda^2}{\mu^2} - \log\frac{\mu^2}{2\Lambda^2} - 31 \right) + \frac{\Lambda^2\kappa^2}{2\pi^2} \left(1 - \frac{27\kappa^2\mu^2}{\lambda\Lambda^2} \right) \tag{4.1.58}$$

$$\delta\lambda = -\frac{3\lambda^2}{32\pi^2} \left(5 + \log\frac{\mu^2}{2\Lambda^2} \right) + \frac{3\kappa^4}{2\pi^2} \left(\frac{14}{3} + \log\frac{3\kappa^2\mu^2}{2\lambda\Lambda^2} \right). \tag{4.1.59}$$

The renormalized tadpole contribution can be thereafter written as

$$\Pi^{\mathrm{ren}}\varphi^{(0)}(\varphi;x) = \sum_{X\in S,D} \Pi_X(\varphi;x)\varphi^{(0)} + \delta\mu^2\varphi^{(0)} + \frac{\delta\lambda}{3!}{\varphi^{(0)}}^3 - \delta Z\partial_z^2\varphi^{(0)} \tag{4.1.60}$$

with which we can find the renormalized quantum corrections to the bounce, by plugging this in the corrected equation of motion in place of the bare tadpole term. The contributions from the counterterms to the action we will collect and denote by

$$\delta B^{(1)} = \int \mathrm{d}^4x \left[\frac{1}{2}\delta\mu^2({\varphi^{(0)}}^2 - v^2) + \frac{1}{4!}\delta\lambda({\varphi^{(0)}}^4 - v^4) + \frac{1}{2}\delta Z(\partial_z\varphi^{(0)})^2 \right] \tag{4.1.61}$$

The publication [31] contains more details of the above procedure and concludes by performing the explicit numerical computations for the above model however taking N_Ψ copies of the fermionic field and N_χ massless scalar spectator fields, that is scalars with no tree-level mass and an interaction term $\Phi^2\chi_i^2$, explicitly

$$\mathcal{L}_{\mathrm{b.mark}} = \frac{1}{2}(\partial_\mu\Phi)^2 + U(\Phi) + \sum_{i=1}^{N_\Psi} \left[\bar\Psi_i\gamma_\mu\partial_\mu\Psi_i + \kappa\bar\Psi_i\Phi\Psi_i \right] + \sum_{i=1}^{N_\chi} \left[\frac{1}{2}(\partial_\mu\chi_i)^2 + \frac{\alpha}{4}\Phi^2\chi_i^2 \right] \tag{4.1.62}$$

For the following set of parameters:

$$\mu = 1, \lambda = 2, \kappa = 0.5, \alpha = 0.5 \quad \text{and} \quad N_\Psi = N_\chi = 10, \tag{4.1.63}$$

the classical action per bubble surface area yields

$$\bar{B} = \frac{B}{2\pi^2 R^3} = 2.828 \tag{4.1.64}$$

and the results they obtained for the other contributions are summarized in the Table 4.1, where all quantities are expressed by unit of bubble surface are and are thus denoted with a $^-$ on top.

	Homogeneous Contr.	Contr. with Gradients	Absolute error
$\bar{B}_S^{(1)}$	-0.583	-0.585	0.34%
$\bar{B}_{\text{spec}}^{(1)}$	-0.320	-0.324	1.25%
$\bar{B}_D^{(1)}$	1.278	1.345	5.24%
$\bar{B}^{(1)}$	0.375	0.436	16.3%
$\bar{B}^{(2)}$	5.08×10^{-4}	-5.72×10^{-3}	

Table 4.1: The table above displays the different quantities appearing in the exponent of the decay rate formula Eq. (4.1.38) after the renormalization procedure has taken place. The first column shows the results of the homogeneous contributions, the second shows the contributions including gradient effects and the last column the percent absolute error that is made relative to the homogeneous result.

Before moving on to the discussion about the gauge sector, let us make some observations on the results above. Generically, scalar fields give a negative contribution, which means they enhance the decay rate and encourage the vacuum to decay. In contrast, the fermionic one-loop contributions are always positive, which means they suppress the decay and cause the false vacuum to be longer-lived. These statements seem to be independent of whether gradients are considered or not. Additionally, as seen from the factors in front of the one-loop contributions in the 1PI-effective action, a Dirac type field amounts to roughly four times a scalar contribution. This factor is kept even when we have spectators in the model, as can be seen in Table 4.1. Collecting all the gradient contributions leads to corrections to the one-loop effects of up to an order of magnitude or 10%, the fermions accounting for the most significant part. The $B^{(2)}$ dumbbell diagrams contribution, which is formally of order $\hbar^2$, are confirmed to be at least two orders of magnitude smaller when gradients are included.

4.2 The $U(1)$-gauge sector case

In recent years the Green's function self-consistent prescription has been applied to different models, such isolated scalars[30], scale-invariant potentials[85] and the case illustrated above of a scalar sector coupled to a fermionic sector via a Yukawa coupling[36]. We take on the job of applying said methods to the so-far untreated gauge sector.
Many questions arise concerning this case. The first question is, of course, how large can the gradient effects be when a gauge boson is included in the one-loop effective potential.

Second, we would like to be able to systematically be able to estimate the size of such effects without the need to run the whole machinery. This is something we will attempt towards the end of the chapter. The third question, which remains unanswered, is that of the gauge dependence of the results provided by this methodology. Extracting physical information from the effective action cannot depend on the choice of gauge chosen to perform the computation. Several studies [86–92] have attempted to track the influence of the gauge-choice or have stated that observables obtained by using extreme points of the effective action remain gauge-invariant. However, there was no explicit computation of such a case taking into account gradient effects. Although the question of gauge dependence was a driver of our study, we currently only have applied the method to a benchmark point at a fixed gauge and cannot make observations in that regard. Nonetheless, the tools are set for future studies where different gauge parameters may be treated.
Following the program of introducing gradient corrections in the computation of the vacuum tunneling rate, with the long-term objective of addressing the SM, and given the importance of the W and Z gauge bosons in the context of the electroweak vacuum metastability, we address now a gauge sector. With the short term objective of employing the green's function methodology and the self-consistency prescriptions[30, 31, 85], in the simplest gauge theory, we fix the gauge group to be $U(1)$. We expect the current methodology to be applied to more realistic phenomenology considering the group $SU(2)$, or at best the SM itself in the future.
As an explicit and novel application of these methods, we study this sector using a model involving a complex scalar field coupled together to a $U(1)$ gauge boson. A scenario displaying a first-order phase transition requires that the scalar potential, to which the complex scalar field will be subjected, presents at least two different local minima separated by a potential barrier. This must happen to some order, but not necessarily tree-level. We build up such potential and compute the different contributions to the exponent in the decay rate coming from one-loop contributions as well as gradients of the background. We do such computations by employing the self-consistent scheme described at the beginning of this chapter. For a concise presentation of this content, the reader is invited to check the publication [6].

4.2.1 A toy model for the examination of the gauge sector

Let us first introduce the Lagrangian and the scalar potential for the case study. Consider a flat space-time in four dimensions with the Minkowski metric denoted by $\eta_{\mu\nu}$, with signature $(+,-,-,-)$ and a Lagrangian density

$$\mathcal{L}_M = -\frac{1}{4}F^M_{\mu\nu}F^{\mu\nu}_M + (D_\mu\Phi)^\dagger D^\mu\Phi - U(\Phi^*\Phi) + \mathcal{L}^M_{\text{G.F}} + \mathcal{L}^M_{\text{ghosts}}, \tag{4.2.65}$$

where the sup- or sub-index M stands for Minkowski, $F^M_{\mu\nu} = \partial_\mu A^M_\nu - \partial_\nu A^M_\mu$ is the field strength tensor, Φ is a complex scalar field, $D_\mu = \partial_\mu - igA^M_\mu$ is the corresponding covariant derivative, $\mathcal{L}^M_{\text{G.F}}$ is a gauge fixing term and $\mathcal{L}^M_{\text{ghosts}}$ corresponds to the Faddeev-Popov ghost Lagrangian which will be made explicit later on. The simplest polynomial gauge-invariant scalar potential that can be chosen, displaying a meta-stable vacuum separated a potential barrier at tree-level, must be of order no less than 6 in Φ and must not contain any odd powers. For that reason, we consider the following scalar potential

$$U(\Phi) = \alpha|\Phi|^2 + \lambda|\Phi|^4 + \lambda_6|\Phi|^6, \tag{4.2.66}$$

where the parameters α, λ and λ_6 are to be chosen so that the false vacuum lies at $\Phi = 0$, see Fig. (4.2). The last term is crucial for this phenomenon to be present without radiative

corrections and can be motivated by phenomenology beyond SM, where physics at a yet unreached scale stabilizes the vacuum. More comments on possible UV completions leading to this model are discussed later on in the document (see Subsec. 4.2.6).

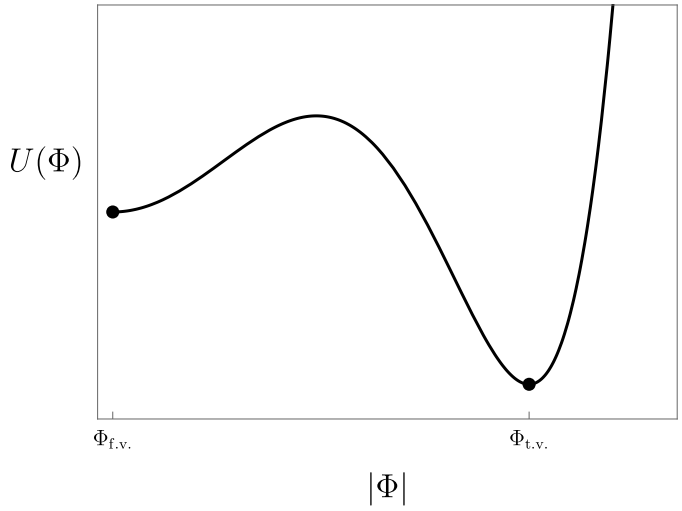

Figure 4.2: Sketch of the tree-level potential showing the different minima separated by a potential barrier.

The first step in computing decay rates associated with quantum tunneling is to calculate the bounce solution, which interpolates between the false vacuum and the true vacuum. For our model, no analytic solution is available, so we resort to a numerical treatment. The problem can be simplified further by employing the so-called thin-wall and the planar wall approximations . We will expand on them later on. For now, we need only know that the first one concerns quasi-degenerate vacua and will allow us to simplify the equation of motion for the bounce. As to remain within the scope of the approximation, we need to ensure that the condition of quasi-degenerate vacua holds at the one-loop level, meaning that in practice, the bounce solution that we employed in this study corresponds to an equation of motion where the potential term is taken from a renormalized CW potential. Let us then differentiate between the configuration that solves the classical Euclidean equations of motion, φ_b, and the configuration solving the Euclidean equation with the renormalized CW potential, φ_0.
First, we compute the corresponding effective action as illustrated in Ch. 1, by first going to Euclidean time and through the addition of external currents and later on expanding around the non-homogeneous background. We remove all the M labels of the Lagrangian in Eq. (4.2.65) and work with Euclidean quantities from now on. This means we have the following Euclidean Lagrangian

$$\mathcal{L} = \frac{1}{4}F_{\mu\nu}F^{\mu\nu} + (D_\mu\Phi)^\dagger D^\mu\Phi + U(\Phi^*\Phi) + \mathcal{L}_{\text{G.F}} + \mathcal{L}_{\text{ghosts}}. \tag{4.2.67}$$

We can write down the path integral, including external currents, as

$$Z[J, K_\mu, \bar{\psi}, \psi] = \int \mathcal{D}\Phi\mathcal{D}A_\mu\mathcal{D}\eta\mathcal{D}\bar{\eta}\ \mathrm{e}^{-\frac{1}{\hbar}\int \mathrm{d}^4x[\mathcal{L} - J(x)\Phi(x) - K_\mu(x)A_\mu(x) - \bar{\psi}(x)\eta(x) - \bar{\eta}(x)\psi(x)]}, \tag{4.2.68}$$

where $\eta, \bar{\eta}$ represent the ghost fields and $J, K_\mu, \bar{\psi}, \psi$, are the external currents corresponding to the scalar, the gauge and the ghosts' fields, respectively. We denote the one-point

expectation value of the fields as a function of external currents as follows:

$$\begin{aligned}
\varphi(x) &= \langle\Omega|\Phi(x)|\Omega\rangle|_{J,K_\mu,\bar\psi,\psi} = \hbar\,\frac{\delta \log Z[J,K_\mu,\bar\psi,\psi]}{\delta J(x)},\\
\mathcal{A}_\mu(x) &= \langle\Omega|A_\mu(x)|\Omega\rangle|_{J,K_\mu,\bar\psi,\psi} = \hbar\,\frac{\delta \log Z[J,K_\mu,\bar\psi,\psi]}{\delta K_\mu(x)},\\
\bar H(x) &= \langle\Omega|\bar\eta(x)|\Omega\rangle|_{J,K_\mu,\bar\psi,\psi} = -\,\hbar\,\frac{\delta \log Z[J,K_\mu,\bar\psi,\psi]}{\delta \psi(x)},\\
H(x) &= \langle\Omega|\eta(x)|\Omega\rangle|_{J,K_\mu,\bar\psi,\psi} = \hbar\,\frac{\delta \log Z[J,K_\mu,\bar\psi,\psi]}{\delta \bar\psi(x)}.
\end{aligned} \tag{4.2.69}$$

We perform the Legendre transform to obtain the exact effective action

$$\Gamma[\varphi,\mathcal{A}_\mu,\bar H,H] = -\hbar\,\log Z[J,K_\mu,\bar\psi,\psi] + J_x\,\varphi_x + K_{\mu;x}\,\mathcal{A}_{\mu;x} + \bar H_x\,\psi_x + \bar\psi_x\,H_x. \tag{4.2.70}$$

where we have used the de Witt notation, to abbreviate the expression, i.e.

$$J_x\varphi_x = \int \mathrm{d}^4x J(x)\varphi(x). \tag{4.2.71}$$

As shown in Ch. 1, the involutive property of the Legendre transform implies the following relations:

$$\begin{aligned}
\frac{\delta\Gamma[\varphi,\mathcal{A}_\mu,\bar H,H]}{\delta\varphi(x)} &= J(x), \quad \frac{\delta\Gamma[\varphi,\mathcal{A}_\mu,\bar H,H]}{\delta\mathcal{A}_\mu(x)} = K_\mu(x),\\
\frac{\delta\Gamma[\varphi,\mathcal{A}_\mu,\bar H,H]}{\delta\bar H(x)} &= \psi(x), \quad \frac{\delta\Gamma[\varphi,\mathcal{A}_\mu,\bar H,H]}{\delta H(x)} = -\bar\psi(x).
\end{aligned} \tag{4.2.72}$$

To investigate tunneling phenomena, we expand the theory around 0 expectation values for all fields except for the scalar, that is we will expand the effective action at $\Gamma[\varphi,\mathcal{A}_\mu = 0,\bar H = 0, H = 0]$ which will be denoted from now on as $\Gamma[\varphi]$, analogously the tree-level action $S[\varphi,\mathcal{A}_\mu = 0,\bar H = 0, H = 0]$ is abbreviated as $S[\varphi]$. From previous studies [29–31, 92, 93] we know that the tunneling rate can be obtained from the truncated effective action through the formula

$$\frac{\gamma}{V} = \frac{2\,|\mathrm{Im}\ \mathrm{e}^{-\Gamma^{(n)}[\varphi^{(n)}]/\hbar}|}{V\mathcal{T}}, \tag{4.2.73}$$

where $\Gamma^{(n)}[\varphi^{(n)}]$ and $\varphi^{(n)}$ are the effective action and corrected bounce at n-loop order

$$\left.\frac{\delta\Gamma^{(n)}[\varphi]}{\delta\varphi_x}\right|_{\varphi_x=\varphi_x^{(n)}} = 0 \tag{4.2.74}$$

Our intention is to obtain the corrected bounce $\varphi^{(1)}$ at one-loop order and the quantum-corrected decay rate $\Gamma^{(1)}$ when evaluated at $\varphi^{(1)}$ through Eq. (4.2.73).
Let us now expand the field Φ around the classical bounce and decompose the higher corrections into a real and an imaginary part, which correspond to a Goldstone boson direction,

$$\Phi = \frac{1}{\sqrt{2}}(\varphi_b + \hat\Phi + \mathrm{i}G), \tag{4.2.75}$$

where φ_b is the bounce and is to be understood as $\varphi^{(0)}$. After this decomposition, we can write down the gauge fixing term for a relatively general family of gauges,

$$\mathcal{L}_{\text{G.F.}} = \frac{1}{2\xi}(\partial_\mu A_\mu - \zeta\, g\, \varphi_b\, G)^2, \tag{4.2.76}$$

where $\zeta = 0$ [94, 95] for the Fermi gauge and $\zeta = 1$ [66] or $\zeta = \xi$ [96] for R_ξ gauges. With every term in the Lagrangian defined, we proceed to expand it up to quadratic order in field fluctuations, given that interaction terms and generically higher-order terms contribute only to higher loop corrections. We have then

$$\begin{aligned}\mathcal{L}^{(2)} = &\frac{1}{2}\,(\partial_\mu\varphi_b)^2 + \frac{\alpha}{2}\,\varphi_b^2 + \frac{\lambda}{4}\,\varphi_b^4 + \frac{\lambda_6}{8}\,\varphi_b^6 + \frac{1}{2}\,\hat{\Phi}\left(-\Delta_4 + \alpha + 3\,\lambda\,\varphi_b^2 + \frac{15\,\lambda_6}{4}\,\varphi_b^4\right)\hat{\Phi} \\ &+ \frac{1}{2}\,A_\mu\left[(-\Delta_4 + g^2\,\varphi_b^2)\,\delta_{\mu\nu} + \frac{\xi-1}{\xi}\,\partial_\mu\partial_\nu\right]A_\nu \\ &+ \frac{1}{2}\,G\left(-\Delta_4 + \alpha + \lambda\,\varphi_b^2 + \frac{3\,\lambda_6}{4}\varphi_b^4 + \frac{\zeta^2\,g^2\,\varphi_b^2}{\xi}\right)G \\ &+ \bar{\eta}\,\left(-\Delta_4 + \zeta\,g^2\,\varphi_b^2\right)\,\eta + \left(\frac{\zeta+\xi}{\xi}\right)\,g\,A_\mu\,(\partial_\mu\varphi_b)\,G + \left(\frac{\zeta-\xi}{\xi}\right)\,g\,\varphi_b\,A_\mu\,(\partial_\mu G),\end{aligned} \tag{4.2.77}$$

where Δ_4 is the four-dimensional Laplacian.
With the expansion of the Lagrangian above, we can obtain the effective action to one-loop order (or equivalently power $\hbar$) evaluated at the classical bounce, as explained in Sec. 1.2 of Ch. 1. Assuming we have set our potential to zero when $\varphi = 0$ by adding the appropriate constant term, we get

$$\begin{aligned}\Gamma^{(1)}[\varphi_b] - \Gamma^{(1)}[0] = S[\varphi_b] + \frac{\hbar}{2}\,\log\frac{\det\mathcal{M}^{-1}_{\hat{\Phi}}(\varphi_b)}{\det\mathcal{M}^{-1}_{\hat{\Phi}}(0)} + \frac{\hbar}{2}\,\log\frac{\det\mathcal{M}^{-1}_{(A_\mu,G)}(\varphi_b)}{\det\mathcal{M}^{-1}_{(A_\mu,G)}(0)} \\ - \hbar\,\log\frac{\det\mathcal{M}^{-1}_{(\bar{\eta},\eta)}(\varphi_b)}{\det\mathcal{M}^{-1}_{(\bar{\eta},\eta)}(0)},\end{aligned} \tag{4.2.78}$$

where the three last terms correspond to the different sectors: scalar, gauge-Goldstone, ghost sector, in that order, and their operators of fluctuations are the following:

$$\begin{aligned}&\mathcal{M}^{-1}_{\hat{\Phi}}(\varphi_b) = -\Delta_4 + \alpha + 3\,\lambda\,\varphi_b^2 + \frac{15\,\lambda_6}{4}\,\varphi_b^4\,, \\ &\mathcal{M}^{-1}_{(A_\mu,G)}(\varphi_b) = \begin{pmatrix}(-\Delta_4 + g^2\,\varphi_b^2)\,\delta_{\mu\nu} + \frac{\xi-1}{\xi}\partial_\mu\partial_\nu & \left(\frac{\zeta+\xi}{\xi}\right)g\,(\partial_\mu\varphi_b) + \left(\frac{\zeta-\xi}{\xi}\right)g\,\varphi_b\,\partial_\mu \\ 2\,g\,(\partial_\nu\varphi_b) + \left(\frac{\xi-\zeta}{\xi}\right)g\,\varphi_b\,\partial_\nu & -\Delta_4 + \alpha + \lambda\,\varphi_b^2 + \frac{3\,\lambda_6}{4}\,\varphi_b^4 + \frac{\zeta^2\,g^2\,\varphi_b^2}{\xi}\end{pmatrix}, \\ &\mathcal{M}^{-1}_{(\bar{\eta},\eta)}(\varphi_b) = -\Delta_4 + \zeta\,g^2\,\varphi_b^2\,.\end{aligned} \tag{4.2.79}$$

where $\mathcal{M}^{-1}_{\hat{\Phi}}$ and $\mathcal{M}^{-1}_{(\eta,\bar{\eta})}$) are seen to be decoupled sectors and pertain only fluctuations of the scalar and the ghosts respectively, while $\mathcal{M}^{-1}_{(A_\mu,G)}$ is a 5×5 matrix operator mixing the gauge field A_μ and the Goldstone G, thus acting on $(A_\mu, G)^T$. By choosing counter-terms accordingly we can make $\Gamma^{(1)}[\varphi = 0] = 0$ as well.

We wish to study the effects of the corrected bounce on the one-loop terms, for which we need to evaluate the effective action at the corrected bounce. This has been done in detail using the method of constrained sources[29] by tracking the difference between saddle points and one point expectation values, leading to

$$\begin{aligned}\Gamma^{(1)}[\varphi^{(1)}] \;&= S[\varphi^{(1)}] + \frac{\hbar}{2}\,\log\frac{\det\mathcal{M}^{-1}_{\hat{\Phi}}(\varphi^{(1)})}{\det\mathcal{M}^{-1}_{\hat{\Phi}}(0)} + \frac{\hbar}{2}\,\log\frac{\det\mathcal{M}^{-1}_{(A_\mu,G)}(\varphi^{(1)})}{\det\mathcal{M}^{-1}_{(A_\mu,G)}(0)} - \\ &\quad -\hbar\,\log\frac{\det\mathcal{M}^{-1}_{(\bar{\eta},\eta)}(\varphi^{(1)})}{\det\mathcal{M}^{-1}_{(\bar{\eta},\eta)}(0)}.\end{aligned} \tag{4.2.80}$$

The equation is now to be evaluated by an expansion on the quantum bounce $\varphi^{(1)}$ around a bounce solution, φ_0 which we take, not to be the tree-level bounce φ_b, but the one computed from the one-loop Coleman-Weinberg potential without any gradient corrections. To make progress in estimating the gradient corrections, we work under the so-called planar wall approximation. Under this assumption, we take the radius of the bubble to be very big so that the terms in the equations, proportional to the Laplacian on the 3-sphere, Δ_3, are taken to be continuous, instead of the commonly discrete eigenvalues corresponding to the four-dimensional version of angular momentum. This means technically that substitute $\ell(\ell+2)/R^2$ with k^2. Geometrically, it means we are taking all directions along the bubble wall to be flat and can therefore employ a Fourier transform for such directions[30]. We will work from now on with operators and Green's functions that depend on the normal direction to the bubble wall, which we take to be $x_4 \to z$, and on momentum, $\mathbf{k}$, running along the bubble wall, denoted with the indices $1,2,3$ and called tangential directions from now on. We furthermore set the center of the bubble wall to be at $z=0$, which we take to be the point of largest gradients of the bubble. Let X correspond to the different sectors, so that $\mathcal{M}^{-1}_X(\varphi^{(0)}$ represents any of the fluctuation operators in Eq. (4.2.79). By employing eigenfunctions as described above, we have

$$\phi_{X;\mathbf{k},i}(x) = \frac{\mathrm{e}^{\mathrm{i}\mathbf{k}\cdot\mathbf{x}}}{(2\pi)^{3/2}}\,f_{X;\mathbf{k},i}(z) \quad \text{with} \quad \mathcal{M}^{-1}_X(\varphi^{(1)})\phi_{X;\mathbf{k},i} = \lambda_{X;\mathbf{k},i}\,\phi_{X;\mathbf{k},i}. \tag{4.2.81}$$

leads to the reduced or planar eigenvalue problem

$$\mathcal{M}^{-1}_{X;\mathbf{k}}(\varphi^{(1)})f_{X;\mathbf{k},i} = \lambda_{X;\mathbf{k},i}\,f_{X;\mathbf{k},i}, \tag{4.2.82}$$

with

$$\mathcal{M}^{-1}_{\hat{\Phi};\mathbf{k}}(\varphi^{(1)}) = -\,\partial_z^2 + \mathbf{k}^2 + \alpha + 3\,\lambda\,\varphi^{(1)2} + \frac{15\,\lambda_6}{4}\,\varphi^{(1)4}, \tag{4.2.83a}$$

$$\mathcal{M}^{-1}_{(A_\mu,G);\mathbf{k}}(\varphi^{(1)}) =$$

$$\begin{pmatrix} M^{-1}_{\mathbf{k}}(\varphi^{(1)})\delta_{ij} + \frac{\xi-1}{\xi}(\mathrm{i}\mathbf{k}_i)(\mathrm{i}\mathbf{k}_j) & \frac{\xi-1}{\xi}(\mathrm{i}\mathbf{k}_i)\partial_z & \frac{\zeta-\xi}{\xi}g\varphi^{(1)}(\mathrm{i}\mathbf{k}_i) \\ \frac{\xi-1}{\xi}(\mathrm{i}\mathbf{k}_j)\partial_z & M^{-1}_{\mathbf{k}}(\varphi^{(1)}) + \frac{\xi-1}{\xi}\partial_z^2 & \left(\frac{\zeta+\xi}{\xi}\right)g(\partial_z\varphi^{(1)}) + \frac{\zeta-\xi}{\xi}g\varphi^{(1)}\partial_z \\ \left(\frac{\xi-\zeta}{\xi}\right)g\varphi^{(1)}(\mathrm{i}\mathbf{k}_j) & 2g(\partial_z\varphi^{(1)}) + \left(\frac{\xi-\zeta}{\xi}\right)g\varphi^{(1)}\partial_z & N^{-1}_{\mathbf{k}}(\varphi^{(1)}) \end{pmatrix}, \tag{4.2.83b}$$

$$\mathcal{M}^{-1}_{(\bar{\eta},\eta);\mathbf{k}}(\varphi^{(1)}) = -\,\partial_z^2 + \mathbf{k}^2 + \zeta\,g^2\,\varphi^{(1)2}. \tag{4.2.83c}$$

with the abbreviations

$$M_{\mathbf{k}}^{-1}(\varphi^{(1)}) = -\partial_z^2 + \mathbf{k}^2 + g^2\,\varphi^{(1)2} \tag{4.2.84}$$

and

$$N_{\mathbf{k}}^{-1}(\varphi^{(1)}) = -\partial_z^2 + \mathbf{k}^2 + \alpha + \lambda\,\varphi^{(1)2} + \frac{3\,\lambda_6}{4}\varphi^{(1)4} + \frac{\zeta^2\,g^2\,\varphi^{(1)2}}{\xi}. \tag{4.2.85}$$

After observing the operator for the (A_μ, G) sector, we will later choose to simplify the computations as much as possible by taking $\chi = 1$ and $\zeta = 1$. Doing this has the effect of decoupling the tangential directions of the gauge field from the Goldstone field. Incidentally, they acquire the same form as the fluctuation operator for the ghosts but will contribute with the opposite sign, as we will see later.
We now show how the terms for the one-loop contributions appearing in the effective action change under this approximation. Given that the fluctuation operators are Hermitian, the eigenfunctions $\phi_{X,\mathbf{k},i}$ are an orthogonal set, and so are the $f_{X;\mathbf{k},i}$, which we assume to be normalized as well. The spectral theorem tells us that the logarithm of a Hermitian and positive-definite operator can be expressed using projectors as

$$\begin{aligned}\log \mathcal{M}_X^{-1}(\varphi^{(1)}; x', x) &= \int \mathrm{d}^3\mathbf{k} \sum\!\!\!\!\!\!\int_i \log(\lambda_{X;\mathbf{k},i})\phi_{X;\mathbf{k},i}(x')\phi^\dagger_{X;\mathbf{k},i}(x) \\ &= \int \frac{\mathrm{d}^3\mathbf{k}}{(2\pi)^3}\,\mathrm{e}^{\mathrm{i}\mathbf{k}\cdot(\mathbf{x}'-\mathbf{x})} \sum\!\!\!\!\!\!\int_i \log(\lambda_{X;\mathbf{k},i}) P_{X;\mathbf{k},i}(z', z),\end{aligned} \tag{4.2.86}$$

with the symbol $\sum\!\!\!\!\!\!\int$ denoting sum over both, the discrete and the possibly continuous part of the spectrum and defining $P_{X;\mathbf{k},i}(z', z) = f_{X;\mathbf{k},i}(z') f^\dagger_{X;\mathbf{k},i}(z)$ and we postpone dealing with possible negative and zero eigenvalues. In this way, we see that the logarithm of the fluctuation operator for sector X can be written as the Fourier transform of the logarithm of a planar fluctuation operator

$$\log \mathcal{M}_X^{-1}(\varphi^{(1)}; x', x) = \int \frac{\mathrm{d}^3\mathbf{k}}{(2\pi)^3}\,\mathrm{e}^{\mathrm{i}\mathbf{k}\cdot(\mathbf{x}'-\mathbf{x})} \log \mathcal{M}_{X;\mathbf{k}}^{-1}(\varphi^{(1)}; z', z). \tag{4.2.87}$$

Analogously one can write down the full Green's function for sector X in terms of the Fourier transform of planar Green's functions

$$\mathcal{M}_X(\varphi^{(1)}; x', x) = \int \frac{\mathrm{d}^3\mathbf{k}}{(2\pi)^3}\,\mathrm{e}^{\mathrm{i}\mathbf{k}\cdot(\mathbf{x}'-\mathbf{x})} \mathcal{M}_{X;\mathbf{k}}(\varphi^{(1)}; z', z). \tag{4.2.88}$$

The one-loop terms in Eq. (4.2.80) are written in terms of the planar fluctuation as follows

$$\begin{aligned}\log\det \mathcal{M}_X^{-1}(\varphi^{(1)}; x, x') &= \mathrm{tr}\,\log \mathcal{M}_X^{-1}(\varphi^{(1)}; x, x') = V \int \mathrm{d}z \frac{\mathrm{d}^3\mathbf{k}}{(2\pi)^3}\,\mathrm{tr}_{\mathrm{dis}} \log \mathcal{M}_{X;\mathbf{k}}^{-1}(\varphi^{(1)}; z, z) \\ &= V \int \frac{\mathrm{d}^3\mathbf{k}}{(2\pi)^3} \log\det \mathcal{M}_{X;\mathbf{k}}^{-1},\end{aligned} \tag{4.2.89}$$

where $\mathrm{tr}_{\mathrm{dis}}$ denotes the trace over possible remaining discrete indices, e.g. Lorentz, spinor, etc. We are now able to rewrite the effective action Eq. (4.2.80) in terms of the planar fluctuations operators. Hence the problem is reduced to dynamics in only one direction,

z.

$$\Gamma^{(1)}[\varphi^{(1)}] = S[\varphi^{(1)}] + \frac{\hbar}{2} V \int \frac{\mathrm{d}^3\mathbf{k}}{(2\pi)^3} \log \frac{\det \mathcal{M}^{-1}_{\hat{\Phi};\mathbf{k}}(\varphi^{(1)})}{\det \mathcal{M}^{-1}_{\hat{\Phi};\mathbf{k}}(0)} + \frac{\hbar}{2} V \,\mathrm{tr} \int \frac{\mathrm{d}^3\mathbf{k}}{(2\pi)^3} \log \frac{\det \mathcal{M}^{-1}_{(A_\mu,G);\mathbf{k}}(\varphi^{(1)})}{\det \mathcal{M}^{-1}_{(A_\mu,G);\mathbf{k}}(0)} - \hbar V \int \frac{\mathrm{d}^3\mathbf{k}}{(2\pi)^3} \log \frac{\det \mathcal{M}^{-1}_{(\bar{\eta},\eta);\mathbf{k}}(\varphi^{(1)})}{\det \mathcal{M}^{-1}_{(\bar{\eta},\eta);\mathbf{k}}(0)}. \tag{4.2.90}$$

Some comments about the above equation are in order. In comparison with $\Gamma^{(1)}[\varphi_0]$, the equation above, Eq. (4.2.90), has additional two-loop contributions. We can also view such equation in terms of traditional Feynman diagrams, in which we have propagators over the background φ_0 forming the usual one-loop diagrams and also presenting new corrections from dumbbell diagrams (See Figs. 4.3 and 4.4). It can be argued that in particular scenarios, these diagrams outweigh other two-loop topologies because of possible sums that happen within the loops, as in the case of color in non-Abelian gauge theories[30]. Although the dumbbell diagrams are not one-particle irreducible, they appear when considering propagators over φ_0 as opposed to $\varphi^{(1)}$. The one-particle irreducibility of $\Gamma[\varphi^{(1)}]$ is preserved if the background is taken to be $\varphi^{(1)}$.
To determine $\varphi^{(1)}$, we need to obtain its equation of motion. For that purpose, we expand Eq. (4.2.90) around φ_0 and organize the different contributions appearing therein as follows:

$$\Gamma^{(1)}[\varphi^{(1)}] = B + \hbar B^{(1)} + \hbar B^{(1)}_{\hat{\Phi};\mathrm{dis}} + \hbar B^{(1)}_{\hat{\Phi}} + \hbar B^{(1)}_{(A_\mu,G)} + \hbar B^{(1)}_{(\bar{\eta},\eta)} + \hbar^2 B^{(2)} + \hbar^2 B^{(2)}_{\hat{\Phi}} + \hbar^2 B^{(2)}_{(A_\mu,G)} + \hbar^2 B^{(2)}_{(\bar{\eta}\,,\eta)}, \tag{4.2.91}$$

where B is the classical action evaluated at φ_0, that is $S[\varphi_0]$, $B^{(1)}$ and $B^{(2)}$ are corrections to B because of the expansion around φ_0, while all the other are the corrections to each sector coming from the gradients in the one-loop terms and the corrections to φ_0; similar to what was done in the Higgs-Yukawa case in the previous section (compare with the exponent of Eq. (4.1.38)). We discuss each one of the terms in detail below.
The fluctuation operator in the scalar sector presents some discrete modes, a negative mode related to tunneling and four zero modes corresponding to spacetime translation. By writing the measure in terms of the eigenfunctions of the operator, we are able to trade the integration over eigenfunctions with integration over translations or collective coordinates as explained in Sec. 2.2. Thus

$$\hbar B^{(1)}_{\hat{\Phi};\mathrm{dis}} = \frac{\mathrm{i}\pi\hbar}{2} - \frac{\hbar}{2} \log \left(\frac{(V\mathcal{T})^2 \alpha^5}{4|\lambda_0|} \left(\frac{B}{2\pi\hbar} \right)^4 \right) \tag{4.2.92}$$

where λ_0 is the negative mode and is taken to be equal to

$$\lambda_0 = -\frac{3}{R^2}, \tag{4.2.93}$$

with R being the radius of the critical bubble in the thin-wall approximation (as done for the Yukawa-Higgs model in Subsec. 4.1.3). A careful analytic continuation and integration over this mode produce an extra factor of $1/2$, relative to the case where it is assumed positive[37]. This is the origin of the $1/2$ in the first term of Eq. (4.2.92) as well as

the factor of 4 accompanying $|\lambda_0|$ in the second term of the same equation. Within the planar wall approximation these discrete modes appear for vanishing momentum running in the tangential directions to the wall, $\mathbf{k} = 0$ and their contribution has been written together with a factor of α on dimensional grounds. We are currently studying whether a non-trivial factor may appear when examining how the measure transforms in more detail. Some basic cases as a quantum mechanical double-well can be seen to give non-unit factors, some more comments can be found in Ref. [36].
The terms with the superscript (1) come from the contributions of the one-loop diagrams over the background φ_0, and they are explicitly given by

$$\hbar B^{(1)}_{\hat{\Phi}} = \frac{\hbar}{2} V \int \frac{\mathrm{d}^3\mathbf{k}}{(2\pi)^3} \log \left| \frac{\det' \mathcal{M}^{-1}_{\hat{\Phi};\mathbf{k}}(\varphi_0)}{\det \mathcal{M}^{-1}_{\hat{\Phi};\mathbf{k}}(0)} \right|, \tag{4.2.94a}$$

$$\hbar B^{(1)}_{(A_\mu,G)} = \frac{\hbar}{2} V \,\mathrm{tr} \int \frac{\mathrm{d}^3\mathbf{k}}{(2\pi)^3} \log \frac{\det \mathcal{M}^{-1}_{(A_\mu,G);\mathbf{k}}(\varphi_0)}{\det \mathcal{M}^{-1}_{(A_\mu,G);\mathbf{k}}(0)}, \tag{4.2.94b}$$

and

$$\hbar B^{(1)}_{(\bar{\eta},\eta)} = -\hbar V \int \frac{\mathrm{d}^3\mathbf{k}}{(2\pi)^3} \log \frac{\det \mathcal{M}^{-1}_{(\bar{\eta},\eta);\mathbf{k}}(\varphi_0)}{\det \mathcal{M}^{-1}_{(\bar{\eta},\eta);\mathbf{k}}(0)}, \tag{4.2.94c}$$

where tr is to be understood as tracing over all remaining variables or indices, and $\det'$ denotes the determinant where the discrete modes are to be omitted. Let us now describe the terms with superscript (2) before diving into how to compute all of them. These correspond to the next order in the semi-classical expansion, and they are obtained through an additional functional variation of the action, them being a consequence of the non-homogeneity of the background. These give

$$\hbar^2 B^{(2)}_{\hat{\Phi}} = \frac{\hbar}{2} V \int \frac{\mathrm{d}^3\mathbf{k}}{(2\pi)^3} \int \mathrm{d}z\, \hbar\delta\varphi(z) \frac{\delta}{\delta\varphi(z)} \log \frac{\det \mathcal{M}^{-1}_{\hat{\Phi};\mathbf{k}}(\varphi)}{\det \mathcal{M}^{-1}_{\hat{\Phi};\mathbf{k}}(0)} \bigg|_{\varphi_0}, \tag{4.2.95a}$$

$$\hbar^2 B^{(2)}_{(A_\mu,G)} = \frac{\hbar}{2} V \int \frac{\mathrm{d}^3\mathbf{k}}{(2\pi)^3} \int \mathrm{d}z\, \hbar\delta\varphi(z) \frac{\delta}{\delta\varphi(z)} \log \frac{\det \mathcal{M}^{-1}_{(A_\mu,G);\mathbf{k}}(\varphi)}{\det \mathcal{M}^{-1}_{(A_\mu,G);\mathbf{k}}(0)} \bigg|_{\varphi_0}, \tag{4.2.95b}$$

and

$$\hbar^2 B^{(2)}_{(\bar{\eta},\eta)} = -\hbar V \int \frac{\mathrm{d}^3\mathbf{k}}{(2\pi)^3} \int \mathrm{d}z\, \hbar\delta\varphi(z) \frac{\delta}{\delta\varphi(z)} \log \frac{\det \mathcal{M}^{-1}_{(\bar{\eta},\eta);\mathbf{k}}(\varphi)}{\det \mathcal{M}^{-1}_{(\bar{\eta},\eta);\mathbf{k}}(0)} \bigg|_{\varphi_0}. \tag{4.2.95c}$$

Additional corrections to order $\hbar^2$ appear from the classical action when evaluated at the quantum corrected bounce as we saw in the Yukawa case. We can derive the corrected equation of motion for the scalar field by functionally differentiating Eq. (4.2.90) with respect to $\varphi^{(1)}$ which results in

$$-\partial_z^2 \varphi^{(1)}(z) + U'_{\mathrm{eff}}(\varphi^{(1)}; z) = 0, \tag{4.2.96}$$

where we have collected the tree-level potential and the tadpole contributions into a single potential function U_{eff}:

$$\begin{aligned} U'_{\mathrm{eff}}(\varphi^{(1)}; z) = U'(\varphi^{(1)}; z) &+ \hbar\, \Pi_{\hat{\Phi}}(\varphi_0; z)\, \varphi_0(z) + \hbar\, \Pi_{(A_\mu,G)}(\varphi_0; z)\, \varphi_0(z) \\ &+ \hbar\, \Pi_{(\bar{\eta},\eta)}(\varphi_0; z)\, \varphi_0(z) \end{aligned} \tag{4.2.97}$$

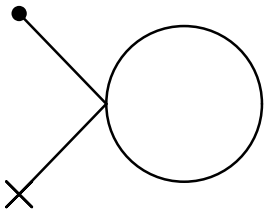

(a) First type of contributions from $\hat{\Phi}$.

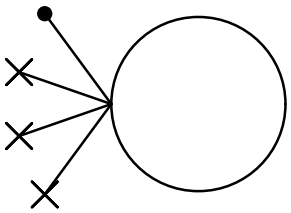

(b) Second tadpole type contribution from $\hat{\Phi}$

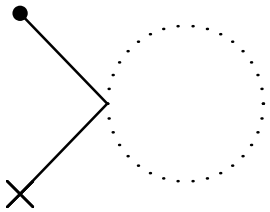

(c) Tadpole contribution coming from the ghost fields $\bar{\eta}, \eta$.

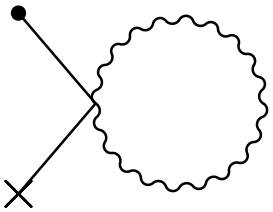

(d) Tadpole contributions from the gauge field components A_1, A_2, A_3 parallel to the bubble wall.

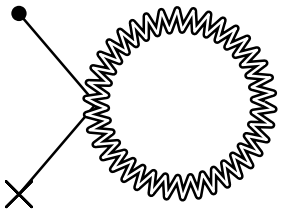

(e) Tadpole contribution coming from the coupled sector of A_4, G.

Figure 4.3: Feynman diagram representation of the tadpole contributions using propagators over the φ_0 background, obtained from the functional derivatives of the one-loop terms, $B_X^{(1)}$, of the effective action. Lines ending with crosses represent insertions of the background φ_0 and lines ending with a dot represent fluctuations around the background.

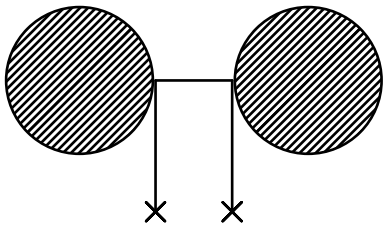

Figure 4.4: Feynman diagram representation of the terms accounted for in Eq. (4.2.80) after the quantum corrected bounce is taken into account, it corresponds to $B_X^{(2)}$ in the effective action. Only one background insertion is depicted per vertex, although more also occur, and the blobs represent any of the tadpoles from Fig. 4.3.

and

$$U(\varphi^{(1)}) = \frac{1}{2}\alpha\varphi^{(1)2} + \frac{\lambda}{4}\varphi^{(1)4} + \frac{\lambda_6}{8}\varphi^{(1)6}. \tag{4.2.98}$$

The tadpole contributions are to be understood as the product of the self-energies $\Pi_{\hat{\Phi}}, \Pi_{(A_\mu,G)}$ and $\Pi_{(\eta,\bar{\eta})}$ together with insertions of the background field. As opposed to the Yukawa-Higgs case treated before, for the potential chosen in this section, the insertions are higher-order polynomials but are otherwise obtained in the same way. These are explicitly seen to be

$$\hbar\,\Pi_{\hat{\Phi}}(\varphi_0;z)\,\varphi_0(z) = \frac{\hbar}{2}\int\frac{\mathrm{d}^3\mathbf{k}}{(2\pi)^3}[6\,\lambda\,\varphi_0(z) + 15\,\lambda_6\,\varphi_0^3(z)]\,\mathcal{M}_{\hat{\Phi};\mathbf{k}}(\varphi_0;z,z), \tag{4.2.99a}$$

$$\hbar\,\Pi_{(A_\mu,G)}(\varphi_0;z)\,\varphi_0(z) = \frac{\hbar}{2}\,\mathrm{tr}\int\frac{\mathrm{d}^3\mathbf{k}}{(2\pi)^3}\,\mathcal{M}_{(A_\mu,G);\mathbf{k}}(\varphi_0;z,z)\,\frac{\partial}{\partial\varphi}\mathcal{M}^{-1}_{(A_\mu,G);\mathbf{k}}(\varphi;z)\Big|_{\varphi_0}, \tag{4.2.99b}$$

$$\hbar\,\Pi_{(\bar{\eta},\eta)}(\varphi_0;z)\,\varphi_0(z) = -2\,\hbar\,\zeta\,g^2\int\frac{\mathrm{d}^3\mathbf{k}}{(2\pi)^3}\,\mathcal{M}_{(\bar{\eta},\eta);\mathbf{k}}(\varphi_0;z,z)\,\varphi_0(z). \tag{4.2.99c}$$

and represent the amputated version of the diagrams shown in Fig. 4.3. This notation allows us to write an abbreviated expression for the order $\hbar^2$ contributions, that is, collecting the definition in Eq. (4.2.95) and the above set of equations gives

$$B_X^{(2)} = V\int\mathrm{d}z\,\delta\varphi(z)\,\Pi_X(\varphi_0;z)\varphi_0(z). \tag{4.2.100}$$

Recalling that our background is not the tree-level bounce φ_b, but φ_0, which is the bounce to be computed from the renormalized CW potential, we must include certain contributions that would normally be zero in the equation for the corrections $\delta\varphi$, viz.

$$\begin{aligned}\mathcal{M}^{-1}_{\hat{\Phi}}(\varphi_0;z)\,\delta\varphi(z) = &\frac{1}{\hbar}\left(\Box\varphi_0 - U'(\varphi_0;z)\right) - \Pi_{\hat{\Phi}}(\varphi_0;z)\,\varphi_0(z) - \Pi_{(A_\mu,G)}(\varphi_0;z)\,\varphi_0(z)\\ &- \Pi_{(\bar{\eta},\eta)}(\varphi_0;z)\,\varphi_0(z).\end{aligned} \tag{4.2.101}$$

We can see that the first term of the right-hand side is an addition coming from the deviations from the φ_b configuration. Inverting the relation above shows how $\delta\varphi$ is given by the tadpole functions supplemented with an additional propagator representing the non-amputated tadpoles of Fig. 4.3, which in turn, when plugged into Eq. (4.2.100) do indeed acquire the representation of the dumbbell diagrams of Fig. 4.4.

Let us next consider the additional terms appearing in the classical action when evaluated at the corrected bounce. Decomposing such additional terms by powers of $\hbar^2$ we have:

$$S[\varphi^{(1)}] = B + \hbar B^{(1)} + \hbar^2\,B^{(2)}, \tag{4.2.102}$$

where $B^{(1)}$ (without subscript) denotes the linear term related to the background φ_0 and its mathematical expression is

$$B^{(1)} = V\int\mathrm{d}z\,\delta\varphi(z)\,\frac{\delta S[\varphi]}{\delta\varphi(z)}\Big|_{\varphi_0} = V\int\mathrm{d}z\,\delta\varphi(z)(-\Box\varphi_0 + U'(\varphi_0;z)). \tag{4.2.103}$$

The quadratic contributions in the corrections of the background can be written down by combining Eqs. (4.2.100),(4.2.101) and Eq. (4.2.103) arriving at

$$\begin{aligned}B^{(2)} &= \frac{1}{2}\int\mathrm{d}^4x\,\delta\varphi(z)\,\mathcal{M}^{-1}_{\hat{\Phi}}(\varphi_0;z)\,\delta\varphi(z) + \mathcal{O}(\hbar^2)\\ &= -\frac{1}{2}\left(B^{(2)}_{\hat{\Phi}} + B^{(2)}_{(A_\mu,G)} + B^{(2)}_{(\bar{\eta},\eta)}\right) - \frac{1}{2\hbar}B^{(1)}.\end{aligned} \tag{4.2.104}$$

For convenience, we group the different contributions for this model so that they can be compared directly with the Yukawa-Higgs case. These final quantities we denote with calligraphic font and are

$$\mathcal{B}^{(0)} = B, \tag{4.2.105}$$

$$\mathcal{B}^{(1)} = B^{(1)}_{\hat{\Phi}} + B^{(1)}_{(A_\mu,G)} + B^{(1)}_{(\bar{\eta},\eta)}, \tag{4.2.106}$$

$$\mathcal{B}^{(2)} = -B^{(2)}. \tag{4.2.107}$$

In terms of the above definitions, we can write the analog of Eq. (4.1.38) for this model

$$\frac{\gamma}{V} = \left(\frac{B}{2\pi\hbar}\right)^2 \sqrt{\frac{\alpha^5}{|\lambda_0|}}\, \exp\left[-\frac{1}{\hbar}\left(\mathcal{B}^{(0)} + \hbar\,\mathcal{B}^{(1)} + \hbar^2\,\mathcal{B}^{(2)}\right)\right], \tag{4.2.108}$$

and the exponent can be found by using the Green's function at the coincident limit, in the same exact way as it was done for the previous model. We will now discuss how we found the Green's functions numerically within specific approximations. Once the Green's functions are specified, we can use the expressions derived in this section to obtain the $\mathcal{B}$'s explicitly.

4.2.2 Choosing the gauge

In order to make progress in the computation of Green's functions, we further opt to study the gauge parameters which produce the simplest Lorentz structure. A glance at Eq. (4.2.83b) is enough to realize that the choice, $\xi = \zeta = 1$, gives rise to a matrix operator which is almost diagonal, namely the only coupled field directions that remain are A_4 and G, i.e.

$$\mathcal{M}^{-1}_{(A_\mu,G);\mathbf{k}}(\varphi^{(1)}) = \begin{pmatrix} M^{-1}_{\mathbf{k}}(\varphi^{(1)})\delta_{ij} & 0 & 0 \\ 0 & M^{-1}_{\mathbf{k}}(\varphi^{(1)}) & 2g(\partial_z\varphi^{(1)}) \\ 0 & 2g(\partial_z\varphi^{(1)}) & N^{-1}_{\mathbf{k}}(\varphi^{(1)}) \end{pmatrix}, \tag{4.2.109}$$

where $M^{-1}_{\mathbf{k}}(\varphi)$ is the same as before and $N^{-1}_{\mathbf{k}}$ is

$$N^{-1}_{\mathbf{k}}(\varphi^{(1)}) = -\partial_z^2 + \mathbf{k}^2 + \alpha + \lambda\,\varphi^{(1)2} + \frac{3}{4}\lambda_6\,\varphi^{(1)4} + g^2\,\varphi^{(1)2}. \tag{4.2.110}$$

Not only the Lorentz structure of the fluctuations' operator for the Gauge-Goldstone sector simplifies with this choice. The directions of the gauge field that are parallel to the wall of the bubble, A_1, A_2 and A_3 take the same form as $\mathcal{M}^{-1}_{(\eta,\bar{\eta});\mathbf{k}}$ and allows us to collect all such contributions in only one term. From here onward, it should be understood that such grouping has been performed so that the remaining one-loop effective action has only terms corresponding to the scalar, the ghost and the (A_4, G) sector as follows:

$$\begin{aligned}\Gamma^{(1)}[\varphi^{(1)}] = \\ S[\varphi^{(1)}] + \frac{\hbar}{2}\,V\int\frac{\mathrm{d}^3\mathbf{k}}{(2\pi)^3}\,\log\frac{\det\mathcal{M}^{-1}_{\hat{\Phi};\mathbf{k}}(\varphi^{(1)})}{\det\mathcal{M}^{-1}_{\hat{\Phi};\mathbf{k}}(0)} + \frac{\hbar}{2}\,V\int\frac{\mathrm{d}^3\mathbf{k}}{(2\pi)^3}\log\frac{\det\mathcal{M}^{-1}_{(A_4,G);\mathbf{k}}(\varphi^{(1)})}{\det\mathcal{M}^{-1}_{(A_4,G);\mathbf{k}}(0)} \\ + \frac{\hbar}{2}\,V\int\frac{\mathrm{d}^3\mathbf{k}}{(2\pi)^3}\log\frac{\det\mathcal{M}^{-1}_{(\bar{\eta},\eta);\mathbf{k}}(\varphi^{(1)})}{\det\mathcal{M}^{-1}_{(\bar{\eta},\eta);\mathbf{k}}(0)},\end{aligned} \tag{4.2.111}$$

where $\mathcal{M}^{-1}_{(A_4,G);\mathbf{k}}$ has been implicitly defined in Eq. (4.2.109) and the factor appearing in front of the ghost contribution is the result of the cancellation with the said gauge field components. Let us denote from now on by $X \in \{\hat{\Phi}, (A_4, G), (\eta, \bar{\eta})\}$ the three different sectors. After these simplifications and choices have been implemented, we can update the expression for the one-loop effective action, Eq. (4.2.91), on the quantum corrected bounce to get

$$\begin{aligned}\Gamma[\varphi^{(1)}] =& B + \frac{\hbar}{2}B^{(1)} + \hbar B^{(1)}_{\hat{\Phi};\mathrm{dis}} + \hbar\, B^{(1)}_{\hat{\Phi}} + \hbar\, B^{(1)}_{(A_4,G)} - \frac{\hbar}{2}\, B^{(1)}_{(\bar{\eta},\eta)} \\ &+ \frac{1}{2}\left(\hbar^2\, B^{(2)}_{\hat{\Phi}} + \hbar^2\, B^{(2)}_{(A_4,G)} - \frac{\hbar^2}{2}\, B^{(2)}_{(\bar{\eta},\eta)}\right),\end{aligned} \tag{4.2.112}$$

with

$$B^{(1)}_{(A_4,G)} = \frac{1}{2}\, V \int \frac{\mathrm{d}^3\mathbf{k}}{(2\pi)^3} \log \frac{\det \mathcal{M}^{-1}_{(A_4,G);\mathbf{k}}(\varphi_0)}{\det \mathcal{M}^{-1}_{(A_4,G);\mathbf{k}}(0)}\,, \tag{4.2.113}$$

$$B^{(2)}_{(A_4,G)} = \frac{1}{2}\, V \int \frac{\mathrm{d}^3\mathbf{k}}{(2\pi)^3} \int \mathrm{d}z\, \delta\varphi(z)\, \frac{\delta}{\delta\varphi(z)} \log \frac{\det \mathcal{M}^{-1}_{(A_4,G);\mathbf{k}}(\varphi)}{\det \mathcal{M}^{-1}_{(A_4,G);\mathbf{k}}(0)}\bigg|_{\varphi_0}\,, \tag{4.2.114}$$

all other terms as defined previously. The potential U_{eff} appearing in the equation of motion for the quantum corrections of the background Eq. (4.2.96), must also be brought up to date

$$\begin{aligned}U'_{\text{eff}}(\varphi^{(1)}; z) = U'(\varphi^{(1)}; z) &+ \hbar\, \Pi_{\hat{\Phi}}(\varphi_0; z)\, \varphi_0(z) + \hbar\, \Pi_{(A_4,G)}(\varphi_0; z)\, \varphi_0(z) \\ &- \frac{\hbar}{2}\, \Pi_{(\bar{\eta},\eta)}(\varphi_0; z)\, \varphi_0(z),\end{aligned} \tag{4.2.115}$$

where the only new quantity is the tadpole contribution corresponding to the reduced coupled sector (A_4, G),

$$\Pi_{(A_4,G)}(\varphi_0; z)\, \varphi_0(z) = \frac{1}{2}\,\mathrm{tr} \int \frac{\mathrm{d}^3\mathbf{k}}{(2\pi)^3}\, \mathcal{M}_{(A_4,G);\mathbf{k}}(\varphi_0; z) \left(\frac{\partial \mathcal{M}^{-1}_{(A_4,G);\mathbf{k}}(\varphi^{(1)}; z)}{\partial \varphi^{(1)}(z)}\right)\bigg|_{\varphi_0}. \tag{4.2.116}$$

With the present gauge choice, we can compute the partial derivative against $\varphi^{(1)}$ appearing above to get:

$$\frac{\partial}{\partial\varphi}\mathcal{M}^{-1}_{(A_4,G);\mathbf{k}}(\varphi; z)\bigg|_{\varphi_0} = \begin{pmatrix} 2g^2\varphi_0(z) & -2g\partial_z \\ -2g\partial_z & 2\lambda\varphi_0(z) + 3\lambda_6\varphi_0^3(z) + 2g^2\varphi_0(z) \end{pmatrix}, \tag{4.2.117}$$

which leads to this expression for the (A_4, G)-sector tadpole function:

$$\begin{aligned}\Pi_{(A_4,G)}(\varphi_0; z)\varphi_0(z) =& \frac{1}{2}\int \frac{\mathrm{d}^3\mathbf{k}}{(2\pi)^3}\Big(2g^2\varphi_0(z)\mathcal{M}_{(A_4,A_4)}(z) - 4g\partial_z\mathcal{M}_{(A_4,G)}(z) \\ &+ (2g^2\varphi_0 + 2\lambda\varphi_0(z) + 3\lambda_6\varphi_0^3(z))\mathcal{M}_{(G,G)}(z)\Big),\end{aligned} \tag{4.2.118}$$

and the following for the quantum corrections of the background:

$$\begin{aligned}\delta\varphi(z) = -\int \mathrm{d}z'\, \mathcal{M}_{\hat{\Phi}}(\varphi_0; z, z')\Big(&\Pi_{\hat{\Phi}}(\varphi_0; z')\varphi_0(z') + \Pi_{(A_4,G)}(\varphi_0; z')\varphi_0(z') \\ &- \frac{1}{2}\Pi_{(\bar{\eta},\eta)}(\varphi_0; z')\varphi_0(z') + \frac{1}{\hbar}(\Box\varphi_0 - U'(\varphi_0; z'))\Big)\end{aligned} \tag{4.2.119}$$

and the different contributions in the exponent of the decay rate are now

$$\mathcal{B}^{(0)} = B, \tag{4.2.120}$$

$$\mathcal{B}^{(1)} = B^{(1)}_{\hat{\Phi}} + B^{(1)}_{(A_4,G)} - \frac{1}{2} B^{(1)}_{(\bar{\eta},\eta)}, \tag{4.2.121}$$

$$\mathcal{B}^{(2)} = - B^{(2)}, \tag{4.2.122}$$

with

$$B^{(2)} = -\frac{1}{2}\left(B^{(2)}_{\hat{\Phi}} + B^{(2)}_{(A_4,G)} - \frac{1}{2} B^{(2)}_{(\bar{\eta},\eta)} \right) - \frac{1}{2\hbar} B^{(1)}, \tag{4.2.123}$$

all else remaining the same as before, so that we only need to plug the $\mathcal{B}$'s into Eq. (4.2.108).

4.2.3 The homogeneous background or CW potential contributions

With the objective of renormalizing the theory and incidentally obtaining a comparison reference for the sizes of the gradient effects, we dedicate this passage to the computation of the CW potential associated with the model in our study case. In the process of deriving the CW potential, we will obtain the corresponding expressions to the Green's functions over an assumed homogeneous background. We solve the Green's equation of the fluctuation operators by direct integration of its Fourier transforms over all directions, which is possible if we keep the background field fixed. After the integration is performed, we can substitute the actual background configuration for the auxiliary fixed value. We will denote such Green's functions by a subscript $\bullet_{\rm hom}$, and for a given sector X they are specifically

$$\mathcal{M}^{-1}_{X;\mathbf{k};\rm hom}(\phi; z, z') = \int \frac{\mathrm{d}k_4}{2\pi}\, \mathrm{e}^{\mathrm{i}k_4(z-z')}(\mathbf{k}^2 + k_4^2 + \mathbf{m^2_X}(\phi)), \tag{4.2.124}$$

where the bold mass term is a place-holder for the effective mass matrix of the X sector. For the choice made in the previous subsection, we have the following effective masses for the three sectors of the model:

$$\begin{aligned} m^2_{\hat{\Phi}}(\phi) &= \alpha + 3\lambda\phi^2 + \frac{15\lambda_6}{4}\phi^4, \\ \mathbf{m^2_{(A_4,G)}}(\phi) &= \begin{pmatrix} g^2\phi^2 & 0 \\ 0 & \alpha + \lambda\phi^2 + \frac{3\lambda_6}{4}\phi^4 + g^2\phi^2 \end{pmatrix}, \\ m^2_{(\bar{\eta},\eta)}(\phi) &= g^2\phi^2. \end{aligned} \tag{4.2.125}$$

The Fourier transform makes the problem of solving for the Green's function a simple algebraic equation and thus

$$\mathcal{M}_{X;\mathbf{k};\rm hom}(\phi; z, z') = \int \frac{\mathrm{d}k_4}{2\pi}\, \mathrm{e}^{\mathrm{i}k_4(z-z')} \frac{1}{\mathbf{k}^2 + k_4^2 + \mathbf{m^2_X}(\phi)} \tag{4.2.126}$$

which after integration and then substitution of ϕ for φ_0 and taking the coincident limit, we have

$$\mathcal{M}_{X;\mathbf{k};\rm hom}(\phi; z, z) = \frac{1}{2\sqrt{\mathbf{k}^2 + \mathbf{m^2_X}(\varphi_0(z))}}. \tag{4.2.127}$$

We can now use these expressions for the Green's functions in the coincident limit to compute the functional determinants as we have shown in Eq. (2.2.49), via deformations of the operators, $\mathbf{k}^2 \to \mathbf{k}^2 + s$:

$$\begin{aligned}\int \mathrm{d}^4x\, U^{(1)}_{\mathrm{CW},X}(\varphi_0) \equiv& \frac{1}{2}V \int \frac{\mathrm{d}^3\mathbf{k}}{(2\pi)^3} \log \frac{\det \mathcal{M}^{-1}_{X;\mathbf{k};\mathrm{hom}}(\varphi_0)}{\det \mathcal{M}^{-1}_{X;\mathbf{k};\mathrm{hom}}(\varphi_0)} \\ =& -\frac{1}{2}\,\mathrm{tr} \int \mathrm{d}^4x \int_0^\infty \mathrm{d}s\, \mathcal{M}_{X;\sqrt{\mathbf{k}^2+s};\mathrm{hom}}(\varphi_0; z, z) - \mathcal{M}_{X;\sqrt{\mathbf{k}^2+s};\mathrm{hom}}(0; z, z).\end{aligned} \tag{4.2.128}$$

We can collect all sectors and the definition above to write the full CW potential extending it to any φ value:

$$\begin{aligned} U^{(1)}_{\mathrm{CW}}(\varphi) =& U^{(1)}_{\mathrm{CW},\hat{\Phi}}(\varphi) + U^{(1)}_{\mathrm{CW},(A_4,G)}(\varphi) + U^{(1)}_{\mathrm{CW},(\bar{\eta},\eta)}(\varphi), \\ U^{(1)}_{\mathrm{CW},X}(\varphi) =& \frac{1}{2}\,\mathrm{tr} \int \frac{\mathrm{d}^4k}{(2\pi)^4} \log\left(\frac{k^2 + \mathbf{m}^{\mathbf{2}}_{\mathbf{X}}(\varphi)}{k^2 + \mathbf{m}^{\mathbf{2}}_{\mathbf{X}}(0)}\right). \end{aligned} \tag{4.2.129}$$

Having the CW potential, we can define the homogeneous version of the tadpole functions, which will be useful when comparing with the gradient effects

$$\Pi_{X;\mathrm{hom}}(\varphi; z)\varphi(z) = \frac{\partial U^{(1)}_{\mathrm{CW},X}(\varphi(z))}{\partial \varphi(z)}. \tag{4.2.130}$$

4.2.4 Renormalizing with MS-scheme

As it is known from the QFT framework, quantities containing radiative corrections from the inclusion of loops are generally divergent, and we must consider renormalizing the theory if we expect to obtain finite physical results. In this study, although Green's functions at the coincident limit for a fixed $\mathbf{k}$ are finite, the complete Green's functions, meaning, after summing over all $\mathbf{k}$, are not. In this section, we follow a similar renormalization scheme to the one described in Sec.1.3.2. Given that we are forced to stop numerical computations at some finite $\mathbf{k}$, it seems natural to use the same hard-cutoff procedure for renormalization. This, together with a gradient expansion method, will suffice to remove all dependencies on the cutoff of our quantities of interest.

The renormalization prescription is split into two pieces, as we have seen in Part.I. The first uses the homogeneous solutions to the Green's equations for every sector to obtain analytical expressions displaying the explicit cutoff dependence, after which we can impose any desired renormalization conditions. The second part involves a gradient expansion method to extract the divergent terms proportional to the wavefunction kinetic term. It must be said that our methodology for numerically finding the Green's functions does not rely on a gradient expansion, implying that the renormalized quantities later obtained contain all derivative corrections to this order in the semi-classical expansion, independently of whether the renormalization procedure does employ a gradient expansion to extract divergences. This last piece of the renormalization procedure led to an independent consideration of the usefulness of such tools to estimate gradient effects not only for a gauge sector but scalar and fermion sectors as well as will be expanded at the end of the chapter.

We begin by introducing counterterms for the wavefunction and for the couplings, namely for the masses and the interactions. In addition, since the potential chosen is not renormalizable, we must include an extra counterterm corresponding to interactions of order 8.

The part of the Lagrangian density containing said local counterterms looks like

$$\mathcal{L}_{\rm ct}[\varphi] = \frac{1}{2}\delta Z(\partial\varphi)^2 + \frac{\delta\alpha}{2}\varphi^2 + \frac{\delta\lambda}{4}\varphi^4 + \frac{\delta\lambda_6}{8}\varphi^6 + \frac{\delta\lambda_8}{16}\varphi^8. \tag{4.2.131}$$

The counterterms can, in turn, be decomposed per sector to study how the different sectors might contribute up to one-loop corrections to the decay rate. With $X \in \{\hat{\Phi}, (A_4, G), (\bar{\eta}, \eta)\}$ we have

$$\mathcal{L}_{\rm ct}[\varphi] = \sum_X \mathcal{L}_{{\rm ct},X}[\varphi] = \sum_X \left(\frac{1}{2}\delta Z_X(\partial\varphi)^2 + \frac{\delta\alpha_X}{2}\varphi^2 + \frac{\delta\lambda_X}{4}\varphi^4 + \frac{\delta\lambda_{6,X}}{8}\varphi^6 + \frac{\delta\lambda_{8,X}}{16}\varphi^8\right). \tag{4.2.132}$$

We can now construct the renormalized term $\mathcal{B}^{(1)\rm ren}$ by adding all renormalized $B^{(1)}$'s as follows:

$$\begin{aligned}\mathcal{B}^{(1)\rm ren} &= B^{(1)\rm ren}_{\hat{\Phi}} + B^{(1)\rm ren}_{(A_4,G)} - \frac{1}{2}B^{(1)\rm ren}_{(\bar{\eta},\eta)} \\ &= B^{(1)}_{\hat{\Phi}} + B^{(1)}_{(A_4,G)} - \frac{1}{2}B^{(1)}_{(\bar{\eta},\eta)} + \int \mathrm{d}^4x\, \mathcal{L}_{\rm ct}[\varphi_0] \equiv \sum_X g_X B^{(1)\rm ren}_X,\end{aligned} \tag{4.2.133}$$

where the coefficients of the linear combination in the last line are obtained after our gauge choice and simplification explained in Subsec. 4.2.2,

$$g_{\hat{\Phi}} = g_{(A_4,G)} = -2g_{(\bar{\eta},\eta)} = 1. \tag{4.2.134}$$

For each sector, we work with integrals that are finite, i.e., independent of the cutoff. This we build in what follows by means of the addition and subtraction from appropriate "reference" homogeneous Green's functions and by introducing an auxiliary kernel that emulates the wavefunction divergence. We explain such a strategy now.
Consider adopting the following cutoffs for the equation resulting of combining Eqs. (4.2.94) and (2.2.49):

$$g_X B^{(1)\rm ren}_X = \int \mathrm{d(Ps)}\ \mathrm{tr}\left(\mathcal{M}_{X;\sqrt{\mathbf{k}^2+s}}(\varphi_0; z, z) - \mathcal{M}_{X;\sqrt{\mathbf{k}^2+s}}(0; z, z)\right) + \int \mathrm{d}^4x\, \mathcal{L}_{{\rm ct},X}[\varphi_0], \tag{4.2.135}$$

where

$$\int \mathrm{d(Ps)} = -\frac{1}{2}\int \mathrm{d}^4x \int_0^{\Lambda_s^2} \mathrm{d}s \int_{B_\Lambda} \frac{\mathrm{d}^3\mathbf{k}}{(2\pi)^3} \tag{4.2.136}$$

We must be careful when using the formulas above for numerical computation since there are different ways in which one could impose the limits of the integrals. We adopt the following convention, which proves to give robust results: the integral over k_4 has been performed from $-\infty$ to ∞, while the integral over $\mathrm{d}^3\mathbf{k}$ will be done assuming spherical symmetry and over a ball B_Λ with radius Λ and similarly the integration over s from 0 to Λ_s^2 which in practice should be taken at least to be $\Lambda^2/2$ and ideally $\Lambda_s \gg \Lambda$. In this sense, we must only choose Λ large enough to ensure that the results are cutoff-independent.
We note that the homogeneous deformed Green's function $\mathcal{M}_{X;\sqrt{\mathbf{k}^2+s};\rm hom}$, matches the numerical solution for the deformed Green's function at false vacuum $\mathcal{M}_{X;\sqrt{\mathbf{k}^2+s}}(0; z, z)$ and is real. Observing as well that the gradient effects can be isolated if we add and

subtract the real part of the homogeneous Green's functions evaluated at the bounce background, $\mathfrak{Re}\mathcal{M}_{X;\sqrt{\mathbf{k}^2+s};\mathrm{hom}}(\varphi_0;z,z)$, we write

$$\begin{aligned} g_X B_X^{(1)\mathrm{ren}} = & \\ & \int \mathrm{d(Ps)}\ \mathrm{tr}\left[\mathcal{M}_{X;\sqrt{\mathbf{k}^2+s}}(\varphi_0;z) - \mathfrak{Re}\mathcal{M}_{X;\sqrt{\mathbf{k}^2+s};\mathrm{hom}}(\varphi_0;z)\right] - K_{s,X}(\mathbf{k})(\partial_z\varphi_0)^2 \\ & + \int \mathrm{d(Ps)}\ \mathrm{tr}\left[\mathfrak{Re}\mathcal{M}_{X;\sqrt{\mathbf{k}^2+s};\mathrm{hom}}(\varphi_0;z) - \mathcal{M}_{X;\sqrt{\mathbf{k}^2+s};\mathrm{hom}}(0;z)\right] \\ & + \int \mathrm{d(Ps)}\, K_{s,X}(\mathbf{k})(\partial_z\varphi_0)^2 + \int \mathrm{d}^4x\, \mathcal{L}_{\mathrm{ct},X}[\varphi_0]. \end{aligned} \tag{4.2.137}$$

where each line is actually cutoff-independent and the in so far unknown kernel $K_{s,X}(\mathbf{k})$ is to be found by demanding that it captures the contributions to the wave-function divergence, i.e., its kinetic term, mathematically

$$\Gamma[\varphi_0] \supset -\int \mathrm{d}^4x\, \frac{1}{2}\delta Z_X(\partial_\mu\varphi_0)^2 = \int \mathrm{d(Ps)}\, K_{s,X}(\mathbf{k})(\partial_z\varphi_0)^2 + \int \mathrm{d}^4x\,(\mathrm{finite}). \tag{4.2.138}$$

We can understand Eq. (4.2.137) by noticing that the first line includes the isolated effects of the gradients, the middle line is nothing else but the CW contributions as computed in Eq. (4.2.128) and the last line takes care of renormalizing the divergences occurring in the previous lines. We employ the following notation

$$g_X B_X^{(1)\mathrm{ren}} = g_X B_X^{(1)\mathrm{ren,hom}} + g_X B_X^{(1)\mathrm{ren,grad}}, \tag{4.2.139}$$

to refer to either the renormalized homogeneous or gradient effects contributions, where

$$\begin{aligned} g_X B_X^{(1)\mathrm{ren,hom}} &= V \int \mathrm{d}z\, \mathfrak{Re}\, U_{\mathrm{CW},X}^{(1)\mathrm{ren}}(\varphi_0(z)), \\ g_X B_X^{(1)\mathrm{ren,grad}} &= \int \mathrm{d(Ps)} K_{s,X}(\mathbf{k})(\partial_z\varphi_0(z))^2 + \frac{V}{2}\int \mathrm{d}z\, \delta Z_X(\partial_z\varphi_0(z))^2 \\ &+ \int \mathrm{d(Ps)}\, \mathrm{tr}\left[\mathcal{M}_{X;\sqrt{\mathbf{k}^2+s}}(\varphi_0;z) - \mathfrak{Re}\mathcal{M}_{X;\sqrt{\mathbf{k}^2+s};\mathrm{hom}}(\varphi_0;z)\right] - K_{s,X}(\mathbf{k})(\partial_z\varphi_0(z))^2. \end{aligned} \tag{4.2.140}$$

We can now see that the job of $K_{s,X}(\mathbf{k})$ is to render the first line of $g_X B_X^{(1)\mathrm{ren,\ grad}}$ equal to zero and thus letting us read the renormalized gradient effects from the second line, which we can actually obtain numerically it being finite.

Unfortunately, the renormalization procedure is not over and we must ensure that the order $\hbar^2$-contributions to the effective action do not present any divergences. We need only recognize that possible divergences in the two-loop contributions are inherited from divergent tadpole functions. Hence obtaining renormalized tadpole functions and writing down the quantum corrections to the bounce in terms of renormalized tadpole functions enables us to get renormalized $\hbar^2$-contributions to the effective action as desired.

The renormalized tadpole functions can then be obtained by functional differentiation as done before, however from the renormalized effective action instead, or put differently, functionally differentiating the Lagrangian density piece having the counterterms. We

arrive to

$$(\Pi_X(\varphi_0;z)\varphi_0(z))^{\rm ren} = \Pi_X(\varphi_0;z)\varphi_0(z) - \delta Z_X \Box\varphi_0(z) + \delta\alpha_X\,\varphi_0(z) + \delta\lambda_X\,\varphi_0(z)^3 + \frac{3\delta\lambda_{6,X}}{4}\,\varphi_0(z)^5 + \frac{\delta\lambda_{8,X}}{2}\,\varphi_0(z)^7. \tag{4.2.141}$$

We can replace the bare tadpole functions appearing in Eq. (4.2.119) for their renormalized versions defined through the formula above, that is

$$\delta\varphi^{\rm ren}(z) = \int \mathrm{d}z'\,\mathcal{M}_{\hat\Phi}(\varphi_0;z,z')\left[\frac{1}{\hbar}(\Box\varphi_0 - U'(\varphi_0;z')) - \sum_X g_X(\Pi_X(\varphi_0;z')\varphi_0(z'))^{\rm ren}\right], \tag{4.2.142}$$

which renormalizes the following two terms in the effective action, as we seek

$$\begin{aligned} B^{(1)\rm ren} =& V\int \mathrm{d}z\,\delta\varphi^{\rm ren}(z)(-\Box\varphi_0 + U'(\varphi_0;z)),\\ B_X^{(2)\rm ren} =& V\int dz\,\delta\varphi^{\rm ren}(z)\,(\Pi_X(\varphi_0;z)\varphi_0(z))^{\rm ren}. \end{aligned} \tag{4.2.143}$$

Collecting all the sectors and using the compressed notation of Eq. (4.2.123) we have simply

$$\mathcal{B}^{(2)\rm ren} = -\,B^{(2)\rm ren} = -\frac{1}{2}\left(B_{\hat\Phi}^{(2)\rm ren} + B_{(A_4,G)}^{(2)\rm ren} - \frac{1}{2}B_{(\bar\eta,\eta)}^{(2)\rm ren}\right) - \frac{1}{2\hbar}B^{(1)\rm ren}. \tag{4.2.144}$$

This almost finishes the renormalization framework. We have only one last task: finding explicit expressions for the counterterms and the missing kernel $K_{s,X}(\mathbf{k})$, which we do in the following subsection.

Counterterms for the interaction couplings

As shown in the mathematical background, we can obtain explicit expressions for the counterterms by considering the CW potential and adopting a renormalization scheme, namely imposing certain renormalization conditions. Recall the expression of the CW potential, evaluated at a constant field configuration ϕ:

$$\begin{aligned} \Gamma_{\rm CW}[\phi] = \int \mathrm{d}^4x\,U_{\rm CW} = S[\phi] + \frac{\hbar}{2}V\int\frac{\mathrm{d}^3\mathbf{k}}{(2\pi)^3}\,\log\frac{\det\mathcal{M}^{-1}_{\hat\Phi;\mathbf{k}}(\phi)}{\det\mathcal{M}^{-1}_{\hat\Phi;\mathbf{k}}(0)}\\ + \frac{\hbar}{2}V\int\frac{\mathrm{d}^3\mathbf{k}}{(2\pi)^3}\log\frac{\det\mathcal{M}^{-1}_{(A_4,G);\mathbf{k}}(\phi)}{\det\mathcal{M}^{-1}_{(A_4,G);\mathbf{k}}(0)} + \frac{\hbar}{2}V\int\frac{\mathrm{d}^3\mathbf{k}}{(2\pi)^3}\log\frac{\det\mathcal{M}^{-1}_{(\bar\eta,\eta);\mathbf{k}}(\phi)}{\det\mathcal{M}^{-1}_{(\bar\eta,\eta);\mathbf{k}}(0)}. \end{aligned} \tag{4.2.145}$$

As we have seen, the log det terms can be computed in the homogeneous field approximation through Eq. (4.2.128). We need to regularize each one of these terms, which we do by following the same convention as the one described in the previous section for the limits of integration (see the comments after Eq. (4.2.135)). The renormalized CW potential is

$$\begin{aligned} U_{\rm CW}^{\rm ren}(\phi) &= U_{\rm CW} - U_{\rm ct}\\ &= U(\phi) + U^{(1)}_{{\rm CW},\hat\Phi}(\phi) + U^{(1)}_{{\rm CW},(A_4,G)} + U^{(1)}_{{\rm CW},(\bar\eta,\eta)} + \frac{\delta\alpha}{2}\phi^2 + \frac{\delta\lambda}{4}\phi^4 + \frac{\delta\lambda_6}{8}\phi^6 + \frac{\delta\lambda_8}{16}\phi^8, \end{aligned} \tag{4.2.146}$$

with $U(\phi)$ the tree-level potential after the original scalar field has been expanded around the simplified bounce. When ignoring gradients, the effective masses are all diagonal, and we can recognize the following three types of integrals

$$\begin{aligned} I_1 &\equiv \frac{\hbar}{2}\int_{B_\Lambda}\frac{\mathrm{d}^3\mathbf{k}}{(2\pi)^3}\int_{-\infty}^{\infty}\frac{\mathrm{d}k_4}{2\pi}\log\frac{k_4^2+\mathbf{k}^2+U''(\phi)}{k_4^2+\mathbf{k}^2+U''(0)},\\ I_2 &\equiv \hbar\int_{B_\Lambda}\frac{\mathrm{d}^3\mathbf{k}}{(2\pi)^3}\int_{-\infty}^{\infty}\frac{\mathrm{d}k_4}{2\pi}\log\frac{k_4^2+\mathbf{k}^2+g^2\phi^2}{k_4^2+\mathbf{k}^2},\\ I_3 &\equiv \frac{\hbar}{2}\int_{B_\Lambda}\frac{\mathrm{d}^3\mathbf{k}}{(2\pi)^3}\int_{-\infty}^{\infty}\frac{\mathrm{d}k_4}{2\pi}\log\frac{k_4^2+\mathbf{k}^2+\alpha+\lambda\phi^2+\frac{3\lambda_6}{4}\phi^4+g^2\phi^2}{k_4^2+\mathbf{k}^2+\alpha}, \end{aligned} \tag{4.2.147}$$

corresponding to the different field sectors in the following combination:

$$U^{(1)}_{\mathrm{CW},\hat{\Phi}} = I_1, \quad U^{(1)}_{\mathrm{CW},(A_4,G)} = \frac{1}{2}I_2 + I_3, \quad U^{(1)}_{\mathrm{CW},(\bar{\eta},\eta)} = \frac{1}{2}I_2. \tag{4.2.148}$$

The integrals can be carried out analytically to arrive at the following expressions (see Eq. (1.3.150) for more details)

$$\begin{aligned} I_1 &= \hbar\left[\frac{\Lambda^2}{16\pi^2}U''(\phi)+\frac{1}{64\pi^2}(U''(\phi))^2\left(\frac{1}{2}+\ln\frac{U''(\phi)}{4\Lambda^2}\right)\right]-(\phi\leftrightarrow 0)+\mathcal{O}\left(\frac{1}{\Lambda}\right),\\ I_2 &= 2\hbar\left[\frac{\Lambda^2}{16\pi^2}g^2\phi^2+\frac{1}{64\pi^2}g^4\phi^4\left(\frac{1}{2}+\ln\frac{g^2\phi^2}{4\Lambda^2}\right)\right]+\mathcal{O}\left(\frac{1}{\Lambda}\right),\\ I_3 &= \hbar\left[\frac{\Lambda^2}{16\pi^2}\left(\alpha+\lambda\phi^2+\frac{3\lambda_6}{4}\phi^4+g^2\phi^2\right)+\frac{1}{64\pi^2}\left(\alpha+\lambda\phi^2+\frac{3\lambda_6}{4}\phi^4+g^2\phi^2\right)^2\times\right.\\ &\quad\left.\times\left(\frac{1}{2}+\ln\frac{\alpha+\lambda\phi^2+\frac{3\lambda_6}{4}\phi^4+g^2\phi^2}{4\Lambda^2}\right)\right]-(\phi\leftrightarrow 0)+\mathcal{O}\left(\frac{1}{\Lambda}\right). \end{aligned} \tag{4.2.149}$$

In this form, it is easy to recognize the divergent pieces, which we see go as Λ^2 and $\log\Lambda$. We will remove this capturing their divergences in the coupling counterterms within a minimal subtraction scheme (MS), where we do not include any finite parts but only a renormalization scale μ accompanying the logs as we have seen in Subsec. 1.3.2. A renormalized CW potential has then the expression

$$U^{\mathrm{ren}}_{\mathrm{CW}}(\phi) = U_{\mathrm{CW}}(\phi) - U_{\mathrm{ct}}(\phi) = U_{\mathrm{CW}}(\phi) - \Lambda^2 C_1(\phi) - \log\left(\frac{\Lambda}{\mu}\right)C_2(\phi), \tag{4.2.150}$$

where we must pick C_1 and C_2 as the coefficients of the diverging pieces, if we want the cancellation to occur. To obtain the coupling counterterms explicitly, it suffices to compare Eqs. (4.2.147) and (4.2.150), by taking derivatives with respect to ϕ and evaluating at $\phi = 0$ we find:

$$\begin{aligned} \delta\alpha &= \frac{1}{8\pi^2}\left[\alpha\left(g^2+4\lambda\right)\log\left(\frac{\Lambda}{\mu}\right)-\Lambda^2\left(3g^2+4\lambda\right)\right],\\ \delta\lambda &= -\frac{1}{8\pi^2}\left[9\lambda_6\Lambda^2-\log\left(\frac{\Lambda}{\mu}\right)\left(9\alpha\lambda_6+3g^4+2g^2\lambda+10\lambda^2\right)\right],\\ \delta\lambda_6 &= \frac{3}{8\pi^2}\left(g^2+16\lambda\right)\lambda_6\log\left(\frac{\Lambda}{\mu}\right),\\ \delta\lambda_8 &= \frac{117}{16\pi^2}\lambda_6^2\log\left(\frac{\Lambda}{\mu}\right). \end{aligned} \tag{4.2.151}$$

We note, we opted for this scheme as opposed to "on-shell like" renormalization schemes, e.g., where one instead imposes renormalization conditions on the effective potential directly, as done in the previous studies [30, 31], because of the simplicity of the expressions for the counterterms in this scheme.
It is useful to compute not only a total tadpole function but a per-sector tadpole function to be able to distinguish the contributions from the different fields involved. To that end, we also need to calculate counterterms for each sector separately. Luckily we can do this easily by following the same steps as above, except that we consider only the CW potential of the sector of interest, that is, we start with $U^{(1)}_{\mathrm{CW,X}}$ and find $C_{1,X}$ and $C_{2,X}$ similarly as above and then we cast such coefficients into a polynomial on ϕ to get

$$\begin{aligned}
\delta\alpha_{\hat{\Phi}} &= \frac{1}{8\pi^2}\left[3\alpha\lambda\log\left(\frac{\Lambda}{\mu}\right) - 3\lambda\Lambda^2\right], \\
\delta\alpha_{(A_4,G)} &= \frac{1}{8\pi^2}\left[\alpha\left(g^2+\lambda\right)\log\left(\frac{\Lambda}{\mu}\right) - \Lambda^2\left(2g^2+\lambda\right)\right], \\
\delta\alpha_{(\bar{\eta},\eta)} &= \frac{-g^2\Lambda^2}{8\pi^2},
\end{aligned} \tag{4.2.152}$$

for the mass or quadratic coupling,

$$\begin{aligned}
\delta\lambda_{\hat{\Phi}} &= \frac{3}{16\pi^2}\left[\left(5\alpha\lambda_6 + 6\lambda^2\right)\log\left(\frac{\Lambda}{\mu}\right) - 5\lambda_6\Lambda^2\right], \\
\delta\lambda_{(A_4,G)} &= \frac{1}{16\pi^2}\left[\left(3\alpha\lambda_6 + 4g^2\lambda + 4g^4 + 2\lambda^2\right)\log\left(\frac{\Lambda}{\mu}\right) - 3\lambda_6\Lambda^2\right], \\
\delta\lambda_{(\bar{\eta},\eta)} &= \frac{g^4}{8\pi^2}\log\left(\frac{\Lambda}{\mu}\right),
\end{aligned} \tag{4.2.153}$$

for the quartic self-interaction coupling,

$$\delta\lambda_{6,\hat{\Phi}} = \frac{45}{8\pi^2}\lambda\lambda_6\log\left(\frac{\Lambda}{\mu}\right), \quad \delta\lambda_{6,(A_4,G)} = \frac{3}{8\pi^2}\lambda_6\left(g^2+\lambda\right)\log\left(\frac{\Lambda}{\mu}\right), \quad \delta\lambda_{6,(\bar{\eta},\eta)} = 0, \tag{4.2.154}$$

for the power six self-interaction coupling and

$$\delta\lambda_{8,\hat{\Phi}} = \frac{225}{32\pi^2}\lambda_6^2\log\left(\frac{\Lambda}{\mu}\right), \quad \delta\lambda_{8,(A_4,G)} = \frac{9}{32\pi^2}\lambda_6^2\log\left(\frac{\Lambda}{\mu}\right), \quad \delta\lambda_{8,(\bar{\eta},\eta)} = 0 \tag{4.2.155}$$

for the additional power eight counterterm. As was described when introducing renormalization, we can keep the logarithms small if we choose a scale μ close to the numerator of the argument of the logarithms, in this case, the cutoff scale Λ. Additionally, we should mention that we do not employ an RG improved potential, so although the couplings run with the scale, we will neglect such behavior and employ the bare quantities for this study.

4.2.5 Wavefunction renormalization

Besides the coupling counterterms, it is also required that we subtract the divergences that are proportional to the kinetic terms that may appear from the higher-order contributions. We will do this by employing a gradient expansion, collecting in this way all terms that contribute to the wavefunction renormalization. As it was known for the toy ϕ^4 model and shown in [31] too, the one-loop contributions from one-loops with scalars running in the loop do not lead to terms proportional to $(\partial_\mu\phi)^2$ that are divergent. Therefore, we

focus on the other possibility; that the gauge-Goldstone sector might be responsible for possible divergent pieces adding to the wavefunction renormalization.
We refer the reader to the last section 4.3 of this chapter for the details on how to obtain the kernel $K_{s,(A_4,G)}$ using the methods described therein. We obtain the following integral kernel for removing the wavefunction renormalization divergences,

$$K_s(\mathbf{k}) \equiv K_{s,(A_4,G)}(\mathbf{k}) = \frac{g^2}{(m_A^2 - m_G^2)} \left(\frac{1}{(m_G^2 + \mathbf{k}^2 + s)^{3/2}} - \frac{1}{(m_A^2 + \mathbf{k}^2 + s)^{3/2}} \right), \tag{4.2.156}$$

which can be used in Eq. (4.2.137) to obtain finite one-loop contributions. We can define with it a wavefunction renormalization counterterm by reading the corresponding coefficient in the effective action:

$$\Gamma[\varphi_0] \supset -\frac{1}{2} \int \mathrm{d}^4x \int_0^\infty \mathrm{d}s \frac{\mathrm{d}^3p}{(2\pi)^3} K_s(\mathbf{k}) (\partial_z \varphi_0)^2 = -\frac{1}{2} \int \mathrm{d}^4x \left(\frac{g^2}{4\pi^2} \log(\Lambda^2) (\partial_z \varphi_0)^2 + \text{finite} \right), \tag{4.2.157}$$

hence we obtain

$$\delta Z = \delta Z_{(A_4,G)} = \frac{g^2}{4\pi^2} \log \frac{\Lambda^2}{\mu^2}, \tag{4.2.158}$$

which accounts for all divergences associated with derivative terms.

4.2.6 Implementation details and Results

After describing the general framework for including the gradient effects of the background, it is desirable to implement the computation for a given set of parameters explicitly. Given the large amount of computation time required to complete the program, we present the results for a single fixed set of parameters which we take as a benchmark.
We give here some more details concerning the computation of the results presented. First, we remind the reader of the assumptions made to arrive at the present results. We have employed the thin-wall approximation which, is valid for potentials exhibiting degenerate minima and lets us ignore linear derivatives (dissipation within the mechanical analogy). We have also employed the planar-wall approximation, which is valid for large enough bubbles where the curvature of the wall does not play a crucial role; this allowed us to treat the radial direction as if it were a flat coordinate. We have then constructed what we called a simplified bounce configuration, φ_0, with boundary conditions such that for $z \to -\infty$ the field is at true vacuum, and at $z \to +\infty$, it sits at false vacuum. Nonetheless, this must be ensured at the one-loop level in the case the degeneracy is broken by loop contributions, thus raising/lowering either of the minima. The effective action would display infinite contributions from the log det terms in the planar-wall limit when approaching true vacuum ($z \to -\infty$), no matter how tiny the difference in energy is with respect to the false vacuum. Therefore we have chosen benchmark parameters where the degeneracy holds as well for the renormalized CW potential (see Fig. 4.5). In general, having degeneracy at tree-level only translates to the degeneracy of the minima in the one-loop effective potential if there is a symmetry enforcing this, as was the case in previous studies [30, 31]. We remark again that this is a requisite only within the planar-wall approximation, without which there are no such issues when integrating over the whole volume.
We adopt units in which $\hbar = 1$, which translates to dimensionless actions. We can also assume that we have chosen the fields and the spacetime coordinates such that the couplings are of order one. Giving all the above comments, we implemented the self-consistent

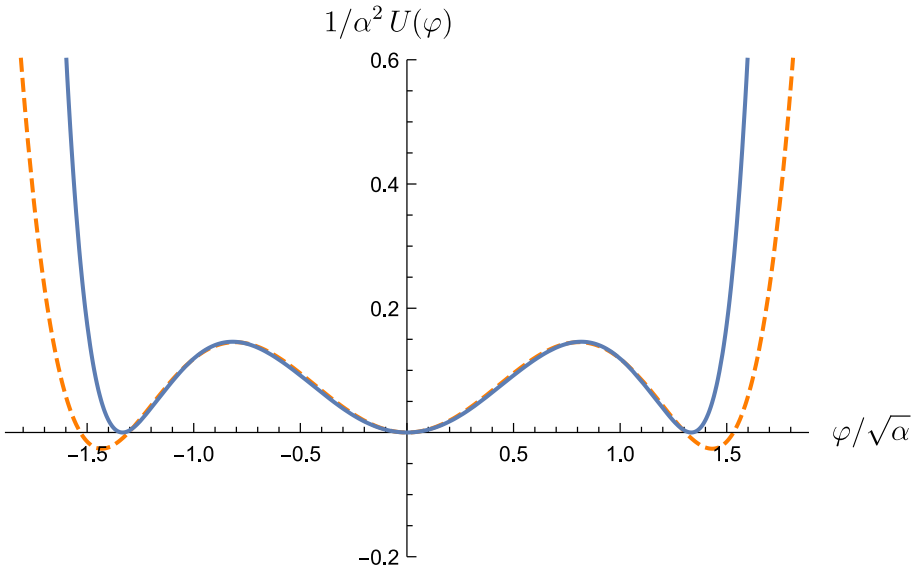

Figure 4.5: Tree-level potential (orange) and real part of the renormalized CW-potential for the benchmark parameters in Eq. (4.2.159) and the cutoff described in-text, chosen to keep the degeneracy of the minima. In particular, the model explores only the right quadrant of the plot as required by the $U(1)$-gauge symmetry.

Green's function program for the following values of the couplings:

$$\alpha = 2, \quad \lambda_6 = \frac{1}{2}, \quad \lambda = -2.0254571, \quad g = \frac{1}{2}, \quad \mu = \frac{1}{2}, \tag{4.2.159}$$

where λ was the only parameter tuned so that the vacua are degenerate at the CW-level. We express all the results of the computations in terms of the dimensionful coupling α. We have fixed a cutoff of $\Lambda = 49 = 34.65\sqrt{\alpha}$ and we have checked that the variation in the region enclosed by the vacua remains below $10^{-13}\alpha^2$ for different cutoffs. Hence we consider it cutoff-independent.

The followed procedure is consistent with the framework of effective field theory under the perspective that our current model can be the low energy theory of certain UV-completions. For a vacuum $\varphi_- \sim \sqrt{2}$, tunneling processes will correspond to field values $\varphi < \varphi_-$ for which we must explain the relevance of the operator $|\Phi|^6$ over higher-dimensional operators $|\Phi|^{2m}$ for $m > 3$, which we have neglected. We give an example of a UV theory that can lead to such a case. Consider the addition of two heavy Dirac fermions ψ and χ, where the former has no charge with respect to the $U(1)$ and the latter has a charge of -1. We can write down a Yukawa type interaction as

$$\mathcal{L}_{\text{heavy}} \supset -y\bar{\Psi}\Phi\chi + \text{c.c.} \tag{4.2.160}$$

Denote the mass of the heavy fermion by M and consider one-loop diagrams with $2m$ insertions of Φ, these produce the following effective interaction

$$\lambda_{2m} \sim \frac{y^{2m}}{16\pi^2 M^{2(m-2)}}. \tag{4.2.161}$$

Relative to the power six operator we used, $m > 3$ and $\varphi \leq \varphi_- \sim \sqrt{\alpha}$ we have

$$\left.\frac{\lambda_n|\Phi|^{2m}}{\lambda_6|\Phi|^6}\right|_{|\Phi|^2=\alpha} = \left(\frac{y\sqrt{\alpha}}{M}\right)^{2(m-3)}. \tag{4.2.162}$$

For the parameters in Eq. (4.2.159), the relation in Eq. (4.2.161) implies $M \sim y^3/(\sqrt{8}\pi)$ if we want to obtain a coupling λ_6 the size used in the numerical implementation. Inserting M in the previous equation together with $\alpha = 2$,

$$\left.\frac{\lambda_n|\Phi|^{2m}}{\lambda_6|\Phi|^6}\right|_{|\Phi|^2=\alpha=2} = \left(\frac{4\pi}{y^2}\right)^{2(m-3)}. \tag{4.2.163}$$

For a perturbative threshold $y < 4\pi$, we conclude that each operator of even and higher-dimension than six is suppressed by a factor of at least $\approx 1/10$, which indicates that we can indeed neglect higher-order operators.
Let us now come to the details of the simplified bounce configuration φ_0. Given that we want to consider the effective potential up to one-loop, we deem the easiest way to find the Green's functions is by employing a bounce configuration computed directly from the real part of the renormalized CW potential. Thus our to-be saddle point configuration must satisfy the bounce's equation of motion with the potential replaced by the renormalized CW potential and reads

$$-\frac{\mathrm{d}^2\varphi}{\mathrm{d}z^2} + \mathrm{Re}(U_{\mathrm{CW}}^{\mathrm{ren}})'(\varphi) = 0, \quad \varphi_0(z)|_{z\to\infty} = 0, \;\; \varphi_0'(z)\big|_{z\to-\infty} = 0. \tag{4.2.164}$$

We can observe that we have at this point already exchanged r with z so that the curvature of the wall is assumed to be flat(planar-wall). Moreover, in the actual implementation, we define the location of the wall to be the point of the field configuration with the steepest slope, which we then set to occur at $z = 0$. Before using the simplified bounce for the computation of any quantity, we transform the coordinate z into a compactified coordinate u, which is more practical for numerical computations. The results for the simplified bounce φ_0 and our benchmark parameters are shown in Fig. 4.6.

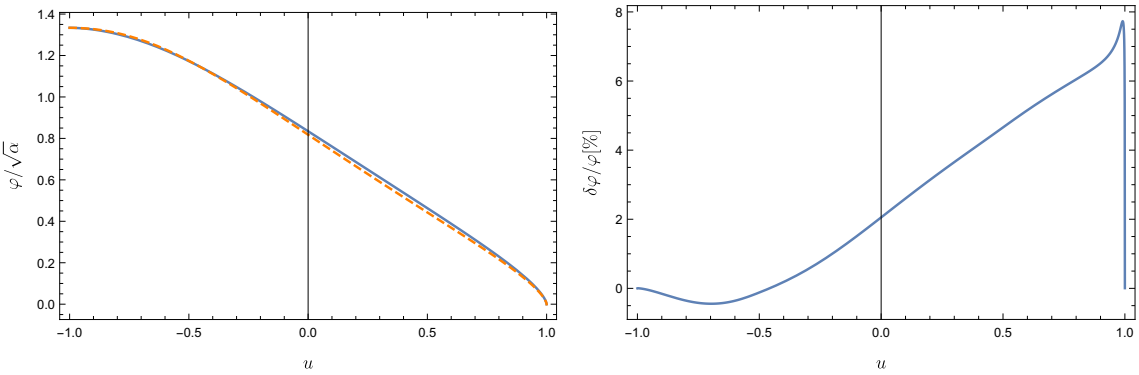

Figure 4.6: Left: Initial approximation to the bounce (dashed orange) and the version including gradient corrections arising from the self-energies computed above (solid blue). Right: relative variation of the bounce induced by gradient corrections.

The whole self-consistent Green's function prescription is implemented by choosing φ_0 as the background.

Solving for the Green's functions using numerical methods

We now take on the task of computing the Green's functions numerically. We employ a combination of methods that have been already partially discussed, together with a separation of momenta regimes. For instance, if we look at the fluctuations operators Eqs. (4.2.83), we realize we can separate the problem into two parts: the first one addresses

solving for the Green's functions for components that are diagonal, i.e., decoupled, the second, developing a different strategy for the remaining coupled sector (A_4, G).
For the components that are diagonal, the strategy followed what was described in Sec. 1.3.2 when explaining the WKB expansion. We exchange a two-point function problem by finding two one-point functions by means of the splitting procedure therein described while implementing appropriate gluing conditions, in our case: continuity and a discontinuity in the first derivative at the coincident point. Thanks to the planar wall assumption, the problem breaks down to a one-dimensional problem for a given value of $|\mathbf{k}|$, which we need to scan over. That is, for a fixed magnitude of the momentum parallel to the bubble walls, we can solve for these functions numerically by simply using straightforward differential equation solvers. We use, for example, `NDSolve` in Wolfram's Mathematica[97] and obtain good results. Some of the codes used for the following sections are collected in the Appendix B. We iterate such procedure for a wide range of $|\mathbf{k}|$, to be able to reconstruct the full Green's function of each diagonal sector.
We review the details of the strategy used to solve for the Green's function for the coupled (A_4, G) sector. After observing the form of the corresponding fluctuations operator $\mathcal{M}^{-1}_{(A_4,G);\mathbf{k}}$ in Eq. (4.2.109), we decide to separate the problem into two regimes. This separation is dictated by the size of the off-diagonal components of the operator.

Case $\mathbf{k}^2 \lesssim g\partial_z\varphi_0$

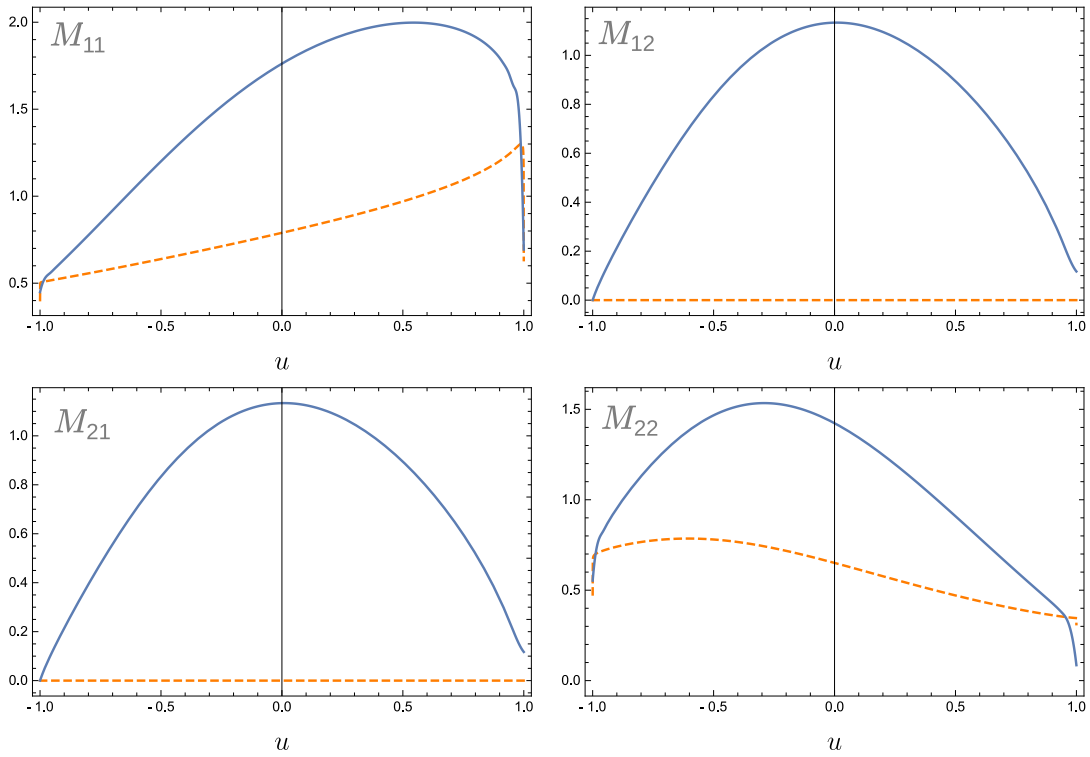

Figure 4.7: Coincident Green's functions of the (A_4, G) sector obtained by directly solving the coupled system numerically with $|\mathbf{k}| = 0.3$, as explained in the present section. The dashed orange line corresponds to the case with a homogeneous background, while the continuous blue line represents the correction to the homogeneous solution by the inclusion of gradients.

In this case, the terms appearing in the off-diagonal dominate the equation and a per-

turbative approach is bound to fail. This means that as long as $\mathbf{k}^2$ remains smaller than $g\partial_z\varphi_0(z)$, we are forced to attempt a direct numerical solution. Explicitly, we want to solve an equation of the form

$$\mathcal{M}^{-1}(z)\mathcal{M}(z,z') = \delta(z-z')\mathbb{1}_2. \tag{4.2.165}$$

To do so, we write down the matrix Green's function by components

$$\mathcal{M}(z,z') = \begin{pmatrix} M_{11}(z,z') & M_{12}(z,z') \\ M_{21}(z,z') & M_{22}(z,z') \end{pmatrix}, \tag{4.2.166}$$

and then further split each component at a given z' point with the aid of Heaviside step functions $\Theta(z)$,

$$M_{ij}(z,z') = \Theta(z-z')M_{ij}^R(z) + \Theta(z'-z)M_{ij}^L(z). \tag{4.2.167}$$

The problem has then been transformed to finding the two functions $M_{ij}^L(z)$ and $M_{ij}^R(z)$ for each component. We impose the following boundary conditions:

$$M_{ij}^L(-\infty) = M_{ij}^R(\infty) = 0, \tag{4.2.168a}$$

$$M_{ij}^L(z') = M_{ij}^R(z'), \tag{4.2.168b}$$

$$M_{ij}'^L(z') - M_{ij}'^R(z') = \frac{1}{1-z'^2}, \tag{4.2.168c}$$

where the first one has no consequence, since the normalization through the Wronskian defines the scale, and the second and third conditions follow from demanding continuity on the coincident point and integrating around the coincident point to obtain the discontinuity of the first derivative, respectively.
In the actual computer implementation, it is convenient to compactify the domain of all functions. To achieve this, we make use of the transformation

$$u = \tanh(z), \tag{4.2.169}$$

so that the working domain for all codes will be $[-1,1]$, with certain established tolerance when approaching the edges. As we have seen, certain quantities, such as determinants and tadpoles, only depend on the coincident limit, so instead of reconstructing the full functions, we take 1000 points for u' in the interval $[-1,1]$ at a distance of 10^{-5} from the edges and compute the above for each point. Hence we obtain all the entries of the matrix $\mathcal{M}(u,u')$ at $u=u'$. An example of the output of this procedure can be seen in Fig. 4.7, where the methodology is successful. A second example with a slightly larger value of $\mathbf{k}^2$ is also illustrated in Fig. 4.8, where it can already be witnessed how the method has trouble around the edges, such figure was produced for a value of $\mathbf{k}^2$ which is of the order $g\partial_z\varphi(z)$ for the parameters chosen (see Eq. 4.2.159).

Case $\mathbf{k}^2 \gtrsim g\partial_z\varphi_0$

Within this regime, the off-diagonal components are small relative to the momentum flowing parallel to the bubble wall, allowing us to use perturbative methods. To do this,

we decompose the fluctuations operator into a diagonal matrix piece and an off-diagonal piece, viz.

$$\mathcal{M}_0^{-1}(z) = \begin{pmatrix} M_{\mathbf{k}}^{-1}(\varphi_0(z)) & 0 \\ 0 & N_{\mathbf{k}}^{-1}(\varphi_0(z)) \end{pmatrix} \tag{4.2.170}$$

and

$$\delta\mathcal{M}^{-1}(z) = \begin{pmatrix} 0 & 2g(\partial_z\varphi_0) \\ 2g(\partial_z\varphi_0) & 0 \end{pmatrix}. \tag{4.2.171}$$

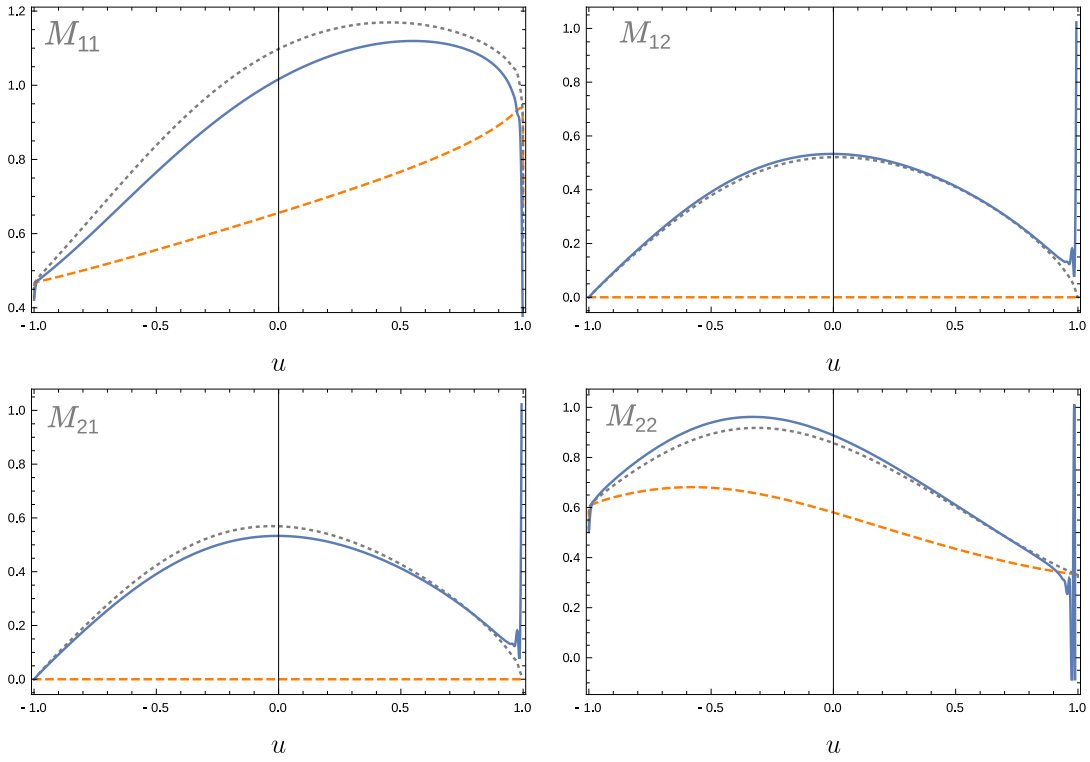

Figure 4.8: Coincident Green's functions of the (A_4, G) sector obtained with the two methods described in the text for $|\mathbf{k}| = 0.5$. The dashed orange line corresponds to the case with a homogeneous background, the continuous blue line represents the exact numerical solution of the previous subsection and the dotted line depicts the solutions obtained using the present perturbative methodology suitable for larger tangential momenta.

In this way, the fluctuations operator, which is just the sum of the above, can be solved by using a perturbative expansion and by using an Ansatz for the Green's function that consists of a series of progressively smaller terms, which we book-keep by ϵ. The expanded Green's function equation is then

$$(\mathcal{M}_0^{-1}(z) + \delta\mathcal{M}^{-1}(z))(\mathcal{M}^{(0)} + \epsilon\mathcal{M}^{(1)} + \epsilon^2\mathcal{M}^{(2)} + \cdots) = \delta(z - z')\mathbb{1}, \tag{4.2.172}$$

where we can collect terms of the same order assuming $\epsilon \sim \delta\mathcal{M}$, leading to an equation

for an arbitrary order in this perturbation expansion:

$$\begin{aligned}
\mathcal{M}_0^{-1}(z)\mathcal{M}^{(0)}(z,z') &= \delta(z-z'),\\
\mathcal{M}_0^{-1}(z)\mathcal{M}^{(1)}(z,z') + \delta\mathcal{M}^{-1}(z)\mathcal{M}^{(0)}(z,z') &= 0,\\
\mathcal{M}_0^{-1}(z)\mathcal{M}^{(2)}(z,z') + \delta\mathcal{M}^{-1}(z)\mathcal{M}^{(1)}(z,z') &= 0,\\
&\vdots\\
\mathcal{M}_0^{-1}(z)\mathcal{M}^{(n+1)}(z,z') + \delta\mathcal{M}^{-1}(z)\mathcal{M}^{(n)}(z,z') &= 0.
\end{aligned} \tag{4.2.173}$$

In our implementation of this algorithm, we can observe how the corrections coming from each iteration become smaller with each increasing order. We compute corrections for each value of $\mathbf{k}$ up to order n. This ensures the difference between the corrections of order n and $n-1$ differ by less than 10^{-5}. We observe when running the algorithms in our numerical implementation that the convergence es slower for values of $\mathbf{k}^2$ close to the threshold, but improve quickly with growing $\mathbf{k}^2$, which agrees with what is expected from a perturbation method based on a perturbation which remains constant while the diagonal keeps growing. A useful cross-check of the quality of our solutions has been the symmetry of the Green's function itself, meaning we know from the theory that $\mathcal{M}_{12} = \mathcal{M}_{21}$, such relation is violated slightly when the size of the diagonal terms approaches the size of the off-diagonal, which confirms that indeed this perturbation method ceases to work for low values of $\mathbf{k}^2$, a small deviation can thus be seen in the $\mathcal{M}_{12}$ and $\mathcal{M}_{21}$ components in Fig. 4.8.

We also illustrate the results for a higher value of $\mathbf{k}^2$ in Fig. 4.9, produced for the same benchmark set of parameters (Eq.(4.2.159)) after 14 iterations of the algorithm, there we can observe that the symmetry of the off-diagonal components is preserved and we include the 0-th order solutions for comparison.

The code for computing the Green's functions and dealing with the data output is included in the Appendix B. with a more extended explanation of how to use them.

In the final implementation, the code to obtain the Green's functions for this coupled-sector scans over the values of $|\mathbf{k}|$ starting at 0 up to $|\mathbf{k}_{\max}| = 50$ with variable spacing and using the threshold for the case described to be $|\mathbf{k}_{\text{thr}}| = 0.5$. For the values of $|\mathbf{k}| > |\mathbf{k}_{|rmthr}|$ we have observed that the number of iterations needed to achieve a given level of convergence decreases with increasing values of momenta along the wall. The scalar and ghost sectors pose no difficulties and can be solved with the direct method of Sec. 4.2.6. Then we are able to take the coincident limit for each of the sectors and obtain the deformed Green's function for every sector, $\mathcal{M}_{X;\sqrt{\mathbf{k}^2+s}}(\varphi_0)$. Afterwards we can use Eqs. 4.2.139 and 4.2.140 to get $B_X^{(1)\text{ren}}$.

In the practice the solutions are useful up to $|\mathbf{k}| \leq \Lambda 49 = 34.65\sqrt{\alpha}$ for the momentum parallel to the bubble's wall. The s integral can be performed without the need of new data up to $\Lambda_s^2 \sim \Lambda^2/2$ after which we extrapolate the behavior for high enough values of s with a power-law fit as to be able to perform the integral all the way up to $s \to \infty$ to ensure the validity of Eq. (2.2.49). Collecting all results for $B^{(1)\text{ren}}$ of all sectors, we get $\mathcal{B}^{(1)\text{ren}}$ from Eq. 4.2.133.

The renormalized tadpole functions are readily computed using the Green's functions for all sectors and using Eqs. (4.2.99) and (4.2.141). Thereafter the renormalized corrections to the background configurations can be retrieved from Eq. (4.2.142). After which the term $\mathcal{B}^{(2)\text{ren}}$ is computable via(4.2.143) and Eq.(4.2.144).

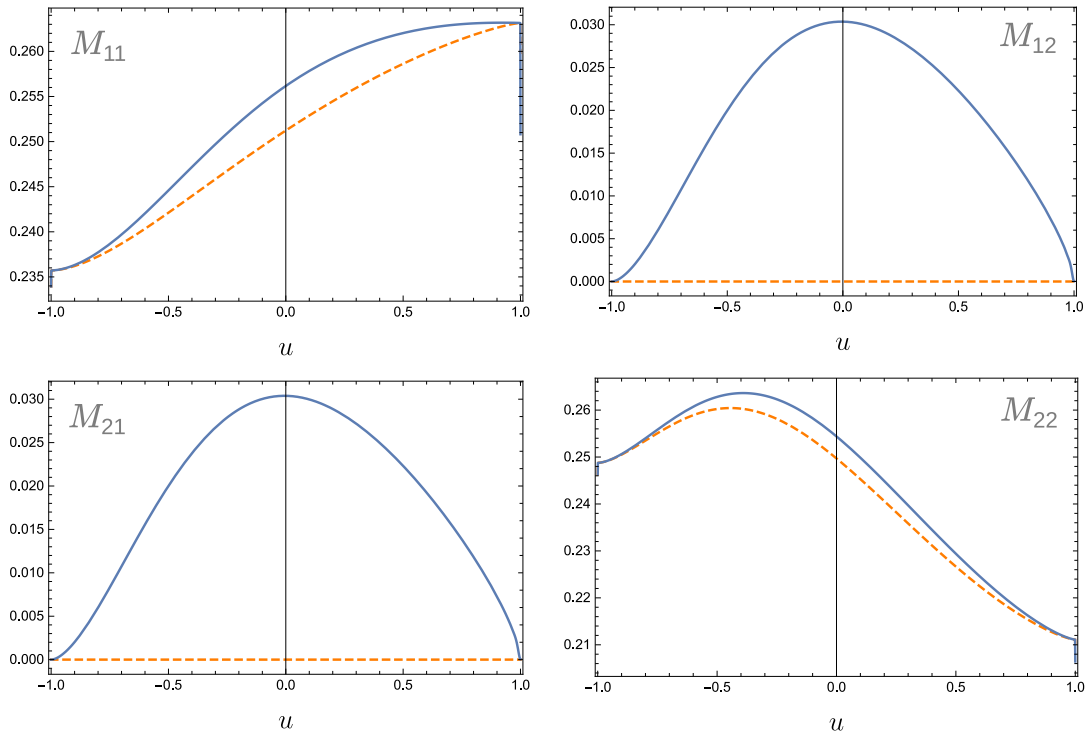

Figure 4.9: Coincident Green's functions of the (A_4, G) sector obtained with perturbative method, for $|\mathbf{k}| = 1.9$. The dashed orange line corresponds to the case with a homogeneous background, while the continuous blue line represents the exact numerical solution of the previous subsection.

Additional numerical subtleties and details

In the process of calculating the deformed coincident Green's function for the scalar sector $\mathcal{M}_{\hat{\Phi};\sqrt{\mathbf{k}^2+s}}$ we have encountered a divergence,

$$\mathcal{M}_{\hat{\Phi};\sqrt{\mathbf{k}^2+s}}(\varphi_0; z, z) \sim \frac{\varphi_-(z)^2}{\mathbf{k}^2 + s - \lambda_-} + O((\mathbf{k}^2 + s - \lambda_-)^0) \text{ for } \lambda_- = 0.21933. \tag{4.2.174}$$

This feature corresponds to the displacement of the negative eigenvalue of the Green's function, namely

$$\mathcal{M}^{-1}_{\hat{\Phi};\mathbf{k}=0}(\varphi_0)\varphi_-(z) = -\lambda_-\varphi_-(z), \tag{4.2.175}$$

which appears as a positive discrete mode in the deformation, as shown above. The existence of the negative eigenvalue is expected when dealing with eigenmodes of fluctuations operators that are written over backgrounds that are associated with tunneling, as we have seen in all previous cases. Fortunately, we still have convergent $|\mathbf{k}|$ integrals within $g_X B_X^{(1)}$ and the tadpole functions $g_X \Pi_X(\varphi_0)\varphi_0$ thanks to the fact that the integral around the singularity is

$$\int_{b-\delta}^{b+\delta} \mathrm{d}|\mathbf{k}| \frac{\mathbf{k}^2}{\mathbf{k}^2 - b^2} = \frac{1}{2}\left(4\delta + b \log\left(\frac{2b-\delta}{2b+\delta}\right)\right). \tag{4.2.176}$$

When integrating any quantity of interest over the singularity in practice, we numerically integrate over the quantity with the divergent piece subtracted, which renders the integrand finite and integrable and the divergent contribution is later added alone by using the expression Eq. (4.2.176), which is nothing else than the principal value.

Following the construction presented, specifically under the degeneracy requirement at the one-loop level, it happens that only the contributions from the renormalized effective action to one-loop is actually finite, mathematically: the sum $(\mathcal{B}^{(0)}+\mathcal{B}^{(1)\text{ren}}/V$ is finite, but not necessarily the summands. We are able to report the numerical result of the sum and to isolate gradient and homogeneous contributions from one another. Using Eqs. (4.2.133), (4.2.139) and (4.2.140) we split the contributions as

$$\mathcal{B}^{(1)\text{ren}} = \mathcal{B}^{(1)\text{ren,hom}} + \mathcal{B}^{(1)\text{ren,grad}}, \tag{4.2.177}$$

where

$$\mathcal{B}^{(1)\text{ren,hom}} = \sum_X g_X B^{(1)\text{ren,hom}}, \quad \mathcal{B}^{(1)\text{ren,grad}} = \sum_X g_X B^{(1)\text{ren,grad}}. \tag{4.2.178}$$

Then the renormalized homogeneous contributions from the effective action to one-loop is explicitly

$$\frac{1}{V}(\mathcal{B}^{(0)} + \mathcal{B}^{(1)\text{ren,hom}}) = \int dz \left(\frac{1}{2}(\partial_z\varphi_0(z))^2 + \text{Re}\, U^{\text{ren}}_{\text{CW}}(\varphi_0)\right). \tag{4.2.179}$$

This expression is, in actuality, the one extremized by the simplified bounce configuration φ_0 and is indeed checked to be finite. The same property holds for the piece containing the gradient effects, $\mathcal{B}^{(1)\text{ren,grad}}$; its integration over spacetime is independent of the cutoff Λ.

We now present several plots showing the results of our numerical implementation together with some of our observations. We begin by considering Fig. 4.10 which illustrates the total tadpole function corresponding to the sum of Eqs. (4.2.99), hence capturing gradients, simultaneously plotted with the homogeneous analog Eq. (4.2.130). Before renormalization has been done, the cutoff-dependent pieces dominate and explain the similarity of both functions. In spite of that, it still reveals that the divergent pieces are properly captured by both functions. In order to be able to observe the gradient effects, we plot the ratio of the two lines in the graph below. Applying the renormalization procedure of subsec. (4.2.4) we construct Fig. 4.11 which displays the total renormalized tadpole function and the derivative with respect to the scalar field of the renormalized effective potential, which serves to highlight the impact of the gradient effects.

The information contained in the first plot of Fig. 4.11 can be as well analyzed on a per-sector basis as done in Fig. 4.12. At first glance, we can already state that the scalar sector possesses the largest contributions to the tadpole functions. When comparing the impact of gradients, we learn that the sectors where the gradients of the background have the biggest impact are the $\hat{\Phi}$ and the (A_4, G) sectors. These observations, pertaining to the scalar field, we can understand from the relative size of g and λ in Eq. (4.2.159). We can also point out the need of correctly renormalizing the wavefunction, without which, we would have obtained the gray line in the right lower plot of Fig. 4.12 which are too large. With have thus witnessed that the gradient corrections are, across sectors, of order 100% of the homogeneous one-loop contributions and slightly larger for the gauge-Goldstone sector, indicating that they are as relevant as their, traditionally accounted for, homogeneous counterparts.

The lower plot of Figure 4.11 provides a cross-check in relation to the boundary conditions. It depicts the functional derivative with respect to the scalar field of the renormalized one-loop effective potential evaluated at φ_0, that is, $U'(\varphi_0) + \sum_X (\Pi_X(\varphi_0)\varphi_0)^{\text{ren}}$. We expect that at $z \to \pm\infty$, the simplified bounce configuration approaches the vacua and remains close to constant. Therefore the derivative of the renormalized effective potential that

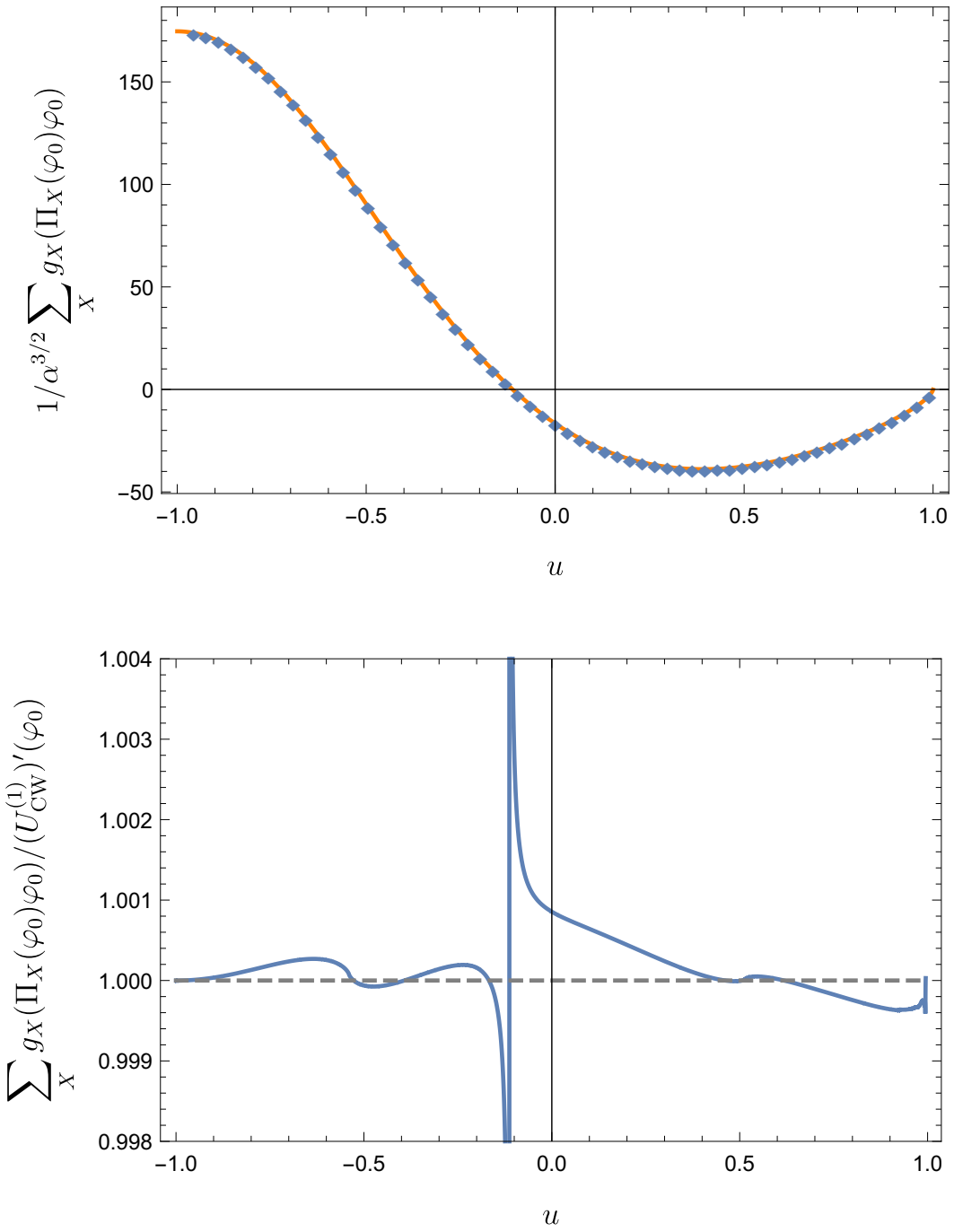

Figure 4.10: Above: tadpole $\sum_X \Pi_X(\varphi_0(u);u)\varphi_0(u)$ with gradient effects (diamonds) and tadpole $(U^{(1)}_{\rm CW})'(\varphi_0) = \sum_X \Pi_{X;\rm hom}(\varphi_0(u);u)\varphi_0(u)$ without gradient effects (solid). Below: Ratio of the total tadpole contribution over its counterpart without gradient effects. The cutoff is taken as $\Lambda = 34.65\sqrt{\alpha}$

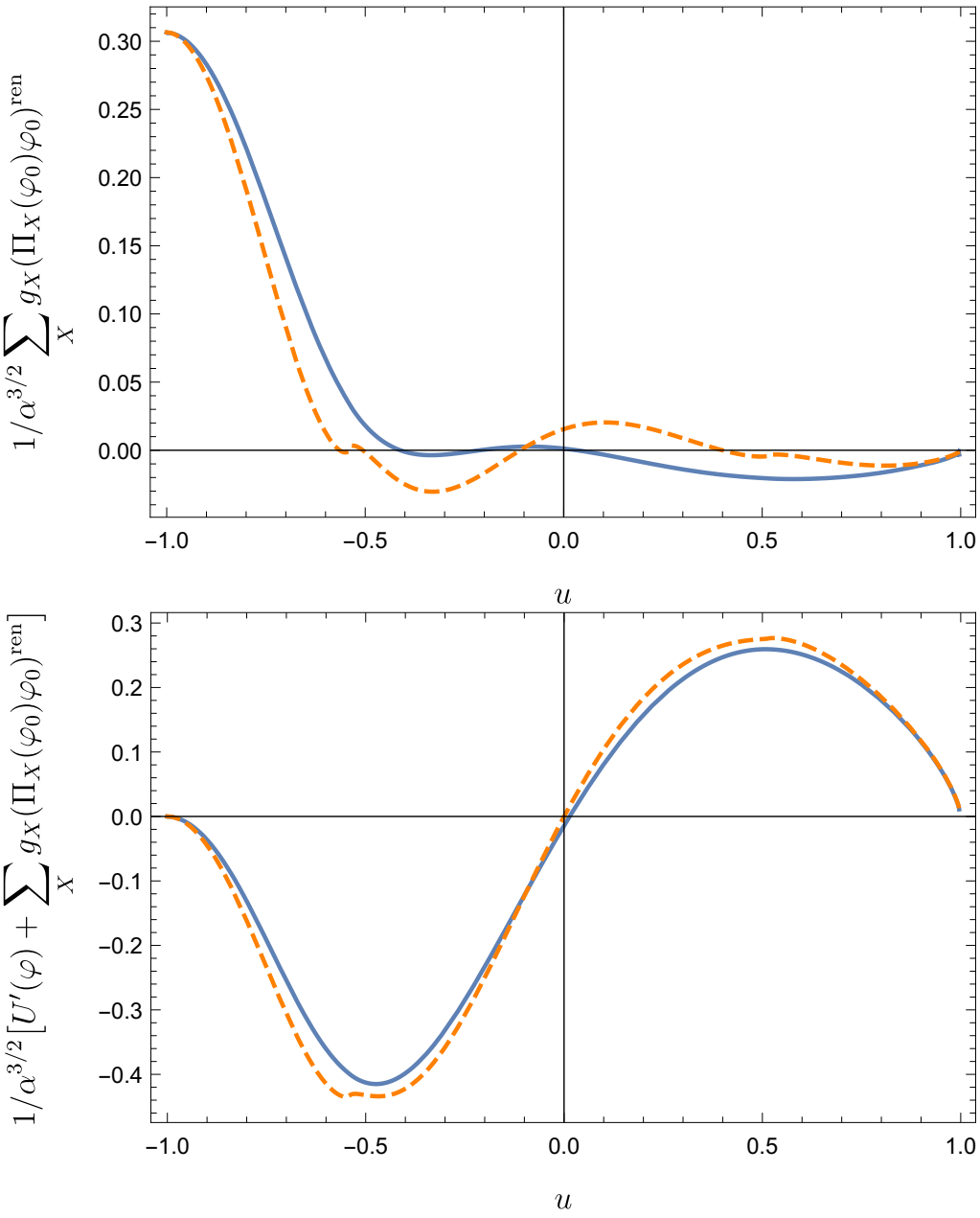

Figure 4.11: Above: Total renormalized tadpole $\sum_X(\Pi_X(\varphi_0(u);u)\varphi_0(u))^{\rm ren}$ (solid blue line), and its approximation neglecting gradients, $(U_{\rm CW}^{(1)\rm ren})'(\varphi_0) = \sum_X(\Pi_{X;\rm hom}(\varphi_0(u);u)\varphi_0(u))^{\rm ren}$ (dashed orange), as a function of the compactified radial coordinate u. Below: Analogous plot, adding the tree-level tadpole contribution $U'(\varphi)$ so as to obtain the one-loop functional derivative of the effective action at the bounce φ_0. The cutoff is taken as $\Lambda = 34.65\sqrt{\alpha}$.

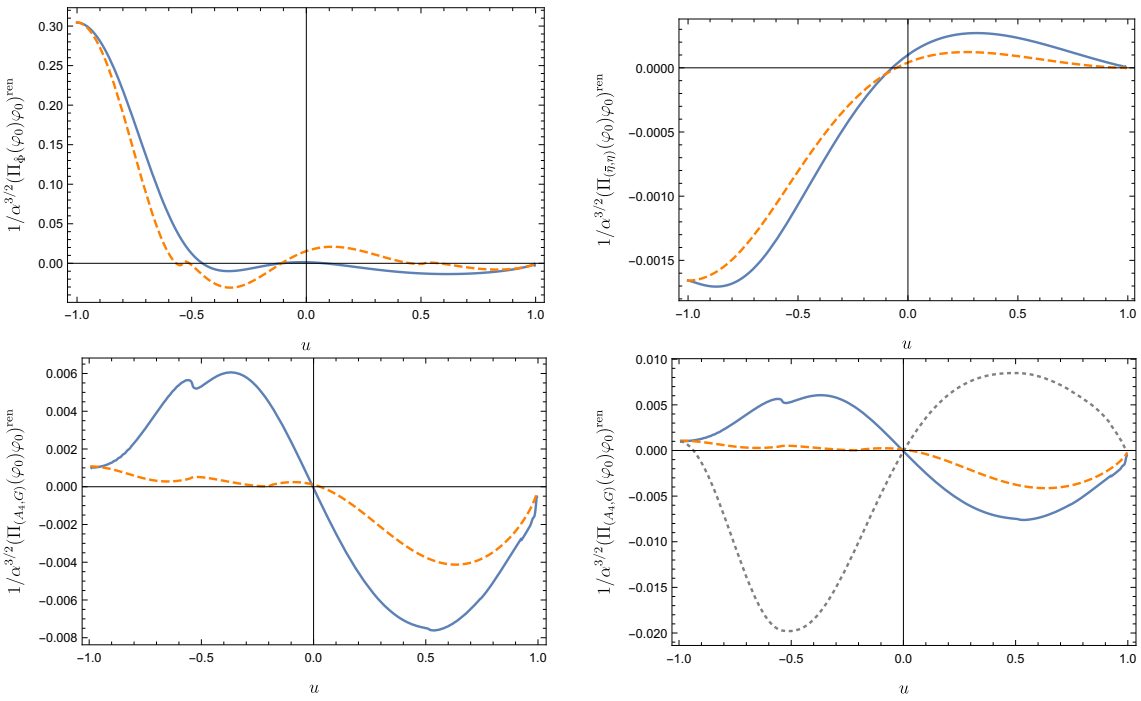

Figure 4.12: For $\Lambda = 34.65\sqrt{\alpha}$, renormalized tadpoles $(\Pi_X(\varphi_0(u);u)\varphi_0(u))^{\rm ren}$ for each set of fields (solid blue) and the corresponding terms ignoring gradient effects, $(U^{(1)}_{\rm CW,X})'(\varphi_0) = (\Pi_{X;\rm hom}(\varphi_0)\varphi_0)^{\rm ren}$ (dashed orange). From upper left to lower right we have $X = \Phi, (\bar\eta,\eta), (A_4,G), (A_4,G)$. The lower right plot includes an extra dotted gray curve illustrating the result in the (A_4,G) sector when one ignores wave-function renormalization. Note that this latter curve is cutoff dependent because the logarithmic divergent wave-function renormalization has not been subtracted.

was used to build the simplified bounce configuration should vanish when $z \to \pm\infty$ or equivalently $u \to \pm 1$, this we confirm in said plot.

The comparison of the simplified bounce φ_0 (dashed orange line) and the quantum corrected bounce (solid blue line) is possible after the renormalized tadpole contributions have been taken into account, which is how Figure 4.6 was obtained. With our construction, all gradient effects are included in the quantum corrected configuration and are seen to be of the order of a few percent, which when compared to previous studies[30, 31, 93] seem to be larger. Our current understanding is that a bounce configuration computed for the one-loop effective potential, with a relative loop factor and couplings of order one, leads to percent corrections, which matches, in this case, the size of the gradient corrections, this we confirm when examining the renormalized tadpoles.

With the availability of all renormalized quantities, we can report the results for all the $\mathcal{B}^{(i)}$'s appearing in the exponent in the formula for the decay rate Eq. (4.2.108), we do this in Table 4.3. Additionally, we provide the results for the renormalized gradient part of the one-loop terms in Table 4.2 separated by sector, and the last column of the table shows the percentage associated with gradients by comparison with the corresponding homogeneous part of the effective potential. Here we can reinstate our conclusion that gradient effects in this model appear to be of order 1% of the full effective one-loop potential, that is, the same size as the corrections we expect from homogeneous one-loop contributions.

When comparing the contributions for the different loop orders in Table4.3, we observe that the one-loop with gradients contributions are two orders of magnitude from the tree-

	Value $[\times\alpha^{-3/2}]$	Value/$((\mathcal{B}^{(0)}+\mathcal{B}^{(1)\mathrm{ren}})/V)$ [%]
$g_{\hat{\Phi}}B^{(1)\mathrm{ren,grad}}_{\hat{\Phi}}/V$	0.00139	0.29
$g_{(\bar{\eta},\eta)}B^{(1)\mathrm{ren,grad}}_{(\bar{\eta},\eta)}/V$	0.0000748	0.016
$g_{(A_4,G)}B^{(1)\mathrm{ren,grad}}_{(A_4,G)}/V$	0.00332	0.70
$\sum_X g_X B^{(1)\mathrm{ren,grad}}_X/V$	0.00479	1.0

Table 4.2: Numerical results for the gradient part of the one-loop contributions to the effective action.

level result, in agreement with what perturbation theory tells us for couplings of order one. Moreover, we can see that the two-loop order contributions from $\mathcal{B}^{(2)\mathrm{ren}}$ certainly fall four orders of magnitude below the tree-level as they should.

	Value $[\times\alpha^{-3/2}]$
$(\mathcal{B}^{(0)}+\mathcal{B}^{(1)\mathrm{ren}})/V$	0.473
$\mathcal{B}^{(2)\mathrm{ren}}/V$	-0.000345
$(\mathcal{B}^{(0)}+\mathcal{B}^{(1)\mathrm{ren}}+\mathcal{B}^{(2)\mathrm{ren}})/V$	0.474

Table 4.3: Numerical results for the renormalized contributions to the effective action.

4.3 Estimations by means of Gradient Expansion Techniques

In this last section, we comment on insofar unpublished work aimed at developing procedures to estimate gradient corrections coming from the inhomogeneity of the background. We expect the method will have a twofold purpose. Firstly, this will allow us to compute the divergences associated with the wavefunction, i.e., it will complete the renormalization program and at the same time will provide us with rough estimates for the sizes of the gradients for the different sectors without going through the trouble of requiring a full numerical simulation in a case by case basis.

The main idea is to consider a careful gradient expansion of the 1PI terms appearing in the effective action evaluated on a classical configuration. The different ingredients leading to our procedure appear already indirectly in several Refs. [98–104]. With the aim of illustrating the steps we follow, we consider first the scalar sector of our model, where we expect to find only finite contributions from terms proportional to the kinetic term, as shown in Sec. 1.3. Let us consider the 1PI terms as in Eq. (4.2.78), first for the scalar. Instead of using a planar wall decomposition, let us change to the four-momentum basis by assuming the fluctuation operator $\mathcal{M}^{-1}$ is invariant under translations, then

$$\Gamma[\varphi_b] \supset \frac{1}{2}\,\mathrm{tr}\log\mathcal{M}^{-1}(x,y;\varphi_b) = \frac{1}{2}\,\mathrm{tr}\int \mathrm{d}^4x\frac{\mathrm{d}^4p}{(2\pi)^4}\,\mathrm{e}^{\mathrm{i}px}\log\mathcal{M}^{-1}(x,x;\varphi_b)\,\mathrm{e}^{-\mathrm{i}px}, \quad (4.3.180)$$

where the functional trace is taken over position and we have translated the operator via plane waves as in [99]. Observing that the effect of conjugation by plane waves is simply

a translation in the operator sense,

$$\mathrm{e}^{\mathrm{i}px}\partial_\mu \,\mathrm{e}^{-\mathrm{i}px} = \partial_\mu - \mathrm{i}p_\mu \equiv \mathrm{i}(\Pi - p)_\mu, \tag{4.3.181}$$

where we have defined de operator Π in the last step for a cleaner notation in what follows. The conjugation means we can translate the derivatives appearing in $\mathcal{M}^{-1}$ by an amount $-\mathrm{i}p_\mu$. This implies, in turn, that for a fluctuation operator depending on the spacetime point, either explicitly or through an effective mass, and possible derivatives, we have that the above operation gives

$$\mathrm{e}^{\mathrm{i}px}\mathcal{M}^{-1}(x^\mu, \partial_\mu)\,\mathrm{e}^{-\mathrm{i}px} = \mathcal{M}^{-1}\left(x^\mu, -\mathrm{i}p^\mu\right) \tag{4.3.182}$$

And for a typical fluctuation operator consisting of a Laplacian (in the Euclidean case) and an effective mass which depends on the spacetime point

$$\mathrm{e}^{\mathrm{i}px}\mathcal{M}^{-1}(x^\mu, \partial_\mu)\,\mathrm{e}^{-\mathrm{i}px} = (\Pi - p)^2 + m^2_{\mathrm{eff}}\left(x^\mu\right). \tag{4.3.183}$$

We can use the formula above directly through the log, which can be seen by using a Taylor expansion and realizing one can insert pairs of exponentials between each factor, thus

$$\mathrm{e}^{\mathrm{i}px}\log\mathcal{M}^{-1}(x^\mu, \partial_\mu)\,\mathrm{e}^{-\mathrm{i}px} = \log\left[(\Pi - p)^2 + m^2_{\mathrm{eff}}\left(x^\mu\right)\right], \tag{4.3.184}$$

also holds. We can conjugate additionally by $\mathrm{e}^{\Pi\cdot\frac{\partial}{\partial p}}$ (see Ref.[102]) which as operators they can be understood as acting on the identity either to the right or via integration by parts to the left without changing anything in the expression[104], then the full 1PI term looks like

$$\Gamma \supset \frac{1}{2}\,\mathrm{tr}\int \mathrm{d}^4x \frac{\mathrm{d}^4p}{(2\pi)^4}\,\mathrm{e}^{\Pi\cdot\frac{\partial}{\partial p}}\log\left[(\Pi - p)^2 + m^2_{\mathrm{eff}}(x^\mu)\right]\,\mathrm{e}^{-\Pi\cdot\frac{\partial}{\partial p}}. \tag{4.3.185}$$

It can be shown that

$$\log\,\mathrm{e}^{\mathcal{O}_1}\mathcal{M}^{-1}\,\mathrm{e}^{-\mathcal{O}_1} = \log\left(\mathrm{e}^{\mathrm{ad}_{\Pi\cdot\frac{\partial}{\partial p}}}\mathcal{M}^{-1}\right), \tag{4.3.186}$$

where

$$\mathrm{ad}_{\Pi\cdot\frac{\partial}{\partial p}}\,\mathcal{O} \equiv \left[\Pi\cdot\frac{\partial}{\partial p}, \mathcal{O}\right]. \tag{4.3.187}$$

We can compute what happens to the kinetic term

$$\begin{aligned}
\mathrm{e}^{\Pi\cdot\frac{\partial}{\partial p}}(\Pi_\mu - p_\mu)\,\mathrm{e}^{-\Pi\cdot\frac{\partial}{\partial p}} &= \mathrm{e}^{\Pi\cdot\frac{\partial}{\partial p}}\Pi_\mu\,\mathrm{e}^{-\Pi\cdot\frac{\partial}{\partial p}} - e^{\Pi\cdot\frac{\partial}{\partial p}}p_\mu e^{-\Pi\cdot\frac{\partial}{\partial p}} \\
&= \Pi_\mu - p_\mu - \sum_{n=1}^{\infty}\frac{1}{n!}\left(\mathrm{ad}_{\Pi\cdot\frac{\partial}{\partial p}}\right)^{n-1}\Pi_\mu \\
&= \Pi_\mu - p_\mu - \Pi_\mu - \sum_{n=2}^{\infty}\frac{1}{n!}\left(\mathrm{ad}_{\Pi\cdot\frac{\partial}{\partial p}}\right)^{n-1}\Pi_\mu \\
&= -p_\mu.
\end{aligned} \tag{4.3.188}$$

Let us introduce some useful notation to deal with the effective mass term. For a spacetime point dependent function $f(x)$, we have

$$f(x) + \delta f(x) \equiv e^{\Pi\cdot\frac{\partial}{\partial p}}f(x)e^{-\Pi\cdot\frac{\partial}{\partial p}} = \sum_{n=0}^{\infty}\frac{1}{n!}\prod_{i=1}^{n}\mathrm{ad}_{\Pi_{\mu_i}}f(x)\frac{\partial}{\partial p_{\mu_i}}, \tag{4.3.189}$$

where the deviation from $f(x)$ was implicitly defined above by simply extracting the 0-th order term, thus

$$\delta f(x) = \sum_{n=1}^{\infty} \frac{1}{n!} \prod_{i=1}^{n} \mathrm{ad}_{\Pi_{\mu_i}} f(x) \frac{\partial}{\partial p_{\mu_i}} = \sum_{n=1}^{\infty} \frac{(-i)^n}{n!} (\partial_{\mu_1} \partial_{\mu_2} \cdots \partial_{\mu_n} f(x)) \frac{\partial^n}{\partial p_{\mu_1} \partial p_{\mu_2} \cdots \partial p_{\mu_n}}, \tag{4.3.190}$$

where $\partial_{\mu_i} = \partial/(\partial x^{\mu_i})$. With this notation, we have so far

$$\Gamma \supset \frac{1}{2} \,\mathrm{tr} \int \mathrm{d}^4 x \frac{\mathrm{d}^4 p}{(2\pi)^4} \log \left[p^2 + m^2_{\mathrm{eff}}(x) + \delta m^2_{\mathrm{eff}} \right], \tag{4.3.191}$$

where the last term presents a different number of momentum derivatives that act to the right. To deal with the logarithm, we consider introducing an auxiliary integral with respect to m^2 and using the derivative of the logarithm as the integrand instead:

$$\begin{aligned} \Gamma \supset & \frac{1}{2} \,\mathrm{tr} \int \mathrm{d}^4 x \frac{\mathrm{d}^4 p}{(2\pi)^4} \int \mathrm{d}(m^2_{\mathrm{eff}}) \frac{1}{p^2 + m^2_{\mathrm{eff}}(x) + \delta m^2_{\mathrm{eff}}(x)}, \\ = & \frac{1}{2} \,\mathrm{tr} \int \mathrm{d}^4 x \frac{\mathrm{d}^4 p}{(2\pi)^4} \int \mathrm{d}(m^2_{\mathrm{eff}}) \frac{1}{(p^2 + m^2_{\mathrm{eff}}(x))[1 + (p^2 + m^2_{\mathrm{eff}}(x))^{-1} \delta m^2_{\mathrm{eff}}(x)]} \end{aligned} \tag{4.3.192}$$

Consider $A^{-1} = p^2 + m^2_{\mathrm{eff}}(x)$ and $B = \delta m^2_{\mathrm{eff}}$, then we have the following relation for generic operators

$$\begin{aligned} (A^{-1}[1 + AB])^{-1} &= [1 + AB]^{-1} A = (1 - AB + ABAB - ABABAB + \cdots) A \\ &= A - ABA + ABABA - \cdots, \end{aligned} \tag{4.3.193}$$

which leads to a final series expression in terms of gradients for the one-loop term of the effective potential:

$$\begin{aligned} \Gamma \supset \frac{1}{2} \,\mathrm{tr} \int \mathrm{d}^4 x \frac{\mathrm{d}^4 p}{(2\pi)^4} \int \mathrm{d}(m^2_{\mathrm{eff}}) \Bigg[& \frac{1}{p^2 + m^2_{\mathrm{eff}}} - \frac{1}{p^2 + m^2_{\mathrm{eff}}} (\delta m^2_{\mathrm{eff}}) \frac{1}{p^2 + m^2_{\mathrm{eff}}} \\ & + \frac{1}{p^2 + m^2_{\mathrm{eff}}} (\delta m^2_{\mathrm{eff}}) \frac{1}{p^2 + m^2_{\mathrm{eff}}} (\delta m^2_{\mathrm{eff}}) \frac{1}{p^2 + m^2_{\mathrm{eff}}} - \cdots \Bigg] \end{aligned} \tag{4.3.194}$$

The expansion above will enable us to compute gradient effects for the different sectors that have been already mentioned in the previous sections.

4.3.1 Scalar sector

Let us first consider the scalar sector. Collecting terms that are quadratic in gradients, we should be able to corroborate that the contributions are finite. We will later evaluate the expression for the cases in Sec. 4.1 and Sec. 4.2. Terms quadratic in gradients come from two types of terms:

1. the second term of $\delta m^2_{\mathrm{eff}}$ appearing between two A terms.
2. products of two order one terms of $\delta m^2_{\mathrm{eff}}$ in between three factors of A.

We consider each case separately, starting with the lowest term in factors of A., namely

$$\Gamma \supset I_S^{(2,2)} \equiv -\frac{1}{2} \,\mathrm{tr} \int \mathrm{d}^4 x \frac{\mathrm{d}^4 p}{(2\pi)^4} \int \mathrm{d}(m^2_{\mathrm{eff}}) \frac{1}{p^2 + m^2_{\mathrm{eff}}} \delta^{(2)} m^2_{\mathrm{eff}} \frac{1}{p^2 + m^2_{\mathrm{eff}}}, \tag{4.3.195}$$

where $I_S^{(2,2)}$ has superscripts indicating the order of the terms considered: second term in δm^2_{eff} and two inverse propagators A, and with

$$\delta^{(2)} m^2_{\text{eff}}(x) = \frac{(-\mathrm{i})^2}{2} \partial_{\mu_1}\partial_{\mu_2} m^2_{\text{eff}}(x) \frac{\partial^2}{\partial p_{\mu_1}\partial p_{\mu_2}}, \tag{4.3.196}$$

and we keep the effective mass as general as possible. The action of the derivatives on A can be computed directly and gives

$$\frac{\partial^2}{\partial p_{\mu_1}\partial p_{\mu_2}} \frac{1}{p^2 + m^2_{\text{eff}}} = \frac{-2\delta_{\mu_1\mu_2}}{(p^2 + m^2_{\text{eff}})^2} + \frac{8 p_{\mu_1} p_{\mu_2}}{(p^2 + m^2_{\text{eff}})^3}, \tag{4.3.197}$$

Plugging the above back into $I_S^{(2,2)}$ leads to

$$I_S^{(2,2)} = -\frac{1}{4} \operatorname{tr} \int \mathrm{d}^4x \frac{\mathrm{d}^4p}{(2\pi)^4} \int \mathrm{d}(m^2_{\text{eff}}) \frac{2 m^2_{\text{eff}} \partial^2 m^2_{\text{eff}}}{(p^2 + m^2_{\text{eff}})^4}. \tag{4.3.198}$$

For comparison with the previous sections, we need to perform the integral over momentum in an analogous manner, viz., we consider the p_4 direction as planar and integrate into $\mathbb{R}$ while the remaining directions are integrated assuming spherical symmetry. We have in this sense that

$$\begin{aligned} I_S^{(2,2)} &= -\frac{1}{2}\frac{5}{32} \int \frac{\mathrm{d}^3\vec{p}}{(2\pi)^3}\, \mathrm{d}^4x\, \mathrm{d}m^2_{\text{eff}} \left(\frac{m^2_{\text{eff}} \partial^2 m^2_{\text{eff}}}{(\vec{p}^2 + m^2_{\text{eff}})^{7/2}} \right) \\ &= -\frac{1}{192\pi^2} \int \mathrm{d}^4x\, \mathrm{d}m^2_{\text{eff}} \left(\frac{\partial^2 m^2_{\text{eff}}}{m^2_{\text{eff}}} \right) = -\frac{1}{192\pi^2} \int \mathrm{d}^4x (\partial^2 m^2_{\text{eff}}) \log m^2_{\text{eff}} \\ &\approx \frac{1}{192\pi^2} \int \mathrm{d}^4x \frac{(\partial m^2_{\text{eff}})^2}{m^2_{\text{eff}}}, \end{aligned} \tag{4.3.199}$$

where we integrated by parts to arrive at the last line.
Let us now compute the second contribution. We collect the first term of two factors of δm^2_{eff} and three inverse propagators A,

$$\Gamma \supset I_S^{(2,3)} \equiv \frac{1}{2} \operatorname{tr} \int \mathrm{d}^4x \frac{\mathrm{d}^4p}{(2\pi)^4} \mathrm{d}(m^2_{\text{eff}}) \frac{1}{p^2 + m^2_{\text{eff}}} (\delta^{(1)} m^2_{\text{eff}}) \frac{1}{p^2 + m^2_{\text{eff}}} (\delta^{(1)} m^2_{\text{eff}}) \frac{1}{p^2 + m^2_{\text{eff}}}, \tag{4.3.200}$$

where the first term in δm^2_{eff} is (see Eq. (4.3.190)),

$$\delta^{(1)} m^2_{\text{eff}} = -\mathrm{i}\partial_{\mu_1} m^2_{\text{eff}} \frac{\partial}{\partial p_{\mu_1}}. \tag{4.3.201}$$

We will need first to compute the following derivative before performing the integrals:

$$\begin{aligned} \frac{\partial}{\partial p_{\mu_1}} \left(\frac{1}{p^2 + m^2_{\text{eff}}} \frac{\partial}{\partial p_{\mu_2}} \frac{1}{p^2 + m^2_{\text{eff}}} \right) &= -2 \frac{\partial}{\partial p_{\mu_1}} \left(\frac{p_{\mu_2}}{(p^2 + m^2_{\text{eff}})^3} \right) \\ &= \frac{\delta_{\mu_1\mu_2}(p^2 - 2m^2_{\text{eff}})}{(p^2 + m^2_{\text{eff}})^4}, \end{aligned} \tag{4.3.202}$$

where $p_{\mu_1}p_{\mu_2}$ was rewritten as $p^2\delta_{\mu_1\mu_2}/4$ since the expression stands within an integral over four-momentum. We can straightaway compute the pending integrals.

$$\begin{aligned} I_S^{(2,3)} &= -\frac{1}{2}\,\mathrm{tr}\int \mathrm{d}^4x \frac{\mathrm{d}^4p}{(2\pi)^4}\,\mathrm{d}m_{\mathrm{eff}}^2\;\partial_\mu m_{\mathrm{eff}}^2\partial^\mu m_{\mathrm{eff}}^2 \frac{p^2-2m_{\mathrm{eff}}^2}{(p^2+m_{\mathrm{eff}}^2)^5} \\ &= \frac{1}{2}\frac{5}{256}\,\mathrm{tr}\int \mathrm{d}^4x \frac{\mathrm{d}^3\vec{p}}{(2\pi)^3}\,\mathrm{d}m_{\mathrm{eff}}^2\;(\partial_\mu m_{\mathrm{eff}}^2)^2 \frac{13m_{\mathrm{eff}}^2-8\vec{p}^2}{(m_{\mathrm{eff}}^2+\vec{p}^2)^{9/2}} \\ &= \frac{1}{384\pi^2}\,\mathrm{tr}\int \mathrm{d}^4x\,\mathrm{d}m_{\mathrm{eff}}^2\;\frac{(\partial_\mu m_{\mathrm{eff}}^2)^2}{m_{\mathrm{eff}}^4} \approx -\frac{1}{384\pi^2}\,\mathrm{tr}\int \mathrm{d}^4x \frac{(\partial_\mu m_{\mathrm{eff}}^2)^2}{m_{\mathrm{eff}}^2} \end{aligned} \tag{4.3.203}$$

Collecting all contributions quadratic in gradients from Eqs. (4.3.199) and (4.3.203) for the case of a field with no internal indices gives

$$\Gamma \supset I_S^{(2,2)} + I_S^{(2,3)} = \frac{1}{384\pi^2}\,\mathrm{tr}\int \mathrm{d}^4x \frac{(\partial_\mu m_{\mathrm{eff}}^2)^2}{m_{\mathrm{eff}}^2} \tag{4.3.204}$$

which coincides exactly with the result in Eq. (4.1.54) when we plugging the effective mass, $m_{\mathrm{eff}}^2 = -\mu^2 + \lambda\varphi^2/2$ used in that model. This expression is not only useful in the theory's renormalization procedure but also allows us to estimate gradient effects roughly.

4.3.2 Fermion sector

We employ the same techniques for the case of a fermion field to arrive at the divergent contributions described in the Higgs-Yukawa model of Sec. 4.1. Almost all the machinery can be recycled after the Dirac operator determinant is squared, as in the right-hand side of the first line of Eq. (4.1.43). We can immediately adapt Eq. (4.3.191)

$$\Gamma \supset -\frac{1}{2}\,\mathrm{tr}\int \frac{\mathrm{d}^4p}{(2\pi)^4}\,\mathrm{d}^4x \log\left[p^2 + m_D^2 + \delta m_D^2 + \not{\partial} m_D + \delta\not{\partial} m_D\right], \tag{4.3.205}$$

and Eq. (4.3.192) subsequently to obtain

$$\Gamma \supset \frac{1}{2}\,\mathrm{tr}\int \mathrm{d}^4x \frac{\mathrm{d}^4p}{(2\pi)^4}\,\mathrm{d}(m_D^2) \frac{1}{(p^2+m_D^2(x))[1+(p^2+m_D^2(x))^{-1}(\delta m_D^2 + \not{\partial} m_D + \delta\not{\partial} m_D)]} \tag{4.3.206}$$

and employing the expansion in Eq. (4.3.193) we have

$$\begin{aligned} \Gamma \supset \frac{1}{2}\,\mathrm{tr}\int \mathrm{d}^4x \frac{\mathrm{d}^4p}{(2\pi)^4}\,\mathrm{d}(m_D^2)\Bigg[&\frac{1}{p^2+m_D^2} - \frac{1}{p^2+m_D^2}(\delta m_D^2 + \not{\partial} m_D + \delta\not{\partial} m_D)\frac{1}{p^2+m_D^2} \\ &+ \frac{1}{p^2+m_D^2}(\delta m_D^2 + \not{\partial} m_D + \delta\not{\partial} m_D)\frac{1}{p^2+m_D^2}(\delta m_D^2 + \not{\partial} m_D + \delta\not{\partial} m_D)\frac{1}{p^2+m_D^2} \\ &- \cdots\Bigg] \end{aligned} \tag{4.3.207}$$

The first contribution quadratic in gradients for the Dirac fermion is after the analogous algebra and integration:

$$\Gamma \supset I_D^{(2,2)} = -4I_S^{(2,2)} = -\frac{4}{192\pi^2}\int \frac{(\partial_\mu m_D^2)^2}{m_D^2} \tag{4.3.208}$$

The second contribution coming from quadratic gradient terms appearing in the second line of Eq. (4.3.206) gives

$$\Gamma \supset I_D^{(2,3)} = \int \mathrm{d}^4x \frac{(\partial_\mu m_D)(\partial_\mu m_D)}{16\pi^2}\left[\log\frac{\Lambda^2}{m_D^2} - 2 + 2\log 2\right] + \frac{(\partial_\mu m_D^2)^2}{96\pi^2 m_D^2}, \tag{4.3.209}$$

where Λ is a momentum cutoff for the three-momentum remaining after the p_4 integration. Adding the two contributions from Eqs. (4.3.208) and (4.3.209) we finally arrive to

$$\Gamma \supset \int \mathrm{d}^4x \frac{(\partial_\mu m_D)(\partial_\mu m_D)}{16\pi^2}\left[\log\frac{\Lambda^2}{m_D^2} + 2\log 2 - \frac{8}{3}\right] \tag{4.3.210}$$

The result matches the one quoted in Eq. (4.1.55). It is important to remark that we get exactly the same finite pieces given that we performed the integration in the exact same way as in Sec. 4.1. Adopting other regularization schemes might lead to differing finite pieces.

4.3.3 Abelian Gauge sector

We can now justify the expression for $K_{s,(A_\mu,G)}$ in Eq. (4.2.157) used in the previous section on the $U(1)$ gauge Higgs sector, Sec. 4.2.1. However, the result obtained here does not match the one published and stated in Sec. 4.2.1 because of a computational mistake. We correct that error here with the current machinery. Consider the fluctuation operator for the mixed sector of A_4 and G studied in Sec. 4.2.1 and split it into the following three contributions given its internal structure

$$\mathrm{e}^{\Pi\cdot\frac{\partial}{\partial p}}\mathcal{M}^{-1}_{(A_\mu,G)}(x;p)\,\mathrm{e}^{-\Pi\cdot\frac{\partial}{\partial p}} = \mathcal{M}_0^{-1}(x) + \delta\mathcal{M}_1^{-1}(x) + \mathcal{M}_2^{-1}(x), \tag{4.3.211}$$

where the terms appearing in the last line are

$$\begin{aligned}
\mathcal{M}_0^{-1}(x) &= \begin{pmatrix} (p^2 + m_A^2(x))\delta_{\mu\nu} & 0 \\ 0 & p^2 + m_G^2(x) \end{pmatrix}, \\
\delta\mathcal{M}_1^{-1}(x) &= \begin{pmatrix} \delta m_A^2(x)\,\delta_{\mu\nu} & 0 \\ 0 & \delta m_G^2(x) \end{pmatrix}, \\
\mathcal{M}_2^{-1}(x) &= \begin{pmatrix} 0 & 2g\,\partial_\mu\varphi + 2g\delta\partial_\mu\varphi \\ 2g\partial_\mu\varphi + 2g\delta\partial_\mu\varphi & 0 \end{pmatrix}.
\end{aligned} \tag{4.3.212}$$

We expand the logarithm directly using first $\log(AB) = \log A + \log B + \mathcal{O}([\log A, \log B])$ and the Taylor series for $\log(1+x)$, explicitly

$$\begin{aligned}
\mathrm{tr}\log\mathcal{M}^{-1}_{(A_\mu,G)}(x;p) &= \mathrm{tr}\log\mathcal{M}_0^{-1} \\
&\quad - \mathrm{tr}\sum_{j=1}^{\infty}\frac{(-1)^j}{j}\left(\mathcal{M}_0(\delta\mathcal{M}_1^{-1} + \mathcal{M}_2^{-1})\right)^j,,
\end{aligned} \tag{4.3.213}$$

where we have neglected commutator terms and higher orders, given that more propagator insertions will render integrals finite and are not important for renormalization but must be

examined for concrete estimations. Let us denote the inverse of the diagonal components of $\mathcal{M}^{-1}_{0(A_\mu,G,p)}(x)$ as

$$\mathcal{M}_0 = \begin{pmatrix} \frac{\delta_{\mu\nu}}{p^2+m_A^2} & 0 \\ 0 & \frac{1}{p^2+m_G^2} \end{pmatrix} \equiv \begin{pmatrix} \Delta_{A,\mu\nu} & 0 \\ 0 & \Delta_G \end{pmatrix} \tag{4.3.214}$$

and start collecting the contributions to the quadratic gradients. From the second term in $\delta\mathcal{M}_1^{-1}$ and the first term in the logarithm expansion, we have

$$\Gamma \supset I^{(1)}_{\text{gauge}} \equiv -\frac{1}{4}\int \mathrm{d}^4x \frac{\mathrm{d}^4p}{(2\pi)^4}\left(\frac{\partial^2\Delta_{A,\mu\mu}}{\partial p_\rho \partial p_\sigma}\partial_\rho\partial_\sigma m_A^2 + \frac{\partial^2\Delta_G}{\partial p_\rho\partial p_\sigma}\partial_\rho\partial_\sigma m_G^2\right), \tag{4.3.215}$$

where integration by parts was done twice on the momentum variable. The derivatives involved can be computed directly to get:

$$\frac{\partial^2\Delta_{A,\mu\mu}}{\partial p_\rho\partial p_\sigma} = \frac{8p_\rho p_\sigma - 2(p^2+m_A^2)\delta_{\rho\sigma}}{(m_A^2+p^2)^3} \xrightarrow{\frac{1}{4}p^2\delta_{\rho\sigma}} \frac{-m_A^2\delta_{\rho\sigma}}{(m_A^2+p^2)^3}, \tag{4.3.216}$$

$$\frac{\partial^2\Delta_G}{\partial p_\rho\partial p_\sigma} = \frac{8p_\rho p_\sigma - 2(p^2+m_G^2)\delta_{\rho\sigma}}{(m_G^2+p^2)^3} \xrightarrow{\frac{1}{4}p^2\delta_{\rho\sigma}} \frac{-m_G^2\delta_{\rho\sigma}}{(m_A^2+p^2)^3}, \tag{4.3.217}$$

The above integrands lead to finite contributions, that is, $I^{(1)}_{\text{gauge}}$ is finite. The other contribution quadratic in background gradients is

$$\Gamma \supset I^{(2)}_{\text{gauge}} \equiv -2g^2\int \mathrm{d}^4x \frac{\mathrm{d}^4p}{(2\pi)^4}\Delta_G\Delta_{A,\mu\nu}(\partial_\mu\varphi)\partial_\nu\varphi. \tag{4.3.218}$$

which comes from the second term in the logarithm series and the first term in $\delta\mathcal{M}_1^{-1}$ appearing twice. We take care of the momentum integration first to arrive at the kernel used in Sec. 4.2.1:

$$\begin{aligned}
\int \frac{\mathrm{d}^4p}{(2\pi)^4}\Delta_G\Delta_{A,\mu\nu} &= \int \frac{\mathrm{d}^4p}{(2\pi)^4}\frac{\delta_{\mu\nu}}{(p^2+m_A^2)(p^2+m_G^2)} \\
&= \int_0^1 \mathrm{d}w \int \frac{\mathrm{d}^4p}{(2\pi)^4}\frac{\delta_{\mu\nu}}{(w(p^2+m_A^2)+(1-w)(p^2+m_G^2))^2} \\
&= \int_0^1 \mathrm{d}w \int \frac{\mathrm{d}^3\mathbf{p}}{(2\pi)^3}\frac{\delta_{\mu\nu}}{4(\mathbf{p}^2+w(m_A^2-m_G^2)+m_G^2)^{3/2}} \\
&= \int_0^\infty \mathrm{d}s\int_0^1 \mathrm{d}w \int \frac{\mathrm{d}^3\mathbf{p}}{(2\pi)^3}\frac{3\delta_{\mu\nu}}{8(\mathbf{p}^2+s+w(m_A^2-m_G^2)+m_G^2)^{5/2}} \\
&= \int_0^\infty \mathrm{d}s\frac{\mathrm{d}^3\mathbf{p}}{(2\pi)^3}\frac{\delta_{\mu\nu}}{4(m_A^2-m_G^2)}\left(\frac{1}{(m_G^2+\mathbf{p}^2+s)^{3/2}} - \frac{1}{(m_A^2+\mathbf{p}^2+s)^{3/2}}\right).
\end{aligned} \tag{4.3.219}$$

From the above equation, we can recognize the kernel in Eq. (4.2.156) we were looking for. Additionally, we can generically write down the results for unspecified gauge parameters ξ and ζ:

$$\Gamma \supset -\frac{1}{16\pi^2}g^2(\zeta+\xi)\log\Lambda^2\int \mathrm{d}^4x(\partial_\mu\varphi)^2. \tag{4.3.220}$$

4.3.4 Comparisons with numerical results

To end the chapter, we provide some comparisons with available numerical results computed using the techniques presented in the first two sections of this chapter. We consider the different models which have been mentioned and studied by our group, and we report on the ratios of homogeneous to gradient contributions in terms of the model field content and the coupling constants of the theory.

$$|S_0| \sim \int \mathrm{d}^4x \, \frac{\lambda}{4!}(\phi^4 - \phi_0^4) \sim \int \mathrm{d}^4x \, \partial_\mu\phi\partial^\mu\phi \tag{4.3.221}$$

where it has been assumed that the factor appearing in front of the kinetic term is of order 1, which is consistent with the cases of a thin-wall approximation or, in the case of a Fubini-Lipatov potential, in which the above equation is actually exact.

Homogeneous one-loop contribution

The homogeneous one-loop terms are computed using the Coleman-Weinberg potential. Assuming we can employ a renormalization scheme which leads to logarithms of order one, this reduces to

$$B_\phi^{(1)\mathrm{hom}} \sim \int \mathrm{d}^4x \, \frac{\lambda^2}{4 \cdot 64\pi^2}\phi^4 \sim \frac{3\lambda}{32\pi^2}S_0 \tag{4.3.222}$$

for the scalar field, to

$$|B_\psi^{(1)\mathrm{hom}}| \sim \int \mathrm{d}^4x \, \frac{\kappa^4}{16\pi^2}\phi^4 \sim \frac{3\kappa^4}{2\pi^2\lambda}S_0 \tag{4.3.223}$$

for a fermionic field coupled to the scalar via a Yukawa coupling κ and

$$|B_G^{(1)\mathrm{hom}}| \sim \int \mathrm{d}^4x \, \dim(\mathfrak{g})\frac{3g^4}{16 \cdot 64\pi^2}\phi^4 \sim \dim(\mathfrak{g})\frac{9g^4}{128\pi^2\lambda}S_0, \tag{4.3.224}$$

for a gauge field with symmetry group G, corresponding Lie algebra $\mathfrak{g}$ with g the coupling constant.

Gradients contributions

Using the gradient expansion presented in this section, specifically Eq. (4.3.194) and its adaption to the different sectors, we can compute the following estimates. For the scalar sector

$$|B_\phi^{(1)\mathrm{grad}}| \sim \int \mathrm{d}^4x \, \frac{\lambda^2}{384\pi^2}\frac{1}{2}\partial_\mu\phi\partial_\mu\phi \sim \frac{\lambda^2}{768\pi^2}S_0 \tag{4.3.225}$$

where the thin-wall tree-level result was used and the result was written in terms of the classical contribution S_0. The fermion sector yields

$$|B_\psi^{(1)\mathrm{grad}}| \sim \int \mathrm{d}^4x \, \frac{\kappa^2}{8\pi^2}\frac{1}{2}\partial_\mu\phi\partial_\mu\phi \sim \frac{\kappa^2}{16\pi^2}S_0 \tag{4.3.226}$$

Similar results can be obtained for the non-Abelian gauge fields through an analogous, however more tedious gradient expansion as for the Abelian case presented above and gives

$$|B_G^{(1)\mathrm{grad}}| \sim \int \mathrm{d}^4x \frac{C^2g^2}{4\pi^2} \cdot \frac{1}{2}(\partial_\mu\phi)^2 \sim \frac{C^2g^2}{8\pi^2}S_0, \tag{4.3.227}$$

where C is the normalization of the Casimir operator for the generators of the group G. Different ratios can be computed to get a rough estimate of the relevance of gradient effects over homogeneous ones. We list some of them here:

$$\frac{|B_{\phi}^{(1)\mathrm{grad}}|}{|B_{\phi}^{(1)\mathrm{hom}}|} \sim \frac{\lambda}{72}, \tag{4.3.228}$$

$$\frac{|B_{\psi}^{(1)\mathrm{grad}}|}{|B_{\psi}^{(1)\mathrm{hom}}|} \sim \frac{\lambda}{24\kappa^2}, \tag{4.3.229}$$

$$\frac{|B_{\psi}^{(1)\mathrm{grad}}|}{|B_{\phi}^{(1)\mathrm{hom}}|} \sim \frac{2}{3}\frac{\kappa^2}{\lambda}\frac{N_f}{N_s}, \tag{4.3.230}$$

where we have included N_f for the number of fermions and N_s for the number of scalars in the model. The expressions above imply that for $N_s = 1$, the scalar gradient effects will never overcome the homogeneous ones if λ is to remain in the perturbative regime, while the possibility of fermion gradient effects dominating the scalar and fermion homogeneous terms is open in scenarios with $N_f \geq 36$ if we demand that gradient effects from fermions are larger than both homogeneous terms, scalar and fermion one. A less demanding scenario occurs within the SM, where we have $\kappa \sim 1$ for the quarks, $N_f = 3$ (heavy quarks), $N_s = 4$ and $|\lambda| \sim 0.1$, hence

$$\frac{|B_{\psi}^{(1)\mathrm{grad}}|}{|B_{\psi}^{(1)\mathrm{hom}}|} \sim 0.004, \tag{4.3.231}$$

$$\frac{|B_{\psi}^{(1)\mathrm{grad}}|}{|B_{\phi}^{(1)\mathrm{hom}}|} \sim 5, \tag{4.3.232}$$

which shows how heavy quarks' field gradients can dominate over homogeneous scalar contributions.

Let us consider the same ratios as above but replacing the fermion with the gauge field. Collecting the Eqs. (4.3.222),(4.3.224) and (4.3.227) we arrive to

$$\frac{|B_{G}^{(1)\mathrm{grad}}|}{|B_{G}^{(1)\mathrm{hom}}|} \sim \frac{16\lambda C^2}{9g^2 \dim \mathfrak{g}}, \tag{4.3.233}$$

$$\frac{|B_{G}^{(1)\mathrm{grad}}|}{|B_{\phi}^{(1)\mathrm{hom}}|} \sim \frac{4g^2C^2}{3\lambda N_s}. \tag{4.3.234}$$

For the weak sector of the SM case we have $g \sim 0.5$ $|\lambda| \sim 0.1$, $\dim \mathfrak{su}(2) = 3$ and $C^2 \sim 3/4$, which implies that both equations above are equal to 0.2, so we can expect $|B_{G}^{(1)\mathrm{grad}}|, |B_{G}^{(1)\mathrm{hom}}|$ and $|B_{\phi}^{(1)\mathrm{hom}}|$ to be roughly of the same order for the case of $SU(2)$. The ratios above are expected to be crude estimates, and it is important to compare them to the exact numerical results for the models that we have presented in Sec. 4.1 and Sec. 4.2.1.

We performed the computation of $|B_{X}^{(1)\mathrm{grad}}|$ for $X \in \{\phi, \psi\}$ but in an MS scheme as done in Sec. 4.2.1. Using the same parameter values, $\mu^2 = 1$, $\lambda = 2$, $\kappa = 0.5$ and a mass scale $\kappa \langle\phi\rangle = \kappa\sqrt{6\mu^2/\lambda}$, the results are shown in Table 4.4. We can see that the estimates give the correct order of magnitude in the last three rows. From the parameters we can

compute the ratios in Eqs. (4.3.228) and (4.3.230) giving:

$$\frac{|B_\phi^{(1)\mathrm{grad}}|}{|B_\phi^{(1)\mathrm{hom}}|} \sim \frac{\lambda}{72} = 0.028 \tag{4.3.235}$$

$$\frac{|B_\psi^{(1)\mathrm{grad}}|}{|B_\psi^{(1)\mathrm{hom}}|} \sim \frac{\lambda}{24\kappa^2} = 0.33, \tag{4.3.236}$$

While the numerical implementation outputs

$$\frac{|B_\phi^{(1)\mathrm{grad}}|}{|B_\phi^{(1)\mathrm{hom}}|} \sim 0.3479, \tag{4.3.237}$$

$$\frac{|B_\psi^{(1)\mathrm{grad}}|}{|B_\psi^{(1)\mathrm{hom}}|} \sim 0.1379. \tag{4.3.238}$$

We observe how at least the first ratio is predicted to the correct order, while the homogeneous scalar fluctuations seem to be an order of magnitude away.

Contribution	Numerical	Gradient Est.
S_0	2.828	–
$B_\phi^{(1)\mathrm{hom}}$	−0.0078	0.0537
$B_\psi^{(1)\mathrm{hom}}$	−0.0094	0.0134
$B_\phi^{(1)\mathrm{grad}}$	0.0027	0.0015
$B_\psi^{(1)\mathrm{grad}}$	0.0013	0.0045

Table 4.4: Results for the different contributions in the Higgs-Yukawa model of Sec. 4.1 in MS scheme and the corresponding estimates performed via the gradient expansion techniques.

We make the last comparison of the ratios estimated via the gradient expansion and the ones obtained numerically for the gauge-Higgs model of Sec. 4.2.1 where the scalar field is subject to a polynomial potential of order six, presenting degenerate minima at the one-loop level. To be able to use the estimates above, we manufacture a tree-level potential that presents the same minima locations and barrier height, so this means that instead of the parameters in Eq. (4.2.159), we use the following set of parameters

$$\begin{aligned} \alpha &= 2.21723 \\ \lambda &= -2.49302 \\ \lambda_6 &= 0.700777 \end{aligned} \tag{4.3.239}$$

and expect to obtain matching results up to orders of magnitude. The classical action for the set of parameters in Eq. (4.3.239) is

$$S_0/V = \int \mathrm{d}z \frac{1}{2}(\partial_z\phi)^2 + V(\phi) = 1.32432 \tag{4.3.240}$$

In units of $\alpha^{3/2}$ we have that $S_0/V = 0.4682$ which is to be compared with $(\mathcal{B}^{(0)} + \mathcal{B}^{(1)\text{ren}})/V = 0.473$ from Table 4.3. Table 4.5 shows the comparison of the numerical results versus the estimates produced from Eqs. (4.3.222), (4.3.225) and (4.3.227) the parameters above which prove to be in decent agreement up to a factor of 2.

Contribution	Numerical $[\alpha^{3/2}]$	Gradient Est. $[\alpha^{3/2}]$
$B_\phi^{(1)\text{hom}}$	0.00478	0.009
$B_\phi^{(1)\text{ren grad}}$	0.00139	0.0005
$B_\psi^{(1)\text{ren grad}}$	0.00332	0.0014

Table 4.5: Results for the different contributions of a similar model described in the text, comparable to the gauge-Higgs model of Sec. 4.2.1, in MS scheme and the corresponding estimates performed via the gradient expansion techniques.

4.4 Summary and conclusions from the case study and estimations made

We have employed the method described in Ref. [30] to compute the gradient corrections to the radiative effects in a false vacuum decay setting. It is the first explicit computation of such effects for a model with a gauge symmetry. Explicitly the phenomenon presented in this chapter is possibly the simplest such scenario, the Abelian case of a $U(1)$-gauge symmetry with two minima at tree-level, forced degeneracy at the one-loop level and zero temperature. To study this tunneling process for a complex scalar, we have written down a polynomial potential of degree 6 exclusively having the combination $\hat{\Phi}^*\Phi$. This model will serve as an illustration of the capabilities of the method from Ref.[30] described again here and paved the way for future application of it to more realistic models as for example, the SM. Besides the purely academic interest, this model can also be considered as an effective field theory coming from certain UV completions, of which one possibility was already mentioned within the text, arguing in favor of neglecting other operators other than $|\hat{\Phi}|^6$. We have also used the thin-wall and planar-wall approximations which have simplified the computation and may be lifted in even more precise future studies.
We have seen how the effects coming from loop-corrections in the scalar and gauge boson sectors contribute positively to the effective action, hence making the decay rate of the false vacuum smaller and its lifetime larger, in agreement with the common knowledge. We obtain results for the gradient corrections that are comparable in size with traditional homogeneous one-loop effects. That is, in order to have full one-loop results, gradient corrections need to be included to all orders. Considering only leading terms from a gradient expansion still keeps the uncertainty at the loop factor level. In this study, we have included all gradient effects up to the one-loop order in the semi-classical approximation and added the contributions from dumbbell diagrams which may come to dominate the $\hbar^2$ term under certain conditions like the presence of colors or spectator fields[31].
After the application of the self-consistent Green's function method also in the thin-will regime, we have obtained larger effects than the ones previously seen in [31]. We are currently trying to find out the origin of said enhancement. It is suspected that the suppressed effects of the previous models come from an emergent $\mathbb{Z}_2$ symmetry related to the interchange of false and true vacuum locations. Whatever the exact reason behind the

difference might be, the relevance of including gradients has also been shown away from the thin-wall limit in a scale-invariant model in [85], supporting the results here reported. The present study extends previous applications by proposing a methodology to obtain the Green's functions for the coupled sector of the gauge and the Goldstone bosons. A general family of gauge choices implies mixing of the different gauge field components and the Goldstone. For the simplest gauge choice possible, we are able to solve the sector numerically by employing the planar-wall approximation and considering two different regimes of momentum flowing parallel to the bubble's wall. For low values of the momentum, we are able to numerically compute exact solutions, while for higher values of $|\mathbf{k}|$, we employ an iterative procedure. The second point of improvement in comparison to previous studies has been the construction of the simplified bounce φ_0, which allows us to avoid possible long-distance divergences appearing from the departures of degeneracy when adopting the one-loop effective potential. We have illustrated how that bounce can contain the details of the tree- and one-loop levels by introducing the appropriate compensating terms to the semi-classical expansion.

The last section about estimations via gradient expansions is also novel and has not yet been published. We plan to fill in details and suppose they will be helpful, for example, for model building or as pointers to models that may feature unaccounted gradient corrections, which are very relevant to topics related to cosmology and phase transitions. We can only expect the techniques described here will find further application to more realistic models, getting closer to the SM. At the implementation level of the Green's functions method, there are clear directions of improvement, such as lifting some of the approximations or considering the impact of different gauge choices on the decay rate of false vacuum in order to make computations more general. If we expect our phenomenological models to be ever more precise and descriptive, we might have to embrace the possibility that gradient effects play a comparable role to homogeneous effects and must be included in particular models.

Part III

Applications to QCD: instantons and the CP-problem

5

QCD review: vacuum structure, phenomenology and related mysteries

As a second application of some of the methods presented in Part I, we consider the impact of fluctuations around a dilute instanton gas in quantum chromodynamics (QCD). This study has led us to interesting conclusions concerning the strong CP problem. In addition, we include alternative arguments supporting the same conclusion using methods not related to perturbation theory or the computation of fluctuations, which we describe in a later chapter.

We will begin by introducing the strong CP problem and the necessary notions to understand the arguments that will be presented in the next chapter. This little journey will take us through, first of all, QCD in isolation, where we will describe its content and some of its symmetries, with a special focus on its chiral properties. We will then naturally speak about anomalies as well as the topological term or $F\tilde{F}$ (read "F F dual") term and its vacuum structure. At that point, we will state the strong CP problem.

In what follows, we give a brief summary of a few phenomenological aspects concerning the θ-angle we saw comes from the vacuum structure. First, we give some comments pertaining to the construction of low-energy QCD theories. More precisely, we will describe the very basics of chiral perturbation theory (chPT) and include important remarks about the matching of the 't Hooft operator[105]. We then give some comments on the mass of the η' particle, which was generally problematic as its mass does not correspond to the size expected for a pseudo-Nambu-Goldstone boson (pNGB) of the $SU(2)_L \times SU(2)_R$ approximate symmetry related to small up and down quark masses (the $U(1)_A$-problem). Lastly, we close the section by relating the above with the so-called topological susceptibility while taking the chance to report current knowledge.

Before we jump into the discussion pertaining to the CP violation/conservation in QCD, we will require to go over some mathematical tools that will also serve to establish the notation. Here instantons will be reviewed from a physical perspective, however, with tinges and small mentions of the beautiful mathematics behind these non-perturbative solutions. In view of all of the above, we hope the reader enjoys the next chapter.

5.1 Quantum Chromodynamics (QCD)

The following presentation of the strong CP problem is based on the following reviews [106–108] which not only introduce the problem but elaborate on different current solu-

tions, especially the possibility of the existence of an Axion particle. We begin with the Lagrangian density for the strong sector of QCD. QCD is the gauge theory of quarks and gluons on Minkowski spacetime, with gauge group $SU(3)$:

$$\mathcal{L}_{\text{QCD}} = -\frac{1}{4}F^{\mu\nu,a}F^a_{\mu\nu} + \sum_{q,a,b}\bar{q}_a(\mathrm{i}\not{D} - m_q\,\mathrm{e}^{\mathrm{i}\alpha_q\gamma^5}\delta_{ab})q_b \tag{5.1.1}$$

where a, b are color indices, q are Dirac fermions in the fundamental representation, come int the different flavors (u, s, d, c, b, t) and where

$$F^a_{\mu\nu} = \partial_\mu A^a_\nu - \partial_\nu A^a_\mu + g_s f^{abc}A^b_\mu A^c_\nu \tag{5.1.2}$$

is the gauge field strength tensor of A^a_μ with g_s the strong coupling parameter. We have parameterized the mass term so that

$$\bar{q}m_q\,\mathrm{e}^{\mathrm{i}\alpha_q\gamma^5}q = m_R\bar{q}q + \mathrm{i}\bar{q}\gamma^5 m_I q. \tag{5.1.3}$$

The model above can be supplemented with the θ-term or topological term:

$$\mathcal{L}_\theta = \theta\,\frac{g_s^2}{64\pi^2}\epsilon^{\mu\nu\lambda\sigma}F^a_{\mu\nu}F^a_{\lambda\sigma} \equiv \theta\frac{g_s^2}{32\pi^2}F^a\tilde{F}^a, \tag{5.1.4}$$

where we have included the definition of the dual field strength tensor implicitly with a $\tilde{}$, which is mathematically known also as the Hodge star (denoted by $*$) of the two-form F, which can be defined formally and in more generality in the language of differential forms. For the present document, it is just important to understand that F and $\operatorname{tr} F{*}F = \operatorname{tr} F^a\tilde{F}^a$ are geometrical objects which are fully independent of the choice of coordinate patches used to describe them and, as we will see, have a deep connection to the topological properties of the spacetime and the gauge group.

We recall the parity transformation P and the charge conjugation C are discrete symmetries, meaning they do not depend on any continuous parameter and in particular they square to the identity. More over, P belongs to the full Lorentz group $O(1,3)$, which acts on spacetime points as follows

$$\mathrm{P}\big((t,\vec{x})\big) = (t,-\vec{x}) \tag{5.1.5}$$

and at the level of spinors a parity transformation exchanges L and R components. In the Weyl representation for the γ^μ, it can be written in short as $\mathrm{P}\big(\psi(t,\vec{x})\big) = \gamma_0\psi(t,-\vec{x})$. C on the other hand can be defined directly by its action on Dirac spinors as

$$\mathrm{C}(\psi) = -\mathrm{i}\gamma_2\psi^*, \tag{5.1.6}$$

where * denotes complex conjugation, and colloquially we say it sends particles to anti-particles.

The terms in Eqs.(5.1.3) and (5.1.4) are actually both responsible of CP violations. In general, we can recognize CP violation by means of the different phases appearing in the different terms of the Lagrangian density. A global phase, where the argument of the CP varying coefficients in the Lagrangian density is the same, creates no interference and implies that such phase is unphysical or not measurable. However, differing phases in these terms imply CP violation processes. This means that in order to study whether there is CP violation or not in the strong sector, we must track down these phases.

We can understand why the θ-term is CP-violating simply by an analogy with the electromagnetic case, where although the gauge group is Abelian and it has no physical consequences, its expression in terms of the classical electric and magnetic fields $\vec{E}, \vec{B}$, is very illustrative. In the case of electromagnetism

$$\epsilon^{\mu\nu\lambda\sigma} F^a_{\mu\nu} F^a_{\lambda\sigma} \propto \operatorname{tr} \vec{E} \cdot \vec{B}. \tag{5.1.7}$$

A parity transformation makes the following exchanges $\vec{E} \to -\vec{E}$ and $\vec{B} \to \vec{B}$, while the charge conjugation turns $E \to -\vec{E}$ and $\vec{B} \to -\vec{B}$, hence a CP transformation of the θ-term takes $\epsilon^{\mu\nu\lambda\sigma} F^a_{\mu\nu} F^a_{\lambda\sigma} \to -\epsilon^{\mu\nu\lambda\sigma} F^a_{\mu\nu} F^a_{\lambda\sigma}$ and the combination CP is not preserved.
In addition to the θ-term, there is an additional possible source of CP violation hidden in the quark mass matrix. They can both display CP violation and with the evidence of the weak sector already violating CP, there is no reason for us to neglect these phases in the absence of a more fundamental principle protecting the CP symmetry. It is nevertheless extremely puzzling why to date, the bounds on CP violation are extremely small. More about the current bounds will be described soon.
Ignoring the two possible CP-violating sources, i.e., masses and the θ-term, $\mathcal{L}_{QCD}$ has the following global symmetry $U(N_f)_R \times U_L(N_f) \simeq SU(N_f)_L \times SU(N_f)_R \times U(1)_L \times U(1)_R$ group, labeled the QCD chiral limit, where N_f specifies the number of flavors and where the symmetries are understood to be approximate given that we know quark masses are not zero. Using a different basis of infinitesimal generators or, said differently, grouping the transformation parameters so that we rotate L and R by the same amount (vector) or L and R by amounts opposite in sign (axial or chiral), we can write down the same symmetry group as $SU(N_f)_V \times SU(N_f)_A \times U(1)_V \times U(1)_A$ which highlights the symmetries that, as we will show, are not actually symmetries at the quantum level, namely they are anomalous, independently of whether we consider a θ-term or not.

The Fujikawa method for computing anomalies

We show here in a reduced version how the chiral anomaly or ABJ-anomaly[8, 9] can be understood from path integral methods. For this we follow textbook expositions[20, 21] and [14] to illustrate Fujikawa's method. For the anomaly computation, we need only consider a simpler model of a single massless fermion and a $U(1)$-gauge field, viz. massless QED. In such a model, the Lagrangian symmetries are enhanced in the absence of masses and one is free to rotate L and R components independently. Hence, in reality, the model has a $U(1)_L \times U(1)_R$ symmetry. This symmetry can be equally well described by $U(1)_V \times U(1)_A$. According to this, the fermion would transform as:

$$\psi \longrightarrow \mathrm{e}^{\mathrm{i}\alpha}\psi, \qquad \text{Vector} \tag{5.1.8}$$

$$\psi \longrightarrow \mathrm{e}^{\mathrm{i}\alpha\gamma^5}\psi. \qquad \text{Axial} \tag{5.1.9}$$

According to Noether's theorem we can define a current for each, which is conserved. One way to obtain them is by assuming the symmetries are local, and considering variations with respect to $\alpha(x)$, we have then

$$j^\mu = \bar{\psi}\gamma^\mu\psi \tag{5.1.10}$$

$$j^{\mu\,5} = \bar{\psi}\gamma^\mu\gamma^5\psi \tag{5.1.11}$$

and classically, we expect the conservation laws

$$\partial_\mu j^\mu = 0 \qquad \text{and} \qquad \partial_\mu j^{\mu\,5} = 0. \tag{5.1.12}$$

Let us consider the above chiral transformation in the context of the path integral for the partition function (with $\hbar = 1$)

$$Z = \int \mathcal{D}\psi\, \mathcal{D}\bar{\psi}\, \mathcal{D}(A_\lambda) \exp\left[\mathrm{i}\int \mathrm{d}^4x \left(-\frac{1}{4}F_{\mu\nu}F^{\mu\nu} + \bar{\psi}\mathrm{i}\not{D}\psi\right)\right]. \tag{5.1.13}$$

The chiral rotation in Eq. (5.1.9) corresponds to the infinitesimal field redefinition

$$\begin{aligned} \psi(x) &\to \psi'(x) = (1 + \mathrm{i}\alpha(x)\gamma^5)\psi(x), \\ \bar{\psi}(x) &\to \bar{\psi}'(x) = \bar{\psi}(1 + \mathrm{i}\alpha(x)\gamma^5), \end{aligned} \tag{5.1.14}$$

where we have promoted the parameter α to a spacetime point dependent function $\alpha(x)$ to obtain the associated axial current. The fermionic part of the action for the transformed fields is, after an integration by parts,

$$\int \mathrm{d}^4x\, \bar{\psi}'(\mathrm{i}\not{D})\psi' = \int \mathrm{d}^4x\, \bar{\psi}(\mathrm{i}\not{D})\psi + \alpha(x)\partial_\mu(\bar{\psi}\gamma^\mu\gamma^5\psi). \tag{5.1.15}$$

However, to compute the variation with respect to $\alpha(x)$ of the partition function itself, we must consider the possible transformation of the measure as suggested by Fujikawa. To properly transform the measure, we use a decomposition of the fermions into eigenfunctions as done in the mathematical background, Part I. For the Dirac equation, we have pairs $\psi_m, \bar{\psi}_m$ which share eigenvalues but are right or left eigenfunctions, respectively,

$$(\mathrm{i}\not{D})\psi_m = \lambda_m\psi_m \qquad \text{and} \qquad \bar{\psi}_m\overleftarrow{(\mathrm{i}\not{D})} = \lambda_m\bar{\psi}_m, \tag{5.1.16}$$

and can be chosen to be orthonormal since $\mathrm{i}\not{D}$ is Dirac-Hermitian (with respect to barred inner-product.) We can then use a spectral decomposition for ψ and $\bar{\psi}$ so that

$$\psi(x) = \sum_m a_m\psi_m(x) \qquad \text{and} \qquad \bar{\psi}(x) = \sum_m \bar{b}_m\bar{\psi}_m(x), \tag{5.1.17}$$

for Grassmann coefficients and c-number eigenfunctions, given the fermionic nature of ψ and $\bar{\psi}$. With this decomposition we can express the measure as an infinite product of measures for each direction and also expand the transformed functions in such basis of functions:

$$\mathcal{D}\psi'\mathcal{D}\bar{\psi}' = \prod_m \mathrm{d}a'_m\, \mathrm{d}b'_m = \det{}^{-2}\mathcal{J}\prod_m \mathrm{d}a_m\, \mathrm{d}b_m = \det{}^{-2}\mathcal{J}\mathcal{D}\psi\mathcal{D}\bar{\psi}, \tag{5.1.18}$$

where $\mathcal{J}$ is the Jacobian corresponding to the coordinate transformation. From the transformation relation in (5.1.14) we know that for coefficients a_m

$$a'_m = a_m + \sum_n \mathrm{i}a_n \int \mathrm{d}^4x\, \bar{\psi}_m(x)\alpha(x)\gamma^5\psi_n(x) \tag{5.1.19}$$

$$\bar{b}'_m = \bar{b}_m + \sum_n \mathrm{i}\bar{b}_n \int \mathrm{d}^4x\, \bar{\psi}_n(x)\alpha(x)\gamma^5\psi_m(x) \tag{5.1.20}$$

The product per direction is then

$$\prod_m \mathrm{d}a'_m\,\mathrm{d}\bar{b}'_m = \prod_m \det{}^{-1}(\delta_{ij} + \mathrm{i}\int \mathrm{d}^4x\,\bar{\psi}_i\alpha(x)\gamma^5\psi_j(x))\,\mathrm{d}a_m \tag{5.1.21}$$

$$\times\ \mathrm{d}\bar{b}_m \det{}^{-1}(\delta_{k\ell} + \mathrm{i}\int \mathrm{d}^4x\,\bar{\psi}_k(x)\alpha(x)\gamma^5\psi_\ell(x)) \tag{5.1.22}$$

$$= \prod_m \mathrm{d}a_m\,\mathrm{d}\bar{b}_m \det{}^{-2}(\delta_{ij} + \mathrm{i}\int \mathrm{d}^4x\,\bar{\psi}_i\alpha(x)\gamma^5\psi_j(x)) \tag{5.1.23}$$

$$= \prod_m \mathrm{e}^{-2\,\mathrm{tr}(\log[1+\mathrm{i}\alpha(x)\gamma^5])}\,\mathrm{d}a_m\,\mathrm{d}\bar{b}_m \tag{5.1.24}$$

$$\approx \mathrm{e}^{-2\mathrm{i}\,\mathrm{tr}[\alpha(x)\gamma^5]} \prod_m \mathrm{d}a_m\,\mathrm{d}\bar{b}_m, \tag{5.1.25}$$

where we have neglected contributions of order α^2 and higher, the Taylor expansion of the log was used, the trace is to be taken by using any basis of functions for the domain of the Dirac operator, e.g. the eigenfunctions $\psi_m, \bar{\psi}_m$. For the computation of the exponent we need to introduce a regulator, otherwise the result diverges linearly as it is known from the computation of the amplitude of the anomaly triangle diagram, e.g. as in the decay $\pi^0 \to 2\gamma$. It is traditional to employ a heat-kernel method[14, 20, 21], which has the advantage of gauge invariant, to regulate this operator. Let M be the regulator scale, thought of as a large mass and make the replacement

$$\mathrm{tr}[\alpha(x)\gamma^5] \longrightarrow \lim_{M\to\infty} \mathrm{tr}[\alpha(x)\gamma^5\,\mathrm{e}^{\frac{(\mathrm{i}\not{D})^2}{M^2}}] = \lim_{M\to\infty}\int \mathrm{d}^4x\,\alpha(x)\sum_n \bar{\psi}_n(x)\gamma^5\,\mathrm{e}^{\frac{(\mathrm{i}\not{D})^2}{M^2}}\psi_n(x). \tag{5.1.26}$$

First we can get rid of the gamma matrices hidden in $\not{D}^2$, by using the identity

$$\not{D}^2 = \gamma^\mu\gamma^\nu D_\mu D_\nu = D_\mu D^\mu + \frac{\mathrm{i}g}{4}[\gamma^\mu,\gamma^\nu]F_{\mu\nu}, \tag{5.1.27}$$

and then use a basis of plane waves instead of the eigenfunctions above

$$\sum_n \bar{\psi}_n(x)\gamma^5\,\mathrm{e}^{\frac{(\mathrm{i}\not{D})^2}{M^2}}\psi_n(x) = \mathrm{tr}\int \frac{\mathrm{d}^4k}{(2\pi)^4}\,\mathrm{e}^{-\mathrm{i}\,kx}\gamma^5\,\mathrm{e}^{-\frac{D^2}{M^2}-\frac{\mathrm{i}g}{4M^2}[\gamma^\mu,\gamma^\nu]F_{\mu\nu}}\,\mathrm{e}^{\mathrm{i}\,kx} \tag{5.1.28}$$

where the trace is over spinor indices. Using the Baker-Campbell-Hausdorff (BCH) formula

$$\mathrm{e}^{(X+Y)/M^2} = \mathrm{e}^{X/M^2}\,\mathrm{e}^{Y/M^2}\,\mathrm{e}^{-[X,Y]/(2M^4)}\ldots \tag{5.1.29}$$

we can split the exponential with the regulator to obtain

$$\sum_n \bar{\psi}_n(x)\gamma^5\,\mathrm{e}^{\frac{(\mathrm{i}\not{D})^2}{M^2}}\psi_n(x) = \mathrm{tr}\int\frac{\mathrm{d}^4k}{(2\pi)^4}\,\mathrm{e}^{-\mathrm{i}\,kx}\gamma^5\,\mathrm{e}^{-\frac{D^2}{M^2}}\,\mathrm{e}^{-\frac{\mathrm{i}g}{4M^2}[\gamma^\mu,\gamma^\nu]F_{\mu\nu}}\,\mathrm{e}^{-\frac{\mathrm{i}g}{2\cdot 4M^4}[D^2,F_{\mu\nu}][\gamma^\mu,\gamma^\nu]}\,\mathrm{e}^{\mathrm{i}\,kx}. \tag{5.1.30}$$

From the properties of the Dirac matrices, we know that we need at least four gamma matrices next to the γ^5 for the trace to be non-zero, hence the lowest order term in powers of M comes from the exponential with just one commutator in the exponent and is

$$\sum_n \bar{\psi}_n(x)\gamma^5\,\mathrm{e}^{\frac{(\mathrm{i}\not{D})^2}{M^2}}\psi_n(x) = \mathrm{tr}\int \frac{\mathrm{d}^4k}{(2\pi)^4}\,\mathrm{e}^{-\mathrm{i}\,kx}\gamma^5\,\mathrm{e}^{-\frac{D^2}{M^2}}\,\mathrm{e}^{\mathrm{i}\,kx}\left(\frac{g^2([\gamma^\mu,\gamma^\nu]F_{\mu\nu})^2}{2!\cdot 16M^4}\right) + \mathcal{O}(M^{-5}). \tag{5.1.31}$$

We can now neglect the gauge field term in the covariant derivative by observing that compared to large M and large k, it can be made arbitrarily small, thus

$$\sum_n \bar{\psi}_n(x)\gamma^5 \,\mathrm{e}^{-\frac{(\mathrm{i}\not{D})^2}{M^2}}\psi_n(x) = \frac{g^2}{32M^4}\,\mathrm{tr}\int \frac{\mathrm{d}^4k}{(2\pi)^4}\,\mathrm{e}^{-\mathrm{i}\,kx}\gamma^5\,\mathrm{e}^{-\frac{\partial^2}{M^2}}\,\mathrm{e}^{\mathrm{i}\,kx}\left([\gamma^\mu,\gamma^\nu][\gamma^\sigma,\gamma^\lambda]F_{\mu\nu}F_{\sigma\lambda}\right). \tag{5.1.32}$$

We can now perform the trace and act with D^2 to the left to arrive to

$$\sum_n \bar{\psi}_n(x)\gamma^5 \,\mathrm{e}^{-\frac{(\mathrm{i}\not{D})^2}{M^2}}\psi_n(x) = \frac{g^2}{32M^4}\int \frac{\mathrm{d}^4k}{(2\pi)^4}\,\mathrm{e}^{\frac{k^2}{M^2}}\,\mathrm{tr}(\gamma^5[\gamma^\mu,\gamma^\nu][\gamma^\sigma,\gamma^\lambda])F_{\mu\nu}F_{\sigma\lambda} \tag{5.1.33}$$

$$= \frac{g^2}{32M^4}(16\mathrm{i}\epsilon^{\mu\nu\sigma\lambda})F_{\mu\nu}F_{\sigma\lambda}\int \frac{\mathrm{d}^4k}{(2\pi)^4}\,\mathrm{e}^{\frac{k^2}{M^2}}. \tag{5.1.34}$$

The last step is to use a Wick rotation ($k^0 \to \mathrm{i}k^4$) to compute the integral above,

$$\sum_n \bar{\psi}_n(x)\gamma^5 \,\mathrm{e}^{-\frac{(\mathrm{i}\not{D})^2}{M^2}}\psi_n(x) = -\frac{g^2}{2M^4}\epsilon^{\mu\nu\sigma\lambda}F_{\mu\nu}F_{\sigma\lambda}\int \frac{k_E^3\,\mathrm{d}k_E}{8\pi^2}\,\mathrm{e}^{\frac{-k_E^2}{M^2}} \tag{5.1.35}$$

$$= -\frac{g^2}{16\pi^2M^4}F_{\mu\nu}\epsilon^{\mu\nu\sigma\lambda}F_{\sigma\lambda}\frac{M^4}{2}, \tag{5.1.36}$$

which can be reorganized and by collecting results from Eqs. (5.1.25),(5.1.15) and (5.1.13) we can write down the transformed partition function after the chiral transformation has taken place

$$Z = \int \mathcal{D}\psi\mathcal{D}\bar{\psi}\mathcal{D}(A_\lambda)\exp\left[\mathrm{i}\int \mathrm{d}^4x\left(-\frac{1}{4}F_{\mu\nu}F^{\mu\nu} + \bar{\psi}\mathrm{i}\not{D}\psi + \alpha(x)\left(\partial_\mu j^{\mu\,5} + \frac{2g^2}{16\pi^2}F_{\mu\nu}\tilde{F}_{\mu\nu}\right)\right)\right]. \tag{5.1.37}$$

Following Noether's procedure, we can conclude by imposing that the partition function is unchanged under global chiral transformations, the above has to vanish for arbitrary $\alpha(x)$, which means

$$\partial_\mu j^{\mu\,5} = -\frac{g^2}{8\pi^2}F_{\mu\nu}\tilde{F}_{\mu\nu}. \tag{5.1.38}$$

Some observations must be made at this point. The result above did not rely on any expansion on couplings and is therefore exact. That is, it is captured by one-loop methods and does not receive corrections from higher-order terms. We notice as well that the result is proportional to the θ-term presented before and that the steps followed to get to it can easily be modified to obtain the non-Abelian version for an arbitrary number of fermions and gauge groups. We remark that the key ingredient for this type of anomalies to occur is the non-cancellation of Jacobians in the path integral, as opposed to the vector transformation cases, where the Jacobian from ψ cancels with that from transforming $\bar{\psi}$. Lastly, we can view this phenomenon as spontaneous symmetry breaking coming from loop corrections since there is no explicit parameter breaking the symmetry explicitly at tree-level or classically, while the non-preservation of the chiral current appears from the anomaly. However, this perspective is misleading. From the point of view of symmetry breaking, we expect the appearance of Nambu-Goldstone bosons (NGBs) every time there is symmetry breaking, but as we have seen from the path integral perspective, the symmetry is not there to begin with, and hence there is no expectation of an NGB[47].

We extend now the result for the case of interest, massless QCD with N_f flavors, where we consider again chiral rotations for the quarks as in Eq. (5.1.9), these are associated to the flavor-singlet axial current:

$$j^{5\,\mu\,(0)} = \sum_f \bar{q}_f \gamma^\mu \gamma^5 q_f. \tag{5.1.39}$$

Redoing the computation for the axial anomaly in massless QED done above, the only difference is that the identity in Eq. (5.1.27) requires some modification, in order to adapt it to the non-Abelian case:

$$\not{D}^2 = \gamma^\mu \gamma^\nu D_\mu D_\nu = D_\mu D^\mu + \frac{\mathrm{i} g_s}{4} \frac{\lambda^a}{2} [\gamma^\mu, \gamma^\nu] F^a_{\mu\nu}, \tag{5.1.40}$$

where the new upper index a is a color index labeling our choice of generators $\lambda^a/2$ of the color group Lie algebra $\mathfrak{su}(3)$, with λ^a the Gell-Mann matrices. So that the term proportional to the set of four Dirac matrices is now

$$\sum_{f,n} \bar{q}_{f_n}(x) \gamma^5 \, \mathrm{e}^{-\frac{(\mathrm{i}\not{D})^2}{M^2}} q_{f_n}(x) = \frac{g_s^2 N_f}{32 M^4} (16 \mathrm{i} \epsilon^{\mu\nu\sigma\lambda}) \frac{\mathrm{tr}(\lambda^a \lambda^b)}{4} F^a_{\mu\nu} F^b_{\sigma\lambda} \int \frac{\mathrm{d}^4 k}{(2\pi)^4} \, \mathrm{e}^{\frac{k^2}{M^2}} \tag{5.1.41}$$

$$= -\frac{g_s^2 N_f}{64 \pi^2} \epsilon^{\mu\nu\sigma\lambda} F^a_{\mu\nu} F^a_{\sigma\lambda}, \tag{5.1.42}$$

so we conclude by considering the Jacobian as before,

$$\partial_\mu j^{5\,\mu\,(0)}(x) = -\frac{g_s^2 N_f}{32 \pi^2} \epsilon^{\mu\nu\sigma\lambda} F^a_{\mu\nu}(x) F^a_{\sigma\lambda}(x). \tag{5.1.43}$$

The Vacuum structure and the invariant $\bar{\theta}$

We attempt here to describe the so-called θ-vacuum without referring to instantons just yet. We describe the ideas originally presented in [109–111] and we follow [47] for this short exposition while adding some details of the mathematical structures involved.

We must first speak about gauge transformations and how they can be classified. This brings us to consider the topology of the geometrical spaces involved. It is particularly relevant for the structure of the QCD vacuum, that the gauge group $SU(3)_{\text{color}}$ of special unitary matrices of dimensions 3×3, allows for different embeddings of the Lie group $SU(2)$ into itself, in other words, we can find different copies of $SU(2)$ inside $SU(3)_{\text{color}}$. At the same time, it is a geometrical fact, that as smooth manifolds, $SU(2)$ and the 3-sphere are diffeomorphic, that is $S^3 \simeq SU(2)$, via the explicit map:

$$\begin{aligned} & f : S^3 \longrightarrow SU(2) \\ & \begin{pmatrix} x^1 \\ x^2 \\ x^3 \\ x^4 \end{pmatrix} \longmapsto \begin{pmatrix} x^4 + \mathrm{i} x^1 & -(x^2 - \mathrm{i} x^3) \\ (x^2 + \mathrm{i} x^3) & x^4 - \mathrm{i} x^1 \end{pmatrix} = x^4 \mathbb{1} + \mathbf{x} \cdot \mathrm{i} \boldsymbol{\sigma}, \end{aligned} \tag{5.1.44}$$

where we are using charts for S^3 such that $x^1, x^2, x^3, x^4 \in \mathbb{R}$ and $x_\mu x^\mu = 1$ for $\mu = 1, 2, 3, 4$, it can be seen that f indeed is smooth, invertible and surjective. So geometrically, when ignoring the Lie group structure, S^3 and $SU(2)$ are indistinguishable.

Coincidentally, Minkowski spacetime has $1 + 3$ dimensions and the 1 representing the time direction serves in flat spacetimes to foliate spacetime with space-like hypersurfaces.

A similar idea can be implemented in Euclidean spacetime, making the relation between gauge transformations and topology completely formal. When we perform a Wick rotation, we bring the line element to Euclidean form and we can thus foliate space by 3-spheres of increasing radius and for each fixed radius r, we have the relation

$$r^2 = (x^1)^2 + (x^2)^2 + (x^3)^2 + (x^4)^2 \tag{5.1.45}$$

among the coordinate components. We see now that a gauge transformation $g(x)$, as a local symmetry, is a mapping taking spacetime points to an element of the gauge Lie group. If we concentrate on the asymptotic behavior alone, the boundary for large r is nothing else than an S^3, and gauge transformations asymptotically map such boundary to the gauge group $SU(3)_{\text{color}}$.

We can then classify gauge transformations according to their asymptotic behavior. It is a known result from topology that the third homotopy group of the 3-sphere is homeomorphic to the integers[112], denoted $\pi_3(S^3) \simeq \mathbb{Z}$. In other words, maps are classified into classes (equivalence classes) up to continuous deformations, with the objective of obtaining a topological invariant. The n-th homotopy group $\pi_n(G)$, for a Lie group[1] G is precisely the group of classes of mappings g,

$$g : S^n \longrightarrow G. \tag{5.1.46}$$

The equivalence class of the identity is that which consists of all maps that can be continuously deformed to a point, i.e. they are contractible. The fact that $\pi_3(SU(3)) \neq 0$, means not all gauge transformations fall in the class of the identity. Those that are not, receive the name of large gauge transformations, an example for $SU(2)$ is[110]

$$g_1(\mathbf{x}) \equiv \left(\frac{\mathbf{x}^2 - d^2}{\mathbf{x}^2 + d^2}\right) \mathbb{1} + \left(\frac{2d}{\mathbf{x}^2 + d^2}\right) \mathbf{x} \cdot \mathrm{i}\boldsymbol{\sigma} \tag{5.1.47}$$

which is independent of the x^4 direction and where d some real parameter and cannot be produced by concatenation of infinitesimal gauge transformations[111], or similarly, it cannot be deformed continuously to a constant element of $SU(2)$, notice how this map is nothing else but a specific case of the embedding f described in Eq. (5.1.44) and we can imagine a bubble-gum bubble wrapped around a sphere, which we cannot reduce into a single point without popping the bubble (see [34] for a more extended discussion). This is precisely related to the important requirement that our allowed gauge transformations are those such that (when working in the specific gauge where $A^4 = 0$)

$$\lim_{|\mathbf{x}| \to \infty} g(\mathbf{x}) = g_\infty, \tag{5.1.48}$$

where g_∞ is a spacetime independent, fixed, element of the gauge group. The condition above ensures that vector potentials of interest fall off as $\frac{1}{|\mathbf{x}|}$ at infinity and without it we would not have the classification described above.

The class to which a given gauge transformation belongs to can be labeled by integers given by what is known as the degree of a continuous map, which for the case of continuous functions between S^1 and itself receives the name of winding number. In physics the term winding number is used generally to mean different things, not only for the case $S^1 \to S^1$ as in mathematics. For the temporal gauge used here it is referred to as the Chern-Simons

[1] The notion is generally defined for topological spaces, but we only require it in application to Lie groups. The groups involved in our applications are also simply connected and there is no need to make reference to base points.

number and is computed out of the spatial parts only. For a given gauge transformation $g(x)$ for the $SU(2)$ case, its degree, or Chern-Simons number for us, is given by

$$\deg[g] = \frac{1}{24\pi^2}\int d^3\mathbf{x}\,\epsilon^{ijk}\,\mathrm{tr}(g^{-1}(\mathbf{x})\partial_i g(\mathbf{x}))(g^{-1}(\mathbf{x})\partial_j g(\mathbf{x}))(g^{-1}(\mathbf{x})\partial_k g(\mathbf{x})), \tag{5.1.49}$$

which is mathematically the wedge product of the Cartan one-form with itself three times in order to produce an integrable 3-form in S^3[113] and is representation independent. It can be proven that as long as the condition in Eq. (5.1.48) holds, the result of the above integration is indeed an integer (see for e.g. Appendix A in [114] for the computations), and is also invariant under continuous deformations, that is all gauge transformations in a given homotopy class have the same winding number. Computing the degree of g_1 as given above is straightforward and gives $\deg[g_1] = 1$. Moreover we can find gauge transformations representative of each homotopy class by exploiting the group structure of $SU(2)$ and operating repeatedly with g_1, so that

$$\deg[g_n] = \deg[(g_1)^n] = n. \tag{5.1.50}$$

Let us remark that this classification applies for gauge transformations that fulfill Eq. (5.1.48), which corresponds to finite action as we will see, any transformation changing the winding number must either be discontinuous or violate Eq. (4.2.90) and implies an infinite action. We continue the explanations in this section for Euclidean quantities but do not change the notation as we are not going to be switching from the Minkowski to the Euclidean version here. Let us now connect this classification with the θ-term mentioned in Eq. (5.1.4). For that purpose, we consider a gauge field strength tensor for the $G = SU(2)$, $F^a_{\mu\nu}$ which is finite. As it can be seen from the kinetic term of the Euclidean action,

$$S^E_{\text{gauge}} = \frac{1}{4g_s^2}\int \mathrm{d}^4x\, F^a_{\mu\nu}F^{\mu\nu\,a}, \tag{5.1.51}$$

with A_μ written in units of the coupling g_s, a necessary condition for the action to be finite is that $F \sim \mathcal{O}(r^{-m})$ with r as in Eq. (5.1.45) and $m > 2$. This implies for the corresponding vector potential in Eq. (5.1.2) that it must decay as $A^a_\mu \sim \mathcal{O}(r^{-m'})$, with $m' > 1$. There are however gauge field configurations which in certain gauge, seem to decay at infinity exactly as r^{-1}, whose field strength still leads to a finite result which we will compute in Sec. 5.3. For now let us consider rewriting the θ-term as the divergence of a current. We can give the current here explicitly

$$K_\mu = \epsilon^{\mu\nu\lambda\sigma}\left[A^a_\nu F^a_{\lambda\sigma} - \frac{1}{3}f^{abc}A^a_\nu A^b_\lambda A^c_\sigma\right] \tag{5.1.52}$$

$$= 2\epsilon^{\mu\nu\lambda\sigma}\left[A^a_\nu\partial_\lambda A^a_\sigma + \frac{1}{3}f^{abc}A^a_\nu A^b_\lambda A^c_\sigma\right], \tag{5.1.53}$$

and we can check that

$$F^a_{\mu\nu}\tilde{F}^{\mu\nu\,a} = \partial_\mu K^\mu. \tag{5.1.54}$$

The form given above for K_μ is proportional to the Hodge dual of the Chern-Simons form of A_μ which is what is written within square brackets in Eq. (5.1.53). This means the Euclidean θ-term is thus a boundary term in the action and in the temporal gauge $A_4 = 0$

we can reduce it at for example $t = \infty$:

$$\frac{\mathrm{i}}{32\pi^2}\int \mathrm{d}^4x\, F^a\tilde{F}^a = \frac{\mathrm{i}}{32\pi^2}\int \mathrm{d}^4x\, \partial_\mu K^\mu = \frac{\mathrm{i}}{32\pi^2}\int \mathrm{d}^3\mathbf{x}\, K^4\Big|_{x^4=-\infty}^{x^4=\infty} \tag{5.1.55}$$

$$= \frac{\mathrm{i}}{48\pi^2}\int \mathrm{d}^3\mathbf{x}\, \epsilon^{ijk} f^{abc} A_i^a(x) A_j^b(x) A_k^c(x)\Big|_{x^4=-\infty}^{x^4=\infty} \tag{5.1.56}$$

$$= \frac{\mathrm{i}}{24\pi^2}\int \mathrm{d}^3\mathbf{x}\, \epsilon^{ijk}\,\mathrm{tr}\left(\boldsymbol{A}_i(x)\boldsymbol{A}_j(x)\boldsymbol{A}_k(x)\right)\Big|_{x^4=-\infty}^{x^4=\infty} \tag{5.1.57}$$

where we used $f^{abc} = \frac{1}{4}\,\mathrm{tr}(\mathrm{i}\lambda^a[\mathrm{i}\lambda^b, \mathrm{i}\lambda^c])$, and have written the fields as $\boldsymbol{A}_\mu = \mathrm{i}\frac{\lambda^a}{2}A_\mu^a$, so that we recover a representation independent expression.
It is useful now to remember how the gauge field and its field strength tensor transform under gauge transformations. Using matrix notation the transformations under an element $g \in G$ are

$$\boldsymbol{A}_\mu \to g^{-1}\boldsymbol{A}_\mu g + g^{-1}\partial_\mu g \tag{5.1.58}$$

$$\boldsymbol{F}_{\mu\nu} \to g\boldsymbol{F}_{\mu\nu}g^{-1}. \tag{5.1.59}$$

We observe that if $\boldsymbol{F}_{\mu\nu}$ vanishes, there is certainly a gauge where $\boldsymbol{A}_\mu$ is a pure gauge configuration, that is $\boldsymbol{A}_\mu = g^{-1}\partial_\mu g$. Or in other words, the vector potential is 0 modulo a gauge transformation. In that case we can choose to represent $\boldsymbol{A}_\mu$ at a fixed x^4, using the gauge group element $g_1 \in SU(2) \subseteq SU(3)$ in Eq. (5.1.47) we have

$$\boldsymbol{A}_i = g_1^{-1}(\mathbf{x})\partial_i g_1(\mathbf{x}) \quad \text{and} \quad A_4 = 0. \tag{5.1.60}$$

So let assume for the time being[2] that there are field configurations such that for $x^4 = -\infty$ the are $\boldsymbol{A}_\mu = 0$ while at $x^4 = \infty$ they are $\boldsymbol{A}_i = g_1^{-1}(\mathbf{x})\partial_i g_1(\mathbf{x})$. Then as we can see from Eq. (5.1.57), and by comparison with Eq. (5.1.49), that the Euclidean θ-term becomes i times an integer, explicitly for the case of an asymptotic behavior as g_1 we have

$$\mathrm{i}\theta\frac{g_s^2}{32\pi^2}\int \mathrm{d}^4x\, F^a\tilde{F}^a = \mathrm{i}\theta(n_\infty - n_{-\infty}) = \mathrm{i}\theta. \tag{5.1.61}$$

So we can understand the θ-term as keeping track of the *total winding number*[47] of a gauge field configuration, which will call a *topological sector* to avoid confusion with the winding- or Chern-Simons-number obtained from the spatial part of the gauge field in temporal gauge.
As we have seen, the classification of gauge transformations implies that the topological sectors can only take on integer values. However, through gauge transformations, in particular large gauge transformations, we can move around where the charge associated with K_μ is concentrated. Hence, the associated charge commonly receives the name of topological charge and when these are concentrated at $x^4 = \pm\infty$ as we have seen above, we call this the *regular gauge* description. Alternatively, the topological charge can be placed at the origin of coordinates via a large transformation that brings the gauge field to its *singular gauge* expression.
Some essential highlights at this point are that gauge transformations cannot change the topological sector, it being a gauge-invariant quantity of a given gauge field configuration

[2] We will see in the next section that such configurations do exist.

as can be seen by using the rule in Eq. (5.1.59) on the θ-term. Second, the arguments here given also apply to the QCD in Minkowski spacetime through a Wick rotation.
Within the regular gauge, we can go further and even apply the canonical quantization formalism as argued by Callan, Dashen and Gross[109] and Jackiw and Rebbi[110, 111], to introduce gauge non-invariant vacuum states, $|n\rangle$, for each $n \in \mathbb{Z}$, which produce a configuration with Chern-Simons n when acted on with the operator-valued gauge field. Since they are modified by large gauge transformations, they cannot be a proper vacuum of the theory and we label them pre-vacuum states. Using the Hamiltonian language and the path integral as we have been doing in the document, we can write

$$\langle n|\, \mathrm{e}^{-HT}|m\rangle \underset{T\to\infty}{=} \int \mathcal{D}[A_\mu]_{n-m}\, \mathrm{e}^{-S^E_{\text{gauge}}[A_\mu]+S_{\text{gf}}}, \tag{5.1.62}$$

where we have included a gauge fixing term. In this sense, these configurations represent possible tunneling phenomena connecting the different pre-vacua. So we face a situation similar to that in quantum mechanics in a setting where there are at least two degenerate potential wells. States that are localized near either well minimum will have energies close to the ground state, while the ground state itself is known to be a superposition of the localized states.
To define the true vacuum of these models, let us look at the zero energy states, that is, at vanishing field strengths and consider that gauge symmetry is supposed to leave the vacuum unchanged. It follows that by using Eq. (5.1.47) or its iterations, we can build vector potentials with different winding numbers, all corresponding to zero-field strength. Given the existence of tunneling configurations, known as instantons, which we will describe in Section 5.3, that shift these pre-vacua

$$U|n\rangle = |n+1\rangle, \tag{5.1.63}$$

where U represents the action of such configuration, we conclude these pre-vacuum states cannot be the true vacuum state. The way out is to superimpose all pre-vacua. The simplest possibility then would be to sum all $|n\rangle$ with a constant coefficient. However, the most general superposition that remains stable under the action of Q_K is the θ-vacuum

$$|\theta\rangle = \sum_n \mathrm{e}^{\mathrm{i}n\theta}|n\rangle. \tag{5.1.64}$$

In this context, θ can take any value and the fact that the vacuum of the theory requires us to fix such parameter externally, meaning every choice of θ corresponds to a different theory, is known as a super-selection rule.
Having introduced the θ-vacuum in a particular gauge and in the canonical context, let us see how it enters the game in the path integral. For that we look at the generic computation of some observable $\mathcal{O}$ in an Euclidean theory with Lagrangian density $\mathcal{L}$,

$$\langle\theta|\mathcal{O}|\theta\rangle = \sum_{n_1,n_2} \mathrm{e}^{\mathrm{i}\theta(n_2-n_1)}\, \langle n_2|\mathcal{O}|n_1\rangle \;=\; \sum_{\Delta n, n_1} \mathrm{e}^{\mathrm{i}\theta\Delta n}\, \langle n_1+\Delta n|\mathcal{O}|n_1\rangle$$

$$\begin{aligned}
\langle\theta|\mathcal{O}|\theta\rangle &= \sum_{\Delta n,n_1} \exp\left\{-\theta\int \mathrm{d}^4x\, \frac{1}{32\pi^2}F\tilde{F}\right\} \langle n_1+\Delta n|\mathcal{O}|n_1\rangle \\
&= \sum_{\Delta n}\int \mathcal{D}[A_\mu]\, \mathcal{O}\exp\left\{-\int \mathrm{d}^4x\, \left(\mathcal{L}[A_\mu]+\frac{\theta}{32\pi^2}F\tilde{F}\right)\right\}\delta\left(\Delta n - \int \mathrm{d}^4x\, \frac{\mathrm{i}}{32\pi^2}F\tilde{F}\right) \\
&= \int \mathcal{D}[A_\mu]\, \mathcal{O}\exp\left\{-\int \mathrm{d}^4x\, \left(\mathcal{L}[A_\mu]+\frac{\theta}{32\pi^2}F\tilde{F}\right)\right\}
\end{aligned}$$

and we learn that to compute expectation values on the θ-vacuum, all we need to do is include the θ-term in the action.
We can collect the results we have, adapt them to actual QCD and introduce the $\bar{\theta}$ invariant as well as the strong CP problem. In the SM, quarks gain their mass through the Higgs mechanism via their Yukawa coupling terms. Current observations tell us that the Yukawa coupling matrices mix different generations and thus flavors, as we saw in PartII. That means that after the EW symmetry breaking has taken place, the masses of the quarks are not diagonal and moreover may have residual phases that are CP-violating even after the Lagrangian is written in the mass basis and all the mixing encapsulated in the CKM-matrix. Paraphrasing Dine [106], CP violation discussions usually begin with counting parameters of the transformations on the quarks (or leptons), bringing us to the mass basis and comparing it with the number of possible redefinitions of the quark (or lepton) fields. This we will do in a way for the rest of the document.
Given the lack of a global symmetry implying CP conservation in the weak sector as has been known since the detection of $K_L \to 2\pi$ in 1964 and confirmed in different processes since, we believe CP should not be a symmetry ad-hoc imposed on the strong sector. Also arguments exist, pointing out that even starting with a CP conserving model, such condition is not stable with respect to renormalization effects[115]. With that in mind and the vacuum structure described above, we consider the effects of the θ-term. Let us then consider the QCD Lagrangian of Eq. (5.1.1), supplemented with a θ-term Eq. (5.1.4),

$$\mathcal{L}_{\text{QCD}} = -\frac{1}{4}F^{\mu\nu,a}F^a_{\mu\nu} + \sum_f \bar{\psi}_f(\mathrm{i}\not{D} - m_f\,\mathrm{e}^{\mathrm{i}\alpha_f\gamma^5})\psi_f + \theta\frac{g_s^2}{32\pi^2}F^a\tilde{F}^a, \tag{5.1.65}$$

where we have omitted color indices and renamed quarks with ψ.
Let us consider as well what we have learned about anomalies, and attempt a chiral rotation to get rid of whatever phases appear in the masses. A chiral transformation on each flavor, $\psi_f \to \mathrm{e}^{-\mathrm{i}\alpha_f\gamma^5/2}\psi_f$, implies $\bar{\psi}_f \to \bar{\psi}_f\,\mathrm{e}^{-\mathrm{i}\alpha_f\gamma^5/2}$ and because of the anomaly, we know the effect of the chiral rotation is a non-trivial Jacobian with a contribution that looks exactly like the θ-term, Eq. (5.1.43), but with twice the chiral rotation angle, then the term proportional to $F\tilde{F}$ in our Lagrangian is now

$$\mathcal{L}_{\text{QCD}} \subset \left(\theta - \sum_f \alpha_f\right)\frac{g_s^2}{32\pi^2}\epsilon^{\mu\nu\sigma\lambda}F^a_{\mu\nu}(x)F^a_{\sigma\lambda}(x), \tag{5.1.66}$$

which seems to indicate that we can have real masses if we change $\theta \to \theta - \sum_f \alpha_f$ and in general for whatever chiral rotation by an angle $+\alpha_f$ we have that $\theta \to \theta + 2\sum \alpha_f$. Therefore it is more useful to define an invariant quantity that accounts for CP violation contributions,

$$\bar{\theta} = \theta + \arg\det M, \tag{5.1.67}$$

where M represents here the quark mass matrix. So defined $\bar{\theta}$ is independent of where the phases are accumulated by chiral rotations. Colloquially, whatever phase factor stands in front of the θ-term plus whatever overall phase stands with the masses remains constant. Which is just the statement of the fact that we have just seen that, field redefinitions alone cannot get rid of possible CP violating terms.
It happens that current experimental bounds to $\bar{\theta}$ are very stringent and show that $\bar{\theta}$ must be really tiny, as we will describe in what follows. The fact that, out of all possible values of θ, nature appears to have picked parameters such that $\bar{\theta} = 0$ begs for an explanation. Why that is so is what we know as the strong CP problem.

5.2 A brief history of QCD and related phenomenology

After defining an invariant which does not depend on how we define the fields, we can ask whether we can measure it. What do experiments have to say about CP violation in the strong sector? As Hook[107] puts it, the strong CP problem is mainly a problem about the neutron, specifically the neutron's electric dipole moment (nEDM) which provides stringent experimental bounds to $\bar{\theta}$. There are other processes, such as $\eta \to 2\pi$, that are also affected by θ and have to be considered when placing bounds on the $\bar{\theta}$-invariant. However, we focus on the case of the EDMs for illustration. We must say nonetheless; from QCD as presented in the previous section to the nEDM, there is still some way to be traveled.
The neutron is a hadron, made up of three valence quarks, which makes it a composite particle and hence requires some effective field theory to describe its interactions. We need then to understand how effective field theories for low-energy QCD processes are constructed. Computations of the nEDM using, for example, the MIT bag model can be used to find[115],

$$d_n = 8.2 \times 10^{-16} \bar{\theta}\, e.\text{cm}. \tag{5.2.68}$$

Other computations attempt to improve on the bag model but lead to similar expressions in orders of magnitude[116]. From the experimental side, the best bound on the nEDM itself is currently provided by [117] where it is concluded that

$$|d_n| < 1.8 \times 10^{-26}\, e.\text{cm}. \tag{5.2.69}$$

To our knowledge, the symmetry breaking pattern is dictated by instanton effects, through a 't Hooft operator, which encodes those non-perturbative effects[105]. Although operators violating CP can be written in terms of the masses of quarks on symmetry grounds for a theory of pions and kaons, as in chiral perturbation theory (ChPT), their coefficients, also called low-energy constants (LECs), should be fixed via matching with the high energy theory, QCD.
We review briefly the very basics of how low energy QCD theories look like before we expand on the details of instantons and our computation concerning the matching of the effective CP-violating operator coefficients à la 't Hooft.

5.2.1 Low energy QCD and the $\eta\prime$ mass

At low energies, the phenomenon of confinement takes place and we are only able to see hadrons, so QCD no longer directly describes the relevant degrees of freedom. However, for our purposes, it is enough to understand how an effective theory for mesons formed by the lightest three quarks, u, d and s, which are the constituents of the pions π, kaons K, η and η', is built up. The guiding principle to build an effective theory for these mesons is chiral symmetry. By using a parametrization for the meson fields that realizes the chiral symmetry $SU_L(3) \times SU_R(3)$ for the fundamental representation of $SU(3)$, we can obtain a successful field theory for the mesons which are the lightest composites states. We note in passing that other representations can be used to build effective Lagrangians for other hadrons like baryons. Lagrangians manufactured under this principle fall generally under what has been called ChPT[118, 119] and deserves a book of their own. We try to state here the most relevant points that pertain to our studies and refer the interested reader to primers and textbooks on it, cf.[47, 120–124].

We begin by realizing that masses can be seen as chiral symmetry breaking parameters, which lock the angles of the independent chiral rotations, allowing only for vector rotations. This description is viable as long as the masses are seen to be small compared to $\Lambda_{\rm QCD} \approx 250$MeV. Mesons are then understood to be the pNGBs appearing after symmetry breaking due to quark non-zero masses. With quarks appearing in the fundamental representation, a theory for "bound" pairs of quarks with the corresponding quantum numbers of the constituents is then built out of a tensor product representation of the fundamental and the anti-fundamental (or conjugate) representations. Deeper and more formal considerations on symmetries fall out of the scope of this document and we will not dwell into representation theory of Lie groups and algebras, the interested reader is referred to [125–127]. A non-linear realization[120, 121] of such product of $SU(3)$ displaying $8+1$ NGBs is then given by

$$U = U_0\, \mathrm{e}^{\frac{\mathrm{i}}{F_0}\boldsymbol{\lambda}\cdot\boldsymbol{\Phi}(x)}\ \mathrm{e}^{\frac{\mathrm{i}}{F_0}\sqrt{\frac{2}{3}}\eta'(x)}, \tag{5.2.70}$$

for U_0 satisfying $\langle U\rangle = U_0$ and where

$$\boldsymbol{\lambda}\cdot\boldsymbol{\Phi}(x) + \sqrt{\frac{2}{3}}\eta'(x) = \begin{pmatrix} \pi^0 + \frac{1}{\sqrt{3}}\eta + \sqrt{\frac{2}{3}}\eta' & \sqrt{2}\,\pi^+ & \sqrt{2}\,K^+ \\ \sqrt{2}\,\pi^- & -\pi^0 + \frac{1}{\sqrt{3}}\eta + \sqrt{\frac{2}{3}}\eta' & \sqrt{2}\,K^0 \\ \sqrt{2}\,K^- & \sqrt{2}\,\bar{K}^0 & -\frac{2}{\sqrt{3}}\,\eta + \sqrt{\frac{2}{3}}\eta' \end{pmatrix}, \tag{5.2.71}$$

with $\boldsymbol{\lambda}$ a vector of Gell-Mann matrices and F_0 the decay constant of the NGBs, included for dimensional reasons, and the independent addition of the η', neglecting the mixing between η_8 and η_0 (see e.g. [47]). One can compute chiral rotations for $R \in SU_R(3)$ and $L \in SU_L(3)$ by left and right multiplication of U, i.e.

$$U \longrightarrow RUL^\dagger. \tag{5.2.72}$$

We can now build a phenomenological effective Lagrangian with the symmetry $SU(3)_L \times SU(3)_R \times U(1)_V$ by including all operators that respect the transformation in Eq. (5.2.72), this way we ensure that quantum numbers match observation and QCD. To lowest order in derivatives the, only consistent kinetic term can be shown to be

$$\mathcal{L}_{\rm ChPT,0} = \frac{F_0^2}{4}\,\mathrm{tr}\left(\partial_\mu U(x)\,\partial^\mu U^\dagger\right). \tag{5.2.73}$$

Expanding the above exponential, we can obtain a canonically normalized kinetic term, together with an infinite number of higher-order interaction terms. This Lagrangian requires explicit symmetry-breaking terms to account for the quark masses. We recall the mass terms for the u, d and s quarks can be in general written as

$$\mathcal{L}_{u,d,s\,\rm mass} = -\bar{q}_L \boldsymbol{M} q_R - \bar{q}_R \boldsymbol{M}^\dagger q_L \tag{5.2.74}$$

for $q = (u, d, s)$ and in the case all the CP violating phases are accumulated in the θ-term, the mass matrix would contain the bare quark masses in the diagonal, viz.

$$\boldsymbol{M} = \begin{pmatrix} m_u & 0 & 0 \\ 0 & m_d & 0 \\ 0 & 0 & m_s \end{pmatrix}. \tag{5.2.75}$$

The way to include and implement the symmetry breaking process from the masses is to consider the matrix $\boldsymbol{M}$ as a spurious field, spurions in the literature, and demand that it transforms under the same realization of the group as the NGBs

$$\mathcal{L}_{\mathrm{ChPT},\,2} = \frac{F_0^2}{4}\mathrm{Tr}\,\partial_\mu U\partial^\mu U^\dagger + \frac{F_0^2 B_0}{2}\,\mathrm{Tr}(\boldsymbol{M}U + U^\dagger \boldsymbol{M}^\dagger) \tag{5.2.76}$$

and where B_0 is related to the scalar singlet quark condensate $\langle\bar{q}q\rangle$.
Withal, the above effective Lagrangian remains incomplete in the sense that it requires the addition of all higher-order operators consistent with the realization and does not explain the experimental absence of a ninth NGBs, which here we have written as the η'. If we were to take $\mathcal{L}_{\mathrm{ChPT},\,2}$ at face value, we would get that η' is the singlet of the representation $8 \oplus 1$ and thus will have a mass of the same order as the pions and kaons. In reality, the η' has the correct quantum numbers but a higher mass as expected. This issue was considered a big problem in the early developments of QCD and ChPT and was dubbed the $U_A(1)$ problem[128], therein Weinberg was able to place a bound on the mass of missing pNGB which disagreed with the experimentally observed mass for the η' of $m_{\eta'} \approx 960\mathrm{MeV/c^2}$. Secondly, this Lagrangian does not yet contain any coupling to nucleons such as the neutron, which is our window to measuring CP violation. At this point, there are two stories to be told: we need to provide a connection of the nEDM as promised at the beginning of the subsection and we need to understand how the $U_A(1)$ problem was solved historically.
We take care of the former story concerning the nEDM. In order to include the effects of the θ-term in such interactions we still need an effective description how the masses break the symmetry. From our classical understanding of an electric dipole, $\vec{d_n} = \sum_i q_i\vec{r_i}$ is vector and hence as an invariant property of the neutron it can only be proportional to its spin, so we expect as well that the potential energy of the nEDM in an electric field $\vec{E}$, coincides with the classical expression $U = -\vec{d_n}\cdot\vec{E}$. For a the relativistic case, the Hamiltonian density

$$\mathcal{H}_{d_n} = \mathrm{i}\frac{d_n}{2}\bar{\psi}\sigma^{\mu\nu}\gamma^5\psi F_{\mu\nu} \tag{5.2.77}$$

reduces to the correct classical expression. The general structure of the computation for the nEDM is then

$$\begin{aligned}\mathrm{i}d_n\bar{u}_n(\mathbf{p}')\sigma^{\mu\nu}(p'-p)_\nu\gamma^5 u_n(\mathbf{p}) &= T\left\langle \mathbf{p}'\left| J^\mu_{\mathrm{EM}}(0)\int \mathrm{d}^4x\,\mathcal{L}_{\mathrm{eff\,CP}}(x)\right|\mathbf{p}\right\rangle \\ &= \mathrm{i}\sum_X \left\langle n(\mathbf{p}')|\mathcal{L}_{\mathrm{eff\,CP}}|X\right\rangle \frac{1}{E_N - E_X}\left\langle X|J^\mu_{\mathrm{EM}}|n(\mathbf{p})\right\rangle,\end{aligned} \tag{5.2.78}$$

where X are intermediate stable hadronic states and $\mathcal{L}_{\mathrm{eff\,CP}}$ is the CP violating part of the Lagrangian density. In order to carry out the computation for the expression above we first need to obtain $\mathcal{L}_{\mathrm{eff\,CP}}$ in relation to $\bar{\theta}$.
The following argument is attributed to Baluni[115], and relates the $\bar{\theta}$ invariant parameter to a CP odd operator for the quarks. Consider the model in Eq. (5.1.65), employing chiral rotations as we have described, we may move all the phase factors to the quark mass terms and thus making the θ-term disappear, we can write

$$\mathcal{L}_{\mathrm{QCD}} \supset \bar{\psi}\boldsymbol{M}\psi + \mathrm{i}\eta\bar{\psi}K\gamma^5\psi = \bar{\psi}_L\tilde{M}\psi_R + \bar{\psi}_R\tilde{M}^\dagger\psi_L, \tag{5.2.79}$$

where $\boldsymbol{M}$ is the diagonal mass matrix in Eq. (5.2.75), η is a small parameter expected to be proportional to $\bar{\theta}$, to be specified and K is determined to be the identity matrix under stability considerations, i.e. avoid linear terms that might render the theory unbounded from below. From Eq. (5.1.67) in this case we have

$$\bar{\theta} = \arg\det\tilde{M} = \arg[(m_u + \mathrm{i}\eta)(m_d + \mathrm{i}\eta)(m_s + \mathrm{i}\eta)], \tag{5.2.80}$$

which can be expanded for small η to arrive to

$$\eta \approx \bar{\theta}\left(\frac{m_u m_d m_s}{m_u m_d + m_u m_s + m_d m_s}\right). \tag{5.2.81}$$

We can conclude then that

$$\mathcal{L}_{\text{eff CP}} = \mathrm{i}\bar{\theta}\left(\frac{m_u m_d m_s}{m_u m_d + m_u m_s + m_d m_s}\right)\left(\sum_{f=u,s,d}\bar{q}_f\gamma^5 q_f\right). \tag{5.2.82}$$

To make contact with the effective theory for pions and kaons, we could as Crewther et. al.[116] do, consider the theory for nucleons interacting only with u and d quarks according to

$$\mathcal{L}_{N\pi\pi} = \vec{\pi}\cdot\vec{\sigma}\bar{N}(\mathrm{i}\gamma^5 g_{_{\pi NN}} + \bar{g}_{_{\pi NN}})N, \tag{5.2.83}$$

and proceed to compute $\bar{g}_{_{\pi NN}}$ using soft-pion theorems and current algebra and a reduced version of Eq. (5.2.82) to the u and d quarks. After the observation that the leading contribution to d_n, as in Eq. (5.2.78), come from $|X\rangle = |N\pi\rangle$ and that

$$\left\langle\pi^-(p+k)|J^\mu_{\text{EM}}(0)|\pi^-(p)\right\rangle = -(2p+k)^\mu + \mathcal{O}(k^2). \tag{5.2.84}$$

The computation of d_n from Eq. (5.2.78) is given by the amplitudes of one-loop Feynman diagrams that involve intermediate pions (see Figure 5.1), using Eq. (5.2.84) and the interaction in Eq. (5.2.83), and ends in

$$d_n = \frac{g_{_{\pi NN}}\bar{g}_{_{\pi NN}}}{4\pi^2 M_N}\log\left(\frac{M_N}{m_\pi}\right) \approx 5.2\times10^{-16}\,\bar{\theta}\text{ cm}, \tag{5.2.85}$$

as reported back then[116].

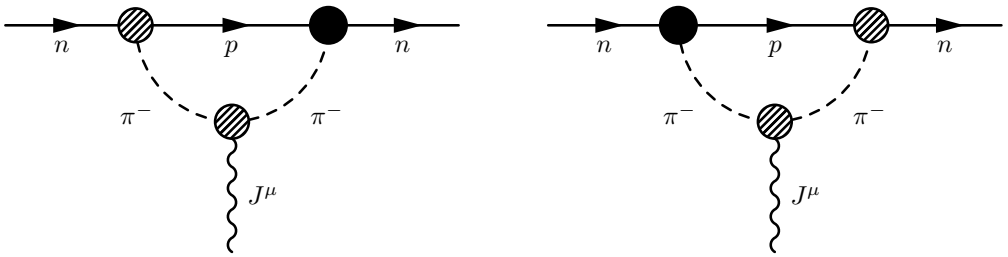

Figure 5.1: Feynman diagrams depicting the possible nEDM contributions from the matrix elements in Eqs. (5.2.84) and (5.2.83), the dark blob indicates the CP violating vertex.

A review emphasizing the different theoretical values obtained to that date for d_n is[129], obtained via the same effective operator derived through the arguments in [130] or Baluni's[115],

where the latter also provides at the same time an estimate for d_n therein using the MIT bag model. Both ways to argue in favor of Eq. (5.2.82) build the operator by employing certain physically motivated constraints but not necessarily from first principles.
We come now to the second story, the $U_A(1)$ problem, which we tell from the perspective of 't Hooft[10] and will serve only as an introduction to our calculations which resemble 't Hooft's ideas very much. The mystery of the mass of the η' was understood as an issue with the $U_A(1)$ axial symmetry, which when taken naively would imply masses for the η' of the same order of the kaon masses, it being a pNGB. With the finding of non-perturbative spacetime localized solutions to the field equations in vacuum[7], called instantons nowadays, the picture changed. It was first understood how computations using instantons as background could be done[131] and how their contributions could lead then to explicit symmetry breaking and an effective theory[105, 132], thus describing the mass of the η' properly and also leading to the vacuum structure we described before [109].
The technical details of instantons will be described in the next subsection. All that we need to understand at this level is that non-perturbative contributions can account for an effective operator, the 't Hooft operator, which is schematically

$$\mathcal{L}_{\mathrm{t'H}} \propto g_s^{-8}\, \mathrm{e}^{-\frac{8\pi^2}{g_s^2}}\, \det \bar{q}_{f_i}(1+\gamma^5)q_{f_j} + \mathrm{h.c.} = g_s^{-8}\, \mathrm{e}^{-\frac{8\pi^2}{g_s^2}}\, \det U + \mathrm{h.c.}, \tag{5.2.86}$$

where the last equality uses the notation of the low-energy theory for pNGBs. This operator is responsible for violating the chiral charge conservation (the charge associated with the classical conservation of $j^{\mu\,5}$) as the anomaly did in the high-energy theory. Namely, it can flip the chirality of any incoming quark of any flavor. The constant of proportionality in the expression above is a central point of the studies that are presented in the next chapter. In 't Hooft's version[105], the proportionality constant contains the phase θ, however by following almost the same computation done there, we advocate for a different result.
The chiral perturbation theory Lagrangian we have been building, can be complemented with the 't Hooft operator

$$\begin{aligned}\mathcal{L}_{\mathrm{ChPT},\,2+\mathrm{t'H}} = \frac{F_0^2}{4}\mathrm{Tr}\,\partial_\mu U \partial^\mu U^\dagger + \frac{F_0^2 B_0}{2}\mathrm{Tr}(\boldsymbol{M}U + U^\dagger \boldsymbol{M}^\dagger) + |\lambda|\mathrm{e}^{-\mathrm{i}\xi}F_0^4 \det U \\ + |\lambda|\mathrm{e}^{\mathrm{i}\xi}F_0^4 \det U^\dagger\,.\end{aligned} \tag{5.2.87}$$

where the constants and the phases appearing in front of the determinants are to be determined by matching with the high-energy theory (cf. [133, 134]). It is common to expand the determinants in terms of traces while keeping the first terms, after for example integrating out auxiliary fields[135], this being a specific case of the Lagrangian above. Let us for now recall the impact of a chiral rotation of quarks transformation on the different quantities appearing in the Lagrangian above:

$$U \to \mathrm{e}^{2\mathrm{i}\beta}U \;\Rightarrow\; \det U \to \mathrm{e}^{2\mathrm{i}N_f\beta}\det U, \qquad \boldsymbol{M} \to \mathrm{e}^{-2\mathrm{i}\beta}\boldsymbol{M}, \qquad \theta \to \theta + 2N_f\beta. \tag{5.2.88}$$

It seems to us that the minimal requirement on the phase ξ is that it is periodic and compatible with the rules above, this leaves us with two options. The traditional option $\xi = \theta$ or $\xi = -\bar{\alpha}$, with $\bar{\alpha}$ the accumulated phase in the masses. Will attempt to derive ξ from the high-energy theory by employing path integral methods over an instanton background.
We must now mention how the Lagrangian in Eq. (5.2.87) together with the matrix of pNGBs in Eq. (5.2.70) can be expanded to find out their masses because the 't Hooft operator does not vanish for quark masses going to zero because of the cancellation of

mass terms, as we will show in the next chapter. So that in the case of $\xi = -\bar{\alpha}$ we get the relation

$$m_{\eta'}^2 = 8|\lambda|F_0^2 \tag{5.2.89}$$

for the mass of the η'-meson.
It is also possible to make contact with the CP violating decay modes of the η' by realizing that in the case of a diagonal $\boldsymbol{M}$ (cf. Ref. [136]), the expectation value of U is also diagonal

$$\langle U \rangle = U_0 = \mathrm{diag}(\, \mathrm{e}^{\mathrm{i}\varphi_u}, \, \mathrm{e}^{\mathrm{i}\varphi_d}, \, \mathrm{e}^{\mathrm{i}\varphi_s}) \tag{5.2.90}$$

and expanding the Lagrangian with the 't Hooft operator for $|lambda| \gg B_0 F_0^2 m_i$ for $i = u, d, s$, with the relation

$$m_i \varphi_i = \left(\frac{m_u m_d m_s}{m_u m_d + m_u m_s + m_d m_s} \right) (\xi \alpha_u + \alpha_d + \alpha_s), \tag{5.2.91}$$

which holds for $\xi\alpha_u + \alpha_d + \alpha_s \ll 1$, we obtain the following interaction term associated with CP violation,

$$-\frac{\mathrm{i}B_0}{F_0}\sqrt{\frac{2}{3}} \left(\frac{m_u m_d m_s}{m_u m_d + m_u m_s + m_d m_s} \right) \eta'(\pi^0\pi^0 + 2\pi^+\pi^-), \tag{5.2.92}$$

which explicitly show that the decays $\eta' \to 2\pi$ are CP violating. To date there is also very strong bounds on the corresponding branching ratio, at the such decays can be consider essentially non-detected[49].

The topological susceptibility

We will end the current historical section by giving some comments on what is known as the topological susceptibility, denoted by χ. As indicated by its name, the idea is to quantify the response of a system to a perturbation. In this particular context of QCD, we are interested in the response of the system when the parameter θ is changed. Mathematically the Euclidean χ is defined as the second derivative with respect to θ, of the free energy, as introduced by Witten[137]:

$$\chi(x) \equiv \frac{1}{|VT|} \frac{1}{Z(0)} \frac{\mathrm{d}^2}{\mathrm{d}\theta^2}\bigg|_{\theta=0} Z(\theta) = \frac{1}{|VT|} \int \mathrm{d}^4x \, \langle T[Q(x)Q(0)] \rangle \,, \tag{5.2.93}$$

where VT is the Euclidean spacetime volume, with

$$Q(x) = \frac{1}{32\pi^2} F^{\mu\nu\, a}(x) \tilde{F}^a_{\mu\nu}(x), \tag{5.2.94}$$

and differs from the Minkowski analogue by a factor of i[138]. It constitutes an important physical observable capable of giving us information on the relevance of the θ-term for physical observables coming from non-perturbative contributions to the theory, given that it vanishes in any perturbative treatment of QCD.
The topological susceptibility can be linked to the mass of the η' meson via arguments of current algebra and large number of colors, or large N expansion[137],

$$m_{\eta'}^2 = \frac{4N_f}{F_\pi^2} \chi_\infty \tag{5.2.95}$$

where ∞ denotes the chiral limit (quark masses going to zero) or more realistically by the Witten-Veneziano formula[139]:

$$\chi = \frac{F_0^2}{4N_f}(m_\eta^2 + m_{\eta'}^2 - 2m_K^2) \approx (212\,\mathrm{MeV})^4, \tag{5.2.96}$$

where the number of colors is assumed large and the approximation has been obtained with current values for the masses involved and using the pion decay constant $F_\pi = 130\,\mathrm{MeV}$. The topological susceptibility is an important observable not only because of its intrinsic relation to θ and the η' mass but also the fact that it can be estimated by studying QCD in a lattice from first principles. Attempts exist since [140], and they have become more precise and sophisticated over time, and more are still pursued[141, 142]. Approaches using ChPT and including corrections up to NNLO have also been published[143] and aim to estimate the mass of a possible Axion solving the strong CP problem.

5.3 Review of Instantons

We have seen how the θ-term is related to the low-energy theory and violation of the chiral symmetry, which connects with the instanton solutions. Having summarized the relevance of understanding the chiral symmetry mechanisms, its connection to the strong CP problem, the mass of the η' meson and the topological susceptibility, we recall here the mathematical details of the instantons, which play an instrumental role in this story. Instantons seem remarkably beautiful, both from the mathematical and the physical perspective. Since their discovery[7], they have attracted much attention in both fields. We will present here what we require for the computations of the next chapter while taking the chance to add certain mathematical comments when appropriate.

5.3.1 The quest for saddle-points

Instantons are an important part of the non-perturbative features of QCD. However, they do not only appear there. We have already seen a configuration related to the instantons in Part II when we spoke about the bounce. The bounce is a type of soliton with specific boundary properties, while instantons are in the same spirit higher-dimensional analogs. One of its notable features is that its action, in the context of Yang-Mills theories, is proportional to the inverse square of the gauge coupling, making them non-perturbative objects. As we will see, they are as well saddle-points of the Euclidean action, making them excellent candidates for semi-classical approximations.
Our goal is, therefore, to employ the machinery developed in Part I to compute correlation functions over a background filled with instantons. To get there, we must first understand the configurations appearing in the background very well. Furthermore, depending on the interest of the reader, she can approach the topic of instantons by choosing any point between pure mathematics and physics' phenomenology without any fear of missing out on any of the exciting things about them. For the mathematically inclined, instantons appear within differential geometry and topology, particularly in relation to the construction of principal fiber bundles[113, 144], where they played a role in Donaldson's work and his Fields Medal. A mathematical physics version can be found in[145], which has the advantage of being more updated. The book by Nakahara[146] stands in the middle. It presents advanced mathematical structures with the rigor of a physicist and presents their relation to physics. On the theoretical physics side, which we will mostly follow, interesting reviews are those by Vainshtein et al. [147] and Vandoren and Nieuwenhuizen[114]. A

review specifically oriented to instantons in QCD is[148], which also includes applications to finite temperature and supersymmetry, which we will not treat here. More recently, not only describing instantons, there is the book by Shuryak[134], which is even closer to the phenomenology of the QCD vacuum.

For the discussion of the instantons, we will remain in Euclidean spacetime, $\mathbb{R}^4$ with a positive-definite metric, and we need only consider a pure Yang-Mills theory with gauge group $SU(2)$ (although $SU(3)$ is the physically relevant group in QCD), we will later discuss the impacts on the fermion sector. Let us begin by motivating the instanton solutions from the point of view of the action, by looking for gauge field configurations of finite action:

$$S_{\mathrm{YM}} = \frac{1}{4g_s^2}\int \mathrm{d}^4x\, F^{\mu\nu\,a}(x)F^a_{\mu\nu}(x) < \infty, \tag{5.3.97}$$

where the trace over the generator of the group has already taken place following the choices

$$\mathrm{tr}(T^aT^b) = -\frac{1}{2}\delta_{ab} \quad \text{and} \quad [T^a, T^b] = f^{abc}T^c, \tag{5.3.98}$$

with f^{abc} a fully anti-symmetric set of structure constants. As we saw already briefly in Sec. (5.1), we can require that the gauge field $\boldsymbol{A}_\mu$ becomes pure gauge, that is $\boldsymbol{A}_\mu \to U^{-1}\partial_\mu U$ when $|x|^2 \to \infty$ for some $U \in SU(2)$. This will ensure that $\boldsymbol{F}_{\mu\nu}$ vanishes fast enough at infinity rendering the action finite. Although our focus before was only on classifying gauge transformations, we can apply the same concept of the winding number to classify gauge field configurations with the above property. Notice how the very classification relies on the action being finite in $\mathbb{R}^4$, in the last chapter this point will play a role on deciding how to take certain limits.

From the mathematical point of view, the geometrical structures describing Yang-Mills theories are principal G-bundles, where G is the gauge group. Each gauge field configuration provides a connection and its field strength corresponds to its curvature. Minimizing the Yang-Mills action can be interpreted as looking for the flattest connections[145]. Considering variations of the gauge field A_μ in the Yang-Mills action, S_{YM}, that way we can obtain the corresponding Euler-Lagrange equations, or classical equations of motion (e.o.m.),

$$(D^\mu \boldsymbol{F}_{\mu\nu})^a = \partial^\mu F^a_{\mu\nu} + g f^{abc} A^{\mu\,b} F^c_\mu \nu = 0, \tag{5.3.99}$$

where $D_\mu = \partial_\mu + g[\boldsymbol{A}_\mu, \cdot]$ is the covariant derivative in terms of the Lie bracket. As a Lie algebra valued tensor, the field strength tensor also automatically fulfills a Bianchi identity which provides a second set of equations of motion

$$D_\mu \tilde{\boldsymbol{F}}^{\mu\nu} = 0. \tag{5.3.100}$$

Together Eqs. (5.3.99) and (5.3.100), constitute the Yang-Mills equations and determine sufficient conditions for a gauge field configuration to be an extremum of S_{YM}.

Instantons are defined in Yang-Mills theories in general as solutions to the e.o.m.'s Eqs. (5.3.99) and (5.3.100) with finite action, which means we can label them by an integer k, their winding number. However, to be able to use such solutions as a sensible background, we will require that they minimize the action as well. Let us start by deriving a bound for the action, known as the BPS bound[149, 150], as done in[114]. First, we rewrite the action,

$$S_{\mathrm{YM}} = -\frac{1}{2g_s^2}\int \mathrm{d}^4x\ \mathrm{tr}\,\boldsymbol{F}^2 = -\frac{1}{4g_s^2}\int \mathrm{d}^4x\ \mathrm{tr}(\boldsymbol{F} \mp \tilde{\boldsymbol{F}})^2 \mp \frac{1}{2g_s^2}\int \mathrm{d}^4x\,\mathrm{tr}\,\boldsymbol{F}^{\mu\nu}\,\tilde{\boldsymbol{F}}_{\mu\nu}, \tag{5.3.101}$$

where $\operatorname{tr} \tilde{\boldsymbol{F}}^2 = \operatorname{tr} \boldsymbol{F}^2$ was used. In such form we drop the first term after the last equal sign, which is positive, and obtain the BPS bound:

$$S_{\mathrm{YM}} \geq \mp \frac{1}{2g_s^2} \int \mathrm{d}^4x \ \operatorname{tr} \boldsymbol{F}^{\mu\nu} \tilde{\boldsymbol{F}}_{\mu\nu}. \tag{5.3.102}$$

At this point, we can see the relation with what we know about the winding numbers, so we observe that solutions with the property

$$\boldsymbol{F}(x) = \pm \tilde{\boldsymbol{F}}(x), \tag{5.3.103}$$

named (anti) self-dual configurations, will satisfy all of our requirements (provided they are asymptotically pure gauge): they will satisfy the Yang-Mills equation (classical e.o.m.'s), will have a finite action and will moreover saturate the BPS bound. It is worth adding that configurations that have a finite action may exist that are not necessarily (anti)self-dual for different gauge groups. For the case of $SU(2)$ and $SU(3)$, it is known that they must be saddle-points, but necessarily local minima, and are proven to exist only for $SU(2)$ (see [114] and references therein). Using what we learned in Eq. (5.1.61), we can immediately evaluate the action for (anti)self-dual configurations

$$S_{\mathrm{YM}} = -\frac{1}{2g_s^2} \int \mathrm{d}^4x \ \operatorname{tr} \boldsymbol{F}^2 = \mp \frac{1}{2g_s^2} \int \mathrm{d}^4x \ \operatorname{tr} \boldsymbol{F}^{\mu\nu} \tilde{\boldsymbol{F}}_{\mu\nu} = \mp \frac{8\pi^2}{g_s^2} k, \tag{5.3.104}$$

where A_μ has been written in units of g as opposed to Eq. (5.1.61) and the trace of the generators of the Lie algebra was used and where $k \in \mathbb{Z}$ denotes the winding number of the asymptotic configuration of A_μ. This means in order to find this gauge field configurations we only need to solve the (anti)self-dual equation Eq. (5.3.103). This can be done employing a clever Ansatz and some algebra as shown in[114], the details are not vital for our discussion and we just quote the results. In the regular gauge the instanton field configuration is

$$A^a_\mu(x; x_0, \rho) = 2\eta^a{}_{\mu\nu} \frac{(x - x_0)^\nu}{(x - x_0)^2 + \rho^2}\,, \tag{5.3.105}$$

where $\eta^a{}_{\mu\nu}$ is the 't Hooft symbol and is defined as

$$\eta^a{}_{\mu\nu} = \begin{cases} \epsilon^a{}_{\mu\nu}, & \mu, \nu = 1, 2, 3 \\ -\delta^a{}_\nu, & \mu = 4 \\ \delta^a{}_\mu, & \nu = 4 \\ 0, & \mu = \nu = 4 \end{cases}, \tag{5.3.106}$$

where x_0 and ρ are collective coordinates corresponding to the location and the size of the instanton. A barred symbol is defined, $\bar{\eta}^a{}_{\mu\nu} \equiv (-1)^{\delta^4_\mu + \delta^4_\nu} \eta^a_{\mu\nu}$, to described anti-instantons. The symbols have the property of being (anti)self-dual,

$$\eta^a{}_{\mu\nu} = \frac{1}{2} \epsilon_{\mu\nu\lambda\sigma} \eta^{a\ \lambda\sigma} \qquad \text{and} \qquad \bar{\eta}^a{}_{\mu\nu} = -\frac{1}{2} \epsilon_{\mu\nu\lambda\sigma} \bar{\eta}^{a\ \lambda\sigma}. \tag{5.3.107}$$

The set of matrices specified through the 't Hooft symbol are a basis for the anti-symmetric 4×4 matrices and can be related to the generators of the Lorentz group. We verify that the equation above has a field strength equal to

$$F^a_{\mu\nu}(x; x_0, \rho) = -4\eta^a{}_{\mu\nu} \frac{\rho^2}{((x - x_0)^2 + \rho^2)^2} \tag{5.3.108}$$

and we can corroborate its contribution to the action by direct computation, without loss of generality we can take $x_0 = 0$ and together with the use of the integral

$$\int \mathrm{d}^4x \, \frac{(x^2)^n}{(x^2+\rho^2)^m} = \pi^2(\rho^2)^{n-m+2}\frac{\Gamma(n+2)\Gamma(m-n-2)}{\Gamma(m)}, \tag{5.3.109}$$

we have

$$S_{\mathrm{YM}} = \frac{1}{4g_s^2}\int \mathrm{d}^4x \, \boldsymbol{F}_{\mu\nu}\boldsymbol{F}^{\mu\nu} = \frac{48}{g_s^2}\rho^4\,\frac{\pi^2}{\rho^4}\frac{1}{3!} = \frac{8\pi^2}{g_s^2} \tag{5.3.110}$$

which confirms the field configuration in Eq. (5.3.105) corresponds to $k = 1$. The above expressions correspond to regular gauge, they are well defined at $x_0 = 0$ as long as $\rho > 0$. An alternative gauge describing the same physics is found in the literature as the singular gauge,

$$A^a_\mu = -\bar{\eta}^a{}_{\mu\nu}\partial^\nu \log\left(1 + \frac{\rho^2}{(x-x_0)^2}\right). \tag{5.3.111}$$

The above form is connected to Eq. (5.3.105) via a large gauge transformation and is thus equivalent in physical terms. However, computing the topological charge in each case gives the same result, but the contributions to the charge come from different regions. In regular gauge, the singularity is moved to infinity and it is thus the regions close to infinity which contain the charge. On the contrary, in the singular gauge description, the singularity is located at the origin. Hence the contributions to the topological charge would come from the origin.

These differences are very elegantly explained in the context of fiber bundles (cf. [113, 146]). We discuss them in this paragraph; however, they are not essential to understand the physical picture. Geometrical objects such as (well-defined) vector fields, 1-forms and other tensors are global objects and they acquire different local forms depending on the coordinate patch used to describe them. It turns out that our pure gauge Euclidean theory initially written over $\mathbb{R}^4$ when supplemented with the asymptotic condition on the gauge fields Eq. (5.1.48), is indistinguishable from a theory written over S^4, which is the one-point compactification of $\mathbb{R}^4$, given the conformal invariance of the pure Yang-Mills action. As it is known from differential geometry, S^4 cannot be described using only a single chart of coordinates, at the very least, we need two open sets. A simple choice for this is to employ the upper and lower hemispheres of the four-sphere, explicitly, let p_N and p_S represent the "north" and "south" pole, the hemispheres can be taken to be the following open sets

$$U_N = S^4 \setminus \{p_S\} \qquad \text{and} \qquad U_S = S^4 \setminus \{p_N\}. \tag{5.3.112}$$

The gauge fields correspond to connections on a bundle with $SU(2)$ fibers, connections can be specified by means of 1-forms, which have to be consistent in the sense that going from one coordinate patch to the other is done through the compatibility condition of charts, which can be seen to be Eq. (5.1.60). Under this perspective, it is clear that all points play the same role, including the point at infinity. Local descriptions are what is written in Eqs. (5.3.105) and (5.3.111), and their singularities lie exactly in the point which was removed to build the open sets above.

Let us come back to physics and expand on the collective coordinates of the (anti)instanton configurations. Besides the five collective coordinates associated with the location and the size of the configuration, we must consider the remaining orientations within $SU(2)$ as

well as the inequivalent embeddings into $SU(3)$ to be able to translate the above solutions to the case of QCD. The issue of the orientation within $SU(2)$ is understood as rigid rotations of the asymptotic gauge configuration[151], according to

$$A_\mu(x; x_0, \rho, \vec{\theta}) = U^{-1}(\vec{\theta}) A_\mu(x; x_0, \rho) U(\vec{\theta}), \tag{5.3.113}$$

and leading to additional collective coordinates[114]. Considering (anti)instanton configurations, modulo the above remaining rotations, conform what is known as the *moduli space*[113], which is extremely interesting from the mathematical point of view. About the second issue, we focus on the $k = \pm 1$ configurations exclusively, for which it is known only two different embeddings of the generators of $SU(2)$ into $SU(3)$ exist[152], depending on how we choose to make the correspondence.

Comments on the vacuum structure and the dilute instanton gas

As we have seen, the discovery of instantons and with them a whole non-perturbative approach to QCD led to a more complicated vacuum structure than expected. In short, we have seen that an infinite set of pre-vacua are to be superimposed to obtain the true vacuum of the theory, in an analogous way to the case of a periodic potential with several degenerate minima in quantum mechanics. Since, different phenomenological models for the vacuum itself have been proposed (cf. [134]), which have evolved and become more sophisticated over time.

After the discovery of instantons and their interpretation as tunneling solutions connecting different pre-vacua, they adopted a central role in modeling the vacuum itself. It is argued that when in the regime of a weak enough coupling, multiple instanton configurations provide the leading contributions to the path integral in semi-classical approximations. Among the simplest examples of multi-instanton configurations, we can find the dilute instanton gas approximation. Nevertheless, we must observe that we cannot expect a semi-classical treatment to describe the QCD-vacuum accurately since all length scales are involved. In a theory like QCD, the coupling runs with the energy scale or equivalently with the length scale and it does not lie within a perturbative regime throughout the energy spectrum. We can thus only hope to extract patterns and estimations of orders of magnitude of these methods, however for certain problems, that might be good enough.

As we will later employ a version of dilute instanton gas, we describe such a model here. Pictorially we imagine vacuum as being populated with instantons and anti-instantons at all possible locations and with a wide range of sizes. They are taken to be diluted in the sense that the centers of the (anti-)instantons must be well separated from each other, and it is said to be gas-like in the sense that any interaction between them is to be neglected. This idea was first introduced by Callan, Dashen and Gross[153, 154], it has since been used for different purposes[10] and has been made more specialized by considering even liquid-like distributions. More comments can also be found in the pedagogical review "ABC of Instantons"[147].

The result of the above picture is that within the small-distance regime, the path integral can be interpreted as the partition function corresponding to a gas of instantons whose degrees of freedom can be taken to be the locations, the sizes, the orientation and the embeddings, or as we have referred to them before: collective coordinates. In its original formulation, we choose a density for instantons of each size and use a cutoff for the sizes, thus filtering relevant scales and ensuring that the gas is sufficiently dilute. In this context, it is exactly the size of the phase space available to instantons that can lead to large tunneling amplitudes even at very small coupling in contrast to the quantum

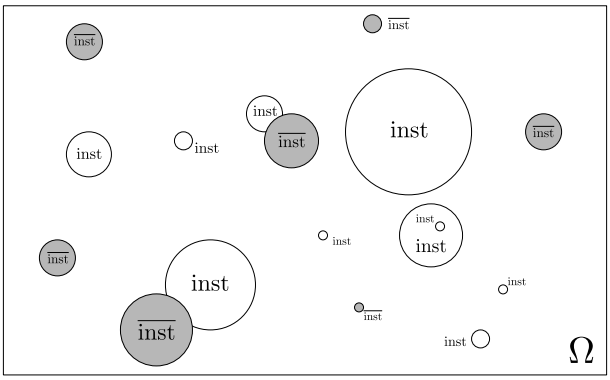

Figure 5.2: Caricature of an instanton gas in a bounded spacetime region Ω. The label "inst" refers to an instanton and "$\overline{\text{inst}}$" to an anti-instanton. Interactions are neglected meaning overlaps may occur without any energy cost.

mechanical case where tunneling contributions can generally be neglected. An estimation of the instanton density in the small size regime, using a light quark condensate can be found in [155]. Moving to larger distances (lower energies), the density of instantons increases, the mutual interactions should not be neglected any longer, and models become more complicated.

Our implementation of the idea of a dilute gas is slightly different at certain points. We will consider configurations of instantons that are transparent with respect to each other (see Figure 5.2). Not only will they not interact with each other, but they will also be allowed to exist at all possible locations independent of their size. Although it is known that integration over instanton sizes diverges for large sizes[105]

$$\langle\theta|\theta\rangle \propto \int \frac{\mathrm{d}\rho}{\rho^5}\, \mathrm{e}^{-\frac{8\pi^2}{g^2(\rho)}} \underset{\rho\to 0}{\longrightarrow} \infty, \tag{5.3.114}$$

the issue requires detailed attention and we assume some mechanism, e.g., a gauge-invariant cutoff, is used to perform such averages. We will build multi-instanton configurations by writing down superpositions of only $k = \pm 1$ instanton solutions as in Eq. (5.3.105) and will consider contributions coming from all possible combinations of instantons and anti-instantons. Namely, we will weigh in the path integral configurations that include n instantons and $\bar{n}$ anti-instantons to which it corresponds a total winding number of $\Delta n = n - \bar{n}$. We then consider Δn taking all possible integer values.

The theory of QCD over a dilute instanton gas described needs to include the effects of the fermions in the theory. Following the semi-classical expansion to the next order, we include fluctuations about such a gas coming from all sectors in order to compute correlation functions between quarks. This with the aim of tracking down CP-violating phases. This is the task we have undertaken in our manuscript[156] which we expand on in the next chapter. As we will see, the interaction of instantons and fermions involves zero-modes, which are delocalized. From a phenomenological perspective[134], this may enable quarks to hop along (anti-)instantons for large distances, which relates to the formation of a quark condensate and allows for contact from lattice results, for example.

6

Path integral and Cluster decomposition methods to study CP violation

The computations and conclusions presented in this chapter are products of the combination of the mathematical tools presented before and the considerations initially oriented at finding Minkowski analogs of particular objects such as correlation functions. This path led us to consider tracking down the possible CP-violating phases appearing in QCD. Our discussion has been described in[156] which we elaborate on in this chapter.
Our arguments are split into two parts. First, by using the path integral formulation over a dilute instanton gas, we were able to compute the possible interference arising between the topological term and the quark mass matrix. Alternatively, we confirm the results with a second approach that considers constraints coming from the cluster decomposition principle and parity. Our conclusions are presented at the end, together with some comments on the impact these may have on the current particle physics knowledge.
We rederive the 't Hooft operator, paying particular attention to the complex phases that appear therein in order to determine the parameter ξ in Eq. (5.2.87). We employ semi-classical methods over a dilute instanton background, as described in the previous chapter, and compute the gauge, fermion and ghosts fluctuations about it.

6.1 Partition function with sum over topological sectors

Semi-classical methods in the context of the path integral and QFT require that we employ some method to stabilize the exponential containing the action. We usually use a Wick rotation in order to analytically continue certain quantities into the full complex plane and later perform integrals along the imaginary time axis. The effects of a Wick rotation are quite complex, bringing the Lorentzian metric to a Euclidean one, which describes very different physics regarding causality. Therefore, we adopt a pragmatic approach in which analytic continuation provides a useful mathematical tool that allows us to have a correspondence of certain quantities. The Wick rotation specifically turns out to be a specific way of extending integrals to the complex plane. However, some features are lost in the process; instantons are one example of such. As we have seen, instanton configurations are minima of the Euclidean Yang-Mills action, which enjoy at least a $O(4)$ symmetry. Nevertheless, these configurations do not correspond to the minima of the action in the Minkowskian world, the real world. Modern analytical tools, like the Picard-Lefschetz theory[157] are used in order to build upon this idea of a dictionary between Euclidean

and Minkowski[36, 158–162]. With the objective of having a full Euclidean and Minkowski version of the theory, we must review how quantities must be transformed. This will include γ-matrices, gauge fields, Green's functions, etc. In the first few subsections, we establish the necessary relations between Euclidean and Minkowskian quantities.
Within this section, we study fermions in the fundamental representation of $SU(2)$ in the background of a $k = -1$ BPST anti-instanton. We label quantities in the Euclidean theory with a superscript E and use Latin sub- and super- indices to denote their components.

6.1.1 Translations from Euclidean to Minkowski

Let us begin by writing down the action for Euclidean QCD,

$$S_{\mathrm{E}} = \int \mathrm{d}^4x \left[\frac{1}{4g^2} F^{\mathrm{E}a}{}_{mn} F^{\mathrm{E}a}{}_{mn} + \psi_i^{\mathrm{E}\dagger} \left(\gamma_m^{\mathrm{E}} D_m^{\mathrm{E}} + M_{ij} \right) \psi_j^{\mathrm{E}} \right] . \tag{6.1.1}$$

where $x_m^{\mathrm{E}} = \{\vec{x}, x_4\}$ and $m, n \in \{1, 2, 3, 4\}$. We denote the Euclidean metric by using the Kronecker delta δ_{mn} which serves to raise and lower indices in principle, although there are no sign changes in the Euclidean case. The Euclidean field strength tensor is

$$F^{\mathrm{E}a}{}_{mn} \equiv \partial_m A^{\mathrm{E}a}{}_n - \partial_n A^{\mathrm{E}a}{}_m + f^{abc} A^{\mathrm{E}b}{}_m A^{\mathrm{E}c}{}_n, \tag{6.1.2}$$

the Euclidean Dirac operator $\not{D}^{\mathrm{E}} \equiv \gamma_m D^{\mathrm{E}}{}_m$, with the Euclidean version of the Dirac matrices in the Weyl representation which will prove to be the most convenient,

$$\gamma_m^{\mathrm{E}} = \begin{pmatrix} 0 & -\mathrm{i}\sigma_m^{\mathrm{E}} \\ \mathrm{i}\bar{\sigma}_m^{\mathrm{E}} & 0 \end{pmatrix}, \quad \gamma^5 = \begin{pmatrix} -\mathbb{1}_2 & 0 \\ 0 & \mathbb{1}_2 \end{pmatrix}, \tag{6.1.3}$$

which satisfy $\{\gamma_m, \gamma_n\} = 2\delta_{mn}$, and the extended Pauli matrices appearing within defined as $\sigma^{\mathrm{E}}{}_m = (\vec{\sigma}, \mathrm{i}\mathbb{1}_2)$ and $\bar{\sigma}_m^{\mathrm{E}} = (\vec{\sigma}, -\mathrm{i}\mathbb{1}_2)$. The covariant derivative explicitly reads

$$D_m^{\mathrm{E}} \psi_i^{\mathrm{E}} = \left(\partial_m - \mathrm{i} A^{\mathrm{E}a}{}_m T^a \right) \psi_i^{\mathrm{E}} \tag{6.1.4}$$

where $T^a = \sigma^a/2$ are hermitian generators for $SU(2)$ when exponentiated with an i. The instanton configuration is the same as the one in Eq. (5.3.105) but with current notation we have

$$A^{\mathrm{E}a}{}_m(\vec{x}, x_4) = 2\eta^a{}_{mn} \frac{x_n}{(x^{\mathrm{E}})^2 + \rho^2}, \tag{6.1.5}$$

in terms of the 't Hooft symbol defined in Eq. (5.3.106). The field configuration corresponding to winding number $k = -1$ is obtained via the parity operator P, in practice it replaces $\eta^a{}_{mn}$ with $\bar{\eta}^a{}_{mn}$. A continuous family of rotations, or analytical continuations can be obtained through the following transformation, following the techniques of[36].

$$x_4 \to \mathrm{e}^{-\mathrm{i}(\vartheta - \frac{\pi}{2})} t, \tag{6.1.6}$$

for $t, \vartheta \in \mathbb{R}$. Different values of the parameter ϑ lead either Euclidean or Minkowski time, explicitly we have $\vartheta = \pi/2$ corresponds to $t \to x^4$, i.e. Euclidean time, and approaching 0 from above, $\vartheta \to 0^+$, means $t \to x^0$, i.e. Minkowski time. This prescription enforces that the vacuum-to-vacuum transition amplitude is properly captured[36]. In the case of Minkowski spacetime, we utilize Greek letters for the indices and they will take on values between 0 and 3 with the index 0 representing time as is conventional. The ϑ dependence

can then be carried along to any other quantity by using Eq. (6.1.6). Observe that the convention used here differs by a sign with respect to the one used in earlier parts of this document, more details concerning arbitrary rotations can be found in Appendix C.. For the edge cases, we reserve the superscript "E" for quantities in Euclidean space, and no subscript will indicate their Minkowskian analogs.
Let us first consider the two different metrics. A glance at our transformation rule affirms the relation $\delta_{mn} \to -\eta_{\mu\nu}$ where $\eta_{\mu\nu}$ is the Minkowski metric tensor with signature $\mathrm{diag}(1,-1,-1,-1)$. The gauge field in matrix form $\boldsymbol{A}_\mu$ we transform as

$$\boldsymbol{A}_0(x^0,\vec{x}) = \mathrm{i}\boldsymbol{A}_4^{\mathrm{E}}(\vec{x}, x_4 = \mathrm{i}x^0)\ ,\ \ \boldsymbol{A}_i(x^0,\vec{x}) = \boldsymbol{A}_i^{\mathrm{E}}(\vec{x}, x_4 = \mathrm{i}x^0) \qquad \text{for } i = 1,2,3\,. \quad (6.1.7)$$

We keep the generators of the group unchanged, meaning that analytically continuing real Euclidean gauge field components to Minkowski makes them in general complex. This means in particular that for the (anti-)instanton solution, the local minimum is displaced away from the real line and the integration path must be adjusted if one wants to employ a saddle-point expansion and steepest-descent[157, 158]. If we were then to compute bosonic fluctuations in Minkowski spacetime around instantons, we would require the techniques of Picard-Lefschetz theory in [36]. That issue does not present itself for the fermionic fluctuations whose saddle-point remains 0.
The usual Dirac matrices are related to the Euclidean spacetime version through:

$$\gamma^0 = \gamma_4^{\mathrm{E}} \quad \text{and} \quad \gamma^i = \mathrm{i}\gamma_i^{\mathrm{E}} \text{ for } i = 1,2,3\,. \quad (6.1.8)$$

while $\gamma^5 = \gamma_1^{\mathrm{E}}\gamma_2^{\mathrm{E}}\gamma_3^{\mathrm{E}}\gamma_4^{\mathrm{E}} = \mathrm{i}\gamma_0\gamma_1\gamma_2\gamma_3$ and thus retains its explicit form. Using the above conventions we can transform the Euclidean Dirac operator into its Minkowski analogue:

$$\begin{aligned} \not{D}^{\mathrm{E}} = (\not{\partial}_m^{\mathrm{E}} - \mathrm{i}\gamma_m^{\mathrm{E}}\boldsymbol{A}_m^{\mathrm{E}}) &\to -\mathrm{i}\frac{\partial}{\partial x^0}\gamma_4^{\mathrm{E}} + \vec{\gamma}^{\mathrm{E}}\cdot\nabla - \mathrm{i}\gamma_4^{\mathrm{E}}\boldsymbol{A}_4^{\mathrm{E}}(\vec{x}, x_4 = \mathrm{i}x^0) - \mathrm{i}\vec{\gamma}^{\mathrm{E}}\cdot\vec{\boldsymbol{A}}^{\mathrm{E}}(\vec{x}, x_4 = \mathrm{i}x^0) \\ &= -\mathrm{i}\left(\frac{\partial}{\partial x^0}\gamma^0 + \vec{\gamma}\cdot\nabla - \mathrm{i}\gamma^0\boldsymbol{A}_0(x^0,\vec{x}) - \mathrm{i}\vec{\gamma}\cdot\vec{\boldsymbol{A}}(x^0,\vec{x})\right) = -\mathrm{i}\not{D}\,, \end{aligned} \quad (6.1.9)$$

where " $\cdot$ " indicates a positive definite sum over the indices $1,2,3$. We can consider complex masses for which the transformation rule gives the correct Dirac operator in Minkowski space,

$$\not{D}^{\mathrm{E}} + m_{\mathrm{R}} + \mathrm{i}\gamma^5 m_{\mathrm{I}} \to -\left(\mathrm{i}\not{D} - m_{\mathrm{R}} - \mathrm{i}\gamma^5 m_{\mathrm{I}}\right)\,. \quad (6.1.10)$$

Let us recall that the Dirac operator above must be supplemented with a factor γ^0 to make it into a Hermitian operator for the traditional case of a real gauge field.
We can now move on and study the corresponding Green's functions. We begin by considering the Green's equation, $S^{\mathrm{E}}(x^{\mathrm{E}}, x'^{\mathrm{E}})$, such that

$$(\not{D}^{\mathrm{E}} + m_{\mathrm{R}} + \mathrm{i}\gamma^5 m_{\mathrm{I}})S^{\mathrm{E}}(x^{\mathrm{E}}, x'^{\mathrm{E}}) = \delta^4(x^{\mathrm{E}} - x'^{\mathrm{E}})\,, \quad (6.1.11)$$

and use the eigenvalues for the massless case,

$$\not{D}^{\mathrm{E}}\hat{\psi}_\lambda^{\mathrm{E}} = \left(\not{\partial}^{\mathrm{E}} - \mathrm{i}\gamma_m^{\mathrm{E}}\boldsymbol{A}_m^{\mathrm{E}}\right)\hat{\psi}_\lambda^{\mathrm{E}} = \lambda^{\mathrm{E}}\hat{\psi}_\lambda^{\mathrm{E}}\,, \quad (6.1.12)$$

to write down a spectral decomposition for S^{E} similarly to the arguments in [163], so tentatively

$$\lim_{m_R, m_I \to 0} S^{\mathrm{E}}(x^{\mathrm{E}}, x'^{\mathrm{E}}) = \sum\!\!\!\!\!\!\int_{\lambda^{\mathrm{E}}} \frac{\hat{\psi}_\lambda^{\mathrm{E}}(x^{\mathrm{E}})\hat{\psi}_\lambda^{\mathrm{E}\dagger}(x'^{\mathrm{E}})}{\lambda^{\mathrm{E}}}\,, \quad (6.1.13)$$

where the eigenvalues are purely imaginary as they correspond to $\not{D}^{\mathrm{E}}$, which is anti-hermitian, however because of the anti-instanton background we have to deal with the appearance of a zero-mode (an eigenvalue takes the values zero). The Atiyah-Singer index theorem[164], as long as we consider the one-point compactification of $\mathbb{R}^4$, relates the winding number of the instanton background with the chirality of the zero-modes, for the case of a $k = -1$ anti-instanton background, the zero-mode is left-handed[165] and explicitly given by

$$\psi^{\mathrm{E}}_{0\mathrm{L}}(x^{\mathrm{E}}) = \begin{pmatrix} \chi^{\mathrm{E}}_0 \\ 0 \\ 0 \end{pmatrix}, \quad \text{where} \quad \chi^{\mathrm{E}\,\alpha a}_0(x^{\mathrm{E}}) = \frac{\rho\epsilon^{\alpha a}}{\pi\left[\rho^2 + (x^{\mathrm{E}})^2\right]^{\frac{3}{2}}}, \tag{6.1.14}$$

where α is a Weyl spinor index and appears mixed with a, that stands for a gauge group index, in a fully anti-symmetric manner, with $\epsilon^{12} = 1$. In the case of $k = 1$, the zero mode is right handed and appears simply in the lower two components of ψ^{E}_{0L}. We can verify that the are correspondingly eigenfunctions of the chiral projectors P_L and P_R respectively.
Including a regulator mass as a perturbation, the zero-mode can be separated from the sum, so that the Green's function's spectral decomposition at first order in the perturbation[166, 167]

$$S^{\mathrm{E}}(x^{\mathrm{E}}, x'^{\mathrm{E}}) = \frac{\hat{\psi}^{\mathrm{E}}_0(x^{\mathrm{E}})\hat{\psi}^{\mathrm{E}\dagger}_0(x'^{\mathrm{E}})}{m\mathrm{e}^{-\mathrm{i}\alpha}} + \sum_{\lambda^{\mathrm{E}}\neq 0} \frac{\hat{\psi}^{\mathrm{E}}_\lambda(x^{\mathrm{E}})\hat{\psi}^{\mathrm{E}\dagger}_\lambda(x'^{\mathrm{E}})}{\lambda^{\mathrm{E}}}, \tag{6.1.15}$$

where all the other eigenvalues are also displaced, are no longer purely imaginary, but can be relabeled and the summation is understood along the displaced line. We will discuss further complex masses and the consequences to the eigenfunctions in the following subsection.
Following the transformation rule in Eq. (6.1.10) we have that the Green's functions are related by simple Wick rotation,

$$S^{\mathrm{E}}(x^{\mathrm{E}}, x'^{\mathrm{E}}) \qquad \underset{x_4=\mathrm{i}x^0,\, x'_4=\mathrm{i}x'^0}{\longrightarrow} \qquad \mathrm{i}S(x, x'), \tag{6.1.16}$$

and the Minkowski version of Green function equation,

$$\left(\mathrm{i}\not{\partial} - m_{\mathrm{R}} - \mathrm{i}\gamma^5 m_{\mathrm{I}}\right)\mathrm{i}S(x, x') = \mathrm{i}\delta^4(x - x'), \tag{6.1.17}$$

is respectively approximately solved for small mass perturbations, which agrees with the analytical continuation of Eq. (6.1.12), when simultaneously changing

$$\delta^4(x^{\mathrm{E}} - x'^{\mathrm{E}}) \to -\mathrm{i}\delta^4(x - x'). \tag{6.1.18}$$

The operators on the left-hand sides of Eqs.(6.1.12) and (6.1.17) appear in their corresponding path integrals, for a background with a single $k = -1$ instanton, which implies that by differentiation with respect to the external sources for the fermions, we can obtain the two-point correlation functions, which in relation to the Green's functions above are

$$S^{\mathrm{E}}(x^{\mathrm{E}}, x'^{\mathrm{E}}) = \langle\psi^{\mathrm{E}}(x^{\mathrm{E}})\psi^{\mathrm{E}\dagger}(x'^{\mathrm{E}})\rangle, \qquad \mathrm{i}S(x, x') = \langle\psi(x)\bar{\psi}(x')\rangle. \tag{6.1.19}$$

We have the following relations between the Euclidean and the Minkowski spinors

$$\psi^{\mathrm{E}}(x^{\mathrm{E}}) \xrightarrow{x_4=\mathrm{i}x^0} \psi(x^0, \vec{x}) \tag{6.1.20}$$

$$\psi^{\mathrm{E}\,\dagger}(x^{\mathrm{E}}) \xrightarrow{x_4=\mathrm{i}x^0} \bar{\psi}(x^0, \vec{x}) \tag{6.1.21}$$

which are compatible with the Eq. (6.1.19). As will see later, however the spectral decomposition requires more attention is not a direct task to translate it to Minkowski spacetime (see [36]).

6.1.2 Euclidean Dirac equation with complex masses

The Euclidean Dirac operator $\not{D}^{\mathrm{E}} + m\,\mathrm{e}^{\mathrm{i}\alpha\gamma^5} = \not{D}^{\mathrm{E}} + m_R + \mathrm{i}\gamma^5 m_I$ has among others, the following two properties under hermitian conjugation,

$$\not{D}^{\mathrm{E}} \xrightarrow{\ \dagger\ } -\not{D}^{\mathrm{E}} \tag{6.1.22}$$

$$(\not{D}^{\mathrm{E}} + m) \xrightarrow{\ \dagger\ } \gamma^5(\not{D}^{\mathrm{E}} + m)\gamma^5. \tag{6.1.23}$$

With a direct computation we can see how the massless eigenfunctions are still eigenfunctions when we perturb with a real mass and the pairing of spinors $\hat{\psi}^{\mathrm{E}}_\lambda$ and $\gamma^5\hat{\psi}^{\mathrm{E}}_\lambda$ is kept:

$$\left(\not{D}^{E} + m_{\mathrm{R}}\right)\hat{\psi}^{\mathrm{E}}_\lambda = (\lambda^{\mathrm{E}} + m_{\mathrm{R}})\hat{\psi}^{E}_\lambda\,, \tag{6.1.24}$$

$$\left(\not{D}^{\mathrm{E}} + m_{\mathrm{R}}\right)\gamma^5\hat{\psi}^{\mathrm{E}}_\lambda = \gamma^5\left(-\not{D}^{\mathrm{E}} + m_{\mathrm{R}}\right)\hat{\psi}^{\mathrm{E}}_\lambda = (-\lambda^{\mathrm{E}} + m_{\mathrm{R}})\gamma^5\hat{\psi}^{\mathrm{E}}_\lambda\,, \tag{6.1.25}$$

so that the spectral decomposition in Eq. (6.1.15) applies for $\alpha = 0$. We see how the pair $\hat{\psi}^{\mathrm{E}}_\lambda$ and $\gamma^5\hat{\psi}^{\mathrm{E}}_\lambda$ corresponds to eigenvalues $(\pm\lambda^{\mathrm{E}} + m_{\mathrm{R}}) \neq 0$ and are thus orthogonal. For a complex mass term, the spinor structure becomes more complicated and we must diagonalize the massless case eigenfunctions to obtain a spectral decomposition that holds for a general mass term. For that purpose we first write the operator in matrix form acting on a Dirac spinor and its chiral pair

$$\begin{pmatrix} \not{D}^{\mathrm{E}} + m_{\mathrm{R}} + \mathrm{i}\gamma^5 m_{\mathrm{I}} & 0 \\ 0 & \not{D}^{\mathrm{E}} + m_{\mathrm{R}} + \mathrm{i}\gamma^5 m_{\mathrm{I}} \end{pmatrix}\begin{pmatrix} \hat{\psi}^{\mathrm{E}}_\lambda \\ \gamma^5\hat{\psi}^{\mathrm{E}}_\lambda \end{pmatrix} = \begin{pmatrix} \lambda^{\mathrm{E}} + m_{\mathrm{R}} & \mathrm{i}m_{\mathrm{I}} \\ \mathrm{i}m_{\mathrm{I}} & -\lambda^{\mathrm{E}} + m_{\mathrm{R}} \end{pmatrix}\begin{pmatrix} \hat{\psi}^{\mathrm{E}}_\lambda \\ \gamma^5\hat{\psi}^{\mathrm{E}}_\lambda \end{pmatrix}. \tag{6.1.26}$$

and proceed to find its eigenvalues, which are found to be

$$\xi^{\mathrm{E}}_\pm(\lambda^{\mathrm{E}}) = m_{\mathrm{R}} \pm \sqrt{(\lambda^{\mathrm{E}})^2 - m_{\mathrm{I}}^2}, \tag{6.1.27}$$

with their corresponding eigenvectors,

$$\psi^{\mathrm{E}}_{\xi\pm} = \frac{1}{\sqrt{2\lambda^{\mathrm{E}}}}\left(\frac{m_{\mathrm{I}}}{\sqrt{\lambda^{\mathrm{E}} \mp \sqrt{(\lambda^{\mathrm{E}})^2 - m_{\mathrm{I}}^2}}}\hat{\psi}^{\mathrm{E}}_\lambda + \mathrm{i}\sqrt{\lambda^{\mathrm{E}} \mp \sqrt{(\lambda^{\mathrm{E}})^2 - m_{\mathrm{I}}^2}}\gamma^5\hat{\psi}^{\mathrm{E}}_\lambda\right). \tag{6.1.28}$$

which are orthogonal to each other given that they belong to different eigenvalues, as long as $\lambda^{\mathrm{E}} \neq 0$. The zero-mode is still an eigenvector after the mass perturbation and contributes to the spectral decomposition. Including the above diagonalization we have

$$S^{\mathrm{E}}(x^{\mathrm{E}}, x^{\mathrm{E}\prime}) = \frac{\psi^{\mathrm{E}}_0(x)\psi^{\mathrm{E}\dagger}_0(x'^{\mathrm{E}})}{m\mathrm{e}^{-\mathrm{i}\alpha}} + \sum\!\!\!\!\!\!\int_{\lambda^{\mathrm{E}}/\mathrm{i}>0}\sum_\pm \frac{\psi^{\mathrm{E}}_{\xi\pm}(x^{\mathrm{E}})\psi^{\mathrm{E}\dagger}_{\xi\pm}(x^{\mathrm{E}\prime})}{\xi^{\mathrm{E}}_\pm}\,. \tag{6.1.29}$$

Given that $(\lambda^{\mathrm{E}})^2 - m_I^2 < 0$ the coefficients of $\hat{\psi}^{\mathrm{E}}_\lambda$ and $\gamma^5\hat{\psi}^{\mathrm{E}}_\lambda$ in Eq. (6.1.28) can be taken to have the same phase by an appropriate choice of complex root. This means the eigenvector also diagonalize the hermitian conjugate operator

$$\begin{pmatrix} (\not{D}^{\mathrm{E}} + m_{\mathrm{R}} + \mathrm{i}\gamma^5 m_{\mathrm{I}})^\dagger & 0 \\ 0 & (\not{D}^{\mathrm{E}} + m_{\mathrm{R}} + \mathrm{i}\gamma^5 m_{\mathrm{I}})^\dagger \end{pmatrix} \begin{pmatrix} \hat{\psi}^{\mathrm{E}}_\lambda \\ \gamma^5\hat{\psi}^{\mathrm{E}}_\lambda \end{pmatrix} = \begin{pmatrix} -\lambda^{\mathrm{E}} + m_{\mathrm{R}} & -\mathrm{i}m_{\mathrm{I}} \\ -\mathrm{i}m_{\mathrm{I}} & \lambda^{\mathrm{E}} + m_{\mathrm{R}} \end{pmatrix} \begin{pmatrix} \hat{\psi}^{\mathrm{E}}_\lambda \\ \gamma^5\hat{\psi}^{\mathrm{E}}_\lambda \end{pmatrix},$$

with eigenvalues $(\xi^{\mathrm{E}}_\pm)^*$.

We can verify the divergence of the anomalous chiral current through direct computation with the decompositions we have. Consider the trace of one mode of the scalar axial current

$$\begin{aligned}
&\partial^{\mathrm{E}}_m \, \psi^{\mathrm{E}\dagger}_{\xi\pm}(x^{\mathrm{E}})\gamma^5\gamma^{\mathrm{E}}_m\psi^{\mathrm{E}}_{\xi\pm}(x^{\mathrm{E}}) \\
&\quad = \partial^{\mathrm{E}}_m \,\mathrm{tr}\; \gamma^5\gamma^{\mathrm{E}}_m\psi^{\mathrm{E}}_{\xi\pm}(x^{\mathrm{E}})\psi^{\mathrm{E}\dagger}_{\xi\pm}(x^{\mathrm{E}}) \\
&\quad = \mathrm{tr}\Big\{\gamma^5\left[\left(\not{D}^{\mathrm{E}} + \mathrm{i}\gamma^{\mathrm{E}}_m \boldsymbol{A}^{\mathrm{E}}{}_m\right)\psi^{\mathrm{E}}_{\xi\pm}\right]\psi^{\mathrm{E}\dagger}_{\xi\pm} - \gamma^5\psi^{\mathrm{E}}_{\xi\pm}\left[\left(\not{D}^{\mathrm{E}} + \mathrm{i}\gamma^{\mathrm{E}}_m \boldsymbol{A}^{\mathrm{E}}{}_m\right)\psi^{\mathrm{E}}_{\xi\pm}\right]^\dagger\Big\} \\
&\quad = \mathrm{tr}\Big\{\gamma^5\left[\left(\not{D}^{\mathrm{E}} + m\,\mathrm{e}^{\mathrm{i}\alpha\gamma^5} + \mathrm{i}\gamma^{\mathrm{E}}_m \boldsymbol{A}^{\mathrm{E}}{}_m - m\,\mathrm{e}^{\mathrm{i}\alpha\gamma^5}\right)\psi^{\mathrm{E}}_{\xi\pm}\right]\psi^{\mathrm{E}\dagger}_{\xi\pm} \\
&\qquad\qquad - \gamma^5\psi^{\mathrm{E}}_{\xi\pm}\left[\left(\not{D}^{\mathrm{E}} - m\,\mathrm{e}^{-\mathrm{i}\alpha\gamma^5} + \mathrm{i}\gamma^{\mathrm{E}}_m \boldsymbol{A}^{\mathrm{E}}{}_m + m\,\mathrm{e}^{-\mathrm{i}\alpha\gamma^5}\right)\psi^{\mathrm{E}}_{\xi\pm}\right]^\dagger\Big\} \\
&\quad = \mathrm{tr}\left\{2\gamma^5\xi^{\mathrm{E}}_\pm\psi^{\mathrm{E}}_{\xi\pm}\psi^{\mathrm{E}\dagger}_{\xi\pm} - 2\gamma^5 m\,\mathrm{e}^{\mathrm{i}\alpha\gamma^5}\psi^{\mathrm{E}}_{\xi\pm}\psi^{\mathrm{E}\dagger}_{\xi\pm}\right\},
\end{aligned} \tag{6.1.30}$$

where we have omitted the spacetime point after the first line, have used the cyclicity of the trace and the commutation relation of γ^5 with γ^{E}_m and used the fact that changing the sign and phase of the mass term leads to the conjugated eigenvalue (see Eq. (C.19)), which also holds for the zero-modes by changing the eigenvalues. The above relation can also be employed for the zero-modes by changing the eigenvalue accordingly. We can compute now the divergence of the full current by using the spectral decomposition in Eq. (6.1.29) to get

$$\partial^{\mathrm{E}}_m \mathrm{tr}\,\gamma^5\gamma^{\mathrm{E}}_m S^{\mathrm{E}}(x^{\mathrm{E}}, x^{\mathrm{E}}) = 2\psi^{\mathrm{E}\dagger}_0(x^{\mathrm{E}})\gamma^5\psi^{\mathrm{E}}_0(x^{\mathrm{E}}) + 2m\left\langle \psi^{\mathrm{E}\dagger}(x^{\mathrm{E}})\gamma^5\,\mathrm{e}^{\mathrm{i}\alpha\gamma^5}\psi^{\mathrm{E}}(x^{\mathrm{E}})\right\rangle, \tag{6.1.31}$$

where the term with contributions of non-zero modes containing a single γ^5 gives zero when taking the trace. We can see that we indeed recover the anomalous divergence of the axial current, the first term coming from the zero-mode in the instanton background and accounting for the anomaly and the second term coming from the symmetry breaking mass term. This equation coincides with Eq. (5.1.38) when masses are taken to be 0 and extends it for mass perturbations and has the same interpretation as before of representing a change in chiral charge by +2 units, corresponding for example to the conversion of a left-handed mode to a right-handed mode.

Functional determinant of the Euclidean Dirac operator

We observe that the phase of the determinant of the operator $\not{D}^{\mathrm{E}} - m_R - \mathrm{i}\gamma^5 m_I$ is determined by the zero-modes of the massless operator. For the case of a single-instanton

background with $k = \pm 1$ we have

$$\det(-\not{D}^{\mathrm{E}} - m_{\mathrm{R}} - \mathrm{i}\gamma^5 m_{\mathrm{I}}) = \det(-\not{D}^{\mathrm{E}} - m\,\mathrm{e}^{\mathrm{i}\alpha\gamma_5}) = -m\,\mathrm{e}^{\mathrm{i}k\alpha} \prod_{\lambda^{\mathrm{E}}/\mathrm{i}>0} \xi_+^{\mathrm{E}}(\lambda^{\mathrm{E}})\xi_-^{\mathrm{E}}(\lambda^{\mathrm{E}})$$
$$= -m\,\mathrm{e}^{\mathrm{i}k\alpha} \prod_{\lambda^{\mathrm{E}}/\mathrm{i}>0} (m^2 + |\lambda^{\mathrm{E}}|^2)\,, \tag{6.1.32}$$

which we can summarize as

$$\det(-\not{D}^{\mathrm{E}} - m\,\mathrm{e}^{\mathrm{i}\alpha\gamma^5}) = -\,\mathrm{e}^{\mathrm{i}k\alpha} |\det(-\not{D}^{\mathrm{E}} - m\,\mathrm{e}^{\mathrm{i}\alpha\gamma^5})|. \tag{6.1.33}$$

This agrees with the fact that the backgrounds are related to each other via a parity transformation, or in practice by $\alpha \to -\alpha$. The same arguments show that the determinant of the background-free operator $-\not{\partial}^{\mathrm{E}} - m_R - \mathrm{i}\gamma^5 m_I$ is already real and positive, that is

$$\det(-\not{\partial}^{\mathrm{E}} - m\,\mathrm{e}^{\mathrm{i}\alpha\gamma^5}) = |\det(-\not{\partial}^{\mathrm{E}} - m\,\mathrm{e}^{\mathrm{i}\alpha\gamma^5})|\,. \tag{6.1.34}$$

More properties and details concerning the eigenvectors and eigenvalues of this diagonalization can be found in the Appendix C..

6.1.3 Minkowski Dirac fermions with complex mass

In this section, we study the Green's function in the Minkowski spacetime. All quantities are, therefore, to be understood to be written over Minkowski spacetime unless otherwise specified. Our objective is to set the Ansatz for the Green's function that will be employed later in the instanton gas and find out the relation between the functional determinants of the Dirac operator in Euclidean and Minkowski spacetime. The results presented here can be obtained by employing our general analytic continuation techniques presented in Appendix C.. The Minkowski Dirac operator is

$$\mathrm{i}\not{D} - m_{\mathrm{R}} - \mathrm{i}\gamma^5 m_{\mathrm{I}}, \tag{6.1.35}$$

and is Dirac-hermitian, that is, the operator $\mathrm{i}\gamma^0\not{D}$ is hermitian in the usual sense, i.e., when computing the dagger or adjoint operator, when the gauge field is real. We want to prioritize Lorentz invariance in spinor products such as $\psi\bar{\psi}$. To do this, although we would be tempted to use the Dirac adjoint throughout our computations while keeping the Dirac operator as above, it is not possible. In doing this, we learn that the Dirac adjoint leads to an ill-defined inner-product so that the spectral decomposition of the Dirac operator must be obtained through the ϑ-adjoint instead; a topic we expand on in the Appendix C.. The ϑ-adjoint induces a well-defined inner-product and allows us to keep the spectral decomposition for the Dirac operator without the γ^0, hence more adequate for S-matrix elements which always appear with barred non-barred combinations. Moreover, as we have seen, analytically continuing the instanton fields, we no longer have a Dirac-adjoint hermitian operator and must find a workaround. Denoting the ϑ-adjoint with a tilde, let the spectral decomposition of the Dirac operator of Eq. (6.1.35) be

$$\left(\mathrm{i}\not{D} - m_{\mathrm{R}} - \mathrm{i}\gamma^5 m_{\mathrm{I}}\right)_{x,x'} = \sum\!\!\!\!\!\!\int_{\xi} \xi\psi_\xi(x)\tilde{\psi}_\xi(x')\,, \quad \mathrm{i}S(x,x') = \mathrm{i}\sum\!\!\!\!\!\!\int_{\xi} \frac{\psi_\xi(x)\tilde{\psi}_\xi(x')}{\xi}\,. \tag{6.1.36}$$

We have focused our interest in the fermion zero mode, defined as the eigenfunction corresponding to the zero eigenvalue for the massless Dirac operator since it plays an

important role in this study in relation to the anomaly. We do not pursue further the study of the continuous part of the spectrum, which is left to further examination.
When considering the addition of a complex mass, we observe all the eigenvalues are shifted by the size of the mass added. As a consequence, the zero-mode of the massless operator will now have an eigenvalue $\xi_{0R/L} = -m\,\mathrm{e}^{\mathrm{i}\alpha}$, where R/L is a reminder that such modes are strictly right- or left-handed modes. By analytically continuing the zero-modes of the Euclidean operator, we obtain the corresponding zero-modes without any change to their chirality, meaning that we get one right-handed zero-mode for the $k = 1$ instanton background and a left-handed zero-mode for the $k = -1$ anti-instanton. Using transformation rule in Eq. (C.31) we have for the anti-instanton case:

$$\psi_{0\mathrm{L}}(x^0, \vec{x}) \equiv \sqrt{\mathrm{i}}\,\varphi_{0\mathrm{L}}(x^0, \vec{x}) = \sqrt{\mathrm{i}}\,\psi^{\mathrm{E}}_{0\mathrm{L}}(\vec{x}, \mathrm{i}x^0)\,, \tag{6.1.37}$$

where

$$\varphi_{0\mathrm{L}}(x) = \begin{pmatrix} \chi_0(x) \\ \begin{pmatrix} 0 \\ 0 \end{pmatrix} \end{pmatrix}, \quad \chi_0^{\mathrm{E}\,\beta a}(x^{\mathrm{E}}) = \frac{\rho\epsilon^{\beta a}}{\pi\,(\rho^2 - x^2)^{\frac{3}{2}}}, \tag{6.1.38}$$

and from the ϑ-adjoint (see Eq. (C.34) and Eq. (C.35)) and the time reflection symmetry of the zero-mode:

$$\tilde{\psi}_{0\mathrm{L}}(x) = \sqrt{\mathrm{i}}\,(\varphi_{0\mathrm{L}}(x))^\dagger\,. \tag{6.1.39}$$

This way we can arrive to a spectral decomposition of the propagator in terms of φ_{0L} and $\varphi^\dagger_{0L}$ which clearly displays how the propagator encodes the breaking of the axial symmetry at the quantum level. In a background with an anti-instanton located at x_0 we expect the Green's function to be dominated by the zero mode close to its location, while everywhere else it should roughly coincide with the propagator over an empty background, explicitly

$$\begin{aligned} \mathrm{i}S(x, x') &= \mathrm{i}S_{\mathrm{cont}}(x, x') + \frac{\varphi_{0\mathrm{L}}(x - x_0)\,\varphi^\dagger_{0\mathrm{L}}(x' - x_0)}{m\,\mathrm{e}^{-\mathrm{i}\alpha}} \\ &\approx \mathrm{i}S_\varnothing(x, x') + \frac{\varphi_{0\mathrm{L}}(x - x_0)\,\varphi^\dagger_{0\mathrm{L}}(x' - x_0)}{m\,\mathrm{e}^{-\mathrm{i}\alpha}}\,, \end{aligned} \tag{6.1.40}$$

where he have replaced the continuous part of the spectrum by the empty background Green's function (see Appendix D. for its derivation)

$$\mathrm{i}S_\varnothing(x, x') = (-\gamma^\mu\partial_\mu + \mathrm{i}m\mathrm{e}^{-\mathrm{i}\alpha\gamma^5}) \int \frac{\mathrm{d}^4p}{(2\pi)^4}\,\mathrm{e}^{-\mathrm{i}p(x-x')}\frac{1}{p^2 - m^2 + \mathrm{i}\epsilon}, \tag{6.1.41}$$

which only has a continuous spectrum, so we expect indeed $\mathrm{i}S_\varnothing \approx \mathrm{i}S(x, x')$ for $x^2, x'^2 \gg \rho^2$. We observe that the expression above leads to the Feynman propagator through the $\mathrm{i}\epsilon$-prescription choice, but other choices are possible depending on the application.
Let us now generalize our Ansatz for the propagator in Eq. (6.1.40), to a background consisting of n instantons labeled by ν and $\bar{n}$ anti-instantons labeled by $\bar{\nu}$, at different locations $x_{0,\nu}$ and $x_{0,\bar{\nu}}$ respectively. For one instanton background we need only replace $\varphi_{0\mathrm{L}}$ with $\varphi_{0\mathrm{R}}$ and α with $-\alpha$. For a dilute instanton gas in our sense, we superimpose the deviations due to the presence of each instanton as follows:

$$\mathrm{i}S_{n,\bar{n}}(x, x') \approx \mathrm{i}S_\varnothing(x, x') + \sum_{\bar{\nu}=1}^{\bar{n}} \frac{\varphi_{0\mathrm{L}}(x - x_{0,\bar{\nu}})\varphi^\dagger_{0\mathrm{L}}(x' - x_{0,\bar{\nu}})}{m\,\mathrm{e}^{-\mathrm{i}\alpha}} + \sum_{\nu=1}^{n} \frac{\varphi_{0\mathrm{R}}(x - x_{0,\nu})\varphi^\dagger_{0\mathrm{R}}(x' - x_{0,\nu})}{m\,\mathrm{e}^{\mathrm{i}\alpha}}\,. \tag{6.1.42}$$

We finish this section with the relation between the functional determinants of the Euclidean and Minkowski Dirac operators, as well as by establishing the notation that will be employed later on. Using the methods of [36] the Euclidean functional determinant is transformed to Minkowski spacetime according to the transformation $T^{\mathrm{E}} \to \mathrm{i}T$ of the observed spacetime region:

$$\det(\mathrm{i}\not{D} - m\,\mathrm{e}^{\mathrm{i}\alpha\gamma^5}) = \det(-\not{D}^{\mathrm{E}} - m\,\mathrm{e}^{\mathrm{i}\alpha\gamma^5})\big|_{T^{\mathrm{E}}\to \mathrm{i}T}\,. \tag{6.1.43}$$

As we have seen in many examples in the document, functional determinants are regulated by normalizing them against their free versions, taking the ratio cancels the T dependence. This is shown in detail in [36], it is related to the time-translation zero-mode and will be confirmed later on here as well. We have therefor

$$\frac{\det(\mathrm{i}\not{D} - m\,\mathrm{e}^{\mathrm{i}\alpha\gamma^5})}{\det(\mathrm{i}\not{\partial} - m\,\mathrm{e}^{\mathrm{i}\alpha\gamma^5})} = \frac{\det(-\not{D}^{\mathrm{E}} - m\,\mathrm{e}^{\mathrm{i}\alpha\gamma^5})}{\det(-\not{\partial}^{\mathrm{E}} - m\,\mathrm{e}^{\mathrm{i}\alpha\gamma^5})}\,. \tag{6.1.44}$$

Using the results from the previous section, Eq. (6.1.33) and the ratio above let us abbreviate

$$\frac{\det(\mathrm{i}\not{D} - m\,\mathrm{e}^{\mathrm{i}\alpha\gamma^5})}{\det(\mathrm{i}\not{\partial} - m\,\mathrm{e}^{\mathrm{i}\alpha\gamma^5})} \equiv -\,\mathrm{e}^{\mathrm{i}k\alpha}\Theta \qquad \text{for} \quad k = \pm 1, \tag{6.1.45}$$

where

$$\Theta = \left|\frac{\det(\mathrm{i}\not{D} - m\,\mathrm{e}^{\mathrm{i}\alpha\gamma^5})}{\det(\mathrm{i}\not{\partial} - m\,\mathrm{e}^{\mathrm{i}\alpha\gamma^5})}\right| = \left|\frac{\det(-\not{D}^{\mathrm{E}} - m\,\mathrm{e}^{\mathrm{i}\alpha\gamma^5})}{\det(-\not{\partial}^{\mathrm{E}} - m\,\mathrm{e}^{\mathrm{i}\alpha\gamma^5})}\right|\,. \tag{6.1.46}$$

6.2 Fermion correlation functions via a dilute instanton gas

We have now collected the quantities needed to compute correlation functions using the path integral method in Minkowski space. First, we illustrate how to do this for the case of a model with a single quark flavor, then we generalize the result to a multi-flavor setting. We start by considering the two-point correlation function for the fermion in the single-flavor theory whose action is S_{single}. For theories such as QCD with non-Abelian gauge groups, we must consider the vacuum structure, as explained in Sec. 5.1. This we do by including a θ-term in the action. We want to consider a dilute instanton gas containing an arbitrary number of instantons, the computation will be then broken down into a computation for a fixed total number of instantons, which we refer to as topological sector, and later on, we consider the possible interference between the different sectors.

6.2.1 Path integration restricted to a topological sector

The full two-point correlation function for the fermionic field in Minkowski spacetime is formally obtained through

$$\langle\psi(x)\bar{\psi}(x')\rangle = \frac{1}{Z}\int \mathcal{D}A\,\mathcal{D}\bar{\psi}\,\mathcal{D}\psi\;\psi(x)\bar{\psi}(x')\,\mathrm{e}^{\mathrm{i}S_{\text{single}}}\,, \tag{6.2.47}$$

where Z is the partition function and is concretely

$$Z = \int \mathcal{D}A\mathcal{D}\bar{\psi}\mathcal{D}\psi\;\mathrm{e}^{\mathrm{i}S}\,, \tag{6.2.48}$$

A sensible saddle-point expansion must require that the action is finite at those points and hence all the instanton technology that we have described in the preparation to this chapter can be applied. Specifically, we remind the reader that this implies that the topological sectors (or total number of instantons and anti-instantons) Δn is an integer number and we will generate these sectors by a superposition of $k = \pm 1$ (anti-)instantons, ignoring any interaction between them. That is we may have n instantons and $\bar{n}$ anti-instantons in the Δn sector, provided that $\Delta n = n - \bar{n}$. Throughout the whole computation, we will make use of the regular gauge, where the instanton solutions, Eq. (5.3.105), accumulates the topological charge asymptotically at $t \to \pm\infty$. If we then choose to include the θ-term in the action and keep the label of the pre-vacua by using the asymptotic topological charge or Chern-Simons number, we have that the ket describing the vacuum of the theory is[109, 110]

$$|\mathrm{vac}\rangle = \sum_{n_{\mathrm{CS}}} |n_{\mathrm{CS}}\rangle \,. \tag{6.2.49}$$

We note how the different topological sectors force the background gauge field to fulfill different boundary conditions, which effectively means we have to deal with a path integral per sector. And for the topological charges to be properly captured, this means the limit $VT \to \infty$ has to be taken for each sector. This argument of ours will have very interesting consequences, as we shall see.

Let us write down the functional determinant for the fermion fluctuations over a background populated with n instantons with $k = 1$ and $\bar{n}$ anti-instantons with $k = -1$,

$$\begin{aligned}
&\det(\mathrm{i}\not{D} - m\,\mathrm{e}^{\mathrm{i}\alpha\gamma^5})_{n,\bar{n}} \\
&\quad = \det(\mathrm{i}\not{\partial} - m\,\mathrm{e}^{\mathrm{i}\alpha\gamma^5}) \left(\frac{\det(\mathrm{i}\not{D}_{k=1} - m\,\mathrm{e}^{\mathrm{i}\alpha\gamma^5})}{\det(\mathrm{i}\not{\partial} - m\,\mathrm{e}^{\mathrm{i}\alpha\gamma^5})}\right)^{n} \left(\frac{\det(\mathrm{i}\not{D}_{k=-1} - m\,\mathrm{e}^{\mathrm{i}\alpha\gamma^5})}{\det(\mathrm{i}\not{\partial} - m\,\mathrm{e}^{\mathrm{i}\alpha\gamma^5})}\right)^{\bar{n}} \\
&\quad = |\det(-\not{\partial}^{\mathrm{E}} - m\,\mathrm{e}^{\mathrm{i}\alpha\gamma^5})|\Big|_{T^{\mathrm{E}}\to \mathrm{i}T}\ \mathrm{e}^{-\mathrm{i}(\bar{n}-n)\alpha}(-\Theta)^{\bar{n}+n}\,,
\end{aligned} \tag{6.2.50}$$

where the first det factor on the right-hand side in the first line, which remains unpaired, counts appropriately fluctuations of the regions far away from the instantons in analogy to Eq. (6.1.42). To obtain the last line we have used the definitions and results of Eqs. (6.1.34), (6.1.43) and (6.1.45). The functional determinant for the gauge and ghost fields gives

$$\det{}'_{\bar{A}_{n,\bar{n}}} = \det{}_{\bar{A}=0} \left(\frac{\det{}'_{\bar{A}}}{\det{}_{\bar{A}=0}}\right)^{n+\bar{n}} \equiv \det{}_{\bar{A}=0}\, R^{-2(n+\bar{n})}, \tag{6.2.51}$$

in analogy with the fermion case, where the $'$ denotes the omission of zero-modes in the functional determinant and the background gauge configuration is indicated in the subscript. We collect therein, within the parenthesis, the fluctuations of the gauge field and the ghosts in the $k = \pm 1$ instanton background, which are the same. We have also taken the chance to introduce abbreviated notation for square root of the above ratio of functional determinants, which will be useful in what follows.

To compute the correlation function for a given topological sector, Δn, we must sum over all possible transitions of pre-vacua with difference in charge of Δn, or in the language of the path integral consider all the combinations of instantons and anti-instantons that give

Δn:

$$\begin{aligned}\langle\psi(x)\bar{\psi}(x')\rangle_{\Delta n} &= \sum_m {}_{\rm out}\langle m+\Delta n|\psi(x)\bar{\psi}(x')|m\rangle_{\rm in}\\ &= \sum_{\substack{\bar{n},n\geq 0\\ n-\bar{n}=\Delta n}} \int \mathcal{D}A_{\bar{n},n}\mathcal{D}\bar{\psi}\mathcal{D}\psi\,\psi(x)\bar{\psi}(x')\,\mathrm{e}^{\mathrm{i}S_{\rm single}}\\ &= \sum_{\substack{\bar{n},n\geq 0\\ n-\bar{n}=\Delta n}} |\det(-\partial\!\!\!/^{\rm E}-m\,\mathrm{e}^{\mathrm{i}\alpha\gamma^5})|\Big|_{T^{\rm E}\to \mathrm{i}T}\frac{1}{\sqrt{\det_{\bar{A}=0}}}\int\frac{1}{\bar{n}!n!}\mathscr{D}_{\bar{n}}\bar{c}\,\mathscr{D}_n c\,\mathrm{i}S_{n,\bar{n}}(x,x')\\ &\quad\times(-\mathrm{e}^{-S^{\rm E}_{k=1}}R\Theta)^{\bar{n}+n}\,\mathrm{e}^{\mathrm{i}\Delta n(\alpha+\theta)},\end{aligned}\tag{6.2.52}$$

where $\mathcal{D}A_{n,\bar{n}}$ restricts the integral to fluctuations about a setting with n instantons and $\bar{n}$ anti-instantons, $S^E_{k=1}=8\pi^2/g^2$ is the classical instanton contribution to the action and where we have use the following definitions for the measure,

$$\begin{aligned}\mathscr{D}_{\bar{n}}\bar{c} &\equiv \prod_{\bar{\nu}=1}^{\bar{n}}\mathrm{d}^4x_{0,\bar{\nu}}\mathrm{d}\Omega_{\bar{\nu}}J_{\bar{\nu}},\\ \mathscr{D}_n c &\equiv \prod_{\nu=1}^{n}\mathrm{d}^4x_{0,\nu}\mathrm{d}\Omega_{\nu}J_{\nu},\end{aligned}\tag{6.2.53}$$

corresponding to the pending integration over collective coordinates of the zero-modes over the whole spacetime region VT, centers, sizes and gauge-orientations, and with J the respective Jacobians, computed in [105, 168], for the Euclidean case, appearing here in their Minkowski version. We note that they become purely imaginary in Minkowski spacetime[36]. The factors $1/(n!\bar{n}!)$ in Eq. (6.2.52) is included to account for exchanges of the n instantons among themselves (their locations) and the $\bar{n}$ anti-instantons among themselves. We have also used the results of [36] concerning complex integration over thimbles, to write the determinant over bosonic fluctuations in terms of its Euclidean version. We also observe that possible plane waves in the fluctuations do not alter the θ-term integration result.

We take care now of the integration over the the locations, which concern only the propagator $S_{n,\bar{n}}(x,x')$. Using our Ansatz in Eq. (6.1.40), an integration over the location yields a background-free part proportional to the spacetime region, VT and an additional anomalous term,

$$\begin{aligned}\int_{VT}\mathrm{d}^4x_{0,\bar{\nu}}\;\mathrm{i}S_{n,\bar{n}}(x,x') &\approx \int_{VT}\mathrm{d}^4x_{0,\bar{\nu}}\left[\mathrm{i}S_{\varnothing}(x,x')+\frac{\varphi_{0\rm L}(x-x_{0,\bar{\nu}})\varphi^\dagger_{0\rm L}(x'-x_{0,\bar{\nu}})}{m\,\mathrm{e}^{-\mathrm{i}\alpha}}+\cdots\right]\\ &= VT\,(\mathrm{i}S_{\varnothing}(x,x')+\cdots)+m^{-1}\,\mathrm{e}^{\mathrm{i}\alpha}h(x,x')P_{\rm L}\,,\end{aligned}\tag{6.2.54}$$

where we define $h(x,x')$ as a block diagonal matrix with two blocks given by

$$h(x,x')P_{\rm L}\equiv\int_{VT}\mathrm{d}^4x_{0,\bar{\nu}}\,\varphi_{0\rm L}(x-x_{0,\bar{\nu}})\varphi^\dagger_{0\rm L}(x'-x_{0,\bar{\nu}})\tag{6.2.55}$$

$$h(x,x')P_{\rm R}\equiv\int_{VT}\mathrm{d}^4x_{0,\nu}\,\varphi_{0\rm R}(x-x_{0,\nu})\varphi^\dagger_{0\rm R}(x'-x_{0,\nu})\,.\tag{6.2.56}$$

We were not able to obtain an analytic expression for h as a function solely of $(x-x')^2$, so we leave the function unevaluated, however without consequences for our conclusions. Note as well that most of the contributions to h come from the neighborhood of the center $x_{0,\bar{\nu}}$ and we can thus take h to be essentially VT independent, however it still depends on the size ρ of the (anti-)instanton in the background, we *assume* we can write expressions from here onward in terms of the average over sizes and orientations

$$\bar{h}(x,x') \equiv \int \mathrm{d}\Omega_{\bar{\nu}}\, \mathrm{d}\Omega_{\nu}\, h(x,x') \Big/ \int \mathrm{d}\Omega_{\bar{\nu}}\, \mathrm{d}\Omega_{\nu}. \tag{6.2.57}$$

Employing $\bar{h}(x,x')$ we can get rid of the collective coordinates integration and neglecting coincident locations of the (anti-)instanton composition we arrive to

$$\begin{aligned}\left\langle \psi(x)\bar{\psi}(x')\right\rangle_{\Delta n} = \begin{pmatrix}\text{free}\\ \text{dets}\end{pmatrix} \sum_{\substack{\bar{n},n\geq 0\\ n-\bar{n}=\Delta n}} \frac{1}{\bar{n}!n!}(\mathrm{i}\kappa)^{\bar{n}+n}(-1)^{n+\bar{n}}\,\mathrm{e}^{\mathrm{i}\Delta n(\alpha+\theta)}\Big[\mathrm{i}S_{\varnothing}(x,x')\,(VT)^{\bar{n}+n} \\ +\ \bar{h}(x,x')\left(\frac{\bar{n}}{m\,\mathrm{e}^{-\mathrm{i}\alpha}}P_{\mathrm{L}}+\frac{n}{m\,\mathrm{e}^{\mathrm{i}\alpha}}P_{\mathrm{R}}\right)(VT)^{\bar{n}+n-1}\Big],\end{aligned} \tag{6.2.58}$$

where

$$\mathrm{i}\kappa = \int \mathrm{d}\Omega\, J\ \Theta\, R\ \mathrm{e}^{-S^{\mathrm{E}}_{k=1}} \tag{6.2.59}$$

with $\kappa > 0$– J has a factor i and $\Theta \in \mathbb{R}$– and where we have compressed the free determinants that can be factorized as

$$\begin{pmatrix}\text{free}\\ \text{dets}\end{pmatrix} \equiv |\det(-\not{\partial}^{\mathrm{E}} - m\,\mathrm{e}^{\mathrm{i}\alpha\gamma^5})|\Big|_{T^{\mathrm{E}}\to \mathrm{i}T} \frac{1}{\sqrt{\det_{\bar{A}=0}}}. \tag{6.2.60}$$

The series appearing in Eq. (6.2.58) above can be recognized as modified Bessel function of the first kind, which are denoted by $I_{\alpha}(x)$, we get

$$\begin{aligned}\left\langle \psi(x)\bar{\psi}(x')\right\rangle_{\Delta n} = \begin{pmatrix}\text{free}\\ \text{dets}\end{pmatrix} (-1)^{\Delta n}\,\mathrm{e}^{\mathrm{i}\Delta n(\alpha+\theta)}\Big[I_{\Delta n}(2\mathrm{i}\kappa VT)\mathrm{i}S_{\varnothing}(x,x') \\ +\left(\mathrm{e}^{\mathrm{i}\alpha}I_{\Delta n+1}(2\mathrm{i}\kappa VT)P_{\mathrm{L}} + \mathrm{e}^{-\mathrm{i}\alpha}I_{\Delta n-1}(2\mathrm{i}\kappa VT)P_{\mathrm{R}}\right)\frac{\mathrm{i}\kappa}{m}\,\bar{h}(x,x')\Big],\end{aligned} \tag{6.2.61}$$

The partition function for a fixed topological sector is computed in an analogous way, but omitting the factor $\psi(x)\bar{\psi}(x')$,

$$\begin{aligned}Z_{\Delta n} &= \sum_{m} {}_{\mathrm{out}}\langle m+\Delta n|m\rangle_{\mathrm{in}} = \sum_{\substack{\bar{n},n\geq 0\\ n-\bar{n}=\Delta n}} \int \mathcal{D}A_{\bar{n},n}\mathcal{D}\bar{\psi}\mathcal{D}\psi\ \mathrm{e}^{\mathrm{i}S_{\mathrm{single}}} \\ &= \sum_{\substack{\bar{n},n\geq 0\\ n-\bar{n}=\Delta n}} \begin{pmatrix}\text{free}\\ \text{dets}\end{pmatrix} \int \frac{1}{\bar{n}!n!}\mathscr{D}_{\bar{n}}\bar{c}\,\mathscr{D}_n c\,(-\mathrm{e}^{-S^{\mathrm{E}}_{k=1}}R\Theta)^{\bar{n}+n}\,\mathrm{e}^{\mathrm{i}\Delta n(\alpha+\theta)},\end{aligned} \tag{6.2.62}$$

where we have left the integration over collective coordinates undone, although we could extract factors of VT from the integration over the locations, however the integration

over sizes is, as we know, divergent and we leave undone. As seen from the expression after the first equal sign above, we interpret the path integral as computing all possible transitions of Δn units of Chern-Simons charge between all pre-vacua. We also note that the functional determinants of the free operators do not depend on collective coordinates or the population of (anti-)instantons in the background and can be factorized. When taking the ratio of Eq. (6.2.52) and Eq. (6.2.62), they will drop out. Performing the remaining sums gives a Bessel function as for $\langle\psi(x)\bar{\psi}(x')\rangle_{\Delta n}$:

$$Z_{\Delta n} = \begin{pmatrix} \text{free} \\ \text{dets} \end{pmatrix} I_{\Delta n}(2\mathrm{i}\kappa VT)\,(-1)^{\Delta n}\,\mathrm{e}^{\mathrm{i}\Delta n(\alpha+\theta)}\,. \tag{6.2.63}$$

We must highlight how for a topological sector, there is a global phase in the expressions in Eq. (6.2.61) and Eq. (6.2.63), which is always given by $\mathrm{e}^{\mathrm{i}\Delta n(\alpha+\theta)}$, so that any operator computed using the path integral will have the same feature since phases come from the fermion determinant and instanton effects, we illustrate this in the sketch shown in Figure 6.1. This, of course, means that the global phase will cancel when taking the ratio within a fixed topological sector.

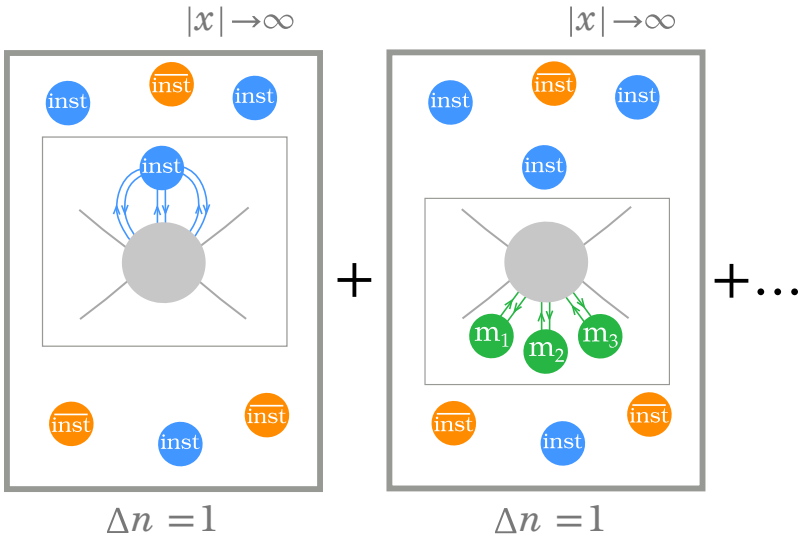

Figure 6.1: Scheme showing different contributions to a four-point correlation function in a multi-instanton background. The contribution in the left is the analogue of $\bar{h}$ in a 3 flavor scenario appearing from a six-point function. The contribution from the right has the same structure but comes from fermion mass terms, as $S_{\varnothing}$ in the single flavor case. When computing such interaction with the path integral in an infinite spacetime region, the phases from both contributions is the same, $\Delta n(\bar{\alpha}+\theta)$.

6.2.2 Computation of full correlation functions

In this subsection, we use the results for the two-point correlation function at a fixed topological sector and build with it a total partition function and a final result for the two-point fermion correlation function. First let us consider a truncated partition function which sums topological sectors from $\Delta n = -N$ to $\Delta n = N$,

$$Z(N,VT) = \sum_{\substack{m,n \\ |m-n|\leq N}} {}_{\text{out}}\langle m|n\rangle_{\text{in}} = \sum_{\Delta n=-N}^{N} \sum_{m} {}_{\text{out}}\langle m+\Delta n|m\rangle_{\text{in}} = \sum_{\Delta n=-N}^{N} Z_{\Delta n}(VT). \tag{6.2.64}$$

We keep both N and VT finite and we study carefully their limits later on. Using this notation the complete fermion two-point correlation function can be expressed as

$$\begin{aligned}\langle\psi(x)\bar{\psi}(x')\rangle &= \lim_{\substack{N\to\infty\\ N\in\mathbb{N}}}\lim_{VT\to\infty}\frac{1}{Z(N,VT)}\sum_{\substack{m,n\\ |m-n|\leq N}}{}_{\text{out}}\langle m|\psi(x)\bar{\psi}(x')|n\rangle_{\text{in}}\\ &= \lim_{\substack{N\to\infty\\ N\in\mathbb{N}}}\lim_{VT\to\infty}\sum_{\Delta n=-N}^{N}\sum_{n}{}_{\text{out}}\langle n+\Delta n|\psi(x)\bar{\psi}(x')|n\rangle_{\text{in}}\Big/\sum_{\Delta n=-N}^{N}Z_{\Delta n}(VT)\\ &= \lim_{\substack{N\to\infty\\ N\in\mathbb{N}}}\lim_{VT\to\infty}\sum_{\Delta n=-N}^{N}\langle\psi(x)\bar{\psi}(x')\rangle_{\Delta n}\Big/\sum_{\Delta n=-N}^{N}Z_{\Delta n}(VT)\\ &= \mathrm{i}S_{\varnothing}(x,x')+\mathrm{i}\kappa\bar{h}(x,x')m^{-1}\,\mathrm{e}^{-\mathrm{i}\alpha\gamma^5}\,,\end{aligned}\tag{6.2.65}$$

where the last line is obtained by collecting the results of the previous subsection and taking the limits in the order, they appear. We take the infinite spacetime limit first to ensure that the topological charge is properly captured, independently of where it could be accumulated through gauge transformations, which, as we have emphasized in Sec.5.3, depend strongly on the gauge and boundary conditions used, and only make sense as special saddle-points when the condition in Eq. (5.1.60) holds at infinity. The limits above are computed by assuming the numerator and denominator converge, meaning it is equivalent to take the limit of N and VT of the ratios instead of separately. We have also used the property, $\lim_{x\to\infty} I_m(\mathrm{i}x)/I_{m'}(\mathrm{i}x) = 1$, of the Bessel functions, which we can colloquially reword as, all modified Bessel functions of the first kind, I_m, tend to the same function for large imaginary argument, that is they can be considered independent of their order m. This property also holds for real positive arguments, so the same conclusion follows from a Euclidean point of view. The property leads to geometric series in Eqs. (6.2.61) and (6.2.63) which cancel each other for almost all values of $(\alpha+\theta)$. For cases where $(\alpha+\theta) = 2\pi q$ with $q\in\mathbb{Q}$, the partial sums will often take the value zero and the expressions must be deal with more care. We suggest for the vanishing partial sums with upper limit N, consider taking the limit towards the rational point in a sufficiently small neighborhood such that it contains no rational numbers of the form p/N with p relative prime to N. The last point to make concerning Eq. (6.2.65) is that even in the massless limit, we obtain a finite non-perturbative correction given by the last term since κ contains a factor of m, which cancels the overall dependence on the mass of such term.
For the sake of comparison, we consider taking the limits of the sum over topological sectors and the spacetime volume in the inverse order, ignoring our arguments concerning the boundary conditions, we would have for the numerator

$$\begin{aligned}&\sum_{\bar{n},n\geq 0}\frac{1}{\bar{n}!n!}(-\mathrm{i}\kappa)^{\bar{n}+n}\,\mathrm{e}^{\mathrm{i}\Delta n(\alpha+\theta)}\Big[\mathrm{i}S_{\varnothing}(x,x')\,(VT)^{\bar{n}+n}\\ &\qquad\qquad+\bar{h}(x,x')(\bar{n}\,m^{-1}\,\mathrm{e}^{\mathrm{i}\alpha}P_{\mathrm{L}}+n\,m^{-1}\,\mathrm{e}^{-\mathrm{i}\alpha}P_{\mathrm{R}})\,(VT)^{\bar{n}+n-1}\Big]\\ &=\left[\mathrm{i}S_{\varnothing}(x,x')-\left(\mathrm{e}^{-\mathrm{i}\theta}P_{\mathrm{L}}+\mathrm{e}^{\mathrm{i}\theta}P_{\mathrm{R}}\right)\frac{\mathrm{i}\kappa}{m}\bar{h}(x,x')\right]\mathrm{e}^{-2\mathrm{i}\kappa VT\cos(\alpha+\theta)}\end{aligned}\tag{6.2.66}$$

and for the limit of the truncated partition function:

$$Z\xrightarrow{VT\to\infty}\sum_{n,\bar{n}}\frac{1}{n!\bar{n}!}(-\mathrm{i}\kappa VT)^{\bar{n}+n}\,\mathrm{e}^{\mathrm{i}\Delta n(\alpha+\theta)}=\mathrm{e}^{-2\mathrm{i}\kappa VT\cos(\alpha+\theta)}.\tag{6.2.67}$$

The expression above is usually interpreted as the projection onto the ground state of the theory which reveals the dependence of θ of the vacuum energy density. It can be read to be $E(\theta)/V = 2\kappa\cos\bar{\theta}$, with $\kappa > 0$ and is compatible with the pure-gauge traditional expression $E(\theta)/V = -2\kappa'\cos\theta$, with $\kappa' > 0$, when taking into account the computed expressions for the fermion fluctuations in Eqs.(6.1.33) and (6.1.45) and a shift in θ or α by an amount π.

We can compare the two expression obtained for the correlation functions, Eqs. (6.2.65) and (6.2.66), we observe the difference in the chiral structures therein. In the latter there is an opposite phase in front of each chirality while not in the former. The origin of the difference can be attributed to the leading contributions of the binomial sums coming from $|\Delta n| \ll \bar{n} + n$, in Eq. (6.2.58)– and hence in Eq. (6.2.65)– when $VT \to \infty$[166], which results in no phase difference between the $\bar{h}$ and the $\mathrm{i}S_\varnothing$ terms. We interpret this to mean that CP-violating effects over backgrounds where $|\Delta n| \ll \bar{n} + n$ muffled by the volume of spacetime.

The phases appearing in Eq. (6.2.65) are of particular relevance, as it can be seen from the background-free propagator piece, Eq. (6.1.41), the phases in the correlation function appear to be the same, in front of the mass as well as in front of $\bar{h}$. The consequence is that $\langle\psi(x)\bar{\psi}(x')\rangle$ does not violate CP.

Instanton effects are often introduced in effective field theories through the addition of a 't Hooft operator, which we described in Sec. 5.1[105, 132], we recall its modification

$$\mathcal{L} \to \mathcal{L} - \bar{\psi}(x)\Gamma\,\mathrm{e}^{\mathrm{i}\alpha\gamma^5}\psi(x)\,, \tag{6.2.68}$$

where Γ can be understood as a LEC to lowest order and has to be inferred from the high-energy theory. The result in Eq. (6.2.65) can be used for that after the issue of instanton size is addressed. In the one flavor setting, this is nothing else but an effective mass with the same exact phase as the one appearing in the Dirac operator. We shall see that within ChPT, the remaining phase can be removed through a field redefinition, hence displaying no CP-violating effects. This would be in agreement with the tight bounds on the nEDM[117] or the decay $\eta' \to 2\pi$[49].

The above phenomenological observations must be contrasted with the effective operator obtained if we exchanged the limits

$$\mathcal{L} \to \mathcal{L} + \bar{\psi}(x)\Gamma\,\mathrm{e}^{-\mathrm{i}\theta\gamma^5}\psi(x)\,, \tag{6.2.69}$$

which leads to a difference in phases between the one in the mass term and the one above and it cannot be removed using chiral rotations. That would mean that a fermion line is CP-odd. The parameters α and θ have been kept general throughout our derivation and follow the transformation rules corresponding to chiral rotations through an angle β and the axial anomaly,

$$\psi \to \mathrm{e}^{\mathrm{i}\beta\gamma^5}\psi, \qquad \bar{\psi} \to \bar{\psi}\,\mathrm{e}^{\mathrm{i}\beta\gamma^5}, \qquad \alpha \to \alpha - 2\beta, \qquad \theta \to \theta + 2\beta, \tag{6.2.70}$$

so the result in Eq. (6.2.68) is compatible with the associated Ward identities.

6.2.3 Generalization to many flavors

In this subsection we generalize the computation made before to the case of multiple flavors. We consider a theory with N_f Dirac fermions, ψ_i, transforming according to the fundamental representation of $SU(3)$, each with a complex mass parameterized by

$m_j\, \mathrm{e}^{\mathrm{i}\alpha_i\gamma^5}$ and we consider a $2N$-point correlation function

$$\left\langle \prod_{j=1}^{N} \psi_{\sigma(j)}\bar{\psi}_{\sigma(j)} \right\rangle = \frac{1}{Z}\int \mathcal{D}A \left(\prod_{k=1}^{N_f} \mathcal{D}\bar{\psi}_k \mathcal{D}\psi_k\right) \left(\prod_{j=1}^{N} \psi_{\sigma(j)}\bar{\psi}_{\sigma(j)}\right) \mathrm{e}^{\mathrm{i}S_{N_f}}\,, \tag{6.2.71}$$

where the spacetime points have been omitted, $\sigma : \mathbb{Z}_{N_f} \to \mathbb{Z}_{N_f}$ is an arbitrary function representing the choice of flavors, and S_{N_f} is the QCD action with N_f flavors. We compute the correlation function following the same procedure as before, by first considering the correlation for a fixed topological sector Δn, then summing over the different sectors and taking the $VT \to \infty$ at the end. We thus have

$$\begin{aligned}\left\langle \prod_{j=1}^{N} \psi_{\sigma(j)}\bar{\psi}_{\sigma(j)} \right\rangle_{\Delta n} = \begin{pmatrix}\text{free}\\ \text{dets}\end{pmatrix} \sum_{\substack{\bar{n},n\geq 0\\ n-\bar{n}=\Delta n}} \frac{1}{\bar{n}!n!}\int \mathscr{D}_{\bar{n}}\bar{c}\,\mathscr{D}_n c \left(\prod_{j=1}^{N} \mathrm{i}S^{\sigma(j)_{n,\bar{n}}}\right) \mathrm{e}^{\mathrm{i}\Delta n(\bar{\alpha}+\theta)} \\ \times \left[(-1)^{N_f} R\bar{\Theta}\, \mathrm{e}^{-S^{\mathrm{E}}_{k=1}}\right]^{(\bar{n}+n)},\end{aligned} \tag{6.2.72}$$

where $S^{\sigma(j)}_{n,\bar{n}}$ is a propagator as in Eq. (6.1.42) built up of modes of the field $\psi_\sigma(j)$, we have used Eq. (6.2.53), defined $\bar{\Theta} = \prod_{j=1}^{N_f} \Theta_j$ using Eq. (6.1.45) for each flavor and with

$$\bar{\alpha} = \arg\det \boldsymbol{M} = \sum_{j=1}^{N_f} \alpha_j, \tag{6.2.73}$$

where $\boldsymbol{M}$ is in general the mass matrix and the last equality holds for our parametrization. The partition function generalizes to

$$\begin{aligned} Z_{\Delta n} &= \begin{pmatrix}\text{free}\\ \text{dets}\end{pmatrix} \sum_{\substack{\bar{n},n\geq 0\\ n-\bar{n}=\Delta n}} \frac{1}{\bar{n}!n!}\int \mathscr{D}_{\bar{n}}\bar{c}\,\mathscr{D}_n c\; \mathrm{e}^{\mathrm{i}\Delta n(\bar{\alpha}+\theta)} \left[(-1)^{N_f} R\bar{\Theta}\, \mathrm{e}^{-S^{\mathrm{E}}_{k=1}}\right]^{(\bar{n}+n)} \\ &= \begin{pmatrix}\text{free}\\ \text{dets}\end{pmatrix} \sum_{\substack{\bar{n},n\geq 0\\ n-\bar{n}=\Delta n}} \frac{1}{\bar{n}!n!} (\mathrm{i}\bar{\kappa}VT)^{\bar{n}+n}\, (-1)^{N_f\Delta n}\; \mathrm{e}^{\mathrm{i}\Delta n(\bar{\alpha}+\theta)} \\ &= \begin{pmatrix}\text{free}\\ \text{dets}\end{pmatrix} I_{\Delta n}(2\mathrm{i}\bar{\kappa}VT)\, (-1)^{N_f\Delta n}\; \mathrm{e}^{\mathrm{i}\Delta n(\bar{\alpha}+\theta)}\,, \end{aligned} \tag{6.2.74}$$

where $\mathrm{i}\bar{\kappa} = \int \mathrm{d}\Omega\, J\bar{\Theta}R\, \mathrm{e}^{-S^{\mathrm{E}}_{k=1}}$ is the analogue of the single flavor κ in Eq. (6.2.59).
We comment now on the different terms that appear in the correlation function after we plug in the propagator Ansatz in Eq. (6.1.42) and perform the same average over locations and sizes as in the case of a single flavor. We identify three kinds of terms:

- empty background terms: have only products of $\mathrm{i}S_\varnothing$
- diagonal terms: products of zero-modes from the same (anti-)instanton, and possible $\mathrm{i}S_\varnothing$ factors
- off-diagonal terms: mixed products of zero-modes belonging to different (anti-) instantons, and possible $\mathrm{i}S_\varnothing$ factors.

For the empty background terms, the integration over locations may be carried out and leads to a contribution which is simply the product $Z_{\Delta n}\prod_j \mathrm{i}S_{\varnothing}^{\sigma(j)}$. Diagonal terms get a factor of $(\bar{n})$ n from the summation over (anti-)instantons as in the single flavor case, and schematically these terms are for the case of a shared instanton,

$$\left(\prod_{m=1}^{p}\mathrm{i}S_{\sigma_p(m),\varnothing}\right)\left(\prod_{j=1}^{q}\frac{P_{\mathrm{R}\sigma_q(j)}}{m_{\sigma_q(j)}\,\mathrm{e}^{\mathrm{i}\alpha_{\sigma_q(j)}}}\right)\bar{h}_q\sum_{\substack{\bar{n},n\geq 0\\ n-\bar{n}=\Delta n}}\frac{n}{\bar{n}!n!}\,(VT)^{\bar{n}+n-1}(\mathrm{i}\bar{\kappa})^{\bar{n}+n}\,(-1)^{N_f\Delta n}\,\mathrm{e}^{\mathrm{i}\Delta n(\bar{\alpha}+\theta)}$$

$$=\left(\prod_{m=1}^{p}\mathrm{i}S_{\sigma_p(m),\varnothing}\right)\left(\prod_{j=1}^{q}\frac{P_{\mathrm{R}\sigma_q(j)}}{m_{\sigma_q(j)}\,\mathrm{e}^{\mathrm{i}\alpha_{\sigma_q(j)}}}\right)\mathrm{i}\bar{\kappa}\bar{h}_q I_{\Delta n-1}(2\mathrm{i}\bar{\kappa}VT)\,(-1)^{N_f\Delta n}\,\mathrm{e}^{\mathrm{i}\Delta n(\bar{\alpha}+\theta)}\,, \tag{6.2.75}$$

where $\sigma_p:\mathbb{Z}_p\to\mathbb{Z}_p$ and $\sigma_q:\mathbb{Z}_q\to\mathbb{Z}_q$ such that $p+q=N$ and agree with the initial σ in Eq. (6.2.72), while $\bar{h}_q$ is the average over the q zero-modes' locations and sizes, capturing the possible overlaps. If we consider our proposal for the computation of the correlation functions, i.e. we sum over topological sectors first and then $VT\to\infty$, we have from the diagonal terms:

$$\left\langle\prod_{j=1}^{N}\psi_{\sigma(j)}\bar{\psi}_{\sigma(j)}\right\rangle\supset\mathrm{i}\bar{\kappa}\left(\prod_{m=1}^{p}\mathrm{i}S_{\sigma_p(m),\varnothing}\right)\left(\prod_{j=1}^{q}\frac{P_{\mathrm{R}\sigma_q(j)}}{m_{\sigma_q(j)}\,\mathrm{e}^{\mathrm{i}\alpha_{\sigma_q(j)}}}\right)\bar{h}_q. \tag{6.2.76}$$

We can see the exponential with phase $\bar{\alpha}+\theta$ cancels and as in the single flavor case, the remaining phases in the correlation function are determined from those in the mass matrix.

In the case of N_f flavors, the transformations caused by performing a chiral rotation by an angle β simultaneously on all fermions is

$$\psi_j\to\mathrm{e}^{\mathrm{i}\beta\gamma^5}\psi_j,\quad \bar{\psi}_j\to\bar{\psi}_j\,\mathrm{e}^{\mathrm{i}\beta\gamma^5}\iff\alpha_j\to\alpha_j-2\beta,\quad\theta\to\theta+2N_f\beta\,, \tag{6.2.77}$$

so that effective operators related to correlation functions from the high-energy theory should comply with the above.

The 't Hooft vertex that we have discussed, corresponds to diagonal terms of an $2N_f$-point correlation function with $p=0$ and $q=N_f$, leading to effective vertices

$$\mathcal{L}\to\mathcal{L}-\Gamma_{N_f}\,\mathrm{e}^{-\mathrm{i}\bar{\alpha}}\prod_{j=1}^{N_f}(\bar{\psi}_j P_{\mathrm{L}}\psi_j)-\Gamma_{N_f}\,\mathrm{e}^{\mathrm{i}\bar{\alpha}}\prod_{j=1}^{N_f}(\bar{\psi}_j P_{\mathrm{R}}\psi_j), \tag{6.2.78}$$

where Γ_{N_f} are constants to lowest order. We observe that the phases appearing in front of the operators can be removed again by a chiral rotation as we saw in the single flavor case but we point out, this would not be the case if our prescription for taking the $VT\to\infty$ is not followed. Concerning the mass factors $m_{\sigma_q(j)}^{-1}$, they cancel exactly with those from the fermion zero modes in $\bar{\Theta}$.

Other diagonal terms with $N<N_f$ produce effective interactions proportional to masses and involving less fermions, however compatible with the transformation in Eq. (6.2.77), (see [169]). Off-diagonal terms involve different instanton and can be categorized by specifying the number of propagators associated to a given (anti-)instanton. The different ways in which this can happen is a combinatorial factor $\binom{n}{m}$ where m is the different

instantons involved. For $m = 1$ for example, we recover what we have said about the diagonal terms. An off-diagonal contribution from m different instantons is then

$$\sum_{\substack{\bar{n},n\geq 0\\ n-\bar{n}=\Delta n}} \frac{1}{\bar{n}!n!}\binom{n}{m}(VT)^{\bar{n}+n-m}(\mathrm{i}\bar{\kappa})^{\bar{n}+n}(-1)^{N_f\Delta n}\,\mathrm{e}^{\mathrm{i}\Delta n(\bar{\alpha}+\theta)} = \frac{(\mathrm{i}\bar{\kappa})^m}{m!}I_{\Delta n-m}(2\mathrm{i}\bar{\kappa}VT)(-1)^{N_f\Delta n}\,\mathrm{e}^{\mathrm{i}\Delta n(\bar{\alpha}+\theta)}\,. \tag{6.2.79}$$

These however appear with a higher power of $\mathrm{e}^{-S^{\mathrm{E}}_{k=1}}$, through $\bar{\kappa}$, and are sub-leading. Taking the ratio with the partition function, the limit $VT \to \infty$ and summing over topological sectors, we lose the θ dependence and in general, we obtain a modified Bessel function multiplied by a certain power of $\bar{\kappa}$ and inverse powers of VT which is the reason why this type of terms are not the dominant ones.
We finish this subsection with some remarks regarding the full partition function. With our construction, the full partition function is to be computed using the formula

$$Z = \lim_{\substack{N\to\infty\\ N\in\mathbb{N}}} \lim_{VT\to\infty} \sum_{\Delta n=-N}^{N} Z_{\Delta n}, \tag{6.2.80}$$

with $Z_{\Delta n}$ as in Eq. (6.2.63) and where the limits are to be computed strictly from right to left. When considering an arbitrarily large spacetime, $VT \to \infty$, we obtain asymptotically

$$Z \sim I_0(2\mathrm{i}\bar{\kappa}VT) \lim_{\substack{N\to\infty\\ N\in\mathbb{N}}} \sum_{|\Delta n|\leq N} \mathrm{e}^{\mathrm{i}\Delta n(\bar{\alpha}+\theta+N_f\pi)}\,. \tag{6.2.81}$$

The above corresponds only formally to a Dirac delta distribution on $\bar{\alpha} + \theta + N_f\pi$ and is maximal when $\theta = -\bar{\alpha} - N_f\pi$ which agrees with the arguments in [170]. However such statement is only formal as the sum results in Z not being analytic. In contrast the partition function usually found in the literature is

$$\lim_{VT\to\infty} \lim_{\substack{N\to\infty\\ N\in\mathbb{N}}} \sum_{\Delta n=-N}^{N} Z_{\Delta n} = \mathrm{e}^{2\mathrm{i}\bar{\kappa}VT\cos(\bar{\alpha}+\theta+N_f\pi)}, \tag{6.2.82}$$

whose Euclidean version is maximal at $\theta = -\bar{\alpha} - N_f\pi$ and remains analytic. We nonetheless see no issues in this regard, given that the partition function itself is not observable and the correlation functions computed using are well defined in the limits we suggest. Some more comments around this point where already made in[137] where it is seen that θ's periodicity is connected to non-analytical behavior of Z. In the present context we have already recognized that such property of θ comes from the homotopic classification of gauge transformations. We will later elaborate on the consequences of these results for experimental observables where we will refer back to the analytic properties indicated here.

Expectation values for arbitrary operator

We can extend the methods used for the computation of correlation functions to expectation values of other types of operators, including possibly loop corrections. We compute the vacuum energy density from the perspective of the stress-energy tensor.
For illustration purposes, we need only consider a single flavor model of QCD. Let us consider the expectation value of some operator $\mathcal{O}$ and use the path integral over a dilute

instanton gas as we have done before to write down the expectation value of the operator $\mathcal{O}$ in a fixed topological sector:

$$\begin{aligned}&\langle\mathcal{O}(z_1,\dots,z_t)\rangle_{\Delta n}\\&=\sum_{\substack{\bar n,n\geq 0\\ n-\bar n=\Delta n}}\frac{1}{\bar n!n!}\int\mathscr{D}_{\bar n}\bar c\,\mathscr{D}_n c\,(-R\Theta\,\mathrm{e}^{-S^{\mathrm{E}}_{k=1}})^{\bar n+n}\,\mathrm{e}^{\mathrm{i}\Delta n(\alpha+\theta)}\int\mathrm{d}^4z_1'\cdots\mathrm{d}^4z_u'\mathcal{F}\left(z_1',\dots,z_u';z_1,\dots,z_t\right),\end{aligned}$$

where $\mathcal{F}$ is a sum of products of Green's functions, and possibly their derivatives, over the multi-instanton background, which can be pictured as Feynman diagrams with propagators on the background. These Green's functions will depend on two points and can in turn be approximated with expressions resembling Eq. (6.1.42), i.e. the superposition of a background-free part and peaked terms at the locations of background (anti-)instantons and may include other fields other than fermions, for which we also express the propagator in the analogous way. We also denote by z_i' spacetime variables appearing in loops and proceed to perform the integration over collective coordinates to get

$$\begin{aligned}&\langle\mathcal{O}(z_1,\dots,z_t)\rangle_{\Delta n}\\&\quad=\sum_{\substack{\bar n,n\geq 0\\ n-\bar n=\Delta n}}\frac{(-1)^{n+\bar n}}{\bar n!n!}(\mathrm{i}\kappa)^{\bar n+n}\,\mathrm{e}^{\mathrm{i}\Delta n(\alpha+\theta)}\int\mathrm{d}^4z_1'\cdots\mathrm{d}^4z_u'\Big[\mathcal{G}_\varnothing\left(z_1',\dots,z_u';z_1,\dots,z_t\right)(VT)^{\bar n+n}\\&\qquad+\left(\bar n\,\bar{\mathcal{G}}_{\bar 1}\left(z_1',\dots,z_u';z_1,\dots,z_t\right)+n\,\bar{\mathcal{G}}_1\left(z_1',\dots,z_u';z_1,\dots,z_t\right)\right)(VT)^{\bar n+n-1}\Big],\end{aligned}$$

where the expansion is in terms of factors of VT and we have introduced a point function accounting for the background-free part $\mathcal{G}_\varnothing$ and one-instanton contribution functions $\bar{\mathcal{G}}_1$ and $\bar{\mathcal{G}}_{\bar 1}$ accounting for the possible interaction with a single (anti-)instanton. Concretely, the latter are the result of averaging over collective coordinates contributions products of background-free propagator with a single zero-mode projector insertion. Contributions from terms with more than one (anti-)instanton interaction are suppressed exponentially and have been neglected. We are now able to perform the sum over n and $\bar n$ to obtain

$$\begin{aligned}&\langle\mathcal{O}(z_1,\dots,z_t)\rangle_{\Delta n}\\&\quad=\int\mathrm{d}^4z_1'\cdots\mathrm{d}^4z_u'\left[\left(I_{\Delta n+1}(2\mathrm{i}\kappa VT)\bar{\mathcal{G}}_{\bar 1}+I_{\Delta n-1}(2\mathrm{i}\kappa VT)\bar{\mathcal{G}}_1\right)\mathrm{i}\kappa+I_{\Delta n}(2\mathrm{i}\kappa VT)\,\mathcal{G}_\varnothing\right]\\&\qquad\times(-1)^{\Delta n}\,\mathrm{e}^{\mathrm{i}\Delta n(\alpha+\theta)}\,.\end{aligned}\tag{6.2.83}$$

where the arguments of $\mathcal{G}_\varnothing,\bar{\mathcal{G}}_1$ and $\bar{\mathcal{G}}_{\bar 1}$ have not been written explicitly.
We focus now on computing the limit $VT\to\infty$ first. We do this by means of the asymptotic expansion for modified Bessel functions,

$$I_n(x)\sim\frac{\mathrm{e}^x}{\sqrt{2\pi x}}\quad\text{for}\quad|x|\to\infty\quad\text{and}\quad|\arg(x)|<\frac{\pi}{2}\,,\tag{6.2.84}$$

which holds for our analytic continuation, $T\,\mathrm{e}^{-\mathrm{i}0^+}$. Using the expansion above, without including sub-leading terms, we can finish the computation of the expectation value

$$\begin{aligned}\langle\mathcal{O}(z_1,\dots,z_t)\rangle&=\lim_{\substack{N\to\infty\\ N\in\mathbb{N}}}\lim_{VT\to\infty}\frac{\displaystyle\sum_{\Delta n=-N}^{N}\langle\mathcal{O}(z_1,\dots,z_t)\rangle_{\Delta n}}{\displaystyle\sum_{\Delta n=-N}^{N}Z_{\Delta n}}\\&=\int\mathrm{d}^4z_1'\cdots\mathrm{d}^4z_u'\left[\mathcal{G}_\varnothing+\mathrm{i}\kappa(\bar{\mathcal{G}}_{\bar 1}+\bar{\mathcal{G}}_1)\right].\end{aligned}\tag{6.2.85}$$

As in all previous cases, the dependence on the topological sector cancels against the partition function. Recall $\mathcal{O}$ is kept general and may contain chiral phases. These can only come from fermion mass terms and are of the form $\mathrm{e}^{\pm \mathrm{i}\alpha}$. However, in the absence of other sources of CP violation, the α phases can be removed through a chiral rotation. For reference, if we were to exchange the sum over topological sectors and the $VT \to \infty$ limit, we recover possible CP-violating observables

$$\langle \mathcal{O}(z_1, \ldots, z_t) \rangle = \int \mathrm{d}^4 z_1' \cdots \mathrm{d}^4 z_u' \left[\mathrm{i}\kappa\, \bar{\mathcal{G}}_{\bar{1}}\, \mathrm{e}^{-\mathrm{i}(\theta+\alpha)} + \mathrm{i}\kappa\, \bar{\mathcal{G}}_1\, \mathrm{e}^{\mathrm{i}(\theta+\alpha)} + \mathcal{G}_\varnothing \right] , \tag{6.2.86}$$

which exhibits the $\bar{\theta}$-invariant which does not change under chiral rotations as explained in the previous chapter.

We end the present subsection by illustrating how these general expectation values agree and thus can describe the effects of 't Hooft vertices, Eq. (6.2.78). If we consider an operator containing fermion insertions with well enough separated spacetime points z_i', such that we do not incur in large overlaps, $|z_i' - z_j'|^2 \gg \rho^2$, or equivalently if the loop integrals are not too sensitive about ultraviolet effects, the function $\mathcal{F}$ can be well approximated by using single interactions with the instantons while neglecting multiple propagators interacting with the same (anti-)instanton. The functions appearing in Eq. (6.2.83) have the following structure:

$\mathcal{G}_0 = \mathcal{F}(\{\mathrm{i}S^{(i)}\}, ...)$ where all propagators are of the type $\mathrm{i}S_\varnothing$,

$\bar{\mathcal{G}}_{\bar{1}} = \sum_j \mathcal{F}(\{\mathrm{i}S^{(i)}\}, ...)$ where each summand contains one term of the form $\frac{\bar{h}}{m\, \mathrm{e}^{-\mathrm{i}\alpha}} P_{\mathrm{L}}$ all others being $\mathrm{i}S_\varnothing$

$\bar{\mathcal{G}}_1 = \sum_j \mathcal{F}(\{\mathrm{i}S^{(i)}\}, ...)$ where each summand contains one term of the form $\frac{\bar{h}}{m\, \mathrm{e}^{\mathrm{i}\alpha}} P_{\mathrm{R}}$ all others being $\mathrm{i}S_\varnothing$,

where $\bar{h}$ is as in Eq. (6.2.57). Independently of how the limits are taken we arrive to an expression to lowest order in κ which is

$$\langle \mathcal{O}(z_1, \ldots, z_t) \rangle \approx \int \mathrm{d}^4 z_1' \cdots \mathrm{d}^4 z_u' \left[\mathcal{G}_0 + \mathcal{G}_1 \right] , \tag{6.2.87}$$

where $\mathcal{G}_0$ comes from the background-free part and we have collected the (anti-)instanton effects in $\mathcal{G}_1$ which is affected by the order of the limits. With $VT \to \infty$ first we have

$\mathcal{G}_{\bar{1}} = \sum_j \mathcal{F}(\{\mathrm{i}S^{(i)}\}, ...)$ where each summand contains one term of the form $\frac{\mathrm{i}\kappa\bar{h}}{m}\, \mathrm{e}^{-\mathrm{i}\alpha\gamma^5}$ all others being $\mathrm{i}S_\varnothing$,

while summing Δn up to infinity first we obtain

$\mathcal{G}_{\bar{1}} = \sum_j \mathcal{F}(\{\mathrm{i}S^{(i)}\}, ...)$ where each summand contains one term of the form $\frac{\mathrm{i}\kappa\bar{h}}{m}\, \mathrm{e}^{\mathrm{i}\theta\gamma^5}$ all others being $\mathrm{i}S_\varnothing$.

The above can be obtained through the effective operators given in the single-flavor case Eqs. (6.2.68) and (6.2.69), but there is no reason to expect they may work for higher orders of κ. If we were to compute such, we would need to consider again using for a fixed topological sector first, Eq. (6.2.83). If the spacetime points were to be taken too close to each other, the overlaps neglected in Eq. (6.2.83), from multi-instanton interaction, must also be included. Following that same reasoning, we understand the 't Hooft effective vertex, Eq. (6.2.78), as only capturing the contributions to the lowest order in κ or equivalently with at most N_f propagators overlapping with the instanton.

Comments on boundary conditions

Before moving to alternative arguments supporting the conclusions above, we make some comments concerning the boundary conditions. It is essential that we recognize that when considering an infinite spacetime, the only way to distinguish special gauge field configurations is by imposing vanishing fields at the infinity. As we have seen, mathematically, field configurations that vanish at infinity, modulo gauge transformations, are automatically classified into their homotopy classes. The homotopy classes are discretized when the gauge group is $SU(N)$ with $N \geq 2$ and the asymptotic region is diffeomorphic to S^3. On the contrary, if we consider a field theory in a finite spacetime region, there are no natural boundary conditions to be chosen. Therefore field configurations are no longer obviously classified by integers and θ might not even correspond to a periodic variable.

Different geometries can also present a classification of gauge field according to winding numbers, as long as the spacetime has a non-trivial topology, e.g., for a four-dimensional torus[171], such that gluing functions (see comments before Eq. (5.3.113)) between patches live in a space homeomorphic to the gauge group. The geometrical viewpoint portrays Δn as an invariant with no reference to Chern-Simons number and transitions of prevacua. Under this perspective, there is no principle telling us to consider weighted sums of topological sectors. Instead, we see a fixed Δn is a world of its own, with its own equations of motion valid within the sector. This leads, for example, to an nEDM which is Δn dependent but $\bar{\theta}$ independent, and to local interactions to be visible only within the given sector. We can therefore draw parallels between our prescription for taking limits and theories over compact spacetimes with $\Delta n = 0$.

In the following section, we adopt a different point of view, where we pay special attention to the boundary conditions and reach the same conclusions. In the context of the saddle-point expansion and the path integral, it seems inevitable to impose vanishing asymptotic boundary conditions.

6.3 Correlation functions via Cluster Decomposition Principle

In order to support the aforementioned conclusions, we adopt a top to bottom approach that does not rely on expansions about a dilute instanton gas. Here we illustrate how considering the effects of the cluster decomposition principle (CDP), the Index Theorem and parity lead to constraints to correlation functions which show how chiral phases are aligned when the same order of limits is applied as in the previous section. We work exclusively in Euclidean space and consider N_f flavors throughout this section.

We recall an argument by Weinberg[21], in which we can view how the phase $\mathrm{i}\Delta n\theta$ comes into play in a natural way if we use a path integral version of the CDP. Colloquially, the principle says that physics is to remain local, in the sense that expectation values of products of operators evaluated at points far away from each other should factorize into a product of expectation values corresponding to each region. A rigorous version of the theorem in axiomatic QFT is proven in[172]. Let us then consider computing the vacuum expectation value of an operator $\mathcal{O}$ via the path integral formalism in a volume $\Omega = VT$, which we later take to be infinite, and by summing over all topological sectors weighed by

an a priori unknown function $f(\Delta n)$ so that the action does not include any θ-term:

$$\langle \mathcal{O} \rangle = \lim_{\substack{N\to\infty \\ N\in\mathbb{N}}} \lim_{\Omega\to\infty} \frac{\sum_{\Delta n=-N}^{N} f(\Delta n) \int \mathcal{D}_{\Delta n}[\phi]\, \mathcal{O}\ \mathrm{e}^{-S_\Omega[\phi]}}{\sum_{\Delta n=-N}^{N} f(\Delta n) \int \mathcal{D}_{\Delta n}[\phi]\ \mathrm{e}^{-S_\Omega[\phi]}}, \tag{6.3.88}$$

where $\mathcal{D}_{\Delta n}$ denotes that the integration is done restricted to gauge field configurations with winding number Δn resulting from their vanishing at the boundary of the spacetime region $\partial\Omega$ and the subscript under the action specifies the spacetime region of integration. We consider two different regions of spacetime Ω_1 and Ω_2, which we call subvolumes and such that $\Omega = \Omega_1 \cup \Omega_2$ as in Figure 6.1. The winding number Δn then comes from the addition of the would-be winding numbers of the two subvolumes, i.e. $\Delta = \Delta n_1 + \Delta n_2$ with Δn_i the contribution from subvolume Ω_i to the (global) winding number. If we evaluate the operator under consideration, $\mathcal{O}_1$, only on spacetime points lying in Ω_1, we can split the integration as follows

$$\langle \mathcal{O}_1 \rangle = \lim_{\substack{N_2\to\infty \\ N_2\in\mathbb{N}}} \lim_{\substack{N_1\to\infty \\ N_1\in\mathbb{N}}} \lim_{\Omega\to\infty} \frac{\sum_{\substack{\Delta n_1=-N_1 \\ \Delta n_2=-N_2}}^{N_1,N_2} f(\Delta n_1+\Delta n_2) \int \mathcal{D}_{\Delta n_1}[\phi]\, \mathcal{O}_1\ \mathrm{e}^{-S_{\Omega_1}[\phi]} \int \mathcal{D}_{\Delta n_2}[\phi]\ \mathrm{e}^{-S_{\Omega_1}[\phi]}}{\sum_{\substack{\Delta n_1=-N_1 \\ \Delta n_2=-N_2}}^{N_1,N_2} f(\Delta n_1+\Delta n_2) \int \mathcal{D}_{\Delta n_1}[\phi]\ \mathrm{e}^{-S_{\Omega_1}[\phi]} \int \mathcal{D}_{\Delta n_2}[\phi]\ \mathrm{e}^{-S_{\Omega_2}[\phi]}}. \tag{6.3.89}$$

Although there is nothing telling us the Δn_1 and Δn_2 must be integers, we abuse the notation and use summation symbol and neglect possible non-trivial contributions happening at the boundary of the two subvolumes.

If we are to comply with the CDP the path integral should factorize in such a way that the fluctuations of the subvolume Ω_2 will not matter. A glance at the equation above suggest that for such contributions to factor out the weighing functions should satisfy

$$f(\Delta n_1 + \Delta n_2) = f(\Delta n_1) f(\Delta n_2). \tag{6.3.90}$$

This means $f(x) = a^x$ for some a. This, together with the assumption that θ must be an angular variable, to match the more common vacuum structure arguments, means

$$f(\Delta n) = \mathrm{e}^{\mathrm{i}\Delta n\theta} \tag{6.3.91}$$

for some angular variable θ. This provides us with yet another view on how the θ-vacuum can be understood.

6.3.1 CDP, Index Theorem and Parity as constraints for Z

It is possible to further derive constraints for the truncated partition function using this factorization idea. The denominator of Eq. (6.3.88) corresponds to the partition function of the system truncated to sector N and we recall the full partition function over volume

Ω[1], is

$$Z(\Omega, N) = \sum_{\Delta n=-N}^{N} Z_{\Delta n}(\Omega), \quad \text{where} \quad Z_{\Delta n}(\Omega) = f(\Delta n) \int \mathcal{D}_{\Delta n}[\phi]\ \mathrm{e}^{-S_\Omega[\phi]}. \tag{6.3.92}$$

We can use the factorization in Eq. (6.3.89) to rewrite the truncated partition function as a product of two sub-partition functions, one for each region, and in terms of a sum over on of the partial winding numbers, say Δn_1:

$$Z_{\Delta n}(\Omega) = f(\Delta n) \int_{\Delta n} \mathcal{D}[\phi]\ \mathrm{e}^{-S_\Omega[\phi]} = \sum_{\Delta n_1=-\infty}^{\infty} f(\Delta n) \int \mathcal{D}_{\Delta n_1}[\phi]\ \mathrm{e}^{-S_{\Omega_1}[\phi]} \int_{\Delta n-\Delta n_1} \mathcal{D}\phi\ \mathrm{e}^{-S_{\Omega_2}[\phi]}, \tag{6.3.93}$$

The property in Eq. (6.3.90) leads us to the following property at the level of partition functions

$$Z_{\Delta n}(\Omega = \Omega_1 + \Omega_2) = \sum_{\Delta n_1=-\infty}^{\infty} Z_{\Delta n_1}(\Omega_1) Z_{\Delta n-\Delta n_1}(\Omega_2), \tag{6.3.94}$$

where

$$Z_{\Delta n}(\Omega) = \mathrm{e}^{\mathrm{i}\Delta n\theta} z_{\Delta n}(\Omega), \quad \text{and} \quad z_{\Delta n}(\Omega) \equiv \int \mathcal{D}_{\Delta n}\phi\ \mathrm{e}^{-S_X[\phi]}. \tag{6.3.95}$$

The Eq. (6.3.94) is to be understood as a reflection of the CDP for the truncated partition functions and will allow us to constrain the path integral factor, $z_{\Delta n}$, of the partition functions.

Let us first factor out any possible remaining phases in $z_{\Delta n}$. Phases can only come from fermion determinants, since we know that the Euclidean gauge field fluctuations give a real functional determinant. For fixed winding numbers Δn of the background, we can invoke Atiyah-Singer index theorem to see that fermion modes come always in pairs with conjugated eigenvalues, leading to real contributions, and that possible phases may only come from zero-modes, independent of the specific details of the background other than its topology. If we parameterize the mass of the j-th fermion as

$$m_j\, \mathrm{e}^{\mathrm{i}\alpha_j\gamma_5} = m_j\, \mathrm{e}^{\mathrm{i}\alpha_j} P_{\mathrm{R}} + m_j\, \mathrm{e}^{-\mathrm{i}\alpha_j} P_{\mathrm{L}} \equiv \mathfrak{m} P_{\mathrm{R}} + \mathfrak{m}^* P_{\mathrm{L}}, \tag{6.3.96}$$

the topological sector Δn will acquire a phase proportional to Δn and $\bar{\alpha}$ and we can now simply examine the modulus of $z_{\Delta n}$, i.e.

$$z_{\Delta n}(\Omega) = \mathrm{e}^{\mathrm{i}\Delta n\bar{\alpha}} \tilde{z}_{\Delta n}(\Omega), \quad \tilde{z}_{\Delta n}(\Omega) \in \mathbb{R}. \tag{6.3.97}$$

We can further simplify the relation in Eq. (6.3.94) using the factorization above

$$\tilde{z}_{\Delta n}(\Omega_1 + \Omega_2) = \sum_{\Delta n_1=-\infty}^{\infty} \tilde{z}_{\Delta n_1}(\Omega_1) \tilde{z}_{\Delta n-\Delta n_1}(\Omega_2). \tag{6.3.98}$$

The modulus coincides with the fluctuation determinant for real masses, which can be seen simply by taking $\alpha_o i \to 0$. With the assumption that parity relates sectors with opposite charges Δn, we have that for real masses

$$\tilde{z}_{-\Delta n}(\Omega) = \tilde{z}_{\Delta n}(\Omega). \tag{6.3.99}$$

[1]We use such symbol to denote the set of points in the region and its size indistinguishably and must be understood by context

With the objective of finding $\tilde{z}_{\Delta n}$'s satisfying Eq. (6.3.98), consider the limit of 0 volume, from which we can deduce

$$\tilde{z}_{\Delta n}(0) = \sum_{\Delta n_1=-\infty}^{\infty} \tilde{z}_{\Delta n_1}(0)\tilde{z}_{\Delta n-\Delta n_1}(0) \Rightarrow \tilde{z}_{\Delta n}(0) = \delta_{\Delta n 0}, \tag{6.3.100}$$

after which we propose the following form of $\tilde{z}_{\Delta n}$:

$$\tilde{z}_{\Delta n}(\Omega) = \tilde{z}_{|\Delta n|}(\Omega) = \Omega^{|\Delta n|} f_{|\Delta n|}(\Omega^2), \quad f_{|\Delta n|}(0) \neq 0, \tag{6.3.101}$$

where the dependence on $|\Delta n|$ enforces Eq. (6.3.99) and the factor $\Omega^{|\Delta n|}$ ensures that the condition in Eq. (6.3.100) is satisfied which also fixes $f_0(0) = 1$. We can obtain a second condition for $\tilde{z}_{\Delta n}$ through its derivative at zero volume, viz.

$$\tilde{z}'_{\Delta n}(\Omega) = |\Delta n|\, \Omega^{|\Delta n|-1} f_{|\Delta n|}(\Omega^2) + 2\, \Omega^{|\Delta n|+1} f'_{|\Delta n|}(\Omega^2), \tag{6.3.102}$$

and thus

$$\tilde{z}'_{\Delta n}(0) = \delta_{|\Delta n|1}\beta, \tag{6.3.103}$$

for some coefficient $f_1(0) \equiv \beta$. We can obtain a recursive relation for the derivative if we differentiate Eq. (6.3.98) with respect to Ω_1 and evaluate at $\Omega_1 = 0$:

$$\tilde{z}'_{\Delta n}(\Omega_1 + \Omega_2) = \sum_{\Delta n_1=-\infty}^{\infty} \tilde{z}'_{\Delta n_1}(\Omega_1)\tilde{z}_{\Delta n-\Delta n_1}(\Omega_2), \tag{6.3.104}$$

then

$$\tilde{z}'_{\Delta n}(\Omega_2) = \sum_{\Delta n_1=-\infty}^{\infty} \tilde{z}'_{\Delta n_1}(0)\, \tilde{z}_{\Delta n-\Delta n_1}(\Omega_2), \tag{6.3.105}$$

and plugging in the condition in Eq. (6.3.103) we arrive to

$$\tilde{z}'_{\Delta n}(\Omega_2) = \beta(\, \tilde{z}_{\Delta n+1}(\Omega_2) + \tilde{z}_{\Delta n-1}(\Omega_2)). \tag{6.3.106}$$

With the expression above it is possible to compute derivatives of arbitrary order in terms of the initial function. If we relabel Ω_2 by simply Ω, the formula for the derivative of order m is

$$\left.\frac{\mathrm{d}^m \tilde{z}_{\Delta n}}{\mathrm{d}\Omega^m}\right|_{\Omega} = \beta^m \sum_{\ell=0}^{m} \binom{m}{\ell} \tilde{z}_{\Delta n-m+2\ell}(\Omega). \tag{6.3.107}$$

This allows us to obtain all derivatives at $\Omega = 0$ by employing Eq. (6.3.103):

$$\left.\frac{\mathrm{d}^m \tilde{z}_{\Delta n}}{\mathrm{d}\Omega^m}\right|_{\Omega=0} = \begin{cases} \beta^m \binom{m}{\frac{m-\Delta n}{2}} & \text{if } m-\Delta n \text{ is even} \\ 0 & \text{otherwise.} \end{cases} \tag{6.3.108}$$

For an analytic $\tilde{z}_{\Delta n}$ we can use a Taylor expansion to reconstruct the function using the derivatives at 0 volume:

$$\tilde{z}_{\Delta n}(\Omega) = \sum_{m=0}^{\infty} \frac{1}{m!} \left.\frac{\mathrm{d}^m \tilde{z}_{\Delta n}}{\mathrm{d}\Omega^m}\right|_{\Omega=0} \Omega^m. \tag{6.3.109}$$

rewriting the series expansion with the condition that $m = \Delta n + 2\ell$ for $\ell = 0, 1, 2, \cdots$ we have

$$\tilde{z}_{\Delta n}(\Omega) = \sum_{\ell=0}^{\infty} \frac{1}{(|\Delta n| + 2\ell)!} \beta^{|\Delta n|+2\ell} \binom{|\Delta n| + 2\ell}{\ell} \Omega^{|\Delta n|+2\ell}, \tag{6.3.110}$$

which can be identified as the series of a modified Bessel function

$$\tilde{z}_{\Delta n}(\Omega) = \sum_{\ell=0}^{\infty} \frac{1}{\ell!(|\Delta n| + \ell)!} \left(\frac{2\beta\,\Omega}{2}\right)^{|\Delta n|+2\ell} = I_{\Delta n}(2\beta\Omega). \tag{6.3.111}$$

We can write down now the truncated partition function

$$Z_{\Delta n}(\Omega) = \mathrm{e}^{\mathrm{i}\theta\Delta n} z_{\Delta n}(\Omega) = \mathrm{e}^{\mathrm{i}(\theta+\bar{\alpha})\Delta n} \tilde{z}_{\Delta n}(\Omega) = I_{\Delta n}(2\beta\Omega)\ \mathrm{e}^{\mathrm{i}(\theta+\bar{\alpha})\Delta n}, \tag{6.3.112}$$

and verify its agreement with the dilute instanton gas computation through a redefinition of $\theta \to \theta + N_f\pi$, and that $I_{\Delta n}$ satisfies the correct parity requirement. It is possible to verify that indeed the modified Bessel functions of the first kind observe the condition

$$I_{\Delta n}(2\beta(\Omega_1 + \Omega_2)) = \sum_{\Delta n_1=-\infty}^{\infty} I_{\Delta n_1}(2\beta\Omega_1) I_{\Delta n - \Delta n_1}(2\beta\Omega_2), \tag{6.3.113}$$

which we have related here with the CDP.
In the last piece of the present subsection we want to derive the divergence of currents associated to the mass terms in order to compare these with the result using a dilute instanton gas and be able to corroborate whether there is a remaining θ dependence or not. For that purpose recall β still depends on quark masses. However we have that $\tilde{z}_{\Delta n}$ is real and may have powers of $m_j = \sqrt{\mathfrak{m}_j \mathfrak{m}_j^*}$ from zero-modes and powers of $m_j^2 = \mathfrak{m}_j \mathfrak{m}_j^*$ from chiral pairs of non-zero modes. This means that β in Eq. (6.3.112) can only depend on the products $\mathfrak{m}_j \mathfrak{m}_j^*$, so that $\beta = \beta(\mathfrak{m}_j \mathfrak{m}_j^*)$. We can rewrite the sum of phases of the quark masses as

$$\bar{\alpha} = -\frac{\mathrm{i}}{2} \sum_{j=1}^{N_f} \log\left(\frac{\mathfrak{m}_j}{\mathfrak{m}_j^*}\right), \tag{6.3.114}$$

which allows to express the truncated partition function in terms of the holomorphic variables $\mathfrak{m}_j$ and $\mathfrak{m}_j^*$ fully

$$Z_{\Delta n}(\Omega) = \mathrm{e}^{\mathrm{i}\Delta n(\theta - \mathrm{i}/2 \sum_k \log(\mathfrak{m}_k/\mathfrak{m}_k^*))} I_{\Delta n}(2\beta(\mathfrak{m}_k \mathfrak{m}_k^*)\,\Omega). \tag{6.3.115}$$

From the Lagrangian density we can interpret the mass parameters $\mathfrak{m}_j$ and $\mathfrak{m}_j^*$ as external sources to the field composites $\bar{\psi}_i P_{\mathrm{R/L}} \psi_j$ respectively, to wit

$$\mathcal{L} \supset \sum_j \bar{\psi}_j (m_j\, \mathrm{e}^{\mathrm{i}\alpha_j\gamma_5}) \psi_j = \sum_j \bar{\psi}_j (\mathfrak{m}_j P_{\mathrm{R}} + \mathfrak{m}_j^* P_{\mathrm{L}}) \psi_j, \tag{6.3.116}$$

meaning we may use the Euclidean path integral to compute integrated correlation functions in a given topological sector from the truncated partition functions:

$$\int \mathrm{d}^4x\, \langle \bar{\psi}_i P_{\mathrm{R}} \psi_i \rangle_{\Delta n} = -\frac{\partial}{\partial \mathfrak{m}_i} Z_{\Delta n}, \qquad \int \mathrm{d}^4x\, \langle \bar{\psi}_i P_{\mathrm{L}} \psi_i \rangle_{\Delta n} = -\frac{\partial}{\partial \mathfrak{m}_i^*} Z_{\Delta n}. \tag{6.3.117}$$

We can plug in our expression for the truncated partition function in Eq. (6.3.115) in the above to get

$$\int \mathrm{d}^4x\ \langle\bar{\psi}_i P_{\mathrm{R}}\psi_i\rangle_{\Delta n} = -\ \mathrm{e}^{\mathrm{i}\Delta n(\theta+\bar{\alpha})}\left(\frac{\Delta n}{2\mathfrak{m}_i}I_{\Delta n}(2\beta\Omega)+2\Omega\,\mathfrak{m}_i^* I'_{\Delta n}(2\beta\Omega)\frac{\partial}{\partial(\mathfrak{m}_i\mathfrak{m}_i^*)}\,\beta(\mathfrak{m}_k\mathfrak{m}_k^*)\right),$$
$$\int \mathrm{d}^4x\ \langle\bar{\psi}_i P_{\mathrm{L}}\psi_i\rangle_{\Delta n} = -\ \mathrm{e}^{\mathrm{i}\Delta n(\theta+\bar{\alpha})}\left(-\frac{\Delta n}{2\mathfrak{m}_i^*}I_{\Delta n}(2\beta\Omega)+2\Omega\,\mathfrak{m}_i I'_{\Delta n}(2\beta\Omega)\frac{\partial}{\partial(\mathfrak{m}_i\mathfrak{m}_i^*)}\,\beta(\mathfrak{m}_k\mathfrak{m}_k^*)\right). \tag{6.3.118}$$

which may be simplified by means of the properties,

$$\frac{\mathrm{d}}{\mathrm{d}z}I_{\Delta n}(z)=\frac{1}{2}\left(I_{\Delta n+1}(z)+I_{\Delta n-1}(z)\right),\qquad \Delta n I_{\Delta n}(z)=-\frac{z}{2}\left(I_{\Delta n+1}(z)-I_{\Delta n-1}(z)\right), \tag{6.3.119}$$

of the modified Bessel functions. After dividing by a volume factor of $\Omega = VT$ we reach the following averages

$$\begin{aligned}\frac{1}{VT}\int \mathrm{d}^4x\,\langle\bar{\psi}_i P_{\mathrm{R}}\psi_i\rangle_{\Delta n} = &-\mathrm{e}^{\mathrm{i}\Delta n(\theta+\bar{\alpha})}\left(-\frac{\beta}{2\mathfrak{m}_i}(I_{\Delta n+1}(2\beta\Omega)-I_{\Delta n-1}(2\beta\Omega))\right.\\ &\left.+\mathfrak{m}_i^*(I_{\Delta n+1}(2\beta\Omega)+I_{\Delta n-1}(2\beta\Omega))\frac{\partial}{\partial(\mathfrak{m}_i\mathfrak{m}_i^*)}\,\beta(\mathfrak{m}_k\mathfrak{m}_k^*)\right),\\ \frac{1}{VT}\int \mathrm{d}^4x\,\langle\bar{\psi}_i P_{\mathrm{L}}\psi_i\rangle_{\Delta n} = &-\mathrm{e}^{\mathrm{i}\Delta n(\theta+\bar{\alpha})}\left(\frac{\beta}{2\mathfrak{m}_i^*}(I_{\Delta n+1}(2\beta\Omega)-I_{\Delta n-1}(2\beta\Omega))\right.\\ &\left.+\mathfrak{m}_i(I_{\Delta n+1}(2\beta\Omega)+I_{\Delta n-1}(2\beta\Omega))\frac{\partial}{\partial(\mathfrak{m}_i\mathfrak{m}_i^*)}\,\beta(\mathfrak{m}_k\mathfrak{m}_k^*)\right).\end{aligned} \tag{6.3.120}$$

Transformation rules for the mass terms considered as spurion fields can be obtained from Eq. (6.2.77), so that a chiral rotation by an angle ϑ leaves an effective Lagrangian invariant if the complex masses transform as $\mathfrak{m}_j \to \mathrm{e}^{-2\mathrm{i}\vartheta}\mathfrak{m}_j$ and $\mathfrak{m}_j^* \to \mathrm{e}^{2\mathrm{i}\vartheta}\mathfrak{m}_j^*$. We observe that the correlation functions above carry ± 2 units of chiral charge associated to the aforesaid rule.

With the current expressions we cannot draw a direct comparison with the results about the dilute instanton gas since there is no clear way to separate background-free from zero-modes pieces, and here we are computing at the coincident limit. However, β contains both effects. The full spacetime averaged correlation functions at the coincident limit are obtained by summing over all topological sectors and dividing by the total partition function:

$$\frac{1}{VT}\int \mathrm{d}^4x\,\langle\bar{\psi}_i P_{R/\mathrm{L}}\psi_i\rangle = \frac{1}{VT\sum_{\Delta n}Z_{\Delta n}}\sum_{\Delta m}\int \mathrm{d}^4x\,\langle\bar{\psi}_i P_{R/L}\psi_i\rangle_{\Delta m}. \tag{6.3.121}$$

We follow our prescription for the limits: we take first the spacetime volume to infinity and then sum over topological sectors. We use the property of the modified Bessel function $I_{\Delta n}(2\beta\Omega) = I_0(2\beta\Omega)(1+\mathcal{O}(1/\Omega))$ to do so and see that only the terms proportional to

derivatives of β survive:

$$\begin{aligned}\frac{1}{VT}\int \mathrm{d}^4x\,\langle\bar{\psi}_i P_{\mathrm{R}}\psi_i\rangle &= \frac{-\sum_{\Delta m}\,\mathrm{e}^{\mathrm{i}\Delta m(\theta+\bar{\alpha})}2\mathfrak{m}_i^* I_0(2\beta\Omega)\,\partial_{\mathfrak{m}_i\mathfrak{m}_i^*}\beta(1+O(1/\Omega))}{\sum_{\Delta n}\,\mathrm{e}^{\mathrm{i}\Delta n(\theta+\bar{\alpha})}I_0(2\beta\Omega)(1+O(1/\Omega))}\\ &\to -2\mathfrak{m}_i^*\,\partial_{\mathfrak{m}_i\mathfrak{m}_i^*}\beta(\mathfrak{m}_k\mathfrak{m}_k^*),\\ \frac{1}{VT}\int \mathrm{d}^4x\,\langle\bar{\psi}_i P_L\psi_i\rangle &= \frac{-\sum_{\Delta m}\,\mathrm{e}^{\mathrm{i}\Delta m(\theta+\bar{\alpha})}2\mathfrak{m}_i I_0(2\beta\Omega)\,\partial_{\mathfrak{m}_i\mathfrak{m}_i^*}\beta(1+O(1/\Omega))}{\sum_{\Delta n}\,\mathrm{e}^{\mathrm{i}\Delta n(\theta+\bar{\alpha})}I_0(2\beta\Omega)(1+O(1/\Omega))}\\ &\to -2\mathfrak{m}_i\,\partial_{\mathfrak{m}_i\mathfrak{m}_i^*}\beta(\mathfrak{m}_k\mathfrak{m}_k^*).\end{aligned} \tag{6.3.122}$$

As it can be seen from the limits above, there is no θ dependence left in the correlation functions, so that all the remaining phases are coming from the tree-level masses and there is no CP violation.

Correlation functions containing products of spacetime averages of two-point correlation functions of the type displayed above can be computed by taking higher-order derivatives of the truncated partition functions. These will again display Bessel functions $I_{\Delta n}$ whose asymptotic behavior matches I_0. The recursive relations for the derivatives in Eq. (6.3.119) allow us to rewrite any derivative in terms of I_m's directly and possible terms of the form $\Delta^m n I_{\Delta n}$ can be expressed as linear combinations without factors of Δn, so that when taking the limit of $VT\to\infty$, the leading terms are all proportional to I_0 and the θ dependence is canceled when taking the ratio against the partition function.

The claim that the prescription of limits advocated for in this document implies the alignment of the phases appearing in the correlation functions and in the quark mass terms has been commented in a previous study[173]. In that article, no use of instantons is made and only real masses are considered. Their prescription is discarded under the argument that the correlation functions should have a phase θ as obtained from the traditional partition function Eq. (6.2.82). We have seen how our prescription produces a different partition function, reopening the possibility that the current order of limits is the correct one.

In the following two subsections, we discuss the consequences of restricting the computations to a single topological sector versus a full summation in the setting of an infinite spacetime volume and later in a finite one. We will see that it is possible to compute correlations functions in a subvolume $\Omega_1\subset\Omega$, while still reaching the same results as in Ω if the partition function follows the factorization property described in this section. This we will do by considering integrating fluctuations in the complement of Ω_1, $\Omega_1^c=\Omega_2=\Omega\setminus\Omega_1$, to arrive to an effective theory for in Ω_1. We will end up with consistent conclusions regarding CP violation, like the ones from the usage of the dilute instanton gas.

6.3.2 Correlation functions within an infinite volume

We consider rewriting Eq. (6.3.89) in terms of the total winding number and the winding number contributions from subvolume Ω_1:

$$\langle\mathcal{O}_1\rangle_\Omega = \lim_{\substack{N_1\to\infty\\ N_1\in\mathbb{N}}}\lim_{\substack{N\to\infty\\ N\in\mathbb{N}}}\lim_{\Omega\to\infty}\frac{\displaystyle\sum_{\Delta n=-N}^{N}\sum_{\Delta n_1=-N_1}^{N_1} f(\Delta n)\int\mathcal{D}_{\Delta n_1}[\phi]\mathcal{O}_1\,\mathrm{e}^{-S_{\Omega_1}[\phi]}\int\mathcal{D}_{\Delta n-\Delta n_1}[\phi]\,\mathrm{e}^{-S_{\Omega_2}[\phi]}}{\displaystyle\sum_{\Delta n=-N}^{N}\sum_{\Delta n_1=-N_1}^{N_1} f(\Delta n)\int\mathcal{D}_{\Delta n_1}[\phi]\,\mathrm{e}^{-S_{\Omega_1}[\phi]}\int\mathcal{D}_{\Delta n-\Delta n_1}[\phi]\,\mathrm{e}^{-S_{\Omega_2}[\phi]}}\,. \tag{6.3.123}$$

Using our result for the partition function for the subvolume Ω_2, Eq. (6.2.74), gives

$$\langle \mathcal{O}_1 \rangle_\Omega = \lim_{\substack{N_1, N\to\infty \\ N_1, N\in\mathbb{N}}} \lim_{\Omega_2\to\infty} \frac{\displaystyle\sum_{\Delta n=-N}^{N} \sum_{\Delta n_1=-N_1}^{N_1} f(\Delta n) I_{\Delta n-\Delta n_1}(2\kappa\Omega_2)((-1)^{N_f}\, \mathrm{e}^{\mathrm{i}\,\bar{\alpha}})^{\Delta n-\Delta n_1} \int \mathcal{D}_{\Delta n_1}[\phi] \mathcal{O}_1\, \mathrm{e}^{-S_{\Omega_1}[\phi]}}{\displaystyle\sum_{\Delta n=-N}^{N} \sum_{\Delta n_1=-N_1}^{N_1} f(\Delta n) I_{\Delta n-\Delta n_1}(2\kappa\Omega_2)((-1)^{N_f}\, \mathrm{e}^{\mathrm{i}\,\bar{\alpha}})^{\Delta n-\Delta n_1} \int \mathcal{D}_{\Delta n_1}[\phi]\, \mathrm{e}^{-S_{\Omega_1}[\phi]}}, \tag{6.3.124}$$

where phase factors coming out fermion determinants are left explicit. In the case of infinite Ω, and Ω_1 being bounded, we must take the $\Omega_2 \to \infty$ limit. To leading order the Bessel functions above, having Ω_2 as an argument, will asymptotically behave as I_0 without regard to Δn_1. We can then factor out and cancel terms depending on the subvolume Ω_2, namely:

$$\langle \mathcal{O}_1 \rangle_\Omega = \frac{\displaystyle\sum_{\Delta n_1=-\infty}^{\infty} \int \mathcal{D}_{\Delta n_1}[\phi]\, (-1)^{-N_f \Delta n_1}\, \mathrm{e}^{-\mathrm{i}\,\bar{\alpha}\Delta n_1} \mathcal{O}_1\, \mathrm{e}^{-S_{\Omega_1}[\phi]}}{\displaystyle\sum_{\Delta n_1=-\infty}^{\infty} \int \mathcal{D}_{\Delta n_1}[\phi]\, (-1)^{-N_f \Delta n_1}\, \mathrm{e}^{-\mathrm{i}\,\bar{\alpha}\Delta n_1}\, \mathrm{e}^{-S_{\Omega_1}[\phi]}}\,. \tag{6.3.125}$$

The expression above is just a path integral computation of $\langle \mathcal{O}_1 \rangle$. It takes that shape by virtue of the exact cancellation between the remnant phases coming from the bigger volume and those from fermion determinants in Ω_1 for each Δn_1. We thus witness again how the different topological sectors do not interfere with each other as the global phases factor out and cancel as long as we are in the infinite spacetime volume case.

This has the same implication as the correlation functions computed in previous sections. For observables computed via a path integral in the subvolume Ω_1, there will not be any CP violation. Using the Eq. (6.3.125) about a dilute instanton gas can be seen to give the same results as in the dilute instanton gas discussion where there was an explicit θ phase and no phase insertions as in Eq. (6.3.125), entailing that the correlation functions come out aligned with the mass terms either way.

We have considered the limit of $\Omega \to \infty$ with the same reasoning behind our prescription for the order of the limits. The topological classification into integer classes highlights specific saddle-point configurations with a finite action. This particular property is lost when one considers compact spacetimes, where all configurations automatically give a finite action. In the present context of dividing the spacetime volume into subvolumes, it is important to remark that Δn_1 and Δn_2 are not necessarily integers and by assuming they can be treated as such above, we have neglected non-trivial winding of the fields that may occur at the boundary of Ω_1, these, we argue, become small when Ω_1 is small compared to Ω but large enough to capture the physical phenomena of interest.

The result of Eq. (6.3.125) coincides with a computation done in an infinite volume but restricted to a single topological sector, without any violation of the CDP. In what follows, we attempt to address how the CDP is affected by finite volumes.

6.3.3 Correlation functions within a finite volume

Imposing the factorization in the path integration as we have done in Subsec. (6.3.1) has the consequence that information concerning the boundary Ω is immaterial for local

excitations within Ω_1. Following such an idea, we consider a finite but large Ω compared to Ω_1 and examine the consequences of restricting to a single topological sector. In its pure form, the CDP breaks down when translation invariance is absent, for example, in finite volumes. Moreover, unless periodic boundary conditions are imposed, there will be deviations from the factorization given by the CDP. We quantify here how the deviations depend on the size of the spacetime, similar to some of the ideas in [174, 175].
We start by considering the expectation value of some operator $\mathcal{O}_1$ localized in subvolume $\Omega_1 \subset \Omega$ in a large but finite Ω. We consider only one topological sector, as we have seen that summing over Δn does not have any effects under the present conditions. Using our result for the partition function in Eq. (6.2.74) for the complement subvolume $\Omega_2 = \Omega \setminus \Omega_1$ we have

$$\langle \mathcal{O}_1 \rangle_{\Delta n\, \Omega} = \frac{\displaystyle\sum_{\Delta n_1=-\infty}^{\infty} I_{\Delta n-\Delta n_1}(2\kappa\Omega_2) \int \mathcal{D}_{\Delta n_1}[\phi](-1)^{-N_f \Delta n_1}\, \mathrm{e}^{-\mathrm{i}\,\bar{\alpha}\Delta n_1} \mathcal{O}_1\, \mathrm{e}^{-S_{\Omega_1}[\phi]}}{\displaystyle\sum_{\Delta n_1=-\infty}^{\infty} I_{\Delta n-\Delta n_1}(2\kappa\Omega_2) \int \mathcal{D}_{\Delta n_1}[\phi](-1)^{-N_f \Delta n_1}\, \mathrm{e}^{-\mathrm{i}\,\bar{\alpha}\Delta n_1}\, \mathrm{e}^{-S_{\Omega_1}[\phi]}}. \tag{6.3.126}$$

As we already have seen in the previous subsection to leading order in $\kappa\Omega$ the volume dependence disappears and the factors depending on Ω_2 drop out of the calculation. Here we find out how the sub-leading terms depend on $\kappa\Omega_2$. To see this formally, we expand first the following factor appearing in the numerator of Eq. (6.3.126),

$$\int \mathcal{D}_{\Delta n_1}[\phi]\, \mathcal{O}_1\, \mathrm{e}^{-S_{\Omega_1}[\phi]} = \sum_r B_r (-1)^{N_f \Delta n_1}\, \mathrm{e}^{\mathrm{i}\,\bar{\alpha}(\Delta n_1 + m_r)} I_{\Delta n_1 + m_r}(2\kappa\Omega_1)\,, \quad m_r \in \mathbb{Z}\,, \tag{6.3.127}$$

for some finite number coefficients B_r that may contain internal indices and m_r captures the phases coming from possible fermions that are present.
On the other hand, the integration over Ω_1 in the denominator of Eq. (6.3.126) corresponds to the Euclidean version of Eq. (6.2.74)

$$\int \mathcal{D}_{\Delta n_1}[\phi]\, \mathrm{e}^{-S_{\Omega_1}[\phi]} = (-1)^{N_f \Delta n_1}\, \mathrm{e}^{\mathrm{i}\,\bar{\alpha}\Delta n_1} I_{\Delta n_1}(2\kappa\Omega_1). \tag{6.3.128}$$

We can see how in both cases, in the numerator as well as the denominator, the phase factors in Eq. (6.3.126) are canceled by those in Eqs. (6.3.127) and (6.3.128).
We consider expanding the remaining terms by using the asymptotic series

$$I_n(z) \sim \frac{\mathrm{e}^z}{\sqrt{2\pi z}} \sum_{k=0}^{\infty} (-1)^k \frac{a_k(n)}{z^k}, \quad |z| \gg 1, \tag{6.3.129}$$

valid for the modified Bessel functions $I_m(z)$ for $z \in \mathbb{C}$ with $|\arg(z)| < \pi/2$, where

$$a_0(n) = 1, \quad \text{and} \quad a_k(n) = \frac{(4n^2-1^2)(4n^2-3^2)\ldots(4n^2-(2k-1)^2)}{k!8^k}\,, \tag{6.3.130}$$

which leads to the following expression for a product of Bessel functions

$$\begin{aligned} I_{\Delta n-\Delta n_1}(z)\, I_{\Delta n_1+m_r}(z') &= I_0(z) \left(1 + \frac{I_{\Delta n-\Delta n_1}(z) - I_0(z)}{I_0(z)}\right) I_{\Delta n_1+m_r}(z') \\ &= I_0(z) \left(1 - \frac{4(\Delta n - \Delta n_1)^2}{8z} + O\left(\frac{1}{z^2}\right)\right) I_{\Delta n_1+m_r}(z')\,. \end{aligned} \tag{6.3.131}$$

The product above implies that for a given difference $\Delta n - \Delta n_1$ we have

$$I_{\Delta n-\Delta n_1}(2\kappa\Omega_2)\, I_{\Delta n_1+m_r}(2\kappa\Omega_1) \approx I_0(2\kappa\Omega_2)\, I_{\Delta n_1+m_r}(2\kappa\Omega_1) + \mathcal{O}\left(\Omega_2^{-1}\right). \tag{6.3.132}$$

In order to compare the tails of the partial sums, not only in terms of Ω_1, we need to consider the behavior with respect to Δn_1 as well. Partial sums involving large Δn_1 can be understood by means of the asymptotic expansion

$$I_n(z) \sim \frac{1}{\sqrt{2\pi|n|}} \left(\frac{\mathrm{e}z}{2|n|}\right)^{|n|}, \quad |n| \gg 1,\ n \in \mathbb{Z}. \tag{6.3.133}$$

We find now an upper bound for the tails of the partial sums, consider the tail starting at $\Delta n_1 = K$ and assume $|m_r| \ll K$ in the last factors appearing in Eq. (6.3.127)

$$\begin{aligned}\sum_{\Delta n_1=K}^{\infty} I_{\Delta n_1}(z) &\sim \sum_{\Delta n_1=K}^{\infty} \frac{1}{\sqrt{2\pi\Delta n_1}} \left(\frac{\mathrm{e}z}{2\Delta n_1}\right)^{\Delta n_1} < \frac{1}{\sqrt{2\pi K}} \sum_{\Delta n_1=K}^{\infty} \left(\frac{\mathrm{e}z}{2K}\right)^{\Delta n_1} \\ &\leq \frac{1}{\sqrt{2\pi K}} \frac{\left(\frac{\mathrm{e}z}{2K}\right)^K}{1-\frac{\mathrm{e}z}{2K}},\end{aligned} \tag{6.3.134}$$

The numerator of Eq. (6.3.126) can be bounded using the above relations as follows

$$\begin{aligned}&\sum_{\Delta n_1=-\infty}^{\infty} \sum_r B_r\ \mathrm{e}^{\mathrm{i}\bar{\alpha}m_r} I_{\Delta n-\Delta n_1}(z_2) I_{\Delta n_1+m_r}(z_1) \\ &\quad= \sum_r B_r\, \mathrm{e}^{\mathrm{i}\bar{\alpha}m_r} \Big[\sum_{\Delta n_1=-\infty}^{\infty} I_0(z_2) I_{\Delta n_1+m_r}(z_1) + \sum_{\Delta n_1=-K}^{K} \left(I_{\Delta n-\Delta n_1}(z_2) - I_0(z_2)\right) I_{\Delta n_1+m_r}(z_1) \\ &\qquad\qquad - \sum_{|\Delta n_1|>K} \left(I_0(z_2) - I_{\Delta n-\Delta n_1}(z_2)\right) I_{\Delta n_1+m_r}(z_1) \Big] \\ &\quad\leq \sum_{\Delta n_1=-\infty}^{\infty} \sum_r \left[B_r\, \mathrm{e}^{\mathrm{i}\bar{\alpha}m_r} I_0(z_2) I_{\Delta n_1+m_r}(z_1) \left(1 + \mathcal{O}\left(\frac{(|\Delta n|+K)^2}{z_2}\right)\right)\right] \\ &\qquad\qquad + I_0(z_2)\, \mathcal{O}\left(\left[\frac{\mathrm{e}z_1}{2K}\right]^K\right),\end{aligned} \tag{6.3.135}$$

for $z_1 \equiv 2\kappa\Omega_1$ and $z_2 \equiv 2\kappa\Omega_2$ and where we have used that $0 \leq I_0(z_2) - I_{\Delta n-\Delta n_1} \leq I_0(z_2)$ to estimate the last summation in the middle line and expressions (6.3.131) and (6.3.134) to get to the last line. Following a similar approximation for the denominator of Eq. (6.3.126)

we can collect our results as

$$\begin{aligned}\langle\mathcal{O}_1\rangle_{\Delta n\,\Omega} =& \\ &\frac{I_0(z_2)\,\mathcal{O}\left(\left[\frac{\mathrm{e}z_1}{2K}\right]^K\right)+\left(1+O\left(\frac{(|\Delta n|+K)^2}{z_2}\right)\right)\sum_{\Delta n_1=-\infty}^{\infty}\sum_r B_r\,\mathrm{e}^{\mathrm{i}\,\bar\alpha m_r}I_0(z_2)I_{\Delta n_1+m_r}(z_1)}{I_0(z_2)\,\mathcal{O}\left(\left[\frac{\mathrm{e}z_1}{2K}\right]^K\right)+\left(1+\mathcal{O}\left(\frac{(|\Delta n|+K)^2}{z_2}\right)\right)\sum_{\Delta m_1=-\infty}^{\infty}I_0(z_2)I_{\Delta m_1}(z_1)}\cdot \\ &= \frac{\mathcal{O}\left(\left[\frac{\mathrm{e}z_1}{2K}\right]^K\right)+\left(1+O\left(\frac{(|\Delta n|+K)^2}{z_2}\right)\right)\sum_{\Delta n_1=-\infty}^{\infty}\sum_r B_r\,\mathrm{e}^{\mathrm{i}\,\bar\alpha m_r}I_{\Delta n_1+m_r}(z_1)}{\mathcal{O}\left(\left[\frac{\mathrm{e}z_1}{2K}\right]^K\right)+\left(1+\mathcal{O}\left(\frac{(|\Delta n|+K)^2}{z_2}\right)\right)\sum_{\Delta m_1=-\infty}^{\infty}I_{\Delta m_1}(z_1)}\cdot\end{aligned} \tag{6.3.136}$$

The last expression shows how the relation of the volumes and K affects the expectation value. We observe that the Bessel function with the argument containing Ω_2 cancels with the denominator in any case and that by choosing $K > z_1 = 2\kappa\Omega_1$ the terms going like $(\,\mathrm{e}z_1/2K)^K$ become negligible. If more over $z_2 = 2\kappa\Omega_2 \gg K \gg |\Delta n|$ we are back to

$$\langle\mathcal{O}_1\rangle_{\Delta n\,\Omega} \approx \frac{\sum_{\Delta n_1=-\infty}^{\infty}\sum_r B_r\,\mathrm{e}^{\mathrm{i}\,\bar\alpha m_r}I_{\Delta n_1+m_r}(2\kappa\Omega_1)}{\sum_{\Delta m_1=-\infty}^{\infty}I_{\Delta m_1}(2\kappa\Omega_1)}, \tag{6.3.137}$$

which we can interpret back as simply having started with the path integration in the subvolume Ω_1 without any reference to Δn as long as the conditions for the volumes are met, explicitly by using Eqs. (6.3.127) and (6.3.128) we obtain

$$\langle\mathcal{O}_1\rangle_{\Delta n\,\Omega} \approx \frac{\sum_{\Delta n_1=-\infty}^{\infty}\int\mathcal{D}_{\Delta n_1}[\phi]\,(-1)^{-N_f\Delta n_1}\,\mathrm{e}^{-\mathrm{i}\,\bar\alpha\Delta n_1}\mathcal{O}_1\;\mathrm{e}^{-S_{\Omega_1}[\phi]}}{\sum_{\Delta m_1=-\infty}^{\infty}\int\mathcal{D}_{\Delta m_1}[\phi]\,(-1)^{-N_f\Delta m_1}\,\mathrm{e}^{-\mathrm{i}\,\bar\alpha\Delta m_1}\,\mathrm{e}^{-S_{\Omega_1}[\phi]}}. \tag{6.3.138}$$

6.4 Closing comments about θ-angle related observables

Before closing the present chapter, we include here a few comments drawing certain similarities and also highlighting differences to other physical systems. We also discuss the relations to often quoted quantities that appear in lattice QCD simulations and perhaps experiment pertaining to the topological charge. They will serve as basic checks to our computations based on the dilute instanton gas and the CDP.

6.4.1 Comparison with quantum mechanical systems

Several models exist where a similar angular variable as θ exists. It is often assumed these then share certain properties. However, this is not always the case. Models that are often used to argue in apparently supporting directions turn up to be just too different. Here

we briefly include two examples where the vacuum structure is usually compared to that of QCD. More details can be found in Ref. [34].

First, consider a quantum mechanical particle in one dimension subject to a periodic potential. Consider examining the evolution of the system within a finite bounded time window $T \subseteq \mathbb{R}$. In this setting, there are approximate ground states which are Gaussian functions localized around the local minima, denote them by $|j\rangle$ for $j \in \mathbb{Z}$, very similar to our pre-vacua. By studying the model after a Wick rotation, it is also possible to find soliton-like solutions that connect two minima and are exponentially suppressed, therefore interpreted as tunneling processes. These solutions induce transitions between the $|j\rangle$, which are not real eigenstates. A superposition of these, however, has the potential of being the true ground state. A family of superposition compatible with the tunneling processes, actually Bloch waves, is $|\theta_T\rangle = \sum_j \exp(\mathrm{i}\theta_T j)|j\rangle$ where the family has been labeled by the angle θ_T. It turns out that not all superpositions correspond to a minimum of the energy, which can be seen to depend on $\cos\theta_T$. Using concatenated strings of solitons, analogous to our dilute instanton gas, we can compute the transition amplitude between two different $|j\rangle$ states, e.g., $\langle j+m|j\rangle$ for some $m \in \mathbb{Z}$. So that considering the energy dependence, the leading contribution to said amplitude for large T is

$$ {}_{\text{out}}\langle j+m|j\rangle_{\text{in}} \propto {}_{\text{out}}\langle\theta_T|\theta_T\rangle_{\text{in}}|_{\theta_T=0}. \tag{6.4.139} $$

This is different from what happens in the QCD instantons case, where any linear combination of pre-vacua $|n\rangle$ gives the same as the amplitude $\langle n+m|n\rangle$ up to an overall factor. We argue that for large bounded spacetimes and fixed Δn, the truncated partition function $Z_{\Delta n}$ produces correlation functions that match with those obtained by summing over topological sectors in infinite spacetimes for $\theta = 0$[174]. This is not the same as projecting a given θ-vacuum sate onto a $\theta = 0$ one, so these conclusions do not conflict with the conservation of θ; it remains a legitimate quantum number.

To better understand the last statement, we relate θ_T with the crystal momentum of a solid-state system. On the one hand, if the crystal is finite, periodicity is broken. However, on the other hand, if we impose spatially periodic boundary conditions, the number of sectors is automatically rendered finite so that the interchange in limits does not change the result. It is in this sense that the nature of θ differs from the quantum mechanical analogy.

The second comparison we want to draw concerns a quantum mechanical system with a finite number of local minima. The most straightforward example is that of the double potential well. While in the field theory case there is an infinite number of spatial boundary conditions, the quantum mechanical case only allows for states that are associated with a few paths. Specifically, those beginning and ending either in the same well or on the opposite well. For the analogy, let us label the classes by $+$ if the path ends in the same well and by $-$ on the contrary, then the partition function can be seen to give[34]:

$$ Z_\pm = \frac{1}{2}\sqrt{\frac{\omega}{\pi}}\,\mathrm{e}^{-\frac{\omega T}{2}}\left(\mathrm{e}^{\kappa\exp(-S_{\mathrm{E}})T} \pm \mathrm{e}^{-\kappa\exp(-S_{\mathrm{E}})T}\right), \tag{6.4.140} $$

for a natural frequency ω around each well and κ associated to fluctuation determinants. Observe that, instead to the modified Bessel functions obtained in the field theory case,Eq. (6.2.74), here we have a sum of exponential functions. A candidate for comparison to CP effects can be the parity operator P. Computing the expectation value of P for the two possible classes gives

$$ \langle P\rangle_{\text{even/odd}} = \frac{\pm Z_+ + Z_-}{Z_+ \pm Z_-} = \pm 1\,. \tag{6.4.141} $$

This is analogous to the summation over topological sectors we performed in Subsec. 6.2.2, however here, there is only a finite number of classes to sum over and no ambiguity arises when considering the limit of $T \to \infty$.

To wrap everything up, in the gauge field theory case θ is a good quantum label because the boundary conditions and the topology ensure θ is conserved, contrary to the first quantum mechanical example. The second example shows how the question of the order of limits is only relevant in case there is an infinite number of sectors to sum over. Consequently, the θ parameter does not change since the theory does not restrict the interactions to a finite spacetime region and because of gauge invariance, all transitions must be summed up.

6.4.2 The η' and the topological susceptibility

In order to check our theoretical study with some reference observations, it is important to look in two directions: lattice simulations and experimental observations. As we say in Chap. 5 we have the topological susceptibility on the lattice side and the η' on the observational one. They are also mutually connected via the Witten-Veneziano relation, Eq. (5.2.96), so that, at the very least, our ideas should be compatible with them. In this section, we describe some of the consequences of our limit prescription and make contact with the aforementioned quantities.

Lattice simulations are an example where we can find computations generally done within a finite volume, Ω_1 and often a fixed topological sector, Δn. They also employ periodic boundary conditions and require taking the continuum limit to make statements about infinite volumes. The simulations allow them to compute the topological susceptibility in different settings. In the language of sec. 6.3 seems that sampling is done while neglecting completely any effect from the complement of the volume Ω_2, e.g. Refs. [142, 176]. To comply with what we have said in relation to the CDP: to evaluate expressions in the lattice, $\bar{\theta}$ should be taken to be 0, to automatically account for the phases of the complement volume, regardless of the $\bar{\theta}$ appearing in the Lagrangian.

Let us come back to the topological susceptibility in more detail. It was already introduced in Eq. (5.2.93), but we recall its definition adapted to the current context

$$\chi_\Omega = \frac{1}{\Omega}\ \langle \Delta n^2 \rangle\big|_{\bar{\theta}=\theta_0} = \frac{1}{\Omega}\ \left\langle \left(\int_\Omega d^4x\, Q(x) \right)^2 \right\rangle \Bigg|_{\bar{\theta}=\theta_0} . \tag{6.4.142}$$

with Q being as in Eq. (5.2.94) and $\theta_0 \equiv (1-(-1)^{N_f})\pi/2$. This last value is chosen such that the vacuum energy is minimized when summing over topological sector in the case of a finite spacetime, also χ remains positive.

Considering the susceptibility at a fixed topological sector reveals that it vanishes when $\Omega \to \infty$, this result implies that when summing over topological sectors after having taken the infinite spacetime limit also leads to a vanishing χ_Ω, independently of fermion fluctuations. This result, however, does not contradict the relation between the susceptibility and the η' particle's mass in the large color limit(5.2.96). As we showed above, we recover the enhanced mass of the η' via our modified matching of 't Hooft operators.

The computations in [137] are performed using a regulator parameter for the infrared, which can be interpreted as a cutoff in terms of lengths. That is, for the sake of comparison with their result, we should instead consider the topological susceptibility within a subvolume $\Omega_1 \subset \Omega$ in which case our pseudo winding number Δn_1 is not necessarily an integer representing the mobility of charge across the boundary of Ω_1. We can use

Eq. (6.3.125) to compute χ_{Ω_1}:

$$\begin{aligned}\chi_{\Omega_1} &\equiv \frac{1}{\Omega_1}\left\langle\left(\int_{\Omega_1} \mathrm{d}^4x\, Q(x)\right)^2\right\rangle \\ &= \frac{\displaystyle\sum_{\Delta n_1=-\infty}^{\infty}\int \mathcal{D}_{\Delta n_1}[A]\mathcal{D}[\bar\psi]\mathcal{D}[\psi]\int_{\Omega_1}\mathrm{d}^4x\,\mathrm{d}^4x'\,Q(x)Q(x')\,\mathrm{e}^{-S_{\Omega_1}[A_\mu]}(-1)^{-N_f\Delta n_1}\,\mathrm{e}^{-\mathrm{i}\,\bar\alpha\Delta n_1}}{\Omega_1\displaystyle\sum_{\Delta n_1=-\infty}^{\infty}\int \mathcal{D}_{\Delta n_1}[A]\mathcal{D}[\bar\psi]\mathcal{D}[\psi]\,\mathrm{e}^{-S_{\Omega_1}[A_\mu]}(-1)^{-N_f\Delta n_1}\,\mathrm{e}^{-\mathrm{i}\,\bar\alpha\Delta n_1}} \\ &= \frac{1}{\Omega_1}\frac{\displaystyle\sum_{n_1=0}^{\infty}\sum_{\bar n_1=0}^{\infty}\frac{1}{n_1!\bar n_1!}(n_1-\bar n_1)^2(\bar\kappa\Omega_1)^{n_1+\bar n_1}}{\displaystyle\sum_{n_1=0}^{\infty}\sum_{\bar n_1=0}^{\infty}\frac{1}{n_1!\bar n_1!}(\bar\kappa\Omega_1)^{n_1+\bar n_1}} = 2\bar\kappa\,,\end{aligned} \tag{6.4.143}$$

where in Euclidean space we have (see Eq. (6.2.59) and definitions surrounding Eq. (6.2.74) in Sec.6.2)

$$\bar\kappa = \int d\Omega\, J^{\mathrm{E}} R\,\mathrm{e}^{-S_{\mathrm{E}}}\prod_{j=1}^{N_f}\Theta_j, \tag{6.4.144}$$

with $J = \mathrm{i}J^{\mathrm{E}}$, while other quantities do not change.
The result in Eq. (6.4.143) coincides with what we would obtain if we were to consider the usual partition function, obtained by taking the Ω limit last, Eq. (6.2.82) at $\bar\theta = 0$ instead. So the topological susceptibility χ_{Ω_1} is not able to distinguish between both cases. This poses no contradiction with χ_Ω since they are simply different operators and we understand that only χ_{Ω_1} corresponds to the regulated version of [137].
Under the following arguments we can find proportionality to the mass of the η' particle. We expect the Dirac operator to have a single discrete mode zero-mode on an instanton background, while keeping its continuum piece unchanged, thus from Eq. (6.1.46) we can approximate $\Theta_i \approx m_i$, with m_i the moduli of the complex mass parameters of the fermions. We can factor a pure gauge factor, κ^{gauge}, out of $\bar\kappa$, detaching it from the fermion determinant factors, which leads to

$$\bar\kappa \approx \kappa^{\mathrm{gauge}}\prod_{j=1}^{N_f} m_j = \frac{1}{2}\,\chi_{\Omega_1}^{\mathrm{gauge}}\prod_{j=1}^{N_f} m_j, \tag{6.4.145}$$

where Eq. (6.4.143) was used.
We can determine up to constant factors, the parameter λ in Eq. (5.2.87) by matching with the 't Hoof operator in Eq. (6.2.78)

$$|\lambda| \propto \Gamma_{N_f} \propto \frac{\bar\kappa}{\prod_j m_j} = \frac{1}{2}\chi_{\Omega_1}^{\mathrm{gauge}}, \tag{6.4.146}$$

where we can read the factor $\bar\kappa/\prod_i m_i$ from Eq. (6.2.76) (with $p = 0$ and $q = N_f$). Using the relation $m_{\eta'}^2 = 8|\lambda|F_0^2$ from subsec. 5.2.1 we see the desired proportionality

$$m_{\eta'}^2 \propto \chi_{\Omega_1}^{\mathrm{gauge}}. \tag{6.4.147}$$

This shows how the results derived in [137] and [139] for the large N_c limit may be valid in a more general setting as long as the dilute gas approximation holds. Moreover, Eq. (6.3.138) implies that even within a large enough but finite volume and a fixed topological sector, we have a massive η' meson.
Other interesting expectation values to look at include the instanton number density and its variation. Let us first look at the former, $\langle n\rangle/\Omega$, at a fixed topological sector Δm. From Eq. (6.2.74) we have

$$\frac{\langle n\rangle_{\Delta m}}{\Omega} = \bar{\kappa}\frac{I_{\Delta m-1}(2\bar{\kappa}\Omega)}{I_{\Delta m}(2\bar{\kappa}\Omega)} \sim \bar{\kappa}, \tag{6.4.148}$$

and for the ratio of the fluctuations to the density

$$\frac{\sqrt{\langle(n-\langle n\rangle)^2\rangle_{\Delta m}}}{\langle n\rangle_{\Delta m}} = \left(\frac{I_{\Delta m}(2\bar{\kappa}\Omega)^2}{I_{\Delta m-1}(2\bar{\kappa}\Omega)^2} + \frac{\Delta m I_{\Delta m}(2\bar{\kappa}\Omega)}{\bar{\kappa}\Omega\, I_{\Delta m-1}(2\bar{\kappa}\Omega)} - 1\right)^{1/2} \sim \sqrt{\frac{\Delta m}{\bar{\kappa}\Omega}}\,, \tag{6.4.149}$$

where the last expression corresponds to the limit $\Omega \to \infty$. The result in Eq. (6.4.148) does not change if we sum over topological sectors after having taken the spacetime volume limit. However taking the sum first we have

$$\frac{\langle n\rangle}{\Omega} = (-1)^{N_f}\bar{\kappa}\,\mathrm{e}^{\mathrm{i}\bar{\theta}}. \tag{6.4.150}$$

We consider as well the expected topological charge density, $\langle \Delta n\rangle/\Omega$, together with the topological susceptibility and the instanton number density with different combinations of the limits prescription and collect all results in Table 6.1. However, only the instanton density depends on the instanton background. The topological charge and the susceptibility are defined nevertheless.

	Δn free and Ω_∞ first or Δn fixed and Ω_∞	Δn free, Ω_∞ last or Δn free, Ω_{fin}	Δn free, $\Omega_1 \subset \Omega_\infty$ and Ω_∞ first or Δn fixed with $\Omega_1 \subset \Omega_{\text{fin}}, \Omega_\infty$	Δn fixed, Ω_{fin}
χ	0	$2\bar{\kappa}$	$2\bar{\kappa}$	$\Delta n^2/\Omega$
$\frac{\langle n\rangle}{\Omega}$	$\bar{\kappa}$	$(-1)^{N_f}\bar{\kappa}\,\mathrm{e}^{\mathrm{i}\bar{\theta}}$	$\bar{\kappa}$	$\bar{\kappa}\frac{I_{\Delta n-1}(2\bar{\kappa}\Omega)}{I_{\Delta n}(2\bar{\kappa}\Omega)}$
$\frac{\langle \Delta n\rangle}{\Omega}$	0	$2\mathrm{i}(-1)^{N_f}\bar{\kappa}\,\sin\bar{\theta}$	0	$\frac{\Delta n}{\Omega}$

Table 6.1: Results for χ, $\langle n\rangle/\Omega$ and $\langle \Delta n\rangle/\Omega$ as defined in the main text, under different limit prescriptions and spacetime volumes. Ω_∞ denotes an infinite total volume and Ω_{fin} a compact one. Ω_1 is assumed to be finite. The adjectives "first/last" refers to when is the spacetime volume limit taken, either before or after the sum over topological sectors.

The topological susceptibility can also computed for the case where the Ω limit is left undone or performed last, in which case we have

$$\chi_\Omega = \frac{\langle \Delta n^2\rangle}{\Omega} = 2\bar{\kappa}\left(\cos(N_f\pi+\bar{\theta}) - 2\bar{\kappa}\Omega\sin^2(N_f\pi+\bar{\theta})\right)\,, \tag{6.4.151}$$

which seems more obscure, presenting still some volume dependence. The last term however vanishes when the full topological susceptibility is evaluated at $\bar{\theta} = \theta_0$, but cannot be interpreted as $\langle \Delta n^2 \rangle / \Omega$.
When keeping the spacetime volume finite, we get results that are compatible with a Taylor expansion around the parameter θ_0,

$$\frac{\langle \Delta n \rangle}{\Omega} = \mathrm{i}\,(\theta - \theta_0)\,\frac{\langle \Delta n^2 \rangle}{\Omega}\bigg|_{\theta_0} + \mathcal{O}(\theta - \theta_0)^2, \tag{6.4.152}$$

which are familiar from analyticity used in [177]. However, as has been remarked earlier in the text, when considering infinite spacetime volume, the partition function may not be considered analytic everywhere in θ. They also obtain a non-zero susceptibility by means of current algebra theorems and using a regulator, meaning we should compare that result with our finite volume version, with which it is in agreement, Eq. (6.4.143). The present results, however, disagree with the statement that CP violation occurs when they employ Eq. (6.4.152) for an infinite volume. Here we have shown how, by using Eq. (6.3.125), the θ dependence disappears and we are led to conclude there is no CP violation although χ_{Ω_1} is non-vanishing.

6.5 Conclusions

In this last part of this thesis, we have seen how many different elements come into play to address one of the long-standing theoretical puzzles of the last 40 years; the strong CP problem.
We started the discussion by reviewing the relevant aspects of QCD for the present document with emphasis on the non-perturbative effects. This called immediately for a digression about topology and instantons, which turned to be the building blocks for the background used in our discussion. Along with the non-perturbative features of QCD, we review in a somewhat historical manner the strong CP problem and low energy QCD. The former to introduce the problem and the latter to attempt some contact with experiments. We saw how the CP problem, although given the tightness of current constraints is of a purely theoretical nature, is connected to observables such as the nEDM, the mass of the η' meson, the topological susceptibility, etc.
With the purpose of studying that problem, we have exploited the techniques commonly applied to the computation of path integrals. Using a mathematically non-trivial background made up of instantons, we have computed correlation functions for QCD while tracking the possible complex phases that arise. Using such correlation functions, we are able to obtain an effective chiral Lagrangian resembling a σ-model where the effective operators capturing CP effects have complex phases which are aligned with mass terms. This important observation allows us to redefine the quark fields to eliminate any remaining phases, thus rendering the theory CP preserving.
To support our conclusions in a somewhat independent manner, we have considered computing the same correlation functions by means of imposing the CDP on the partition function of the system. This led us to consistent results for the dilute instanton gas and taught us many things concerning the relevance of the size of spacetime and the consideration of different topological sectors. But most importantly, employing our suggestion for performing the limits appearing in the correlation functions led to supporting results.
Currently, there is an active quest for axion-like particles, which are pseudoscalar particles that can be included in the SM, motivated initially by the fact that they dynamically pick

$\theta = 0$, solving the strong CP problem. However, here we have put forward a competing idea for understanding CP-violating phases, which renders the strong CP problem meaningless without requiring new fields but only a proper consideration of instanton effects. We hope this can be a final answer to this conundrum, but if not, the journey on its own has already been rewarding: we have combined and explored the power of different methods and learned about the limits of some others.

Appendices

A. Gaussian Integrals

For completeness and given how ubiquitous Gaußian integrals are, we include the basic proofs for some results in this appendix. More cases can be found in textbooks concerning Gaußian integration such as Refs. [14, 15, 178]). These are all based on generalizing the basic Gaußian integral

$$I_0(\alpha) = \int_{-\infty}^{\infty} \mathrm{d}x\, \mathrm{e}^{-\frac{1}{2}\alpha x^2} = \sqrt{\frac{2\pi}{\alpha}} \qquad \text{for} \quad \alpha > 0. \tag{A.1}$$

We consider different cases in a finite number of dimensions but most results are extrapolated to the case of field path integrals. First, let $\boldsymbol{A}$ be a real symmetric positive-definite matrix of dimensions $n \times n$, i.e., its eigenvalues are real and greater than 0. We want to prove the following result used often:

$$I_1(\boldsymbol{A}) \equiv \int_{-\infty}^{\infty} \mathrm{d}\vec{x}\, \mathrm{e}^{-\frac{1}{2}\vec{x}^T \boldsymbol{A}\vec{x}} = \sqrt{\frac{(2\pi)^n}{\det \boldsymbol{A}}}. \tag{A.2}$$

Proof. Given a real symmetric and positive definite matrix $\boldsymbol{A}$, there exists an orthogonal matrix $\boldsymbol{O}$ such that

$$\boldsymbol{A} = \boldsymbol{O}\boldsymbol{D}\boldsymbol{O}^T, \tag{A.3}$$

with $\boldsymbol{D}$ a diagonal matrix having the eigenvalues, a_i, of $\boldsymbol{A}$ which are real and positive. We can then consider the coordinate transformation

$$\vec{x} = \boldsymbol{O}\vec{y}, \tag{A.4}$$

which for orthogonal $\boldsymbol{O}$ implies $\vec{y}^T = \vec{x}^T\boldsymbol{O}$. The transformation being orthogonal, has a Jacobian equal to 1, $J = |\det \boldsymbol{O}| = 1$, and the integral decouples into n one-dimensional Gaußian integrals:

$$I_1(\boldsymbol{A}) = \prod_{i=1}^{n} \int \mathrm{d}y_i\, \mathrm{e}^{-\frac{1}{2}a_i y_i^2} = \sqrt{\frac{(2\pi)^n}{\prod_{i=1}^n a_i}} = \sqrt{\frac{(2\pi)^n}{\det \boldsymbol{A}}}, \tag{A.5}$$

where we used the basic Gaußian integral for each component. □

We can extend the result of the integral above to the complex symmetric case with positive-definite real part. Let $\boldsymbol{B}$ be such matrix. Using the fact that a complex symmetric matrix can be decomposed as (called Takagi's factorization)

$$\boldsymbol{B} = \boldsymbol{U}\boldsymbol{D}\boldsymbol{U}^T, \tag{A.6}$$

with $\boldsymbol{U}$ a unitary matrix and $\boldsymbol{D}$ a diagonal matrix, we can perform the coordinate change

$$\vec{x} = (\boldsymbol{U}^T)^{-1}\vec{y}, \tag{A.7}$$

to use the result in Eq. (A.2) for the diagonal factor. Explicitly

$$I_1(\boldsymbol{B}) = \int_{-\infty}^{\infty} \mathrm{d}\vec{y} \frac{1}{\det \boldsymbol{U}^T} \mathrm{e}^{-\frac{1}{2}\vec{y}^T \boldsymbol{U}^{-1}\boldsymbol{D}\boldsymbol{U}^T(\boldsymbol{U}^T)^{-1}\vec{y}} \tag{A.8}$$

$$= \frac{1}{\det \boldsymbol{U}^T}\sqrt{\frac{(2\pi)^n}{\det \boldsymbol{D}}} = \sqrt{\frac{(2\pi)^n}{\det \boldsymbol{B}}}, \tag{A.9}$$

where we have used the result in Eq. (A.2) for the diagonal piece and $\det \boldsymbol{B} = \det^2 \boldsymbol{U} \det \boldsymbol{D}$ in the last step. This shows that the integral in Eq. (A.2) applies without modification to complex symmetric matrices with a positive-definite real part.
Now let us include some external source vector $\vec{J}$ and prove the following

$$I_2(\boldsymbol{A}) \equiv \int_{-\infty}^{\infty} \mathrm{d}\vec{x}\, \mathrm{e}^{-\frac{1}{2}\vec{x}^T\boldsymbol{A}\vec{x}+\vec{J}^T\vec{x}} = \sqrt{\frac{(2\pi)^n}{\det \boldsymbol{A}}}\, \mathrm{e}^{\frac{1}{2}\vec{J}^T\boldsymbol{A}^{-1}\vec{J}}, \tag{A.10}$$

for a complex symmetric $n \times n$ matrix $\boldsymbol{A}$ with positive-definite real part.

Proof. We can recycle the decomposition in the proof of I_1, and perform the same coordinate change for $\vec{x}$ while rewriting $\vec{u}^T = \vec{J}^T(\boldsymbol{U}^T)^{-1}$. This way we can write I_2 as

$$\begin{aligned} I_2(\boldsymbol{A}) &\equiv \int_{-\infty}^{\infty} \mathrm{d}\vec{x}\, \mathrm{e}^{-\frac{1}{2}\vec{x}^T\boldsymbol{A}\vec{x}+\vec{J}^T\vec{x}} = \int_{-\infty}^{\infty} \mathrm{d}\vec{y} \frac{1}{\det \boldsymbol{U}^T} \mathrm{e}^{-\frac{1}{2}\vec{y}^T\boldsymbol{D}\vec{y}+\vec{u}^T\vec{y}} \\ &= \frac{1}{\det \boldsymbol{U}^T}\int_{-\infty}^{\infty}\left(\prod_{j=1}^{n}\mathrm{d}y_j\right)\exp\left(-\frac{1}{2}\sum_{j=1}^{n} d_j y_j^2 + u_j y_j\right) \\ &= \frac{1}{\det \boldsymbol{U}^T}\prod_{j=1}^{n}\mathrm{e}^{\frac{u_j^2}{2d_j}}\sqrt{\frac{2\pi}{d_j}} = \frac{1}{\det \boldsymbol{U}^T}\sqrt{\frac{(2\pi)^n}{\det \boldsymbol{D}}}\,\mathrm{e}^{\frac{1}{2}\vec{u}^T\boldsymbol{D}^{-1}\vec{u}} \\ &= \frac{1}{\det \boldsymbol{U}^T}\sqrt{\frac{(2\pi)^n}{\det \boldsymbol{D}}}\,\mathrm{e}^{\frac{1}{2}\vec{J}^T(\boldsymbol{U}^T)^{-1}\boldsymbol{D}^{-1}\boldsymbol{U}^{-1}\vec{J}} = \sqrt{\frac{(2\pi)^n}{\det \boldsymbol{A}}}\,\mathrm{e}^{\frac{1}{2}\vec{J}^T\boldsymbol{A}^{-1}\vec{J}}, \end{aligned} \tag{A.11}$$

where Takagi's factorization was used, Eq. (A.6), for $\boldsymbol{A}$ and we completed the square for each component to get to the previous to last line. □

Gaußian integrals can also be used in the case of $2n$ real variables with holomorphic integrands by using an holomorphic set of variables, z and $\bar{z}$, which are to be considered independent and simply a replacement of say x and y. In this sense, we have, for example, that the basic Gaußian integral is expressed as

$$\frac{1}{2\pi}\int \mathrm{d}x\,\mathrm{d}y\,\mathrm{e}^{-\frac{1}{2}\alpha(x^2+y^2)} = \int \frac{\mathrm{d}z\,\mathrm{d}\bar{z}}{2\mathrm{i}\pi}\,\mathrm{e}^{-\alpha\bar{z}z} = \frac{1}{\alpha}, \qquad \text{for} \quad \alpha > 0, \tag{A.12}$$

where we have employed the coordinate change

$$z = \frac{1}{\sqrt{2}}(x + \mathrm{i}y), \qquad \bar{z} = \frac{1}{2}(x - \mathrm{i}y). \tag{A.13}$$

The last integral we will include and was used in the main text is

$$\int \left(\prod_{i=1}^{n} \frac{\mathrm{d}z_i \, \mathrm{d}\bar{z}_i}{2\mathrm{i}\pi} \right) \exp\left[-A(\bar{\mathbf{z}}, \mathbf{z}) + \bar{\mathbf{b}} \cdot \mathbf{z} + \bar{\mathbf{z}} \cdot \mathbf{b} \right] = \frac{1}{\det \mathbf{A}} \, \mathrm{e}^{\bar{\mathbf{b}} \, \boldsymbol{A}^{-1} \, \mathbf{b}}, \tag{A.14}$$

where bold small-caps letters stand for vectors and the equation holds for a hermitian positive quadratic form $A(\bar{\mathbf{z}}, \mathbf{z}) = \bar{\mathbf{z}}^T \boldsymbol{A} \, \mathbf{z}$.

Proof. For a quadratic form corresponding to a Hermitian positive matrix $\boldsymbol{A}$ we can find unitary $\boldsymbol{U}$ such that

$$\boldsymbol{A} = \boldsymbol{U} \boldsymbol{D} \boldsymbol{U}^\dagger, \tag{A.15}$$

with $\boldsymbol{D}$ real positive and diagonal. By using the coordinate change

$$\mathbf{z}' = \boldsymbol{U}^\dagger \mathbf{z}, \qquad \bar{\mathbf{z}}' = \bar{\mathbf{z}}^T \boldsymbol{U}. \tag{A.16}$$

Each coordinate change contributes a Jacobian factor but in this case $\det U = 1$, so that employing Eq. (A.12) for each direction, we are led immediately to the result valid for $\mathbf{b} = \bar{\mathbf{b}} = 0$.
For the case of non-zero sources, we can employ the coordinate change $\{\mathbf{z}, \bar{\mathbf{z}}\} \to \{\mathbf{v}, \bar{\mathbf{v}}\}$ given by

$$\mathbf{z} = \mathbf{v} + \boldsymbol{A}^{-1} \mathbf{b}, \qquad \bar{\mathbf{z}} = \bar{\mathbf{v}} + \bar{\mathbf{b}} \boldsymbol{A}^{-1}, \tag{A.17}$$

to factor out the source (linear) terms and then use the source-free diagonalization. □

B. Codes

The codes in the following compute the Green's function corresponding to the longitudinal direction of a gauge field and a Goldstone boson for a given set of parameters for the couplings, for a polynomial potential up to order 6 as described in the body of the document in Sec. 4.2.1. It uses the planar-wall approximation to reduce the problem to a radial direction corresponding to the radius of the nucleated bubble and consequently, the only variable on which the bounce solution itself depends on. Tangential components are Fourier transformed and their effects included by means of the momentum vector $\vec{k}$. The gauge choice has been fixed as to decouple the Goldstone mode from all but the longitudinal component of the gauge field, i.e., $\zeta = \xi = 1$.
This appendix contains the following code files which address the remaining coupled sector of A_4 and G:

- exactLowK.m
- facLowerBlock.m
- coinLimitV2.m
- compiler.m

along with the unix scripts:

- compBaseFun.sh
- compIteration.sh

The code was run in TUM's Physics Department cluster using SGE through the command:

```
qsub -j yes -N "batch30-40" submitBatch.sh "compIteration.sh" 30 39 2
```

The j and N are options of `qsub` which allow to obtain a single file containing the standard output and any possible errors. The job is also named as "batch30-40". The job runs then the bash script `submitBatch.sh` with the subsequent options:

- Argument 1: File to be run. Can be either `"compBaseFun.sh"` or `"compIteration.sh"`.
- Argument 2: k_{in} - Initial value of tangential momentum e.g 30.
- Argument 3: k_{end} - Final value of tangential momentum e.g 39 (means up to 40.0)
- Argument 4: Type of background (bounce) to be used. Can be 0 for a constant background, 1 for a linear background or 3 to load a file with a pre-saved solution)

As a default the code computes in between the range of momenta $(k_{\text{in}}, k_{\text{end}} + 1)$ given, with steps of 0.1. It uses a tolerance of 1×10^{-5} and samples 100 points between -1 and 1. Solutions are saved in an external folder in the `.wdx` format readable with `Mathematica` through the command `get`.
The script `compBaseFun.sh` should be run first over the values of momenta that are desired and then one can compute corrections with `compIteration.sh` for as many iterations as needed. The base function takes around 100 MB while the corrections size is around 700 kB each. The files saved contain the complete two point Green's functions for this physical system., therefore, in order to extract coincident limit Green's functions one can use the

file `coinLimitV2.m` as follows:

```
find -name "*k[1-4][0-9].*Iter0.wdx" -exec bash -c 'math
 -run -noprompt <coinLimitV2.m "$1"' - {} \;
```

on an unix console. This will take the base function, add the corrections and compute the coincident limit. It will save a new file with the coincident Green's function.
In order to reconstruct the full coincident Green's function, we collect the data for all **k**s computed above and then interpolate. We do this in two steps. First one uses `compiler.nb` to produce csv files which already include the data from k to $k+1$ (one must introduce the component of the Green's function to be compiled $G_{m,n}$). Then one can use `cat` on a unix console to concatenate all these .csv files, e.g.

```
cat data*-11.csv > dataCompiled11.csv
```

Finally, this file can be loaded, with any statistical software, like Mathematica, to be analyzed and processed. We recommend using interpolations of low order, choosing order one may give better results than Mathematica's default (order 3).
We list the codes mentioned above here:

exactLowK.m

```
(* ::Package:: *)

$HistoryLength=0;
kk = ToExpression[StringJoin[$CommandLine[[-2]]]];
numPoints = ToExpression[$CommandLine[[-1]]];
fileName = StringJoin["exactK",ToString[N[kk,3]]];
Print[StringJoin["Using␣file:␣", fileName, "␣and␣computing␣for␣
    momentum␣", ToString[N[kk]]]];
tol = 1*10^(-5);
myInf = 1;
g = 1/2;
\[Alpha] = 2;
\[Lambda] =
    -2.025457177930057218161330673298321202006040311424295340;
\[Beta] = 1/2;
Print[Directory[]];
F1[h_, u_] = g*h[u];
F2[hPrime_, u_] = g*hPrime[u];
F3[h_, \[Xi]_, \[Zeta]_, u_] = \[Alpha] + \[Lambda]*h[u]^2 +
    (3/4*\[Beta]) h[u]^4 + \[Zeta]^2*F1[h, u]^2/\[Xi];
f2[\[Xi]_, \[Zeta]_] = (\[Zeta] + \[Xi])/\[Xi];
MyHeaviside[x_] = Piecewise[{{HeavisideTheta[x], x != 0}, {1/2, x
    == 0}}];
{bounceInterp, bounceInterpP} = Get["bounceInterps"];
dd = 1*1 + 1;
eq1[A_Symbol, B_Symbol, u_, k_, \[Xi]_, \[Zeta]_] = (2 u A'[u] - (1
     - u^2) A''[u] + (F1[h, u]^2 + k^2)*A[u]/(1 - u^2)) + f2[\[Xi],
    \[Zeta]]*F2[hPrime, u]*B[u] == 0;
eq2[A_Symbol, B_Symbol, u_, k_, \[Xi]_, \[Zeta]_] = f2[\[Xi], \[
    Zeta]]*F2[hPrime, u]*A[u] + (2 u B'[u] - (1 - u^2) B''[u] + (k^2
     + F3[h, \[Xi], \[Zeta], u])*B[u]/(1 - u^2)) == 0;
```

```
24 eqs[G11_Symbol, G12_Symbol, G21_Symbol, G22_Symbol, u_, k_] = {eq1[
       G11, G21, u, k, 1, 1], eq1[G12, G22, u, k, 1, 1], eq2[G11, G21,
       u, k, 1, 1], eq2[G12, G22, u, k, 1, 1]};
25 bdC[B1_Symbol, B2_Symbol, uP_, jump_] = {B1[-myInf + 10 tol] == 0,
       B2[myInf - 10 tol] == 0, B1[uP] == B2[uP], B2'[uP] - B1'[uP] ==
       jump};
26 greenMat = Table[{ToExpression[StringJoin["g", ToString[i],
       ToString[j], "l"]], ToExpression[StringJoin["g", ToString[i],
       ToString[j], "r"]]}, {i, 1, dd}, {j,1, dd}];
27 eqsAll[u_, k_] = Flatten[Table[eqs[greenMat[[1, 1, n]], greenMat
       [[1, 2, n]], greenMat[[2, 1, n]], greenMat[[2, 2, n]], u, k], {n
       , 1, 2}]] /. {h -> bounceInterp, hPrime -> bounceInterpP};
28 bdCs[uP_, jumps_] := Flatten[Table[If[i == j, bdC[greenMat[[i, j,
       1]], greenMat[[i, j, 2]], uP, jumps[[i]]], bdC[greenMat[[i, j,
       1]], greenMat[[i, j, 2]], uP, 0]], {i, 1, dd}, {j, 1, dd}]];
29 greenFuncs[u_] = Table[greenMat[[i, j, n]][u], {i, 1, dd}, {j, 1,
       dd}, {n, 1, 2}];
30 greenCoin[uP_?NumericQ, k_] := Module[{sol,greenSol,u,file},
31 sol = Quiet[NDSolve[Join[eqsAll[u, k], bdCs[uP, {-1/(1 - uP^2),
       -1/(1 - uP^2)}]], Flatten[greenFuncs[u]], {u, -myInf + tol,
       myInf - tol}, Method -> {"EquationSimplification" -> "Solve"},
       WorkingPrecision -> 15]];
32 greenSol = Table[(MyHeaviside[uP - u]*greenFuncs[u][[i, j, 1]] +
       MyHeaviside[u - uP]*greenFuncs[u][[i, j, 2]]), {i, 1, dd}, {j,
       1, dd}] /. sol[[1]];
33 PutAppend[{{{uP,#[[1,1]]},{uP,#[[1,2]]}},{{uP,#[[2,1]]},{uP
       ,#[[2,2]]}}}& /@{greenSol/.u->uP},fileName];
34 file=OpenAppend[fileName];
35 WriteString[file,","];
36 Close[file];
37 Print[uP];];
38 Print["Definitions␣loaded␣properly"];
39
40 file=OpenWrite[fileName];
41 WriteString[file,"{"];
42 Close[file];
43 step = 2(myInf-100tol)/(numPoints-1);
44 Print[StringJoin["Using␣a␣step␣of␣:␣", ToString[N[step]]]];
45 endPointL=-.999`16;
46 endPointR=.999`16-step;
47 Do[greenCoin[x,kk],{x,endPointL,endPointR,step}];
48 greenCoin[endPointR+step,kk];
49 file=OpenAppend[fileName];
50 WriteString[file,"}"];
51 Close[file];
52
53 Quit[];
```

Note that for higher momenta, it is set by default in line 62 that only the first iteration is done, the condition can be removed to compute more iterations on one run.

facLowerBlock.m

```
1 (* ::Package:: *)
2
3 ClearAll[G,x,xP,ggg];
```

```
(* Reading parameters from command line *)
k = ToExpression[$CommandLine[[-4]]];
err = ToExpression[$CommandLine[[-3]]];
numpoints = ToExpression[$CommandLine[[-2]]];
background = ToExpression[$CommandLine[[-1]]];

(*Setting up constants of the problem *)
tol = 1/100000;
myInf = 1;
\[Mu]2 = 2;
\[Lambda] = -2.025457177930057218161330673298321202006040 3`50;
\[Beta] =1/2;
g=1/2;
(* Potential formula U[x_]:= \[Mu]2*x^2/2+\[Lambda]*x^4/4+\[Beta]*x
    ^6/8; *)
\[CurlyPhi][u_]= If[background==0,background,If[background==1,-Sqrt
    [2] (u-1)/2,If[background==2,Get["tunedBouncePhi6.wdx"]/.u->(
    myInf-tol),Get["tunedBouncePhi6.wdx"]/.u->u]]];
MyHeaviside[u_]:=Piecewise[{{HeavisideTheta[u],u!= 0},{1/2,u==0}}];
MOp[f_,k_,\[CurlyPhi]_,u_]:=2u D[f,u]-(1-u^2)D[D[f,u],u]+(k^2 f+ g
    ^2 \[CurlyPhi][u]^2f)/(1-u^2);
NOp[f_,k_,\[CurlyPhi]_,u_]:=MOp[f,k,\[CurlyPhi],u]+(\[Mu]2 f + \[
    Lambda] \[CurlyPhi][u]^2f+3\[Beta] \[CurlyPhi][u]^4 f/4 )/(1-u
    ^2);
eq1[k_,z_]:= MOp[G[z],k,\[CurlyPhi],z];
eq2[k_,z_]:= NOp[G[z],k,\[CurlyPhi],z];

(* For constant backgrounds the working precision must be above 40
    to avoid noise, for non-constant background it is not necessary
    to specify *)
If[background == 0,
sol[k_,pm_,equation_]:=NDSolve[{equation[k,u]==0,G[pm*(myInf-tol)
    ]==0,G'[pm(myInf-tol)]==1},G,{u,-myInf+tol,myInf-tol},
    WorkingPrecision->60,MaxSteps->30000,Method->{"
    StiffnessSwitching",Method->{"ExplicitRungeKutta",Automatic}}],
sol[k_,pm_,equation_]:=NDSolve[{equation[k,u]==0,G[pm*(myInf-tol)
    ]==0,G'[pm(myInf-tol)]==1},G,{u,-myInf+tol,myInf-tol},
    WorkingPrecision->24,AccuracyGoal->12,MaxSteps->50000,
    InterpolationOrder->All,MaxStepSize->4*(myInf-10tol)/numpoints
    ]];
f1less[eq_,k_,u_]:=G[u]/.sol[k,-1,eq][[1]];
f1great[eq_,k_,u_]:=G[u]/.sol[k,1,eq][[1]];
wronsk[eq_,k_,u_]:=-f1less[eq,k,u]*D[f1great[eq,k,u],u] +f1great[eq
    ,k,u]*D[f1less[eq,k,u],u];
green[eq_,k_,u_,uP_]:=(MyHeaviside[uP-u]*f1less[eq,k,u]*f1great[eq,
    k,uP]+MyHeaviside[u-uP]*f1great[eq,k,u]*f1less[eq,k,uP])/(wronsk
    [eq,k,uP](1-uP^2));

(*Interpolating subroutine *)
myInterp[f_,numPoints_]:=Module[{i,j,x,xP,pointTemp,step,points,
    valF,f2,state,ParallelPrint,status=""},
LaunchKernels[];
SetSharedVariable[points];
SetSharedFunction[ParallelPrint];
SetSharedFunction[status];
ParallelPrint[str_]:=PrintTemporary[str];
```

```
41 points={{{},{}},{{},{}}};
42 step=(2myInf-20tol)/numPoints;
43 ParallelDo[
44 For[x=-myInf+10tol,x<=xP,x=x+step,f2=f[x,xP];
45 For[i=1,i<3,i++, For[j=1,j<3,j++, valF =f2[[i,j]]; AppendTo[points
       [[i,j]],{x,xP,valF}]; If[x!=xP,AppendTo[points[[i,j]],{xP,x,valF
       }]]; ]]];
46 state = StringJoin[ToString[N[Length[points[[1,1]]]*100/(numPoints
       +1)^2,3]],"% of interpolation completed"];
47 (* Uncomment the next line to print interpolation status update *)
48 status = ParallelPrint[state];
49 ,{xP,-myInf+10tol,myInf-10tol,step}]; Map[Interpolation[#,
       InterpolationOrder->3,Method->"Spline"]&,points,{2}]];
50
51 (* Integrating and iterating subroutine *)
52 proc[k0_,err_,numPoints_]:=Module[{k=k0,g11,g22,gg0,c,kern,u,uP,
       gggNoInter,gggInterp,i,j,w,t,iter,error,gTemp},
53 g11[u_,uP_]=green[eq1,k,u,uP];
54 g22[u_,uP_]=green[eq2,k,u,uP];
55 gg0[u_,uP_]={{g11[u,uP],0},{0,g22[u,uP]}};
56 Put[gg0[x,xP],StringJoin["bk",ToString[background],"k",ToString[N[k
       ,3]],"ggIter",ToString[0],".wdx"]];
57 Print["0-th Order solution computed"];
58 gTemp[u_,uP_]={{g11[u,uP],0},{0,g22[u,uP]}};
59 ggg[u_,uP_] = gTemp[u,uP];
60 c[w_]={{0,2*g*\[CurlyPhi]'[w]},{2*g*\[CurlyPhi]'[w],0}};
61 iter = 1;
62 error = If[background==0,0,100];
63 While[error>err,
64 t = SessionTime[];
65 kern[u_,w_,uP_]=-gg0[u,w] . c[w] . gTemp[w,uP];
66 gggNoInter[u_?NumericQ,uP_?NumericQ]:=Quiet[Map[NIntegrate[#,{w,-
       myInf+10tol,myInf-10tol},WorkingPrecision->30,AccuracyGoal
       ->15]&,kern[u,w,uP]]];
67 gggInterp=myInterp[gggNoInter,numPoints];
68 Print[StringJoin["Interpolation on iteration number: ",ToString[
       iter], ", computed."]];
69 Print[N[SessionTime[]-t,5]];
70 error=Abs[1-ggg[0,0][[1,1]]/(gggInterp[[1,1]][0,0]+ggg[0,0][[1,1]])
       ]+Abs[1-ggg[0,0][[1,2]]/(gggInterp[[1,2]][0,0]+ggg[0,0][[1,2]])
       ];
71 Print[StringJoin["Current error: ", ToString[InputForm[error*100]]
       , "%"]];
72 gTemp[u_,uP_] = Table[Table[gggInterp[[i,j]][u,uP],{j,1,2}],{i
       ,1,2}];
73 ggg[u_,uP_] = ggg[u,uP] + gTemp[u,uP];
74 Put[gTemp[x,xP],StringJoin["bk",ToString[background],"k",ToString[N
       [k,3]],"gTempIter",ToString[iter],".wdx"]];
75 iter++;
76 ];
77 (* Put[ggg[x,xP],StringJoin["bk",ToString[background],"k",ToString[
       k],"ggIter",ToString[iter-1],".wdx"]]; *)
78 Print[StringJoin["Number of iterations needed: ",ToString[iter
       -1]]];
79 ];
80
```

```
81 (*Executed commands on run *)
82 myPath = StringJoin["/space/ga32buw/k",ToString[N[k,3]],"/"] ;
83 CreateDirectory[myPath];
84 SetDirectory[myPath];
85 Print[StringJoin["Working␣directory␣is␣now", myPath]];
86 Print[StringJoin["Computing␣lower␣block␣Greens'␣func␣for␣k=",
       ToString[N[k,3]],"␣and␣up␣to␣a␣relative␣error␣of␣", ToString[
       InputForm[err]],"␣with␣", ToString[numpoints],"␣points."]];
87 If[background==0,Print["Background␣assumed␣constant."],If[
       background==1,Print["Using␣constant␣slope␣toy-bounce␣as␣
       background."],If[background==2,Print["Using␣homogeneous␣false␣
       vacua"],Print["Using␣saved␣bounce␣for␣Phi^6␣theory."]]]];
88 proc[k,err,numpoints];
89 Print[StringJoin["Out␣saved␣in:␣",myPath, "␣with␣the␣names␣bk",
       ToString[background],"k",ToString[N[k,3]],"ggIter0.wdx"]];
90
91 Exit[];
```

The output of the above codes, as explained above, can be processed by running the code named `coinLimitV2.m`, to obtain an interpolating function which includes corrections and where the coincident limit has been taken, that is the two-point function are evaluated at the same point. The script looks for files in the directory input in line 5, in the variable `baseName` and outputs the functions after adding corrections and taking the coincident limit to the directory specified in line 18.

coinLimitV2.m

```
1  (* ::Package:: *)
2
3  ClearAll[x,u];
4  fileName = StringReplace[ToString[$CommandLine[[-1]]],"./"->""];
5  baseName = "/scratch/VacuumDataRaw/";
6  Print[StringJoin["File:␣",baseName,fileName,"␣opened."]];
7  ggbase[u_,uP_]=Check[Get[StringJoin[baseName,fileName]]/.{x->u,xP->
       uP},Print["File␣Damaged"];Quit[];];
8  iter=1;
9  gCorrections[u_,uP_] ={};
10 fileNameIter = StringReplace[fileName,"ggIter0.wdx"->"gTempIter"];
11 name[iter_] := StringJoin[baseName,fileNameIter,ToString[iter],".
       wdx"];
12 While[FileExistsQ[name[iter]],
13 gTemp[u_,uP_]=Get[name[iter]]/.{x->u,xP->uP};
14 AppendTo[gCorrections[u,uP],gTemp[u,uP]];
15 iter++;
16 ];
17 gg0[u_,uP_]=ggbase[u,uP] +Plus@@gCorrections[u,uP];
18 SetDirectory["/scratch/VacuumData/"];
19 coinName = StringReplace[FileNameTake[fileName],"ggIter0.wdx"->"
       coin.wdx"];
20 gg[x_]=gg0[x,x];
21 Put[gg[x],coinName];
22 Print[StringJoin[coinName,"␣file␣saved␣succesfully."]];
23 Exit[];
```

compiler.m

```
tol=1/10000;
myInf=1;
SetDirectory["/scratch/VacuumData/"];
ClearAll[x];
compile[m0_,n0_]:=Module[{m=m0,n=n0,data,gTemp},
ClearAll[data];
For[j=0,j<1,j++,
data={};
For[i=1,i<10,i++,
gTemp[u_]=Get[StringJoin["bk3k",ToString[j],".",ToString[i],"00coin
    .wdx"]][[m,n]]/.x->u;
data = Join[data,Table[{u,j+i/10,Evaluate[gTemp[u]]},{u,-myInf+tol,
    myInf-tol,1/20}]];
ClearAll[gTemp];];
Export[StringJoin["compiled/data",ToString[j],"-",ToString[m],
    ToString[n],".csv"],data];
Print[StringJoin["Saved k=",ToString[j]]];
];
ClearAll[data];
For[j=1,j<10,j++,
data={};
For[i=0,i<10,i++,
gTemp[u_]=Get[StringJoin["bk3k",ToString[j],".",ToString[i],"0coin.
    wdx"]][[m,n]]/.x->u;
data = Join[data,Table[{u,j+i/10,gTemp[u]},{u,-myInf+tol,myInf-tol
    ,1/20}]];
ClearAll[gTemp];];
Export[StringJoin["compiled/data",ToString[j],"-",ToString[m],
    ToString[n],".csv"],data];
Print[StringJoin["Saved k=",ToString[j]]];
];
ClearAll[data];
For[j=10,j<45,j++,
data={};
For[i=0,i<10,i++,
gTemp[u_]=Get[StringJoin["bk3k",ToString[j],".",ToString[i],"coin.
    wdx"]][[m,n]]/.x->u;
data=Join[data,Table[{u,j+i/10,gTemp[u]},{u,-myInf+tol,myInf-tol
    ,1/20}]];
ClearAll[gTemp];];
Export[StringJoin["compiled/data",ToString[j],"-",ToString[m],
    ToString[n],".csv"],data];
Print[StringJoin["Saved k=",ToString[j]]];
];
ClearAll[data];
For[j=45,j<46,j++,
data={};
For[i=0,i<1,i++,
gTemp[u_]=Get[StringJoin["bk3k",ToString[j],".",ToString[i],"coin.
    wdx"]][[m,n]]/.x->u;
data=Join[data,Table[{u,j+i/10,gTemp[u]},{u,-myInf+tol,myInf-tol
    ,1/20}]];
ClearAll[gTemp];];
Export[StringJoin["compiled/data",ToString[j],"-",ToString[m],
```

```
    ToString[n],".csv"],data];
44 Print[StringJoin["Saved k=",ToString[j]]];
45 ];
46 Quit[];
```

Other scripts useful for using the cluster at the physics department of TUM. The following just runs the above Mathematica which obtains the 0-th iteration, or base function, namely the diagonals of the coupled block.

compBaseFun.sh

```
1 #!/bin/bash
2 #$ -cwd
3 echo -n "Job $JOB_ID running on "
4 hostname
5 date
6 echo "Parameters k=$1, RelativeError=$2, numPoints=$3, background=
    $4"
7 math -run -noprompt -nohup <facLowerBlock.m $1 $2 $3 $4
```

The following calls a similar script to `facLowerBlock.m` which does not compute the base function, but only computes corrections on top of an existing one, this is supposed to be iterated until the precision desired is reached.

compIteration.sh

```
1 #!/bin/bash
2 #$ -cwd
3 echo -n "Job $JOB_ID running on "
4 hostname
5 date
6 echo "Parameters k=$1, RelativeError=$2, numPoints=$3, background=
    $4"
7 math -run -noprompt -nohup <facLoopV4.m $1 $2 $3 $4
```

The above scripts can easily be combined and used by running the following bash script, which takes care of submitting the jobs for a range of tangential momentum $\mathbf{k}$, it can either compute the base functions or iterations, by specifying which of the above two scripts to call for. Additionally, the background can be specified: 0 uses a constant value field equal to 0, 1 uses a toy bounce with a constant gradient and 2 uses the bounce for our model which was computed and saved in `.wdx` format before hand.

submitBatch.sh

```
#!/bin/bash
#$ -cwd
sourceFile=$1
background=$4

for j in `seq $2 $3`;
do
for i in {1..10};
do

        if [ $sourceFile == "compBaseFun.sh" ];
        then
                sleep 2
                qsub -cwd -j yes -N "K$j.$((i))Base" $sourceFile "
                   $j+$i*1/10" "200" 100 $background
        else
                sleep 20
                qsub -r yes -cwd -q longrun -N "K$j.$((i))mom$2" -j
                    yes -l h_vmem=21G -R y -pe smp 7 $sourceFile "
                   $j+$i*1/10" "1" 100 $background
        fi
done
done
```

C. Arbitrary rotations of the time axis and complex fermion masses

Ideas concerning Euclidean analogs of Minkowskian Green's functions, and other quantities appearing in field theory over a Minkowskian metric, have been around for a while[179, 180], specially from a perspective of algebraic quantum field theory and Wightman axioms (see [172]). Although we do not follow an axiomatic and mathematical approach for the construction of the analogs used in the text, we provide here explicit computation and verification of some of the expressions for the objects, decompositions and similar used in Chap. 6.

We present here the details and properties involved when studying the Euclidean analogs required for the spectral decomposition of the Dirac operator about a single instanton background. Consider the Euclidean Dirac operator from Eq. (6.1.11). Let us denote the discrete normalizable modes by ψ_n^{E} with eigenvalues ξ_n^{E}. For these modes, the orthogonality property holds,

$$(\psi_m^{\mathrm{E}}, \psi_n^{\mathrm{E}}) = \int \mathrm{d}^4 x^{\mathrm{E}}\, \psi_m^{\mathrm{E}\dagger}(x^{\mathrm{E}}) \psi_n^{\mathrm{E}}(x^{\mathrm{E}}) = \delta_{mn}\,. \tag{C.18}$$

The continuum part of the spectrum consists in principle of non-normalizable eigenfunctions. These can be taken to be solutions that asymptotically behave as plane waves in the infinite past, when $x_4 \to -\infty$, and which can be characterized by their asymptotic Euclidean four-momentum k_m^{E} with $m = 1, \ldots, 4$. We label these solutions for the continuum part as $\psi_{\{k^{\mathrm{E}}\}}^{\mathrm{E}} = \psi_{\{\vec{k}, k_4\}}^{\mathrm{E}}$ and their corresponding eigenvalues as $\xi_{\{k^{\mathrm{E}}\}}^{\mathrm{E}} = \xi_{\{\vec{k}, k_4\}}^{\mathrm{E}}$. By construction, either the discrete or the continuum modes satisfy

$$\begin{aligned} (\not{D}^{\mathrm{E}} + m\, \mathrm{e}^{\mathrm{i}\alpha\gamma^5})\psi_\xi^{\mathrm{E}}(x^{\mathrm{E}}) &= \xi^{\mathrm{E}} \psi_\xi^{\mathrm{E}}(x^{\mathrm{E}})\,, \\ (\not{D}^{\mathrm{E}} + m\, \mathrm{e}^{\mathrm{i}\alpha\gamma^5})^\dagger \psi_\xi^{\mathrm{E}}(x^{\mathrm{E}}) &= (-\not{D}^{\mathrm{E}} + m\, \mathrm{e}^{-\mathrm{i}\alpha\gamma^5})\psi_\xi^{\mathrm{E}}(x^{\mathrm{E}}) = (\xi^{\mathrm{E}})^* \psi_\xi^{\mathrm{E}}(x^{\mathrm{E}})\,, \end{aligned} \tag{C.19}$$

which can be used to find a Klein-Gordon equation analog

$$|\xi^E|^2 \psi_\xi^{\mathrm{E}} = (\not{D}^{\mathrm{E}} + m\, \mathrm{e}^{\mathrm{i}\alpha\gamma^5})(-\not{D}^{\mathrm{E}} + m\, \mathrm{e}^{-\mathrm{i}\alpha\gamma^5})\psi_\xi^{\mathrm{E}} \tag{C.20}$$

$$= (-(\partial_m - \mathrm{i}A^{\mathrm{E}}{}_m)(\partial_m - \mathrm{i}A^{\mathrm{E}}{}_m) + m^2)\psi_\xi^{\mathrm{E}}\,, \tag{C.21}$$

implying the relation

$$((\partial_m - \mathrm{i}A^{\mathrm{E}}{}_m)(\partial_m - \mathrm{i}A^{\mathrm{E}}{}_m) - m^2 + |\xi^E|^2)\psi_\xi^{\mathrm{E}} = 0\,. \tag{C.22}$$

The continuum eigenfunctions fulfill

$$\psi_{\{k^{\mathrm{E}}\}}^{\mathrm{E}} \sim \mathrm{e}^{\mathrm{i}k_m x_m} \text{ as } x_4 \to -\infty\,, \tag{C.23}$$

so that the relation above leads to

$$|\xi_{\{k^{\mathrm{E}}\}}^{\mathrm{E}}|^2 = m^2 + k_m k_m\,, \tag{C.24}$$

for vanishing background gauge fields, such as the $k = \pm 1$ instanton configuration. Given that for the case of interest, the fields go to zero in the infinite future, we expect a solution with a given asymptotic momentum k_m to behave as the same plane wave at $x_4 \to \infty$ in analogy to scattering problems. The elements of such basis of solutions then observe

$$(\psi_{\{k^{\mathrm{E}}\}}^{\mathrm{E}}, \psi_{\{k^{\mathrm{E}\prime}\}}^{\mathrm{E}}) = \delta^4(k^{\mathrm{E}} - k^{\mathrm{E}\prime})\,. \tag{C.25}$$

As discussed in the text, the eigenvalues of the Euclidean massless Dirac equation are purely imaginary, so that in the massless limit, using Eq. (C.24), we have

$$\lambda^{\mathrm{E}}_{\{k^{\mathrm{E}}\}} \equiv \mathrm{i}\sqrt{k_m k_m}, \tag{C.26}$$

with which we can write the eigenvalues in Eq. (6.1.27) in terms of the asymptotic momenta as

$$\xi^{\mathrm{E}}_{\pm\{k^{\mathrm{E}}\}} = m_{\mathrm{R}} \pm \mathrm{i}\sqrt{k_m k_m + m_{\mathrm{I}}^2}\,. \tag{C.27}$$

We describe now how to generalize the Wick rotation, described above, to arbitrary angles in the complex plane. Our objective here, as in the main text, is to not only be able to perform certain integrals employing a Wick rotation, but to completely rewrite the original field theory in an Euclidean metric. The procedure here described is closely related to that presented in [181] and inspired in previous work by Schwinger[182], Osterwalder and Schrader[179, 180]. However, it is just an adaptation of the methods in [36]. Within this appendix, we use θ as a continuous parameter related to the analytic continuation of the functions herein and is not to be confused with the θ parameter of the main text (see Eq. (6.1.6)). Recall how we define an arbitrary complex rotation

$$x_4 \to \mathrm{e}^{-\mathrm{i}(\theta-\frac{\pi}{2})}t, \tag{C.28}$$

which as a consequence, rotates the quadratic fermion terms in the Lagrangian as

$$-\not{D}^{\mathrm{E}} - m\,\mathrm{e}^{\mathrm{i}\alpha\gamma^5} \;\to\; \mathrm{i}\not{D}^{\theta} - m\,\mathrm{e}^{\mathrm{i}\alpha\gamma^5}\,, \qquad \not{D}^{\theta} = \gamma^{\theta\mu}(\partial_\mu - \mathrm{i}A^{\theta}_{\mu}(x))\,, \tag{C.29}$$

where

$$\begin{aligned} \gamma^{\theta 0} &= \mathrm{e}^{\mathrm{i}\theta}\gamma^0\,, & \gamma^{\theta i} &= \gamma^i\,, \\ A^{\theta 0}(x^0,\vec{x}) &= \mathrm{i}\,\mathrm{e}^{-\mathrm{i}\theta}A^{\mathrm{E}}{}_4(\vec{x}, x_4 = \mathrm{i}\,\mathrm{e}^{-\mathrm{i}\theta}x^0)\,, & A^{\theta i}(x^0,\vec{x}) &= A^{\mathrm{E}}{}_i(\vec{x}, x_4 = \mathrm{i}\,\mathrm{e}^{-\mathrm{i}\theta}x^0)\,. \end{aligned} \tag{C.30}$$

It can be checked that the matrices $\gamma^{\theta\mu}$, still satisfy the same Clifford algebra relation, $\{\gamma^{\theta\mu}, \gamma^{\theta\nu}\} = 2g^{\theta\mu\nu}$, as their Minkowskian analogs, for an accordingly rotated metric $g^{\theta\mu\nu} = \mathrm{diag}\{\mathrm{e}^{2\mathrm{i}\theta}, -1, -1, -1\}$. For the signature we are using in the document, $(+,-,-,-)$, there is an additional factor of i when trying to recover the Euclidean γ-matrices via $\theta = \pi/2$, however the operators appearing in Eq. (C.29) do correspond to each other without caveats for $\theta = \pi/2$.

As it has been studied in [36], the eigenfunctions of the Euclidean Dirac operator may be analytically continued to arbitrary rotations. The discrete part of the spectrum must only be continued by rotation of its time-like coordinate, while the continuum part requires an extra rotation of its fourth-momentum component k_4. Doing this we obtain discrete eigenfunctions, ψ^{θ}_n, with the same eigenvalues as in Euclidean space with the addition of a minus as in Eq. (C.29), compared to the operator used in the main text, explicitly

$$\psi^{\theta}_n(x) = \psi^{\theta}_n(x^0,\vec{x}) = \sqrt{\mathrm{i}\,\mathrm{e}^{-\mathrm{i}\theta}}\,\psi^{\mathrm{E}}_n(\vec{x}, x_4 = \mathrm{i}\,\mathrm{e}^{-\mathrm{i}\theta}x^0)\,, \quad \xi^{\theta}_n = -\xi^{\mathrm{E}}_n\,, \tag{C.31}$$

where the square root in front is a normalization factor and the complex root is taken in the principal branch. For the continuum spectrum, we need to rotate k_4 in order to keep the plane wave behavior at $t \to -\infty$, so we have

$$\psi^{\theta}_{\{k\}}(x) = \psi^{\theta}_{\{k^0,\vec{k}\}}(x^0,\vec{x}) = \psi^{\mathrm{E}}_{\{\vec{k},-\mathrm{i}\,\mathrm{e}^{\mathrm{i}\theta}k_0\}}(\vec{x}, x_4 = \mathrm{i}\,\mathrm{e}^{-\mathrm{i}\theta}x^0)\,, \quad \xi^{\theta}_{\{k^0,\vec{k}\}} = -\xi^{\mathrm{E}}_{\{\vec{k},-\mathrm{i}\,\mathrm{e}^{\mathrm{i}\theta}k_0\}}. \tag{C.32}$$

From now on, we label eigenvalues and eigenfunctions generically by ξ^θ and ψ^θ_ξ, independently of in which part of the spectrum they lie. For the transformations described above, we need to introduce a modified inner-product to keep the relations of orthogonality. We call

$$(\psi^\theta_\xi, \psi^\theta_{\xi'})_\theta = \int \mathrm{d}^4x\, \tilde{\psi}^\theta_\xi(x)\, \psi^\theta_{\xi'}(x)\,, \tag{C.33}$$

the θ-adjoint inner product, where the tilde denotes the following operation

$$\tilde{\psi}^\theta_n(x^0,\vec{x}) = \sqrt{\mathrm{i}\,\mathrm{e}^{-\mathrm{i}\theta}}\,(\psi^{\mathrm{E}}_n(\vec{x},x_4))^\dagger\Big|_{x_4=\mathrm{i}\,\mathrm{e}^{-\mathrm{i}\theta}x^0} = \mathrm{i}\,\mathrm{e}^{-\mathrm{i}\theta}\,(\psi^\theta_n(x^0,\vec{x}))^\dagger\Big|_{x^0\to-\,\mathrm{e}^{-2\mathrm{i}\theta}x^0}\,, \tag{C.34}$$

for the discrete modes and

$$\tilde{\psi}^\theta_{\{k^0,\vec{k}\}}(x^0,\vec{x}) = \Big(\psi^{\mathrm{E}}_{\{\vec{k},k_4\}}(\vec{x},x_4)\Big)^\dagger\Big|_{\substack{x_4=\mathrm{i}\,\mathrm{e}^{-\mathrm{i}\theta}x^0\\ k_4=-\,\mathrm{i}\,\mathrm{e}^{\mathrm{i}\theta}k^0}} = \psi^\theta_{\{k^0,\vec{k}\}}(x^0,\vec{x})^\dagger\Big|_{\substack{x^0\to-\,\mathrm{e}^{-2\mathrm{i}\theta}x^0\\ k^0\to-\,\mathrm{e}^{2\mathrm{i}\theta}k^0}}\,, \tag{C.35}$$

for the continuum modes. Within this definitions, and in order to remove any ambiguities, it is understood that we first perform the hermitian adjoint considering the original arguments and later evaluate them as indicated by the vertical bars. The discrete modes and continuum modes then satisfy orthogonality relations

$$(\psi^\theta_m, \psi^\theta_n)_\theta = \delta_{mn}\,, \tag{C.36}$$

$$(\psi^\theta_{\{k\}}, \psi^\theta_{\{k'\}})_\theta = \delta^4(k-k')\,, \tag{C.37}$$

respectively. For the last the relation, a cancellation occurs between the factors from the rotation and the continuation of the Euclidean Dirac delta. As shown in [36], the completeness of the set of eigenfunctions also follows from the completeness of the Euclidean set. With these properties, it is possible to write down a spectral decomposition for an arbitrarily rotated Dirac operator:

$$\mathrm{i}\not{D}^\theta - m\,\mathrm{e}^{\mathrm{i}\alpha\gamma^5} = \sum\!\!\!\!\!\!\int_{\xi^\theta} \xi^\theta \psi^\theta_\xi(x)\tilde{\psi}^\theta_\xi(x') \tag{C.38}$$

$$= \sum_n \xi^\theta_n\, \psi^\theta_n(x)\tilde{\psi}^\theta_n(x') + \int \mathrm{d}^4k\, \xi^\theta_{\{k\}}\psi^\theta_{\{k\}}(x)\tilde{\psi}^\theta_{\{k\}}(x')\,. \tag{C.39}$$

Similarly, we can expand its Green's function with the same projectors:

$$\begin{aligned} S^\theta(x,x') &\equiv (\mathrm{i}\not{D}^\theta - m\,\mathrm{e}^{\mathrm{i}\alpha\gamma_5})^{-1}(x,x') \\ &= \sum_n \frac{1}{\xi^\theta_n}\psi^\theta_n(x)\tilde{\psi}^\theta_n(x') + \int \mathrm{d}^4k \frac{1}{\xi^\theta_{\{k\}}}\psi^\theta_{\{k\}}(x)\tilde{\psi}^\theta_{\{k\}}(x')\,. \end{aligned} \tag{C.40}$$

This coincides with the analytic continuation of the Euclidean Green's function,

$$S^\theta(x,x') = -\mathrm{i}\,\mathrm{e}^{-\mathrm{i}\theta}S^{\mathrm{E}}(x^{\mathrm{E}},x^{\mathrm{E}\prime})|_{x_4\to\mathrm{i}\,\mathrm{e}^{-\mathrm{i}\theta}x^0,\,x'_4\to\mathrm{i}\,\mathrm{e}^{-\mathrm{i}\theta}x'^0}\,, \tag{C.41}$$

modulo a minus sign, originating in Eq. (C.29), and where the factor in front comes from the normalization of the discrete part and the rotation of the k_4 direction as $k_4 \to -\mathrm{i}\,\mathrm{e}^{\mathrm{i}\theta}k^0$. We observe for $\theta = 0^+$ the relation in Eq. (6.1.16) is confirmed.

D. Checking Minkowski analogues

In this appendix we employ the methods for arbitrary complex rotations, shown in Appendix C., to verify that using the decomposition proposed therein we obtain the usual Minkowski propagator for a complex mass in an empty background.
We consider the operator in Minkowski spacetime

$$\mathrm{i}\not{\partial} - m\,\mathrm{e}^{\mathrm{i}\alpha\gamma^5}\,. \tag{D.42}$$

and begin by proposing a set of plane waves $\{\psi_k\}$, where

$$\psi_k(x) = \frac{1}{(2\pi)^2}\,f(k)\,\mathrm{e}^{-\mathrm{i}kx}\,. \tag{D.43}$$

We will determine the spinor function $f(k)$ as to make the set a complete basis. Each plane wave must satisfy

$$(\mathrm{i}\not{\partial} - m\,\mathrm{e}^{\mathrm{i}\alpha\gamma^5})\psi_k(x) = \xi_k\psi_k(x), \tag{D.44}$$

which simplifies to

$$(\not{k} - m\,\mathrm{e}^{\mathrm{i}\alpha\gamma^5})f(k) = \xi_k f(k)\,. \tag{D.45}$$

We can diagonalize the matrix operator $\not{k} - m\,\mathrm{e}^{\mathrm{i}\alpha\gamma^5}$ to arrive to the following set of eigenvalues:

$$\xi_{k,i} = \left\{-m_\mathrm{R} - \mathrm{i}\sqrt{m_\mathrm{I}^2 - k^2}, -m_\mathrm{R} - \mathrm{i}\sqrt{m_\mathrm{I}^2 - k^2}, -m_\mathrm{R} + \mathrm{i}\sqrt{m_\mathrm{I}^2 - k^2}, -m_\mathrm{R} + \mathrm{i}\sqrt{m_\mathrm{I}^2 - k^2}\right\}, \tag{D.46}$$

which agree via analytical continuation with the spectrum given in the previous appendix (see Eq. (C.27) and Eq. (C.32)). Their eigenvectors are computed and give

$$f_1(k) = \frac{1}{\sqrt{2}}\begin{pmatrix} \dfrac{k^2 + \mathrm{i}k^1}{g(k;m_\mathrm{I})} \\ \dfrac{\mathrm{i}(k^0 - k^3)}{g(k;m_\mathrm{I})} \\ 0 \\ h_+(k;m_\mathrm{I}) \end{pmatrix}, \qquad f_2(k) = \frac{1}{\sqrt{2}}\begin{pmatrix} \dfrac{\mathrm{i}(k^0 + k^3)}{g(k;m_\mathrm{I})} \\ \dfrac{-k^2 + \mathrm{i}k^1}{g(k;m_\mathrm{I})} \\ h_+(k;m_\mathrm{I}) \\ 0 \end{pmatrix},$$

$$f_3(k) = \frac{1}{\sqrt{2}}\begin{pmatrix} -\dfrac{k^2 + \mathrm{i}k^1}{g(k;m_\mathrm{I})} \\ -\dfrac{\mathrm{i}(k^0 - k^3)}{g(k;m_\mathrm{I})} \\ 0 \\ h_-(k;m_\mathrm{I}) \end{pmatrix}, \qquad f_4(k) = \frac{1}{\sqrt{2}}\begin{pmatrix} -\dfrac{\mathrm{i}(k^0 + k^3)}{g(k;m_\mathrm{I})} \\ -\dfrac{-k^2 + \mathrm{i}k^1}{g(k;m_\mathrm{I})} \\ h_-(k;m_\mathrm{I}) \\ 0 \end{pmatrix}, \tag{D.47}$$

with

$$g(k;m_{\rm I}) \equiv \sqrt[4]{m_{\rm I}^2-k^2}\sqrt{\sqrt{m_{\rm I}^2-k^2}+m_{\rm I}}, \tag{D.48}$$

$$h_{\pm}(k;m_{\rm I}) \equiv \frac{\sqrt{\sqrt{m_{\rm I}^2-k^2}\pm m_{\rm I}}}{\sqrt[4]{m_{\rm I}^2-k^2}}. \tag{D.49}$$

The eigenvector written above satisfy orthogonality with the θ-adjoint inner product

$$\tilde{f}_i(k) f_j(k) = \delta_{ij}\,, \tag{D.50}$$

for $\theta \to 0$, that is

$$\tilde{f}_i(k) = f_i(k)^\dagger|_{k_0\to -k_0}\,. \tag{D.51}$$

And the completeness relation can also be verified

$$\sum_{i=1}^{4} f_i(k)\tilde{f}_i(k) = \mathbb{1}_4\,. \tag{D.52}$$

The eigenfunctions in configuration space inherit these properties from the momentum counterparts. First the θ-adjoint is simply

$$\tilde{\psi}_{k,j}(x) = \frac{1}{(2\pi)^2}\,\tilde{f}_j(k)\,\mathrm{e}^{\mathrm{i}kx}\,, \tag{D.53}$$

where the spinor indices have been made explicit, and the inner-product gives

$$\begin{aligned}(\psi_{k,i}(x),\psi_{\{k'\},j}(x)) &= \int \mathrm{d}^4x\tilde{\psi}_{k,i}(x)\psi_{\{k'\},j}(x)\\ &= \frac{1}{(2\pi)^4}\int \mathrm{d}^4x\;\mathrm{e}^{\mathrm{i}(k-k')x}\tilde{f}_i(k)f_j(k)\\ &= \delta_{ij}\delta^4(k-k')\,.\end{aligned} \tag{D.54}$$

The completeness relation can be verified analogously

$$\sum_i \int \mathrm{d}^4k\,\psi_{k,i}(x)\tilde{\psi}_{k,i}(x') = \frac{1}{(2\pi)^4}\int \mathrm{d}^4k\,\mathrm{e}^{-\mathrm{i}k(x-x')}\sum_i f_i(k)\tilde{f}_i(k) = \delta^4(x-x')\mathbb{1}_4\,, \tag{D.55}$$

where we used the completeness relation of the spinors $f(k)$. Collecting these results we can write down the Green's function, or free propagator in this case, as

$$\begin{aligned}S_\varnothing(x,x') &= \sum_i \int \mathrm{d}^4p\,\frac{1}{\xi_{p,i}}\,\psi_{p,i}(x)\tilde{\psi}_{p,i}(x')\\ &= \frac{1}{(2\pi)^4}\int \mathrm{d}^4p\;\mathrm{e}^{-\mathrm{i}p(x-x')}\sum_i \frac{1}{\xi_{p,i}}\,f_i(p)\tilde{f}_i(p)\,.\end{aligned} \tag{D.56}$$

Plugging in the expressions for the eigenvalues found in Eq. (D.46) and eigenvectors in Eq. (D.47) and using the θ-adjoint as in Eq. (D.51) we arrive to

$$S_\varnothing(x,x') = \int \frac{\mathrm{d}^4p}{(2\pi)^4}\;\mathrm{e}^{-\mathrm{i}p(x-x')}\,\frac{(\not{p}+m\,\mathrm{e}^{-\mathrm{i}\gamma^5})}{p^2-m^2+\mathrm{i}\epsilon}\,, \tag{D.57}$$

which agrees with the expression given in Eq. (6.1.41) in the text.

Acknowledgments

With all said and done, I would first of all thank my supervisor Prof. Björn Garbrecht and co-supervisor Dr. Carlos Tamarit, who have accompanied me in the last four years and throughout this tough but nurturing experience that is a PhD. They have been my guides in this journey, so thank you both again first of all for all the knowledge deliberately and unintentionally imparted and for having sustained my insatiable skepticism, questioning, complains, different moods, while enjoying coffee, hiking or simply having lunch together (where I hope we achieved some work-life balance).
For my family, mom, dad and siblings; it has never been more true that "No man is an Iland, intire of it selfe"[183], thank you for supporting me emotionally and financially not lately, but always. I can only hope that you share all my satisfaction and feeling of fulfillment with every step forward.
To all my previous supervisors, teachers and tutors, rest assured that I have learned something from you without exception, for that I am grateful.
I want to also thank the T70 group, for making the PhD experience a more enjoyable one. Thank you Wen-yuan and Juraj for having the patience to teach me many things, specially towards the beginning of this process and for your very interesting questions. Also thanks to my old office colleagues Nico, Philipp, Philip, Patrick, Stefan and Stephan for sharing random questions, thoughts and conversations about everything.
I am only standing on the shoulders of great friends and for that I will always feel thankful. To the guys in Colombia thank you for holding me always down to earth and with a fresh perspective towards life. Thank you Beltrán for proofreading parts of this work. To the guys from LMU: Danu, Alex, Daniel and Max, to whom the MQM experience left a mark, thanks for being my brothers in arms, becoming part of my life and sharing simultaneous perils of all kinds. To my most recent set of friends: Hans, Vishnu, Santiago, Jakob and Uday, thank you for every experience while sharing the apartment, I never felt alone or without a family.
And last but not least, Tami thank you for your immense support in all aspects, for the constant reminder "Du schaffst es", to which I hope I can only answer "Wir haben es geschafft".

Bibliography

[1] Sidney R. Coleman. The Fate of the False Vacuum. 1. Semiclassical Theory. *Phys. Rev.*, D15:2929–2936, May 1977. doi:10.1103/PhysRevD.15.2929. [Erratum: Phys. Rev.D16,1248(1977) doi:10.1103/PhysRevD.16.1248].

[2] Serguei Chatrchyan et al. Observation of a new boson at a mass of 125 GeV with the CMS experiment at the LHC. *Phys. Lett.*, B716:30–61, 2012. doi:10.1016/j.physletb.2012.08.021.

[3] Georges Aad et al. Observation of a new particle in the search for the Standard Model Higgs boson with the ATLAS detector at the LHC. *Phys. Lett.*, B716:1–29, 2012. doi:10.1016/j.physletb.2012.08.020.

[4] M. Tanabashi et al. Review of Particle Physics. *Phys. Rev. D*, 98(3):030001, 2018. doi:10.1103/PhysRevD.98.030001.

[5] Dario Buttazzo, Giuseppe Degrassi, Pier Paolo Giardino, Gian F. Giudice, Filippo Sala, Alberto Salvio, and Alessandro Strumia. Investigating the near-criticality of the higgs boson. *Journal of High Energy Physics*, 2013(12):89, December 2013. ISSN 1029-8479. doi:10.1007/JHEP12(2013)089.

[6] Wen-Yuan Ai, Juan S. Cruz, Björn Garbrecht, and Carlos Tamarit. Gradient effects on false vacuum decay in gauge theory. *Phys. Rev. D*, 102(8):085001, 2020. doi:10.1103/PhysRevD.102.085001.

[7] A.A. Belavin, Alexander M. Polyakov, A.S. Schwartz, and Yu.S. Tyupkin. Pseudoparticle Solutions of the Yang-Mills Equations. *Phys. Lett. B*, 59(1):85–87, October 1975. ISSN 0370-2693. doi:10.1016/0370-2693(75)90163-X. URL `https://www.sciencedirect.com/science/article/pii/037026937590163X`.

[8] Stephen L. Adler. Axial vector vertex in spinor electrodynamics. *Phys. Rev.*, 177: 2426–2438, 1969. doi:10.1103/PhysRev.177.2426.

[9] J.S. Bell and R. Jackiw. A PCAC puzzle: $\pi^0 \to \gamma\gamma$ in the σ model. *Nuovo Cim. A*, 60:47–61, 1969. doi:10.1007/BF02823296.

[10] G. 't Hooft. How Instantons Solve the U(1) Problem. *Phys. Rept.*, 142(6):357–387, September 1986. ISSN 0370-1573. doi:10.1016/0370-1573(86)90117-1.

[11] R. P. Feynman. Space-time approach to non-relativistic quantum mechanics. *Rev. Mod. Phys.*, 20:367–387, April 1948. doi:10.1103/RevModPhys.20.367.

[12] Jean Zinn-Justin. *Quantum field theory and critical phenomena*, volume 77. Clarendon Press, 1989. ISBN 978-0-19-850923-3.

[13] Matthew D. Schwartz. *Quantum Field Theory and the Standard Model*. Cambridge University Press, March 2014. ISBN 978-1-107-03473-0, 978-1-107-03473-0.

[14] Kazuo Fujikawa and Hiroshi Suzuki. *Path Integrals and Quantum Anomalies*. International Series of Monographs on Physics. Oxford University Press, Oxford, 2004. ISBN 978-0-19-852913-2. doi:10.1093/acprof:oso/9780198529132.001.0001.

[15] Jean Zinn-Justin. *Path Integrals in Quantum Mechanics*. Oxford University Press, September 2010. ISBN 9780198566755.

[16] B Osgood, R Phillips, and P Sarnak. Extremals of determinants of Laplacians. *Journal of Functional Analysis*, 80(1):148–211, September 1988. ISSN 0022-1236. doi:10.1016/0022-1236(88)90070-5. URL `https://www.sciencedirect.com/science/article/pii/0022123688900705`.

[17] Steven Weinberg. *The Quantum theory of fields. Vol. 1: Foundations*. Cambridge University Press, June 2005. ISBN 978-0-521-67053-1, 978-0-511-25204-4.

[18] DLMF. *NIST Digital Library of Mathematical Functions*. http://dlmf.nist.gov/, Release 1.1.1 of 2021-03-15, 2021. URL `http://dlmf.nist.gov/`. F. W. J. Olver, A. B. Olde Daalhuis, D. W. Lozier, B. I. Schneider, R. F. Boisvert, C. W. Clark, B. R. Miller, B. V. Saunders, H. S. Cohl, and M. A. McClain, eds.

[19] N. D. Birrell and P. C. W. Davies. *Quantum Fields in Curved Space*. Cambridge University Press, 1 edition, February 1982. ISBN 978-0-521-23385-9 978-0-521-27858-4 978-0-511-62263-2. doi:10.1017/CBO9780511622632. URL `https://www.cambridge.org/core/product/identifier/9780511622632/type/book`.

[20] Michael E. Peskin and Daniel V. Schroeder. *An Introduction to quantum field theory*. Addison-Wesley, Reading, Mass., 1995. ISBN 978-0-201-50397-5. Chap. 7.

[21] Steven Weinberg. *The quantum theory of fields. Vol. 2: Modern applications*. Cambridge University Press, August 2013. ISBN 978-1-139-63247-8, 978-0-521-67054-8, 978-0-521-55002-4.

[22] Sidney Coleman and Erick Weinberg. Radiative corrections as the origin of spontaneous symmetry breaking. *Phys. Rev. D*, 7:1888–1910, March 1973. doi:10.1103/PhysRevD.7.1888.

[23] Ernst Carl Gerlach Stueckelberg de Breidenbach and Andreas Petermann. Normalization of constants in the quanta theory. *Helv. Phys. Acta*, 26:499–520, 1953. doi:10.5169/seals-112426.

[24] Kenneth G. Wilson. Renormalization group and critical phenomena. 1. Renormalization group and the Kadanoff scaling picture. *Phys. Rev. B*, 4:3174–3183, 1971. doi:10.1103/PhysRevB.4.3174.

[25] Kenneth G. Wilson. Renormalization group and critical phenomena. 2. Phase space cell analysis of critical behavior. *Phys. Rev. B*, 4:3184–3205, 1971. doi:10.1103/PhysRevB.4.3184.

[26] Gregor Wentzel. Eine verallgemeinerung der quantenbedingungen für die zwecke der wellenmechanik. *Z. Phys.*, 38(6):518–529, 1926. doi:10.1007/BF01397171.

[27] H. A. Kramers. Wellenmechanik und halbzahlige quantisierung. *Z. Phys.*, 39(10): 828–840, 1926. doi:10.1007/BF01451751.

[28] Léon Brillouin. La mécanique ondulatoire de Schrödinger; une méthode générale de resolution par approximations successives. *Compt. Rend. Hebd. Seances Acad. Sci.*, 183(1):24–26, 1926.

[29] Björn Garbrecht and Peter Millington. Constraining the effective action by a method of external sources. *Nucl. Phys.*, B 906:105–132, 2016. doi:10.1016/j.nuclphysb.2016.02.022.

[30] Björn Garbrecht and Peter Millington. Green's function method for handling radiative effects on false vacuum decay. *Phys. Rev.*, D91:105021, 2015. doi:10.1103/PhysRevD.91.105021.

[31] Wen-Yuan Ai, Björn Garbrecht, and Peter Millington. Radiative effects on false vacuum decay in Higgs-Yukawa theory. *Phys. Rev. D*, 98(7):076014, October 2018. doi:10.1103/PhysRevD.98.076014.

[32] Curtis G. Callan, Jr. Broken scale invariance in scalar field theory. *Phys. Rev. D*, 2:1541–1547, 1970. doi:10.1103/PhysRevD.2.1541.

[33] K. Symanzik. Small distance behaviour in field theory and power counting. *Communications in Mathematical Physics*, 18(3):227–246, September 1970. ISSN 1432-0916. doi:10/fpgwcf.

[34] Sidney Coleman. *Aspects of Symmetry: Selected Erice Lectures*. Cambridge University Press, Cambridge, U.K., 1985. ISBN 978-0-521-31827-3. doi:10.1017/CBO9780511565045.

[35] S. Coleman, V. Glaser, and A. Martin. Action minima among solutions to a class of euclidean scalar field equations. *Comm. Math. Phys.*, 58(2):211–221, 1978. URL `https://projecteuclid.org:443/euclid.cmp/1103901444`.

[36] Wen-Yuan Ai, Björn Garbrecht, and Carlos Tamarit. Functional methods for false vacuum decay in real time. *JHEP*, 12:095, 2019. doi:10.1007/JHEP12(2019)095.

[37] Curtis G. Callan and Sidney Coleman. Fate of the false vacuum. ii. first quantum corrections. *Phys. Rev. D*, 16:1762–1768, September 1977. doi:10.1103/PhysRevD.16.1762.

[38] Jean-Loup Gervais and B. Sakita. Extended Particles in Quantum Field Theories. *Phys. Rev. D*, 11:2943, May 1975. doi:10.1103/PhysRevD.11.2943.

[39] Björn Garbrecht and Peter Millington. Self-consistent radiative corrections to false vacuum decay. *J. Phys. Conf. Ser.*, 873(1):012041, 2017. doi:10.1088/1742-6596/873/1/012041.

[40] J. Baacke and S. Junker. Quantum fluctuations around the electroweak sphaleron. *Phys. Rev. D*, 49:2055–2073, February 1994. doi:10.1103/PhysRevD.49.2055.

[41] J. Baacke and S. Junker. Quantum corrections to the electroweak sphaleron transition. *Mod. Phys. Lett. A*, 8:2869–2874, 1993. doi:10.1142/S0217732393003251.

[42] Jurgen Baacke. One-loop corrections to the instanton transition in the Abelian Higgs model: Gel'fand-Yaglom and Green's function methods. *Phys. Rev. D*, 78:065039, 2008. doi:10.1103/PhysRevD.78.065039.

[43] S. L. Glashow. Partial symmetries of weak interactions. *Nucl. Phys.*, 22:579–588, 1961. doi:10.1016/0029-5582(61)90469-2.

[44] Steven Weinberg. A Model of Leptons. *Phys. Rev. Lett.*, 19:1264–1266, 1967. doi:10.1103/PhysRevLett.19.1264.

[45] A Salam. p. 367 of elementary particle theory, ed. *N. Svartholm (Almquist and Wiksells, Stockholm, 1969)*, 1969.

[46] Marc Sher. Electroweak higgs potentials and vacuum stability. *Phys. Rept.*, 179: 273–418, 1989. doi:10.1016/0370-1573(89)90061-6.

[47] J. F. Donoghue, E. Golowich, and Barry R. Holstein. *Dynamics of the standard model*, volume 2. CUP, 2014. doi:10.1017/CBO9780511524370.

[48] Igor P. Ivanov. Building and testing models with extended higgs sectors. *Prog. Part. Nucl. Phys.*, 95:160–208, 2017. doi:10.1016/j.ppnp.2017.03.001.

[49] P. A. Zyla et al. Review of Particle Physics. *PTEP*, 2020(8):083C01, 2020. doi:10.1093/ptep/ptaa104.

[50] K. Fujikawa, B. W. Lee, and A. I. Sanda. Generalized renormalizable gauge formulation of spontaneously broken gauge theories. *Phys. Rev. D*, 6:2923–2943, 1972. doi:10.1103/PhysRevD.6.2923.

[51] L. Dolan and R. Jackiw. Gauge invariant signal for gauge symmetry breaking. *Phys. Rev. D*, 9:2904, 1974. doi:10.1103/PhysRevD.9.2904.

[52] T. P. Cheng, E. Eichten, and Ling-Fong Li. Higgs phenomena in asymptotically free gauge theories. *Physical Review D*, 9(8):2259–2273, April 1974. doi:10.1103/PhysRevD.9.2259.

[53] D. R. T. Jones. Two loop diagrams in yang-mills theory. *Nucl. Phys. B*, 75:531, 1974. doi:10.1016/0550-3213(74)90093-5.

[54] Mark S. Fischler and Christopher T. Hill. Effects of large mass fermions on m x and sin2 thetaw. *Nucl. Phys. B*, 193:53–60, 1981. doi:10.1016/0550-3213(81)90517-4.

[55] D. R. T. Jones. The two loop beta function for a g(1) x g(2) gauge theory. *Phys. Rev. D*, 25:581, 1982. doi:10.1103/PhysRevD.25.581.

[56] I. Jack and H. Osborn. General two loop beta functions for gauge theories with arbitrary scalar fields. *J. Phys. A*, 16:1101, 1983. doi:10.1088/0305-4470/16/5/026.

[57] Marie E. Machacek and Michael T. Vaughn. Two-loop renormalization group equations in a general quantum field theory (II). Yukawa couplings. *Nuclear Physics B*, 236(1):221–232, April 1984. ISSN 0550-3213. doi:10.1016/0550-3213(84)90533-9.

[58] Marie E. Machacek and Michael T. Vaughn. Two loop renormalization group equations in a general quantum field theory. 3. scalar quartic couplings. *Nucl. Phys. B*, 249:70–92, 1985. doi:10.1016/0550-3213(85)90040-9.

[59] Stephen P. Martin. Two Loop Effective Potential for a General Renormalizable Theory and Softly Broken Supersymmetry. *Phys. Rev. D*, 65:116003, 2002. doi:10.1103/PhysRevD.65.116003.

[60] Stephen P. Martin. Three-Loop Standard Model Effective Potential at Leading Order in Strong and Top Yukawa Couplings. *Phys. Rev. D*, 89(1):013003, 2014. doi:10.1103/PhysRevD.89.013003.

[61] A. V. Bednyakov and A. F. Pikelner. Four-loop strong coupling beta-function in the Standard Model. *Phys. Lett. B*, 762:151–156, 2016. doi:10.1016/j.physletb.2016.09.007.

[62] Colin Poole and Anders Eller Thomsen. Constraints on 3- and 4-loop β-functions in a general four-dimensional Quantum Field Theory. *JHEP*, 09:055, 2019. doi:10.1007/JHEP09(2019)055.

[63] Paul Langacker. Grand unified theories and proton decay. *Physics Reports*, 72(4): 185–385, 1981. ISSN 0370-1573. doi:10/bkjfqg.

[64] Andrei D. Linde. On the Vacuum Instability and the Higgs Meson Mass. *Phys. Lett. B*, 70:306–308, 1977. doi:10.1016/0370-2693(77)90664-5.

[65] Pham Quang Hung. Vacuum instability and new constraints on fermion masses. *Phys. Rev. Lett.*, 42(14):873–876, April 1979. ISSN 0031-9007. doi:10.1103/PhysRevLett.42.873.

[66] Gino Isidori, Giovanni Ridolfi, and Alessandro Strumia. On the metastability of the standard model vacuum. *Nucl. Phys.*, B609:387–409, 2001. doi:10.1016/S0550-3213(01)00302-9.

[67] D0 Collaboration, S. Abachi, et al. Observation of the Top Quark. *Physical Review Letters*, 74(14):2632–2637, April 1995. doi:10/cm6jx2.

[68] CDF Collaboration, F. Abe, et al. Observation of Top Quark Production in $\overline{p}p$ Collisions with the Collider Detector at Fermilab. *Physical Review Letters*, 74(14): 2626–2631, April 1995. doi:10/djhmrz.

[69] Giuseppe Degrassi, Stefano Di Vita, Joan Elias-Miró, José R. Espinosa, Gian F. Giudice, Gino Isidori, and Alessandro Strumia. Higgs mass and vacuum stability in the standard model at nnlo. *Journal of High Energy Physics*, 2012(8):98, August 2012. ISSN 1029-8479. doi:10.1007/JHEP08(2012)098.

[70] J. R. Espinosa and M. Quiros. Improved metastability bounds on the standard model Higgs mass. *Phys. Lett. B*, 353:257–266, 1995. doi:10.1016/0370-2693(95)00572-3.

[71] Jose Ramon Espinosa, John Ellis, Gian Giudice, Andreas Hoecker, and Toni Riotto. The probable fate of the standard model. *PoS*, EPS-HEP2009:255, 2009. doi:10.22323/1.084.0255.

[72] Joan Elias-Miro, Jose R. Espinosa, Gian F. Giudice, Gino Isidori, Antonio Riotto, and Alessandro Strumia. Higgs mass implications on the stability of the electroweak vacuum. *Phys. Lett.*, B709:222–228, 2012. doi:10.1016/j.physletb.2012.02.013.

[73] J R Espinosa, G F Giudice, and A Riotto. Cosmological implications of the higgs mass measurement. *Journal of Cosmology and Astroparticle Physics*, 2008(05):002, May 2008. doi:10.1088/1475-7516/2008/05/002.

[74] Tommi Markkanen, Arttu Rajantie, and Stephen Stopyra. Cosmological aspects of higgs vacuum metastability. *Front. Astron. Space Sci.*, 5:40, 2018. doi:10.3389/fspas.2018.00040.

[75] Arnd Sürig. Selfconsistent treatment of bubble nucleation at the electroweak phase transition. *Phys. Rev. D*, 57:5049–5063, 1998. doi:10.1103/PhysRevD.57.5049.

[76] A.D. Linde. Decay of the False Vacuum at Finite Temperature. *Nucl. Phys. B*, 216(2):421, 1983. ISSN 0550-3213. doi:10.1016/0550-3213(83)90072-X. URL `http://www.sciencedirect.com/science/article/pii/0550321383902936`. [Erratum: Nucl.Phys.B 223, 544 (1983)].

[77] M. E. Shaposhnikov. Baryon Asymmetry of the Universe in Standard Electroweak Theory. *Nucl. Phys. B*, 287:757–775, 1987. doi:10.1016/0550-3213(87)90127-1.

[78] Larry D. McLerran. Can the Observed Baryon Asymmetry Be Produced at the Electroweak Phase Transition? *Phys. Rev. Lett.*, 62:1075, 1989. doi:10.1103/PhysRevLett.62.1075.

[79] Peter Brockway Arnold and Olivier Espinosa. The Effective potential and first order phase transitions: Beyond leading-order. *Phys. Rev. D*, 47:3546, 1993. doi:10.1103/PhysRevD.47.3546. [Erratum: Phys.Rev.D 50, 6662 (1994)].

[80] Greg W. Anderson and Lawrence J. Hall. The Electroweak phase transition and baryogenesis. *Phys. Rev. D*, 45:2685–2698, 1992. doi:10.1103/PhysRevD.45.2685.

[81] S. W. Hawking, I. G. Moss, and J. M. Stewart. Bubble Collisions in the Very Early Universe. *Phys. Rev. D*, 26:2681, 1982. doi:10.1103/PhysRevD.26.2681.

[82] Mark Hindmarsh, Stephan J. Huber, Kari Rummukainen, and David J. Weir. Gravitational waves from the sound of a first order phase transition. *Phys. Rev. Lett.*, 112:041301, 2014. doi:10.1103/PhysRevLett.112.041301.

[83] David J. Weir. Gravitational waves from a first-order electroweak phase transition: A brief review. *Philosophical Transactions of the Royal Society A: Mathematical, Physical and Engineering Sciences*, 376(2114):20170126, March 2018. ISSN 1364-503X, 1471-2962. doi:10.1098/rsta.2017.0126.

[84] R. V. Konoplich. Calculation of Quantum Corrections to Nontrivial Classical Solutions by Means of the Zeta Function. *Theor. Math. Phys.*, 73:1286–1295, 1987. doi:10.1007/BF01041911.

[85] Björn Garbrecht and Peter Millington. Fluctuations about the fubini-lipatov instanton for false vacuum decay in classically scale invariant models. *Phys. Rev. D*, 98(1):016001, July 2018. doi:10.1103/PhysRevD.98.016001.

[86] N.K. Nielsen. On the Gauge Dependence of Spontaneous Symmetry Breaking in Gauge Theories. *Nucl. Phys. B*, 101(1):173–188, 1975. ISSN 0550-3213. doi:10.1016/0550-3213(75)90301-6. URL `http://www.sciencedirect.com/science/article/pii/0550321375903016`.

[87] Reijiro Fukuda and Taichiro Kugo. Gauge Invariance in the Effective Action and Potential. *Phys. Rev. D*, 13:3469, 1976. doi:10.1103/PhysRevD.13.3469.

[88] Dimitrios Metaxas and Erick J. Weinberg. Gauge independence of the bubble nucleation rate in theories with radiative symmetry breaking. *Phys. Rev. D*, 53:836–843, January 1996. doi:10.1103/PhysRevD.53.836.

[89] D. Metaxas. Derivative expansion and gauge independence of the false vacuum decay rate in various gauges. *Phys. Rev. D*, 63:085009, March 2001. doi:10.1103/PhysRevD.63.085009.

[90] Anders Andreassen, William Frost, and Matthew D. Schwartz. Consistent Use of Effective Potentials. *Phys. Rev. D*, 91(1):016009, January 2015. doi:10.1103/PhysRevD.91.016009.

[91] A.V. Bednyakov, B.A. Kniehl, A.F. Pikelner, and O.L. Veretin. Stability of the Electroweak Vacuum: Gauge Independence and Advanced Precision. *Phys. Rev. Lett.*, 115(20):201802, 2015. doi:10.1103/PhysRevLett.115.201802.

[92] Alexis D. Plascencia and Carlos Tamarit. Convexity, gauge-dependence and tunneling rates. *JHEP*, 10(10):099, October 2016. ISSN 1029-8479. doi:10.1007/JHEP10(2016)099.

[93] Björn Garbrecht and Peter Millington. Self-consistent solitons for vacuum decay in radiatively generated potentials. *Phys. Rev.*, D92:125022, 2015. doi:10.1103/PhysRevD.92.125022.

[94] M. Endo, T. Moroi, M. M. Nojiri, and Y. Shoji. False vacuum decay in gauge theory. *JHEP 1711*, 11:074, 2017. doi:10.1007/JHEP11(2017)074.

[95] A. Andreassen, William Frost, and M. D. Schwartz. Scale-invariant instantons and the complete lifetime of the Standard Model. *Phys. Rev.*, D97(5):056006, 2017. doi:10.1103/PhysRevD.97.056006.

[96] Vincenzo Branchina, Emanuele Messina, and Marc Sher. Lifetime of the electroweak vacuum and sensitivity to Planck scale physics. *Phys. Rev*, D 91:013003, 2015. doi:10.1103/PhysRevD.91.013003.

[97] Wolfram Research, Inc. Mathematica, Version 11.3, 2018. Champaign, IL, 2018.

[98] I. J. R. Aitchison and C. M. Fraser. Fermion loop contribution to skyrmion stability. *Physics Letters B*, 146(1):63–66, October 1984. ISSN 0370-2693. doi:10.1016/0370-2693(84)90644-0. URL `https://www.sciencedirect.com/science/article/pii/0370269384906440`.

[99] Lai-Him Chan. Effective-action expansion in perturbation theory. *Phys. Rev. Lett.*, 54:1222–1225, March 1985. doi:10.1103/PhysRevLett.54.1222.

[100] Lai-Him Chan. Derivative expansion for the one-loop effective actions with internal symmetry. *Phys. Rev. Lett.*, 57:1199–1202, September 1986. doi:10.1103/PhysRevLett.57.1199.

[101] Oren Cheyette. Derivative Expansion of the Effective Action. *Phys. Rev. Lett.*, 55: 2394, 1985. doi:10.1103/PhysRevLett.55.2394.

[102] Oren Cheyette. Effective Action for the Standard Model With Large Higgs Mass. *Nucl. Phys.*, B297:183–204, 1988. doi:10.1016/0550-3213(88)90205-2.

[103] M. K. Gaillard. The Effective One Loop Lagrangian With Derivative Couplings. *Nucl. Phys.*, B268:669–692, 1986. doi:10.1016/0550-3213(86)90264-6.

[104] Brian Henning, Xiaochuan Lu, and Hitoshi Murayama. How to use the Standard Model effective field theory. *Journal of High Energy Physics*, 2016(1):23, January 2016. ISSN 1029-8479. doi:10.1007/JHEP01(2016)023.

[105] Gerard 't Hooft. Computation of the Quantum Effects Due to a Four-Dimensional Pseudoparticle. *Phys. Rev. D*, 14:3432–3450, 1976. doi:10.1103/PhysRevD.14.3432. [Erratum: Phys.Rev.D 18, 2199 (1978)].

[106] Michael Dine. TASI Lectures on The Strong CP Problem. November 2000.

[107] Anson Hook. TASI Lectures on the Strong CP Problem and Axions. December 2018.

[108] Luca Di Luzio, Maurizio Giannotti, Enrico Nardi, and Luca Visinelli. The landscape of qcd axion models. *Phys. Rept.*, 870:1–117, 2020. doi:10.1016/j.physrep.2020.06.002.

[109] C. G. Callan, R. F. Dashen, and D. J. Gross. The structure of the gauge theory vacuum. *Physics Letters B*, 63(3):334–340, August 1976. ISSN 0370-2693. doi:10.1016/0370-2693(76)90277-X.

[110] R. Jackiw and C. Rebbi. Vacuum Periodicity in a Yang-Mills Quantum Theory. *Physical Review Letters*, 37(3):172–175, July 1976. doi:10/dp392d.

[111] R. Jackiw. Introduction to the Yang-Mills quantum theory. *Reviews of Modern Physics*, 52(4):661–673, October 1980. ISSN 0034-6861. doi:10.1103/RevModPhys.52.661.

[112] Kiyosi Itō and Nihon Sūgakkai, editors. *Encyclopedic Dictionary of Mathematics*. MIT Press, Cambridge, Mass, 2nd ed., 1st mit press pbk. ed edition, 1993. ISBN 978-0-262-59020-4 978-0-262-09026-1.

[113] G.L. Naber. *Topology, Geometry and Gauge Fields: Foundations*. Texts in Applied Mathematics. Springer New York, 2010. ISBN 978-1-4419-7254-5.

[114] Stefan Vandoren and Peter van Nieuwenhuizen. Lectures on instantons. February 2008.

[115] Varouzhan Baluni. CP -nonconserving effects in quantum chromodynamics. *Physical Review D*, 19(7):2227–2230, April 1979. ISSN 0556-2821. doi:10.1103/PhysRevD.19.2227.

[116] R. J. Crewther, P. Di Vecchia, G. Veneziano, and Edward Witten. Chiral Estimate of the Electric Dipole Moment of the Neutron in Quantum Chromodynamics. *Phys. Lett. B*, 88:123, 1979. doi:10.1016/0370-2693(79)90128-X. [Erratum: Phys.Lett.B 91, 487 (1980)].

[117] C. Abel et al. Measurement of the permanent electric dipole moment of the neutron. *Phys. Rev. Lett.*, 124(8):081803, 2020. doi:10.1103/PhysRevLett.124.081803.

[118] Roger Dashen. Chiral SU(3) $\bigotimes$ SU(3) as a Symmetry of the Strong Interactions. *Physical Review*, 183(5):1245–1260, July 1969. doi:10.1103/physrev.183.1245.

[119] Roger Dashen and Marvin Weinstein. Soft Pions, Chiral Symmetry, and Phenomenological Lagrangians. *Physical Review*, 183(5):1261–1291, July 1969. doi:10.1103/physrev.183.1261.

[120] S. Coleman, J. Wess, and Bruno Zumino. Structure of phenomenological lagrangians. i. *Phys. Rev.*, 177(5):2239–2247, January 1969. doi:10.1103/PhysRev.177.2239.

[121] Curtis G. Callan, Sidney Coleman, J. Wess, and Bruno Zumino. Structure of phenomenological lagrangians. ii. *Phys. Rev.*, 177(5):2247–2250, January 1969. doi:10.1103/PhysRev.177.2247.

[122] A. Pich. Chiral perturbation theory. *Reports on Progress in Physics*, 58(6):563–609, June 1995. ISSN 0034-4885. doi:10.1088/0034-4885/58/6/001.

[123] Howard Georgi. *Weak Interactions and Modern Particle Theory*. Dover Publications, Mineola, N.Y, dover ed., rev. and updated edition, 2009. ISBN 978-0-486-46904-1.

[124] Stefan Scherer and Matthias R. Schindler. *A Primer for Chiral Perturbation Theory*. Springer Berlin Heidelberg, 2012. doi:10.1007/978-3-642-19254-8.

[125] J. F Cornwell. *Group Theory in Physics: An Introduction.* Elsevier, Burlington, 1997. ISBN 978-0-08-053266-0 978-0-12-189800-7. URL `https://public.ebookcentral.proquest.com/choice/publicfullrecord.aspx?p=349344`.

[126] Brian C. Hall. *An Elementary introduction to groups and representations*. Graduate Texts in Mathematics. Springer International Publishing, 2 edition, May 2015. ISBN 978-3-319-13466-6. doi:10.1007/978-3-319-13467-3. URL `https://www.springer.com/gp/book/9783319134666`.

[127] A. Zee. *Group Theory in a Nutshell for Physicists*. In a Nutshell. Princeton University Press, Princeton, 2016. ISBN 978-0-691-16269-0.

[128] Steven Weinberg. The U(1) Problem. *Phys. Rev. D*, 11:3583–3593, 1975. doi:10.1103/PhysRevD.11.3583.

[129] Hai-Yang Cheng. The strong CP problem revisited. *Physics Reports*, 158(1):1–89, January 1988. ISSN 0370-1573. doi:10.1016/0370-1573(88)90135-4.

[130] Roger Dashen. Some Features of Chiral Symmetry Breaking. *Physical Review D*, 3 (8):1879–1889, April 1971. ISSN 0556-2821. doi:10.1103/PhysRevD.3.1879.

[131] R. Jackiw and C. Rebbi. Solitons with fermion number $\frac{1}{2}$. *Physical Review D*, 13 (12):3398–3409, June 1976. ISSN 0556-2821. doi:10.1103/PhysRevD.13.3398.

[132] Gerard 't Hooft. Symmetry Breaking Through Bell-Jackiw Anomalies. *Phys. Rev. Lett.*, 37:8–11, 1976. doi:10.1103/PhysRevLett.37.8.

[133] Michael Creutz. The 't Hooft vertex revisited. *Annals of Physics*, 323(9):2349–2365, September 2008. ISSN 0003-4916. doi:10.1016/j.aop.2007.12.008. URL `https://linkinghub.elsevier.com/retrieve/pii/S0003491607001935`.

[134] Edward V Shuryak. *The QCD Vacuum, Hadrons and Superdense Matter*, volume 71 of *World Scientific Lecture Notes in Physics*. WORLD SCIENTIFIC, second edition, October 2004. ISBN 978-981-238-573-4 978-981-256-569-3. doi:10.1142/5367.

[135] P. Di Vecchia and G. Veneziano. Chiral dynamics in the large N limit. *Nuclear Physics B*, 171:253–272, 1980. ISSN 0550-3213. doi:10.1016/0550-3213(80)90370-3.

[136] Mark Allen Srednicki. *Quantum Field Theory*. Cambridge University Press, Cambridge ; New York, 2007. ISBN 978-0-521-86449-7.

[137] Edward Witten. Current Algebra Theorems for the U(1) Goldstone Boson. *Nucl. Phys. B*, 156:269–283, 1979. doi:10.1016/0550-3213(79)90031-2. URL `https://inspirehep.net/literature/140486`.

[138] Enrico Meggiolaro. Topological susceptibility of QCD: From Minkowskian to Euclidean theory. *Physical Review D*, 58(8):085002, August 1998. doi:10.1103/PhysRevD.58.085002.

[139] G. Veneziano. U(1) without instantons. *Nuclear Physics B*, 159(1):213–224, November 1979. ISSN 0550-3213. doi:10.1016/0550-3213(79)90332-8. URL `http://www.sciencedirect.com/science/article/pii/0550321379903328`.

[140] P. Di Vecchia, K. Fabricius, G. C. Rossi, and G. Veneziano. Preliminary evidence for $u_a(1)$ breaking in QCD from lattice calculations. *Nuclear Physics B*, 192(2): 392–408, December 1981. ISSN 0550-3213. doi:10.1016/0550-3213(81)90432-6. URL `https://www.sciencedirect.com/science/article/pii/0550321381904326`.

[141] Claudio Bonati and Paolo Rossi. The topological susceptibility of two-dimensional $U(N)$ gauge theories. *Physical Review D*, 99(5):054503, March 2019. ISSN 2470-0010, 2470-0029. doi:10.1103/PhysRevD.99.054503.

[142] Andrea Shindler, Thomas Luu, and Jordy de Vries. Nucleon electric dipole moment with the gradient flow: The θ-term contribution. *Physical Review D*, 92(9):094518, November 2015. doi:10.1103/PhysRevD.92.094518. URL `https://link.aps.org/doi/10.1103/PhysRevD.92.094518`.

[143] Marco Gorghetto and Giovanni Villadoro. Topological susceptibility and QCD axion mass: QED and NNLO corrections. *Journal of High Energy Physics*, 2019(3):33, March 2019. ISSN 1029-8479. doi:10.1007/JHEP03(2019)033.

[144] G.L. Naber. *Topology, geometry, and gauge fields: Interactions*, volume 141 of *Applied Mathematical Sciences*. Springer-Verlag, New York, 2 edition, 2011. ISBN 978-1-4419-7894-3. doi:10.1007/978-1-4419-7895-0. URL `https://www.springer.com/gp/book/9781441978943`.

[145] Mark J.D. Hamilton. *Mathematical Gauge Theory: With Applications to the Standard Model of Particle Physics*. Springer Berlin Heidelberg, New York, NY, 1st edition edition, 2017. ISBN 978-3-319-68438-3.

[146] M. Nakahara. *Geometry, Topology and Physics, Second Edition*. Graduate Student Series in Physics. Taylor & Francis, 2003. ISBN 978-0-7503-0606-5.

[147] A.I. Vainshtein, Valentin I. Zakharov, V.A. Novikov, and Mikhail A. Shifman. ABC's of Instantons. *Sov. Phys. Usp.*, 25(4):195, April 1982. ISSN 0038-5670. doi:10.1070/PU1982v025n04ABEH004533.

[148] T. Schaefer and E. Shuryak. Instantons in QCD. *Reviews of Modern Physics*, 70(2): 323–425, April 1998. ISSN 0034-6861, 1539-0756. doi:10.1103/RevModPhys.70.323.

[149] E. B. Bogomolny. Stability of Classical Solutions. *Sov. J. Nucl. Phys.*, 24:449, 1976.

[150] M. K. Prasad and Charles M. Sommerfield. Exact classical solution for the 't hooft monopole and the julia-zee dyon. *Phys. Rev. Lett.*, 35:760–762, September 1975. doi:10.1103/PhysRevLett.35.760.

[151] R. Jackiw and C. Rebbi. Conformal properties of a Yang-Mills pseudoparticle. *Physical Review D*, 14(2):517–523, July 1976. doi:10.1103/PhysRevD.14.517.

[152] Frank Wilczek. Inequivalent embeddings of SU(2) and instanton interactions. *Physics Letters B*, 65(2):160–162, November 1976. ISSN 0370-2693. doi:10.1016/0370-2693(76)90021-6. URL `https://www.sciencedirect.com/science/article/pii/0370269376900216`.

[153] Curtis G. Callan, Roger Dashen, and David J. Gross. Toward a theory of the strong interactions. *Physical Review D*, 17(10):2717–2763, May 1978. doi:10.1103/PhysRevD.17.2717.

[154] Curtis G. Callan, Roger F. Dashen, and David J. Gross. A theory of hadronic structure. *Physical Review D*, 19(6):1826–1855, March 1979. doi:10.1103/PhysRevD.19.1826.

[155] Mikhail A. Shifman, A.I. Vainshtein, and Valentin I. Zakharov. Instanton Density in a Theory with Massless Quarks. *Nucl. Phys. B*, 163:46–56, January 1980. ISSN 0550-3213. doi:10.1016/0550-3213(80)90389-2. URL `https://linkinghub.elsevier.com/retrieve/pii/0550321380903892`.

[156] Wen-Yuan Ai, Juan S. Cruz, Björn Garbrecht, and Carlos Tamarit. Absence of CP violation in the strong interactions. January 2020.

[157] Edward Witten. Analytic Continuation Of Chern-Simons Theory. *AMS/IP Stud. Adv. Math.*, 50:347–446, 2011.

[158] Yuya Tanizaki and Takayuki Koike. Real-time Feynman path integral with Picard–Lefschetz theory and its applications to quantum tunneling. *Annals Phys.*, 351: 250–274, 2014. doi:10.1016/j.aop.2014.09.003.

[159] Aleksey Cherman and Mithat Unsal. Real-Time Feynman Path Integral Realization of Instantons. July 2014.

[160] Anders Andreassen, David Farhi, William Frost, and Matthew D. Schwartz. Precision decay rate calculations in quantum field theory. *Phys. Rev. D*, 95(8):085011, 2017. doi:10.1103/PhysRevD.95.085011.

[161] Zong-Gang Mou, Paul M. Saffin, Anders Tranberg, and Simon Woodward. Real-time quantum dynamics, path integrals and the method of thimbles. *JHEP*, 06:094, 2019. doi:10.1007/JHEP06(2019)094.

[162] Zong-Gang Mou, Paul M. Saffin, and Anders Tranberg. Quantum tunnelling, real-time dynamics and Picard-Lefschetz thimbles. *JHEP*, 11:135, 2019. doi:10.1007/JHEP11(2019)135.

[163] Lowell S. Brown, Robert D. Carlitz, Dennis B. Creamer, and Choonkyu Lee. Propagation functions in pseudoparticle fields. *Physical Review D*, 17(6):1583–1597, March 1978. doi:10.1103/PhysRevD.17.1583.

[164] M. F. Atiyah and I. M. Singer. The Index of Elliptic Operators: I. *Annals of Mathematics*, 87(3):484–530, 1968. ISSN 0003-486X. doi:10.2307/1970715. URL https://www.jstor.org/stable/1970715.

[165] A. S. Schwarz. On regular solutions of Euclidean Yang-Mills equations. *Physics Letters B*, 67(2):172–174, March 1977. ISSN 0370-2693. doi:10.1016/0370-2693(77)90095-8. URL https://www.sciencedirect.com/science/article/pii/0370269377900958.

[166] Dmitri Diakonov and V.Yu. Petrov. A Theory of Light Quarks in the Instanton Vacuum. *Nucl. Phys. B*, 272(2):457–489, July 1986. ISSN 0550-3213. doi:10.1016/0550-3213(86)90011-8. URL https://linkinghub.elsevier.com/retrieve/pii/0550321386900118.

[167] P. V. Pobylitsa. The quark propagator and correlation functions in the instanton vacuum. *Physics Letters B*, 226(3):387–392, August 1989. ISSN 0370-2693. doi:10.1016/0370-2693(89)91216-1. URL https://www.sciencedirect.com/science/article/pii/0370269389912161.

[168] Claude W. Bernard. Gauge Zero Modes, Instanton Determinants, and QCD Calculations. *Phys. Rev. D*, 19(10):3013, May 1979. doi:10.1103/PhysRevD.19.3013.

[169] David G. Cerdeño, Peter Reimitz, Kazuki Sakurai, and Carlos Tamarit. $B + L$ violation at colliders and new physics. *JHEP*, 04:076, 2018. doi:10.1007/JHEP04(2018)076.

[170] Cumrun Vafa and Edward Witten. Parity Conservation in Quantum Chromodynamics. *Physical Review Letters*, 53(6):535–536, August 1984. doi:10.1103/PhysRevLett.53.535.

[171] H. Leutwyler and Andrei V. Smilga. Spectrum of Dirac operator and role of winding number in QCD. *Phys. Rev. D*, 46(12):5607–5632, December 1992. ISSN 0556-2821. doi:10.1103/PhysRevD.46.5607.

[172] R.F. Streater and A.S. Wightman. *PCT, spin and statistics, and all that*. Princeton University Press., 1989. ISBN 978-0-691-07062-9. URL https://www.jstor.org/stable/j.ctt1cx3vcq.1.

[173] J. J. M. Verbaarschot and T. Wettig. Dirac spectrum of one-flavor QCD at $\theta = 0$ and continuity of the chiral condensate. *Physical Review D*, 90(11):116004, December 2014. doi:10.1103/physrevd.90.116004.

[174] R. Brower, S. Chandrasekharan, J. W. Negele, and U. J. Wiese. QCD at fixed topology. *Physics Letters B*, 560(1):64–74, May 2003. ISSN 0370-2693. doi:10.1016/S0370-2693(03)00369-1. URL https://www.sciencedirect.com/science/article/pii/S0370269303003691.

[175] Sinya Aoki, Hidenori Fukaya, Shoji Hashimoto, and Tetsuya Onogi. Finite volume QCD at fixed topological charge. *Physical Review D*, 76(5):054508, September 2007. ISSN 1550-7998, 1550-2368. doi:10.1103/PhysRevD.76.054508.

[176] F.-K. Guo, R. Horsley, U.-G. Meißner, Y. Nakamura, H. Perlt, P. E. L. Rakow, G. Schierholz, A. Schiller, and J. M. Zanotti. Electric Dipole Moment of the Neutron from 2+1 Flavor Lattice QCD. *Physical Review Letters*, 115(6):062001, August 2015. doi:10.1103/PhysRevLett.115.062001. URL `https://link.aps.org/doi/10.1103/PhysRevLett.115.062001`.

[177] M. A. Shifman, A. I. Vainshtein, and V. I. Zakharov. Can confinement ensure natural CP invariance of strong interactions? *Nuclear Physics B*, 166(3):493–506, April 1980. ISSN 0550-3213. doi:10.1016/0550-3213(80)90209-6.

[178] Kerson Huang. *Quantum Field Theory: From Operators to Path Integrals*. Wiley, New York, 1998. ISBN 978-0-471-14120-4.

[179] Konrad Osterwalder and Robert Schrader. Axioms for Euclidean Green's functions. *Communications in Mathematical Physics*, 31(2):83–112, June 1973. ISSN 0010-3616, 1432-0916. doi:10.1007/BF01645738.

[180] Konrad Osterwalder and Robert Schrader. Axioms for Euclidean Green's functions II. *Communications in Mathematical Physics*, 42(3):281–305, October 1975. ISSN 1432-0916. doi:10.1007/BF01608978.

[181] Peter van Nieuwenhuizen and Andrew Waldron. On Euclidean spinors and Wick rotations. *Physics Letters B*, 389(1):29–36, December 1996. ISSN 0370-2693. doi:10.1016/S0370-2693(96)01251-8. URL `https://www.sciencedirect.com/science/article/pii/S0370269396012518`.

[182] Julian Schwinger. Euclidean Quantum Electrodynamics. *Physical Review*, 115(3):721–731, August 1959. doi:10.1103/PhysRev.115.721. URL `https://link.aps.org/doi/10.1103/PhysRev.115.721`.

[183] John Donne, Helen Lush, and John Donne. *No Man Is an Island*. Souvenir, London, 1999. ISBN 978-0-285-62874-8.

Index